# Illuminating The Surgical Field

## Advances in Intraoperative NIR Fluorescence Imaging

Hidde A. Galema

Financial support for the publication of this thesis was generously provided by: The Erasmus University Rotterdam, Erasmus MC department of Surgery and department of Otorhinolaryngology, Head and Neck Surgery, Surgimab, Stöppler Medical, Sirius Medical, Mobula IGM, Coloplast, Erbe, ABN AMRO and Chipsoft.

Cover design: Lorraine Lauwerends

Lay-out: Wouter Aalberts

Print by: RidderPrint

# Illuminating The Surgical Field

Advances in Intraoperative NIR fluorescence Imaging

**Het chirurgische veld oplichten**

Ontwikkelingen in intra-operatieve NIR fluorescentie beeldvorming

**Thesis**

to obtain the degree of Doctor from the
Erasmus University Rotterdam
by command of the rector magnificus

Prof.dr. A.L. Bredenoord

and in accordance with the decision of the Doctorate Board.

The public defence shall be held on
Tuesday, 5 December 2023 at 10:30 hrs

by

**Hidde Ake Galema**

Born in Leiden

**Erasmus University Rotterdam**

**PROMOTIECOMMISSIE**

| | |
|---|---|
| **Promotors** | Prof. dr. C. Verhoef |
| | Prof. dr. R.J. Baatenburg de Jong |
| **Overige leden** | Prof. dr. M. Smits |
| | Prof. dr. C.W.G.M. Löwik |
| | Prof. dr. S. Kruijff |
| **Copromotors** | Dr. D.E. Hilling |
| | Dr. S. Keereweer |

## TABLE OF CONTENTS

# Chapter 1

## General introduction and outline of this thesis

## GENERAL INTRODUCTION

Surgery is still the cornerstone treatment modality for many solid tumours despite modern neoadjuvant therapies. Introduction of these (neo)adjuvant therapies and minimally invasive surgery improved outcomes of most surgically treated patients with solid tumours over the last decades (1-5). Despite these improved outcomes, cancer surgery can still result in unfavourable outcomes such as inadequate resection margins or surgical complications. Inadequate resection margins are associated with a decrease in overall survival for most tumour types and often necessitates burdensome adjuvant therapies (6-8). Feared surgical complications include anastomotic leakage, and iatrogenic injury of vital structures such as bile ducts, ureters, or nerves. Although some complications are rare, most are associated with high morbidity, reoperations, prolonged hospital admission, and in some cases even death (9-12). As inadequate margins and surgical complications require additional treatment, they also increase health-care costs. Both these outcomes can be associated with inadequate identification of structures with conventional white light visualisation and palpation. With the introduction of minimally invasive surgery, identification of vital structures became even more challenging, as tactile feedback is lacking with this approach. Moreover, discriminating tumour tissue from neoadjuvant treatment related fibrosis can be challenging. New intraoperative imaging techniques are therefore warranted to improve visualisation of tumours and vital structures. Near-infrared (NIR) fluorescence imaging is a promising imaging technique that can be used to perform intraoperative imaging of a variety of tissues, including tumours and vital structures (13-15).

### Near-infrared fluorescence imaging

NIR fluorescence imaging requires a dedicated fluorescence camera system and a contrast agent with fluorescent properties in the near-infrared spectrum of light (i.e. a fluorophore). Fluorescence camera systems are composed of a laser that sends a laser light bundle at a wavelength in the NIR spectrum of light (~650 – 900 nanometre). When the fluorophore is reached by the laser light, the fluorophore absorbs and subsequently emits NIR light. The fluorescence camera system is optimised for detection of this emitted light. For NIR fluorescence imaging, exogenous fluorophores are mostly used. However, endogenous tissue also has fluorescent properties and can serve as an endogenous fluorophore, when exited by the appropriate laser light (i.e. autofluorescence). NIR light has a higher wavelength compared to visible white light (~380 – 700 nm), and is therefore invisible to the human eye. In general, when any light is traveling through tissue, it is subject to scattering and absorption (16). Scattering causes the light to change its direction, which can interfere with imaging of the fluorophore of interest. Absorption causes the light to be absorbed by a certain anatomical structure, after which it emits (auto)fluorescent light. Visible white light is more subject to scattering and absorption than NIR Light, which leads to a penetration depth of only 1 – 2 mm. NIR light can travel up to 10 mm deep in human tissue, allowing for imaging of subsurface

tissue. For example, when placing a flashlight on a finger, most of the low wavelength visible light will be scattered or absorbed and only the high wavelength red light will penetrate, which leads to a red glow on the finger. Due to this superior penetration depth, NIR light is mostly used for fluorescence imaging. As a result of its invisibility to the human eye, NIR light will not 'contaminate' the surgical field, which is another advantage. A third advantage of NIR light is that most human tissue has low fluorescent properties in this spectrum, which leads to a higher contrast with the exogenous agent.

### Fluorescent agents

This thesis focusses on NIR fluorescence imaging with exogenous fluorescent contrast agents only. For successful fluorescence imaging with exogenous contrast, it is vital that the fluorophore reaches the lesion of interest. Roughly, two types of exogenous fluorophores exist: targeted and non-targeted fluorophores. Targeted tracers comprise of a targeting agent that targets tumour-specific receptors or micro-environment. This targeting agent is labelled with a fluorophore. Non-targeted agents comprise of a fluorophore that reaches the tissues of interest through a physiological way. Depending on the lesion or structure of interest, fluorescent agents can be administered systemically or locally. Indocyanine green (ICG) and methylene blue are two non-targeted fluorescent agents. ICG has its emission and excitation wavelength around 800 nm and methylene blue around 700 nm. ICG is FDA/EMA approved to intraoperatively assess perfusion status of tissue. Methylene blue is FDA/EMA approved for other purposes, but can be used as an off-label fluorescent agent, for example for pancreatic neuroendocrine tumour identification (17).

### Applications of NIR fluorescence imaging

Nowadays, NIR fluorescence cameras are integrated in open, endoscopic, and robotic camera systems. As such, NIR fluorescence imaging can be used to delineate cancerous tissue and detect vital structures throughout the whole procedure. With the appropriate targeting agent or mechanism, virtually all tissues of interest can be imaged with NIR fluorescence imaging. This thesis covers the two main applications of NIR fluorescence imaging: tumour imaging and tissue perfusion assessment with ICG.

### Tumour imaging

Over the last decade, many studies have been published introducing new tumour-specific fluorescent agents (18). Targeting agents have been described with various size, ranging from large antibodies to nanoparticles. Size of the targeting agent is important as larger agents require a longer time interval between administration and imaging. Shorter time intervals are favourable as they do not require additional hospital visits for administration. Recently, tumour-specific tracers targeting or activated by a tumour environment, such as the PH-grade or necrosis, have also been introduced (19). Intraoperative delineation of tumours

yields two main applications (20). Intraoperatively, occult (white light invisible, fluorescence positive) lesions can be detected. This may be useful for detection of peritoneal metastases in abdominal surgery or occult lesions during lung surgery. Detection of occult metastases can either lead to a more extensive resection, or refraining from surgical resection at all, if there appears irresectable or too extensive metastatic disease. The second application of NIR fluorescence tumour imaging is resection margin assessment. Resection margin assessment is mostly performed by whole specimen imaging in an *ex vivo* setting on the back table or a standardized black-box imaging device. If an inadequate resection margin is detected with NIR fluorescence imaging, an extra resection can be performed. Potentially, tumour-specific imaging leads to more complete resections resulting in less adjuvant therapy, less recurrences, and improved survival.

### Perfusion assessment

Adequate perfusion of tissue is vital in order to prevent surgical complications such as anastomotic leakage with subsequent peritonitis, fistulas, and abscesses. NIR fluorescence imaging with ICG can be used to assess perfusion status of tissue of interest. ICG is a safe and inexpensive non-targeted fluorophore that is designed for perfusion assessment. Intravenous administration of ICG allows for perfusion assessment of tissue as it only reaches well perfused tissue, which results in a fluorescent signal. Absence of this fluorescent signal is usually associated with a poor perfusion status of tissue. Perfusion assessment of any tissue with ICG is called ICG fluorescence angiography (ICG-FA). ICG-FA can assist the surgeon intraoperatively in guiding which tissue should be selected to create an anastomosis. As ICG is commercially available, a high number of retrospective cohort studies on its use to prevent anastomotic leakage (AL) after colorectal surgery are available. Pooled analysis of these studies suggests that using ICG-FA decreases the occurrence of AL (21). However, early randomized controlled trials could not yet show a clear decrease of AL in the ICG-FA group (22, 23). This may be explained by a lack of standardized imaging when performing ICG-FA assessment.

### Challenges of intraoperative NIR fluorescence imaging

The use NIR fluorescence imaging has increased rapidly over the last decade and the first phase 3 trials are currently ongoing (24). This brings the use of NIR fluorescence imaging closer towards demonstrating patient benefit. So far this has only been shown for patients with malignant glioma (25). In order to demonstrate a survival benefit, complication reduction, and improved quality of life, some important challenges need to be overcome. In this thesis, we cover several challenges. For tumour imaging, these challenges include: finding a suitable target and fluorescent tracer for tumour imaging, and assessing targeting of currently available fluorescent tracers to the tumour of interest. For ICG-FA, these challenges include: improving standardization of imaging, and improving quantification and interpreta-

tion of the fluorescence signal. However not studied in this thesis, proving cost-effectiveness is an important requirement when implementing this technique into standard of care. To achieve optimal cost-effectiveness, identification of patients who are likely to benefit from the use of this technique should be the focus of future studies.

## OUTLINE OF THIS THESIS

The aim of this thesis is to further improve clinical implication of intraoperative near-infrared (NIR) fluorescence imaging, with a focus on tumour imaging and perfusion assessment. This may ultimately improve outcomes of surgically treated patients with solid malignancies. In **part I** of this thesis, the current status of the literature on intraoperative NIR fluorescence imaging for colorectal cancer (**chapter 2, chapter 4**) and laryngeal cancer (**chapter 3**) is highlighted. In **part II**, expression of potential targets for imaging on tissue of oesophageal cancer (**chapter 5**) is assessed by performing immunohistochemistry. In **part III**, clinical trials have been performed to assess targeting and efficacy of new fluorescent agents for tumour imaging with a tumour targeted agent for colorectal lung metastases (**chapter 6**) and a non-targeted fluorescent agent for small intestinal neuroendocrine tumours (**chapter 7**). Moreover, pilot studies were conducted in order to further improve standardization and quantification of ICG-FA for perfusion assessment of a colon interposition (**chapter 8**) and gastric conduit (**chapter 9**) after oesophagectomy and bowel tissue after colorectal resection (**chapter 10**).

## References


1. Van der Pas MH, Haglind E, Cuesta MA, Fürst A, Lacy AM, Hop WC, et al. Laparoscopic versus open surgery for rectal cancer (COLOR II): short-term outcomes of a randomised, phase 3 trial. Lancet Oncol. 2013;14(3):210-8.
2. Kang SB, Park JW, Jeong SY, Nam BH, Choi HS, Kim DW, et al. Open versus laparoscopic surgery for mid or low rectal cancer after neoadjuvant chemoradiotherapy (COREAN trial): short-term outcomes of an open-label randomised controlled trial. Lancet Oncol. 2010;11(7):637-45.
3. Bendixen M, Jørgensen OD, Kronborg C, Andersen C, Licht PB. Postoperative pain and quality of life after lobectomy via video-assisted thoracoscopic surgery or anterolateral thoracotomy for early stage lung cancer: a randomised controlled trial. Lancet Oncol. 2016;17(6):836-44.
4. Noordman BJ, Verdam MGE, Lagarde SM, Hulshof M, van Hagen P, van Berge Henegouwen MI, et al. Effect of Neoadjuvant Chemoradiotherapy on Health-Related Quality of Life in Esophageal or Junctional Cancer: Results From the Randomized CROSS Trial. J Clin Oncol. 2018;36(3):268-75.
5. Versteijne E, van Dam JL, Suker M, Janssen QP, Groothuis K, Akkermans-Vogelaar JM, et al. Neoadjuvant Chemoradiotherapy Versus Upfront Surgery for Resectable and Borderline Resectable Pancreatic Cancer: Long-Term Results of the Dutch Randomized PREOPANC Trial. J Clin Oncol. 2022;40(11):1220-30
6. Smits RW, Koljenović S, Hardillo JA, Ten Hove I, Meeuwis CA, Sewnaik A, et al. Resection margins in oral cancer surgery: Room for improvement. Head Neck. 2016;38 Suppl 1:E2197-203.
7. Bao QR, Pellino G, Spolverato G, Restivo A, Deidda S, Capelli G, et al. The impact of anastomotic leak on long-term oncological outcomes after low anterior resection for mid-low rectal cancer: extended follow-up of a randomised controlled trial. Int J Colorectal Dis. 2022;37(7):1689-98.
8. Bundred JR, Michael S, Stuart B, Cutress RI, Beckmann K, Holleczek B, et al. Margin status and survival outcomes after breast cancer conservation surgery: prospectively registered systematic review and meta-analysis. Bmj. 2022;378:e070346.
9. Brisinda G, Chiarello MM, Pepe G, Cariati M, Fico V, Mirco P, et al. Anastomotic leakage in rectal cancer surgery: Retrospective analysis of risk factors. World J Clin Cases. 2022;10(36):13321-36.
10. Barrett M, Asbun HJ, Chien HL, Brunt LM, Telem DA. Bile duct injury and morbidity following cholecystectomy: a need for improvement. Surg Endosc. 2018;32(4):1683-8.
11. Angeramo CA, Dreifuss NH, Schlottmann F, Bun ME, Rotholtz NA. Postoperative outcomes in patients undergoing colorectal surgery with anastomotic leak before and after hospital discharge. Updates Surg. 2020;72(2):463-8.
12. Alanezi K, Urschel JD. Mortality secondary to esophageal anastomotic leak. Ann Thorac Cardiovasc Surg. 2004;10(2):71-5.
13. Vahrmeijer AL, Hutteman M, van der Vorst JR, van de Velde CJ, Frangioni JV. Image-guided cancer surgery using near-infrared fluorescence. Nat Rev Clin Oncol. 2013;10(9):507-18.
14. Martin E, Hom M, Mani L, Rosenthal EL. Current and Future Applications of Fluorescence-Guided Surgery in Head and Neck Cancer. Surg Oncol Clin N Am. 2022;31(4):695-706.
15. Liu D, Liang L, Liu L, Zhu Z. Does intraoperative indocyanine green fluorescence angiography decrease the incidence of anastomotic leakage in colorectal surgery? A systematic review and meta-analysis. Int J Colorectal Dis. 2021;36(1):57-66.

**16.** Keereweer S, Van Driel PB, Snoeks TJ, Kerrebijn JD, Baatenburg de Jong RJ, Vahrmeijer AL, et al. Optical image-guided cancer surgery: challenges and limitations. Clin Cancer Res. 2013;19(14):3745-54.

**17.** Handgraaf HJM, Boogerd LSF, Shahbazi Feshtali S, Fariña Sarasqueta A, Snel M, Swijnenburg RJ, et al. Intraoperative Near-Infrared Fluorescence Imaging of Multiple Pancreatic Neuroendocrine Tumours: A Case Report. Pancreas. 2018;47(1):130

**18.** Schouw HM, Huisman LA, Janssen YF, Slart R, Borra RJH, Willemsen ATM, et al. Targeted optical fluorescence imaging: a meta-narrative review and future perspectives. Eur J Nucl Med Mol Imaging. 2021;48(13):4272-92.

**19.** Voskuil FJ, Steinkamp PJ, Zhao T, van der Vegt B, Koller M, Doff JJ, et al. Exploiting metabolic acidosis in solid cancers using a tumour-agnostic pH-activatable nanoprobe for fluorescence-guided surgery. Nat Commun. 2020;11(1):3257.

**20.** Lauwerends LJ, van Driel P, Baatenburg de Jong RJ, Hardillo JAU, Koljenovic S, Puppels G, et al. Real-time fluorescence imaging in intraoperative decision making for cancer surgery. Lancet Oncol. 2021;22(5):e186-e95.

**21.** Emile SH, Khan SM, Wexner SD. Impact of change in the surgical plan based on indocyanine green fluorescence angiography on the rates of colorectal anastomotic leak: a systematic review and meta-analysis. Surg Endosc. 2022;36(4):2245-57.

**22.** De Nardi P, Elmore U, Maggi G, Maggiore R, Boni L, Cassinotti E, et al. Intraoperative angiography with indocyanine green to assess anastomosis perfusion in patients undergoing laparoscopic colorectal resection: results of a multicenter randomized controlled trial. Surg Endosc. 2020;34(1):53-60.

**23.** Alekseev M, Rybakov E, Shelygin Y, Chernyshov S, Zarodnyuk I. A study investigating the perfusion of colorectal anastomoses using fluorescence angiography: results of the FLAG randomized trial. Colorectal Dis. 2020;22(9):1147-53.

**24.** Vahrmeijer AL. Performance of SGM-101 for the Delineation of Primary and Recurrent Tumour and Metastases in Patients Undergoing Surgery for Colorectal Cancer: ClinicalTrials.gov; [Available from: https://clinicaltrials.gov/ct2/show/NCT03659448.

**25.** Stummer W, Pichlmeier U, Meinel T, Wiestler OD, Zanella F, Reulen HJ, et al. Fluorescence-guided surgery with 5-aminolevulinic acid for resection of malignant glioma: a randomised controlled multicentre phase III trial. Lancet Oncol. 2006;7(5):392-401.

# Part I

## Current status of intraoperative imaging in surgical oncology

# Chapter 2

## Fluorescence-guided surgery in colorectal cancer; a review on clinical results and future perspectives

Hidde A. Galema*, Ruben P.J. Meijer*, Lorraine J. Lauwerends, Cornelis Verhoef, Jacobus Burggraaf, Alexander L. Vahrmeijer, Merlijn Hutteman, Stijn Keereweer‡, Denise E. Hilling‡

*Shared first authorship ‡ Shared senior authorship

European Journal of Surgical Oncology. 2022 Apr;48(4):810-821.

## ABSTRACT

### Background

Colorectal cancer is the fourth most diagnosed malignancy worldwide and surgery is one of the cornerstones of the treatment strategy. Near-infrared (NIR) fluorescence imaging is a new and upcoming technique, which uses an NIR fluorescent agent combined with a specialised camera that can detect light in the NIR range. It aims for more precise surgery with improved oncological outcomes and a reduction in complications by improving discrimination between different structures.

### Methods

A systematic search was conducted in the Embase, Medline and Cochrane databases with search terms corresponding to 'fluorescence-guided surgery', 'colorectal surgery', and 'colorectal cancer' to identify all relevant trials.

### Results

The following clinical applications of fluorescence guided surgery for colorectal cancer were identified and discussed: (1) tumour imaging, (2) sentinel lymph node imaging, (3) imaging of distant metastases, (4) imaging of vital structures, (5) imaging of perfusion. Both experimental and FDA/EMA approved fluorescent agents are debated. Furthermore, promising future modalities are discussed.

### Conclusion

Fluorescence-guided surgery for colorectal cancer is a rapidly evolving field. The first studies show additional value of this technique regarding change in surgical management. Future trials should focus on patient related outcomes such as complication rates, disease free survival, and overall survival.

## INTRODUCTION

Colorectal cancer (CRC) is globally the fourth most common malignancy and the second cause of cancer related mortality with over 550 000 deaths annually (1). In most CRC patients, surgery remains the cornerstone of treatment. Complete surgical resection of the tumour is associated with better overall survival and lower recurrence rates (2, 3). Minimal invasive surgery, laparoscopic or robot-assisted, is increasingly used in the last two decades. Despite it its advantages, this application also brought new technical challenges as it lacks tactile feedback for tumour identification and identification of vital structures. These challenges sparked the interest in novel intraoperative visualisation techniques, such as near-infrared (NIR) fluorescence imaging.

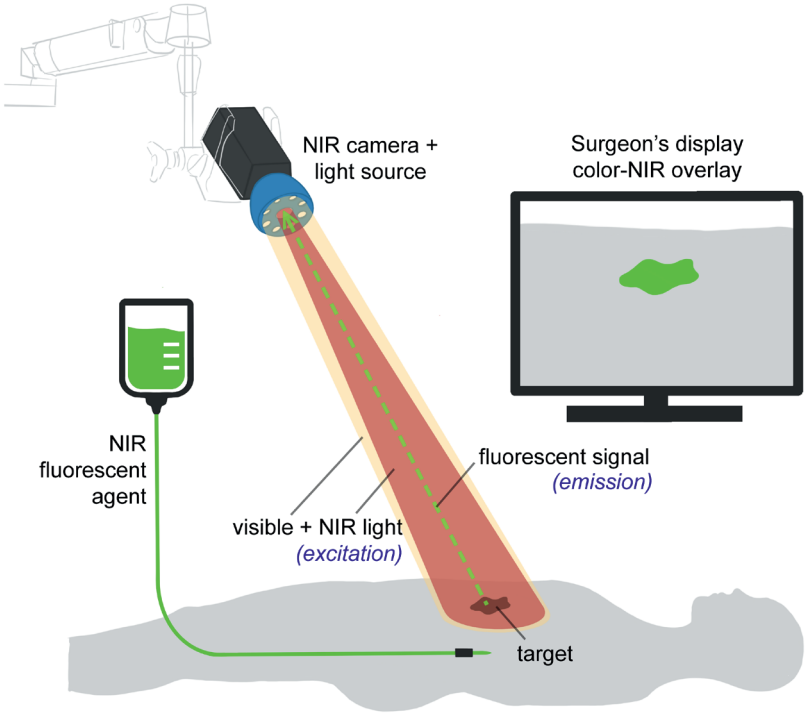


**Figure 1.** The basic principles of fluorescence-guided surgery
*NIR fluorescent agents are administered intravenously or locally. Imaging of the agent is performed using a fluorescence imaging system. Besides a white light source and camera, this system includes a dedicated NIR excitation light, collection optics and filtration, and a camera dedicated to NIR fluorescence emission light. NIR fluorescence output is displayed on a screen in the operating theatre. A simultaneous visible light image, which can be merged with the NIR fluorescence image, is desirable.*

NIR fluorescence imaging is a real-time imaging technique that combines a NIR fluorescent agent with a specialised imaging system (figure 1). These systems can capture light emitted by a fluorescent agent after excitation with an appropriate light source (figure 2). NIR light (650-900 nm) is favourable for intraoperative imaging compared to visible light because of its better depth penetration in tissue (up to 10 mm). Moreover, the fluorescent agents will not interfere with the standard surgical field, as the human eye is unable to detect light within these NIR wavelengths.

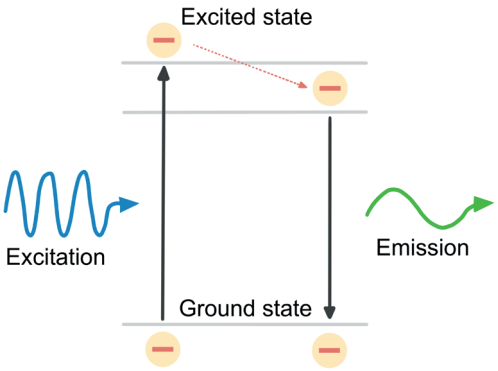


■ **Figure 2.** The basic principles of fluorescence
*NIR fluorescent agents are administered intravenously or locally. Imaging of the agent is performed using a fluorescence imaging system. Besides a white light source and camera, this system includes a dedicated NIR excitation light, collection optics and filtration, and a camera dedicated to NIR fluorescence emission light. NIR fluorescence output is displayed on a screen in the operating theatre. A simultaneous visible light image, which can be merged with the NIR fluorescence image, is desirable.*

NIR fluorescent agents are predominantly injected intravenously and can be divided into two groups: targeted (binding to a specific ligand or activated by the tumour-specific environment) and non-targeted. Currently, various targeted fluorescent agents are tested in phase I-III clinical trials (4). In the group of non-targeted agents, indocyanine green (ICG) and methylene blue (MB) are approved by the United States Food and Drug Administration (FDA) and the European Medicines Agent (EMA), for other purposes. ICG was first used in 1957 to determine hepatic function, but its fluorescent properties (excitation peak around 800 nm), and hence other applications, became known decades later (5). MB on the other hand, is predominantly cleared renally and has its excitation peak around 700 nm (6). Both agents have been proven to be safe for fluorescence utilisation.

There are many applications for NIR fluorescence imaging during colorectal surgery. This review provides an overview of the currently available clinical applications and promising future modalities of fluorescence-guided surgery in the treatment of CRC patients.

## METHODS

Due to heterogeneity in available literature and study phases between the several subjects, this study was not fully conducted according to the PRISMA guidelines.

### Literature search and selection criteria

A systematic search was conducted in the Embase, Medline and Cochrane databases with search terms corresponding to 'fluorescence-guided surgery', 'colorectal surgery', and 'colorectal cancer'. The search strategy was expanded with terms to identify articles reporting on vital structure imaging and colorectal metastases. Supplement 1 shows the search strategies per database and its corresponding hits. The last search was conducted on December 21st, 2020. All articles were independently screened based on title and abstract by two authors (HG and RM). Next, full article screening and reference screening was performed. Inconsistencies were discussed with an additional author (DH). Regarding experimental fluorescent agents, all clinical studies were included in the final reference list. Regarding ICG and MB, the final reference list was generated based on the quality of the article and the amount of scientific evidence available per subject. Articles on the following subjects were included: fluorescence-guided surgery for CRC for the imaging of the primary tumour, lymph nodes, metastases (peritoneal, liver, extra-abdominal), vital structures (nerve, ureter, urethra), and perfusion (anastomosis, omentoplasty). Only articles in English and published after the year 2000 were considered.

### Data extraction

The following data was extracted: tumour type, fluorescent agent, fluorescence imaging application, (optimal) dose, (optimal) dosing interval, optimal TBR, sensitivity, specificity, change in surgical management, and other outcomes.

### Quality assessment

Quality assessment was performed for all studies assessing experimental fluorescent agents. The Methodological index for non-randomized studies (MINORS score) was used for quality assessment. A total score of 16 (for non-comparative studies) or 24 (for comparative studies) could be obtained (7).

## RESULTS

A total of 14 completed clinical studies (supplement 2) and 8 ongoing trials (supplement 3) assessing experimental fluorescent agents for CRC surgery were identified. Figure 3 gives an overview of all clinical applications of FGS for CRC, with the assessed fluorescent agents (table 1). All 14 clinical studies regarding experimental fluorescence agents had a MINORS score of 11 or higher (supplement 4).

## Imaging of the primary tumour and local recurrence

Achieving tumour-negative resection margins is of utmost importance in the surgical treatment of CRC patients, as tumour-positive resection margins are associated with a significant decrease in overall survival (2, 8). Tumour-positive resection margins are reported in 5% of all colon cancer cases, but occur more frequently with increasing tumour stage, with an occurrence of up to 14% in T4 colon cancer (2). Moreover, in primary locally advanced rectal cancer the proportion of tumour-positive resection margins is reported up to 28% (8). This rate is even higher in patients with recurrent rectal cancer, where up to 50% tumour-positive resection margins are reported (9). These high rates in recurrent rectal cancer are likely a consequence of the distorted anatomy and treatment related fibrosis after previous resection and (re-)neoadjuvant treatment. Tumour identification is challenging in these cases due to the difficult distinction (both visual and tactile) between fibrosis and residual tumour tissue.

Preoperative endoscopic tattooing with India ink, a permanent marker injected distal to the tumour, is the current standard of care for intraoperative tumour identification in CRC, with an accuracy rate of 70-88% (10, 11). However, India ink can leak into the abdominal cavity and thereby interfere with the surgical procedure.

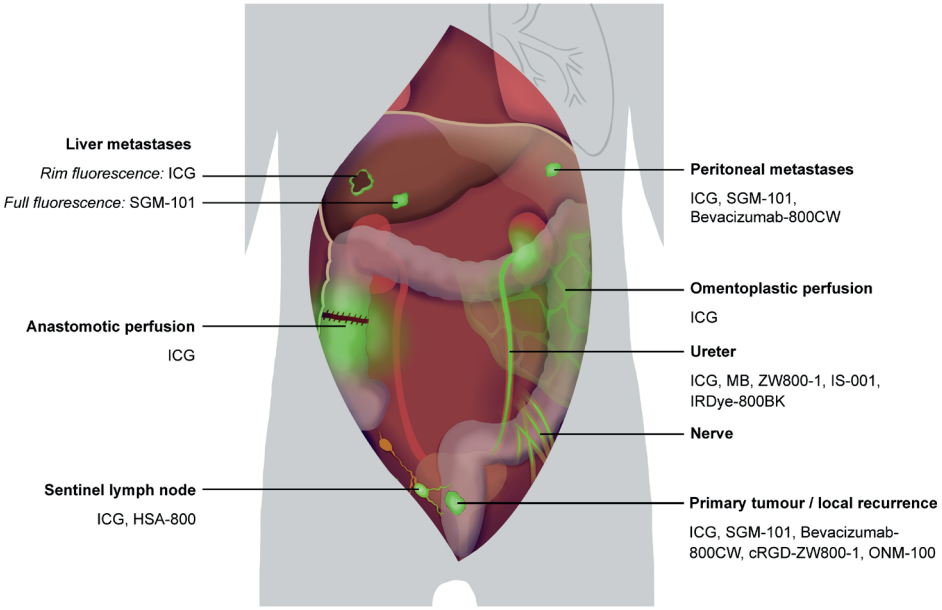


■ **Figure 3.** A schematic overview of all clinical applications of fluorescence guided surgery for colorectal cancer
*Abbreviations: ICG Indocyanine Green | MB: Methylene blue*

*Table 1. overview of all fluorescent agents used for colorectal cancer surgery and their optical properties*

| Fluorescent Agent | Molecular target | Fluorophore | ~Peak absorbance wavelength | ~Peak emission wavelength | Reference |
|---|---|---|---|---|---|
| Bevacizumab-800CW | VEGF-A | IRDye-800CW | 778 nm | 794 nm | 21 |
| cRGD-ZW800-1 | Integrins (αvβ6, αvβ3, αvβ5) | ZW800-1 | 785 nm | 805 - 850 nm | 69 |
| HSA800 | na | IRDye-800CW | 778 nm | 795 nm | 21 |
| ICG | na | ICG | 780 nm | 830 nm | 5 |
| IRDye-800BK | na | IRDye-800BK | 774 nm | 790 nm | 72 |
| IS-001 | na | IS-001 | 780 nm | 815 nm | 70 |
| LUM015 | Cathepsins (K, L, S, B) | Cy5 | 650 nm | 675 nm | 22 |
| MB | na | MB | 667 nm | 685 nm | 6 |
| ONM-100 | Metabolic acidosis* | ICG | 780 nm | 830 nm | 5 |
| SGM-101 | CEA | BM-104 | 685 nm | 705 nm | 19 |
| ZW800-1 | na | ZW800-1 | 785 nm | 805 - 850 nm | 69 |

*Activated in a tumour-specific PH-environment
*Abbreviations: VEGF-A vascular endothelial growth factor alpha | nm nanometre | ICG indocyanine green | MB methylene blue | CEA carcinoembryonic antigen | na not applicable*

In 2009, the first NIR fluorescence imaging technique to identify the primary tumour in CRC was introduced by injecting ICG peritumoural via endoscopy. It has a high tumour identification rate (100%) and minimal adverse events (12, 13). However, a major drawback is the relatively rapid clearance of ICG, as detection rates tend to decrease two to seven days after injection (12). Therefore, patients must undergo an additional endoscopy in the week before surgery, in contrast to the conventional injection of India ink that can be administered at the initial, diagnostic colonoscopy. Because of these drawbacks, peritumoural ICG injection has not been widely implemented for tumour identification. Moreover, this technique will not improve the tumour-negative resection margin rates because it does not differentiate between tumour tissue and benign surrounding tissue, nor does it enable the detection of additional lesions. A potential solution is the use of fluorescent agents that specifically bind to tumour cells.

The number of tumour-targeted fluorescent agents has substantially increased in the past two decades. The use of these agents is aimed to achieve complete tumour resection. This should lead to a decrease in the number of tumour-positive resection margins, detection of additional lesions and avoid unnecessary removal of benign tissue. To quantify fluorescence intensity, most studies use the signal-to-background ratio (SBR) or tumour-to-background ra-

tio (TBR). This is a ratio of the mean fluorescence intensity of the tumour and the surrounding tissue (background). A TBR of at least 1.5 and preferably 2.0 is deemed sufficient for tumour identification. Currently, four tumour-targeted fluorescent agents have been tested in early phase clinical studies for CRC and have shown promising results: SGM-101, cRGD-ZW800-1, bevacizumab-800CW, and ONM-100 (14, 18).

SGM-101 consists of a monoclonal antibody targeting the carcinoembryonic antigen (CEA) bound to the fluorophore BM-104 (19). A phase II study of 37 patients showed an intraoperative TBR of 1.9. Importantly, based on fluorescence assessment, the surgical plan was changed in 9 (24%) patients. In 7 patients, fluorescence led to resection of malignant lesions that were not identified with white light only. In two patients, clinically suspected but non-fluorescent tissue was proven to be benign, which resulted in a less extensive resection (18). These promising results have led to the initiation of 2 phase III trials using SGM-101 (NCT03659448, NCT04642924).

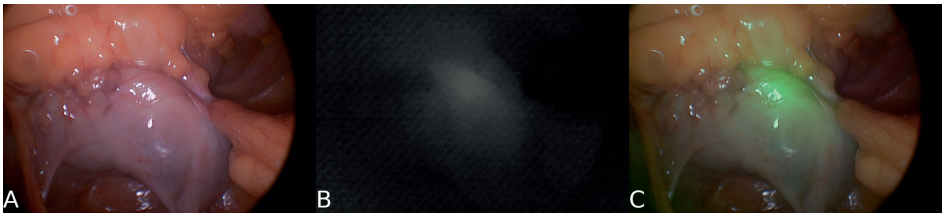


**Fig. 4.** Fluorescence imaging results of primary colon cancer.
*Intraoperative fluorescence imaging result of an adenocarcinoma of the ascending colon (TBR 1.6) using cRGD-ZW800-1. Imaging was performed using the Quest Spectrum laparoscopic imaging system. It shows an image in white light (A), near-infrared (B) and merge of A and B (C).*

cRGD-ZW800-1 is a cyclic pentapeptide (cRGD) conjugated to the 800 nm zwitterionic NIR fluorophore ZW800-1. It targets various integrins that have been shown to be overexpressed on colorectal tumour cells. In the first-in-human study, 12 colon cancer patients were included. Intraoperative fluorescence imaging of the primary tumour was feasible in both open and minimal invasive surgeries (figure 4). The highest mean TBR of 1.6 was found in the highest dosing of 0.05 mg/kg (15).

Bevacizumab-800CW consists of a monoclonal antibody targeting vascular endothelial growth factor A (VEGF-A), bound to IRDye800CW[20, 21]. Bevacizumab-800CW has been studied in eight rectal cancer patients (16). During back table fluorescence assessment of the resection margins on the surgical specimen, a tumour-positive margin was correctly identified in one out of two patients. In the six patients with a tumour-negative resection margin, one (17%) showed a false-positive signal.

ONM-100 is a pH-activatable fluorescent agent that exploits the metabolic microenvironment of solid tumours (17). It does not bind to specific tumour receptors but is activated in the acidic tumour environment. It is a conjugation of a pH-sensitive nanoparticle to ICG, which becomes fluorescent in environments with a pH below 6.9. Thirty patients were studied with this agent, of which three underwent surgery for CRC. All three CRC patients showed a sharply demarcated fluorescent signal during back table imaging. Currently, a phase II study using ONM-100 is ongoing in which patients undergoing surgery for CRC are also included (NCT03735680).

A phase I/II trial will be conducted using LUM015, a novel PEGylated protease-activated fluorescent imaging agent targeting cathepsins, which play a crucial role in mammalian cell turnover (22). The first results of this study, which focuses on intraoperative imaging of CRC, are expected in 2021 (NCT02584244).

Altogether, these early phase clinical trials have shown that tumour-targeted fluorescence imaging is a feasible addition to CRC surgery. The fluorescent agents detected most of the known tumours and SGM-101 even detected additional lesions, which were not detected in white light. To assess the impact on patient related outcomes, future studies should focus on clinical endpoints like tumour-negative resection margin rate and change in surgical management.

## Imaging of the sentinel lymph node

Adequate lymph node staging in CRC patients is crucial; it is an important prognostic feature and determines the need for (neo)adjuvant chemotherapy and/or radiotherapy. The sentinel lymph node (SLN) may be crucial in nodal staging, as it is defined as the first lymph node draining the tumour and is believed to be the first place for lymphogenic metastases. Moreover, one in three patients with stage I and II colon cancer, who are staged as lymph node-negative, still develop distant metastases (23). This might be a consequence of understaging by histopathology, due to lymph nodes with occult malignant cells and micrometastases. Currently, a single paraffin embedded slide per lymph node is reviewed during routine histopathological analysis, increasing the chance of missing tumour cells away from the slide's cutting edge. More extensive histopathological analysis of all resected lymph nodes would improve nodal staging, but this process is time-consuming and expensive (24). Extensive analysis of only the SLN is feasible, and thus unfolds a niche for SLN mapping in CRC. Moreover, tumour-negative SLNs create an opportunity for endoscopic or local resection of early stage tumours (25).

A reason for the absence of SLN mapping in the routine treatment of CRC patients might be a consequence of so-called skip metastases that are reported in up to 22% the patients (26). In these cases, malignant cells are absent in the SLN, but present in other regional lymph nodes. Moreover, the use of blue dye for SLN mapping in CRC appears limited due to its

minimal depth penetration in the mesocolic and mesorectal fat (27). Therefore, the interest in fluorescent dyes, especially the peritumoural injection of ICG, has increased. These fluorescent dyes have already shown to be of additional value for the identification of complete lymph drainage patterns, including aberrant flow (28, 29). Nevertheless, the identification of only the SLN would be a valuable addition.

Various techniques have been used in studies assessing fluorescence-guided SLN mapping in CRC. Agent administration and SLN mapping can be performed before or during the procedure (*in vivo*) or after resection (*ex vivo*). Although *ex vivo* imaging might be easier to adapt in the current surgical or pathological workflow, it has drawbacks. Most importantly, *ex vivo* injection of an agent and identification of the SLN lacks the possibility of finding SLNs in patients with aberrant lymph node drainage patterns (30). Another technical consideration is the site of injection. For *in vivo* SLN mapping, submucosal injection is done endoscopically, prior to surgery. Alternatively, subserosal injection can be performed during surgery, which in laparoscopic surgery demands transcutaneous needle placement. Submucosal injection is preferred over subserosal injection because of better accuracy of injection near the tumour and easier endoscopic needle positioning (31).

ICG is the only fluorescent dye that has been reported for *in vivo* SLN mapping in CRC with cohorts up to 48 patients and success rates of SLN detection ranging from 65.5 to 100% (31-35). The accuracy of this technique seems to diminish with increasing tumour stage (34, 36). Which is most likely a result of the distorted drainage patterns caused by transmural growth of advanced tumours.

*Ex vivo* SLN mapping facilitates the use of experimental agents, like HSA800 (IRDye 800CW conjugated to human serum albumin). HSA800 has shown a potential advantage over ICG, due to its bigger hydrodynamic diameter that results in better retention in the SLN (37). HSA800 has demonstrated successful identification of the SLN in 95-100% of 96 patients (38-40).

Despite high fluorescence-guided SLN identification rates, the SLN itself was associated with a relatively low negative predictive value (74 – 100%) in general, mainly as a result of high false-negative rates (when the SLN did not contain tumour tissue, but other regional lymph nodes did) (31-35, 38, 39). This can be a result of the occurrence of skip metastases (26).

Correct staging is essential for treatment planning in CRC patients and may be improved with SLN mapping. A patient is upstaged when no tumour deposits were seen during conventional histopathology of all lymph nodes, but the SLN showed malignant cells at advanced histopathological analysis using serial sectioning and immunohistochemistry. SLN mapping with ICG and subsequent advanced histopathology resulted in upstaging in 6-23% of the patients

(31-33). Although plausible, it is yet unknown whether upstaged patients with micrometastatic lymph nodes will benefit from subsequent neoadjuvant treatment.

Overall, it can be concluded that fluorescence-guided identification of the SLN is feasible and potentially of additional clinical value. However, a wide variety of techniques for fluorescence-guided SLN identification are currently used. It is recommended to first determine the optimal agent, injection technique and patient population. The high false-negative rate (tumour-negative SLN with tumour-positive regional nodes) remains a major drawback for SLN mapping in CRC in general. Nevertheless, its value in terms of upstaging and the consequence of adjuvant treatment seems enough reason to further explore this field.



## Imaging of distant metastases

*Peritoneal metastases*

Approximately 10% of all CRC patients develop peritoneal metastases during the course of the disease (41). In the past, this diagnosis was considered non-curable with a median overall survival of approximately 12 months (42). These survival rates have improved with the introduction of cytoreductive surgery followed by intraoperative hyperthermic intraperitoneal chemotherapy (HIPEC) (3, 43). Studies have shown that in particular complete cytoreduction plays a major role as it prolongs the long-term survival of patients with peritoneal metastases (3). However, identification of small peritoneal lesions can be challenging, especially after previous abdominal surgery or neoadjuvant therapy with subsequent fibrosis. An accurate PCI is essential as this score plays a crucial role in the decision to perform a HIPEC procedure or not (44). Fluorescence imaging can potentially lead to more complete cytoreductive surgery by more accurately identifying peritoneal lesions.

Intravenous injection of ICG and subsequent fluorescence imaging of peritoneal metastases is primarily based on the enhanced permeability and retention (EPR) effect. The EPR effect is dependent on the porous nature of tumour vasculature and the extended circulation of the fluorescent agent, leading to accumulation in the tumour (45). ICG is administered at the start of the surgical procedure and has shown good intraoperative imaging of peritoneal metastases, which has led to a modification of the surgical plan in 4 out of 14 patients (29%) solely based on the fluorescence assessment (46). Nevertheless, the authors reported limited ability to assess fluorescence in areas with high physiological ICG accumulation such as the liver, as well as a sensitivity of 0% in patients with mucinous tumours (46). Moreover, neoadjuvant treatment resulted in a higher false-negative rate (53.8% vs. 42.9%) and lower sensitivity (65.0% vs 76.3%) compared to patients who did not receive neoadjuvant treatment (47).

To date, two tumour-targeted agents have been used for *in vivo* detection of peritoneal metastases in CRC: bevacizumab-800CW and SGM-101. Bevacizumab-800CW was the first

tumour-targeted fluorescent agent that was reported to yield promising results, identifying additional peritoneal metastases in two out of seven (29%) patients (48). Similar results were achieved in a study with SGM-101, where fluorescence imaging led to a change in PCI in 5 out of 12 (42%) patients (figure 5). Four patients had a higher PCI and one patient a lower PCI, all confirmed by histopathology (49). It is noteworthy that both studies reported a high false-positive rate (38% and 47%, respectively). This could be a result of non-specific localisation of the fluorescent agent or autofluorescence of collagen-rich structures and calcifications (50).

One clinical trial is currently ongoing using LUM015, including patients with peritoneal metastases of gastrointestinal cancer, ovarian cancer, and mesothelioma (NCT03834272). The aforementioned phase III study with SGM-101 will also include patients with peritoneal metastases (NCT03659448).

The feasibility of fluorescence-guided detection of peritoneal metastases has been demonstrated, allowing for detection of peritoneal deposits and potentially also of occult lesions. This is especially valuable knowing that treatment success is primarily determined by complete cytoreduction.

*Liver metastases*

Over the course of the disease, 20 – 30% of CRC patients develop liver metastases (CRLM) (51). Complete resection of these metastases is an important treatment option, with positive resection margins being associated with a two- to three-fold decrease in 5-year survival compared to negative margins. However, positive resection margins occur in approximately 13% of patients (52). In the past, the hepatic surface was palpated for superficial lesions during surgery. With minimal invasive surgery this has become challenging. Nowadays, preoperative magnetic resonance imaging (MRI), computed tomography (CT) and intraoperative ultrasound (IOUS) are the most frequently used imaging modalities for the identification of CRLM (53). Fluorescence imaging offers surgeons another tool for detecting CRLM. It is suitable for detecting small superficial metastases (up to eight mm deep), but also for resection margin assessment. Intravenous ICG doses between 10 - 50 mg are described with injection windows of 1 – 14 days prior to surgery (54). After intravenous injection, ICG is exclusively cleared by the liver. Immature hepatocytes, located at the transition zone between healthy and malignant liver cells, are unable to excrete ICG into bile due to down-regulation of anion transporters, resulting in an accumulation of ICG. This causes CRLM to show a rim of fluorescence (figure 6) (55).

Various studies have reported on fluorescence imaging with ICG for the detection of occult CRLM, but none were randomised (55-57). In one systematic review, six out of nine studies reported a sensitivity exceeding 94% (54). Furthermore, when fluorescence imaging was added to conventional imaging, extra metastases were found and resected in 20 out of 148 patients

(13.5%). Tumour-targeted fluorescence identification of CRLM was previously reported in one study using SGM-101. SGM-101 provided visualisation of all 12 malignant lesions in eight patients with a mean in vivo TBR of 1.7 (58).

It is widely debated if additional resection of small superficial CRLM improves overall survival. One study has retrospectively assessed (disease-free) survival of 86 patients after ICG-guided resection of CRLM (59). Significantly more additional lesions were found when fluorescence-guided resection with ICG was added compared to standard care (25% vs. 13%, p=0.04). However, this was not associated with a significant decrease in local recurrence-free survival (HR: 0.74; 95% CI: 0.42 – 1.28), and overall survival (HR: 0.94; 95% CI: 0.50 – 1.76).

Besides detection of CRLM, fluorescence imaging can also be used for margin assessment and aiding in tumour delineation for CRLM resection. Two small case series with a total of 52 patients achieved 100% tumour-negative resection margins using ICG to determine the precise tumour border (56, 57). Recently, a systematic workflow was proposed to detect or prevent tumour positive margins in CRLM surgery (60). In a selected group of eight patients with initial tumour positive resection margins, the surgeons were able to correctly identify seven out of eight positive margins by using the proposed surgical workflow. The currently ongoing prospective MIMIC-trial will assess whether this surgical workflow can lead to a decrease of tumour-positive resection margins in 186 patients with CRLM (Netherlands trial register: NL7674).

Fluorescence imaging with ICG has been demonstrated to improve intraoperative detection of CRLM. It can also be used for margin assessment and aiding in tumour delineation for CRLM resection. Future trials must confirm this potential and demonstrate whether this technique will improve patient survival.

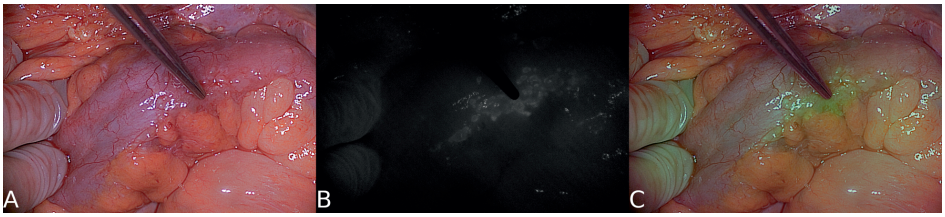


**Figure 5.** Fluorescence imaging result of colorectal peritoneal metastases
*Intraoperative fluorescence imaging result of peritoneal metastases of a mucinous carcinoma with signet ring cell differentiation (TBR 1.8) using SGM-101. Imaging was performed using the Quest Spectrum open imaging system. It shows an image in white light (A), near-infrared (B) and merge of A and B (C)*

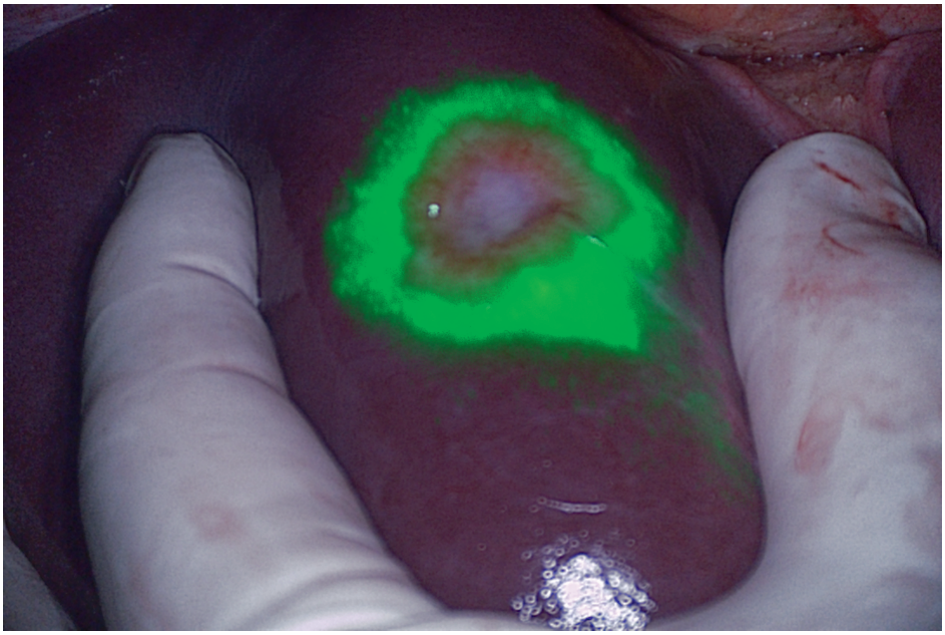

**Figure 6.** Fluorescence imaging result of a liver metastasis
*A colorectal liver metastasis showing clear 'rim fluorescence' after intravenous injection of 10 mg indocyanine green 24 hours prior to surgery. Imaging was performed using the Quest Spectrum open imaging system.*

*Extra-abdominal metastases*

A feasibility study with SGM-101 to identify colorectal lung metastases is currently recruiting (NCT04737213). A similar study with SGM-101 to identify colorectal brain metastases will be conducted soon (NCT04755920).

## Imaging of vital structures

*Ureters*

Iatrogenic ureteral injury is a severe complication in abdominal surgery and has an incidence of up to 5.7% in colorectal surgery. Surgeries on the distal colon and rectum bear the highest risk for ureteral injury (61). Depending on the time of diagnosis, location, and extent of the injury, treatment ranges from minimal invasive transurethral procedures to complex surgical reconstruction. Consequences of (undiagnosed) iatrogenic ureteral injury include kidney failure, sepsis, ureteral stenosis, urinoma, and fistulas (62). The ureter is usually identified through visual inspection and palpation, which can be difficult due to its retroperitoneal location. The introduction of minimal invasive surgery in the last decades has further increased this challenge (61). Intraoperative fluorescence imaging can guide the surgeon in identification of the ureter, which could result in less ureteral injury. ICG and MB have both been studied for ureteral identification. Due to the hepatic clearance of ICG, retrograde intra-ureteral

injection is needed, which makes ureteral identification with ICG a complex procedure (63). Successful ureteral identification using ICG is reported in 94 – 100% of procedures (63-65). As MB is cleared renally, intravenous injection is possible for intraoperative identification of ureters. Outcomes of intravenous MB administration for ureteral identification show variable results (66-68). Fluorescence of the ureters is reported in 50 – 100% of cases and usually between 10 – 90 minutes after injection of MB. Optimal visualisation is achieved with doses between 0.5 mg/kg and 1.0 mg/kg. Most important, in most cases, the ureter could only be identified with fluorescence after it was already adequately identified in white light, thus the clinical benefit was minimal. Overall, MB appears to be suboptimal for ureteral identification.

To date, three experimental fluorophores have been used in clinical studies to image the ureter: ZW800-1, IS-001, and IRDye800BK (69-71). These experimental fluorophores are all fluorescent dyes with peak emission around 800 nm. ZW800-1 is a zwitterionic molecule that shows low non-specific binding and is exclusively renally cleared. ZW800-1 was intravenously administered during abdominopelvic surgery in 12 patients. Using ZW800-1, all ureters became fluorescent within 10 minutes, without dissecting the peritoneum (69). The SBR was 2.7 in the group with 2.5 mg throughout the first hour. The ureters remained visible with NIR during the whole procedure, with the longest procedure being over 3.5 hours. The first clinical study assessing the safety and efficacy of IS-001 included 24 patients who underwent laparoscopic gynaecological surgery[70]. The ureters could be identified in all patients, the highest SBR (3.6) was observed with a dose of 20 mg. Signal intensity decreased rapidly over time, with the peak SBR occurring 30 minutes after injection. The third experimental fluorescent dye that was studied for ureter identification is IRDye800BK, a hydrophilic dye (72). In this trial, the optimal dose of 0.06 mg/kg was administered in 25 patients (71). In all patients, the ureter was visualised within ten minutes. After 90 minutes the ureter was still visible in 89% of the patients. Currently, another clinical trial is ongoing using IRDye800BK, including 40 patients undergoing laparoscopic surgery. (NCT03387410)

ZW800-1, IS-001, and IRDye-800BK appear suitable for ureter identification with NIR fluorescence imaging and have advantages over MB and ICG. Future clinical trials are needed to confirm the promising early results of these experimental fluorescent agents. However, large sample sizes are required for such studies due to relatively low incidence of iatrogenic ureteral injury. Therefore, phase III studies should focus on patients with high risk for intraoperative ureteral injury.

*Urethra*

Besides ureteral injury, the urethra is also at risk for injury during pelvic surgery. Perineal dissection in (low) rectal surgery is an especially high-risk step for urethral injury. One clinical study with urethral administration of ICG during prostatectomies in 12 patients has been

published (73). No intraoperative urethra injury occurred. In another study, ICG was injected in the urethra during a transanal total mesorectal excision in one patient, resulting in successful identification of the urethra (74).

*Nerves*

Sexual and urological dysfunction due to iatrogenic nerve injury are complications of rectal surgery, significantly affecting quality of life. Up to 79% of the patients undergoing rectal surgery acquire some sort of sexual or urological dysfunction (75). The hypogastric, splanchnic, and levator ani nerves are at risk during (colo)rectal surgery[76]. Nerve targeted fluorescence-guided surgery has the potential to improve nerve identification, and therefore prevent injury. Although promising pre-clinical results of nerve specific fluorescence imaging have been reported, the translation to clinical studies has yet to be made (77-79). The main difficulties include fluorescent agents not being able to pass the nerve-blood barrier, and relatively high nonspecific uptake of nerve targeted agents by fat and muscle (79).

## Imaging of perfusion

*Anastomotic perfusion*

Anastomotic leakage is one of the most severe complications in CRC surgery. It often requires additional surgical or radiological intervention, leading to a prolonged hospital stay. Anastomotic leakage is reported up to 13% of patients undergoing CRC surgery with subsequent mortality rates of up to 27% (80, 81). Poor bowel perfusion is thought to play an important role in anastomotic leakage. ICG fluorescence-angiography can provide real-time feedback of bowel perfusion and aid the surgeon in determining the optimal location for the anastomosis. ICG doses between 2 – 20 mg have been reported (82, 83). In general, bowel perfusion can be assessed within 60 seconds after intravenous injection.

Over the years, several cohort studies have been published on the effect of ICG fluorescence angiography use on anastomotic leakage. Studies specifically addressing colonic anastomoses are sporadic and fail to show a significant decrease in anastomotic leakage rates when using ICG fluorescence angiography84, 85. More data has been reported on rectal surgery. Song et al. published the most recent and complete meta-analysis on rectal anastomoses including 2088 patients from nine retrospective studies (86). Their pooled analysis showed an odds ratio for anastomotic leakage of 0.34 (95% CI: 0.22 – 0.52) in favour of ICG fluorescence angiography over standard of care.

Recently, the first randomised controlled trials (RCTs) on ICG fluorescence angiography have been published. One study included 240 patients undergoing left-sided colon or rectal resection and failed to show a significant difference in anastomotic leakage rate between

the ICG fluorescence angiography group and the control group (5% vs 9%; p = 0.2) (87). The second study investigated the value of ICG fluorescence angiography on the occurrence of anastomotic leakage in 377 patients undergoing sigmoid or rectal resection. A significantly lower anastomotic leakage rate was found in the ICG fluorescence angiography group (9.1% vs 16.3%; p = 0.04) (88). However, this difference was predominantly based on the occurrence of anastomotic leakage grade A, which does not alter patient management (89). Thus, minimal clinical benefit was demonstrated as no difference was observed in the number of re-operations or the length of postoperative hospital stay. The third RCT also failed to report a significant decrease of anastomotic leakage in the ICG fluorescence angiography group compared to the control group (9.0% vs 9.6%; p = 0.37) (90). It should be noted that the pre-determined sample size was not achieved due to a decrease in accrual rates. More RCTs have been registered that will include similar or higher amount of patients (NCT02598414, NCT04012645). Noteworthy are the INTACT-trial and the AVOID-trial, both planning to include up to 1000 patients (ISCRN: 13334746, NCT04712032). Also, the prospective IMARI trial is assessing a series of interventions, including ICG fluorescence angiography, and its influence on anastomotic leakage in rectal cancer surgery (Netherlands trial register: NL8261).

In conclusion, ICG fluorescence angiography has potential in the prevention of anastomotic leakage in a safe and simple way. Pooled analysis of cohort studies has demonstrated that ICG fluorescence angiography reduces anastomotic leakage, but high-quality evidence is currently lacking. RCTs with inclusion up to 1000 patients are currently ongoing and might provide with the answer if ICG fluorescence angiography prevents anastomotic leakage in CRC surgery.

*Omentoplastic perfusion*

Perineal wound bed complications occur in almost 50% of the patients undergoing abdominoperineal resection (APR) and carry major morbidity (91). Omentoplasty can be performed for the prevention and management of these complications. It is hypothesised that the transferred omentum prevents dead space formation, has an anti-inflammatory and antibacterial effect, and provides excellent vascularisation to the wound bed (92). However, its clinical benefit in rectal cancer surgery has been disputed. A meta-analysis of 1894 patients showed that omentoplasty did not reduce the risk of postoperative presacral abscesses or perineal complications (93). ICG fluorescence angiography of the transferred omentum was recently assessed in a pilot study (94). Remarkably, ICG fluorescence angiography led to a change in surgical management in 80% of the patients. A follow up study by the same group showed a decrease in pelviperineal non-healing in the ICG group compared to the control group (22% vs 42%; p = 0.051) (95). However non-significant, this study showed a trend towards improved outcomes after ICG fluorescence angiography guided omentoplasty. The reported alteration of the surgical plan in 80% of cases suggests that ‘standard’ omentoplasty is vulnerable to

poor omental perfusion. Further research on ICG fluorescence angiography for omentoplasty is therefore warranted.

## DISCUSSION AND FUTURE PERSPECTIVES

NIR fluorescence-guided surgery is a rapidly evolving technique with various clinical applications in CRC surgery. This review provides an overview of the clinical applications of all fluorescent agents for CRC surgery. ICG, the nonspecific FDA/EMA approved fluorescent agent is already used in a variety of clinical applications of which CRLM resection and ICG fluorescence angiography show the most potential. However, no unequivocal benefits in relevant outcome measures have yet been reported. Over the past years, promising experimental fluorescent agents (targeted and non-targeted) have been investigated. These agents could potentially improve intraoperative fluorescence imaging, ultimately leading to improved detection of tumour tissue, vital structures, and vascularisation. Improving intraoperative detection of tumour could not only lead to more complete resections, but can also lead to better patient selection, as unnecessary surgery could be prevented if the disease is found to be too advanced. On the other hand, false-positive lesions would lead to unnecessary resection of healthy tissue which makes tumour-binding specificity of the fluorescent agent crucial.

Quantification of the fluorescence signal is challenging, with numerous factors such as scattering, absorption, camera angulation and distance, and background light influencing the signal intensity (96). The latest studies on ICG fluorescence angiography for the prevention of anastomotic leakage focus on less subjective perfusion assessment by analysing time-dependent inflow parameters (97, 98). Real-time quantification of the fluorescence signal of tumour-targeted agents, aiding surgeons in deciding whether tissue is malignant or not, has not been reported yet. Most clinical studies report the SBR (or TBR) and change in surgical management as the main parameters in early phase studies. Eventually, trials should report on clinically significant events such as the tumour-negative resection margin rate, detection of occult lesions, surgical complications, and (disease free) survival (99).

Nowadays, a variety of fluorescence camera systems is available in clinical practice. It is important to keep in mind that these camera systems can influence imaging results (21). This also counts for the difference between open- and laparoscopic cameras. Most laparoscopes that are currently clinically available are optimised for ICG at 830 nm. This wavelength is slightly too high for optimal imaging of most experimental fluorescent agents, which have peak emission wavelengths around 800 nm (table 1). Therefore, there is a need for high-quality laparoscopes that are optimised for imaging of specific tumour-targeted fluorescent agents. Fluorescence imaging could account for the lack of tactile feedback in minimal

invasive surgery, as it has the potential to improve visualisation of vital structures (e.g. the ureter, nerves) and tumours. Moreover, fluorescence imaging can be integrated in the laparoscopic field with an overlay view, which is an advantage over open surgery, where an additional handheld camera is needed. Especially in rectal surgery, in the conically shaped (male) pelvis, difficulties are experienced with optimal positioning due to the size of most open cameras. A laparoscope is much smaller and therefore easier to manoeuvre towards an optimal imaging angle.

## CONCLUSION

In conclusion, the field of fluorescence-guided surgery is rapidly evolving with already several clinical applications in CRC surgery. ICG is widely used, and its use appears to be beneficial in specific applications. Many experimental fluorescent agents have been developed and several of these agents are currently being assessed in late phase clinical studies. The most promising applications of these experimental fluorescent agents in CRC surgery are distinguishing between fibrotic and tumour tissue after neo-adjuvant treatment, improving the rate of tumour-negative resection margins in locally advanced and recurrent rectal cancer, detection of occult metastases in cytoreductive surgery for peritoneal metastases, and ureteral imaging in high-risk cases. An essential next step for the implementation of these agents in clinical practice is to show direct patient benefit in terms of change in surgical management, surgical complications, recurrence-free survival, and overall survival.

## Acknowledgements

The authors wish to thank S.T.G. Meertens-Gunput of the Erasmus MC Medical Library for developing and updating the search strategies. Moreover, we thank K.S. de Valk for supplying figure 4 and O.D. Bijlstra for supplying figure 6.

## REFERENCES


1. Bray F, Ferlay J, Soerjomataram I, Siegel RL, Torre LA, Jemal A. Global cancer statistics 2018: GLOBOCAN estimates of incidence and mortality worldwide for 36 cancers in 185 countries. *CA Cancer J Clin* 2018;68(6): 394-424.
2. Amri R, Bordeianou LG, Sylla P, Berger DL. Association of Radial Margin Positivity With Colon Cancer. *JAMA Surg* 2015;150(9): 890-898.
3. Elias D, Gilly F, Boutitie F, Quenet F, Bereder JM, Mansvelt B, Lorimier G, Dube P, Glehen O. Peritoneal colorectal carcinomatosis treated with surgery and perioperative intraperitoneal chemotherapy: retrospective analysis of 523 patients from a multicentric French study. *J Clin Oncol* 2010;28(1): 63-68.
4. Hernot S, van Manen L, Debie P, Mieog JSD, Vahrmeijer AL. Latest developments in molecular tracers for fluorescence image-guided cancer surgery. *Lancet Oncol* 2019;20(7): e354-e367.
5. Fox IJ, Brooker LG, Heseltine DW, Essex HE, Wood EH. A tricarbocyanine dye for continuous recording of dilution curves in whole blood independent of variations in blood oxygen saturation. *Proc Staff Meet Mayo Clin* 1957;32(18): 478-484.
6. Ginimuge PR, Jyothi SD. Methylene blue: revisited. *J Anaesthesiol Clin Pharmacol* 2010;26(4): 517-520.
7. Slim K, Nini E, Forestier D, Kwiatkowski F, Panis Y, Chipponi J. Methodological index for non-randomized studies (minors): development and validation of a new instrument. *ANZ J Surg* 2003;73(9): 712-716.
8. Nagtegaal ID, Quirke P. What is the role for the circumferential margin in the modern treatment of rectal cancer? *J Clin Oncol* 2008;26(2): 303-312.
9. Holman FA, Bosman SJ, Haddock MG, Gunderson LL, Kusters M, Nieuwenhuijzen GA, van den Berg H, Nelson H, Rutten HJ. Results of a pooled analysis of IOERT containing multimodality treatment for locally recurrent rectal cancer: Results of 565 patients of two major treatment centres. *Eur J Surg Oncol* 2017;43(1): 107-117.
10. Conaghan PJ, Maxwell-Armstrong CA, Garrioch MV, Hong L, Acheson AG. Leaving a mark: the frequency and accuracy of tattooing prior to laparoscopic colorectal surgery. *Colorectal Dis* 2011;13(10): 1184-1187.
11. Feingold DL, Addona T, Forde KA, Arnell TD, Carter JJ, Huang EH, Whelan RL. Safety and reliability of tattooing colorectal neoplasms prior to laparoscopic resection. *J Gastrointest Surg* 2004;8(5): 543-546.
12. Satoyoshi T, Okita K, Ishii M, Hamabe A, Usui A, Akizuki E, Okuya K, Nishidate T, Yamano H, Nakase H, Takemasa I. Timing of indocyanine green injection prior to laparoscopic colorectal surgery for tumour localization: a prospective case series. *Surg Endosc* 2020.
13. Watanabe M, Tsunoda A, Narita K, Kusano M, Miwa M. Colonic tattooing using fluorescence imaging with light-emitting diode-activated indocyanine green: A feasibility study. *Surg Today* 2009;39(3): 214-218.
14. Boogerd LSF, Hoogstins CES, Schaap DP, Kusters M, Handgraaf HJM, van der Valk MJM, Hilling DE, Holman FA, Peeters KCMJ, Mieog JSD, van de Velde CJH, Farina-Sarasqueta A, van Lijnschoten I, Framery B, Pèlegrin A, Gutowski M, Nienhuijs SW, de Hingh IHJT, Nieuwenhuijzen GAP, Rutten HJT, Cailler F, Burggraaf J, Vahrmeijer AL. Safety and effectiveness of SGM-101, a fluorescent

antibody targeting carcinoembryonic antigen, for intraoperative detection of colorectal cancer: a dose-escalation pilot study. *Lancet Gastroenterol Hepatol* 2018;3(3): 181-191.

**15.** de Valk KS, Deken MM, Handgraaf HJM, Bhairosingh SS, Bijlstra OD, van Esdonk MJ, Terwisscha van Scheltinga AG, Valentijn R, March TL, Vuijk J, Peeters KC, Holman FA, Hilling DE, Mieog JSD, Frangioni JF, Burggraaf J, Vahrmeijer AL. First-in-Human Assessment of cRGD-ZW800-1, a Zwitterionic, Integrin-Targeted, Near-Infrared Fluorescent Peptide in Colon Carcinoma. *Clin Cancer Res* 2020.

**16.** de Jongh SJ, Tjalma JJJ, Koller M, Linssen MD, Vonk J, Dobosz M, Jorritsma-Smit A, Kleibeuker JH, Hospers GAP, Havenga K, Hemmer PHJ, Karrenbeld A, van Dam GM, van Etten B, Nagengast WB. Back-Table Fluorescence-Guided Imaging for Circumferential Resection Margin Evaluation Using Bevacizumab-800CW in Patients with Locally Advanced Rectal Cancer. *J Nucl Med* 2020;61(5): 655-661.

**17.** Voskuil FJ, Steinkamp PJ, Zhao T, van der Vegt B, Koller M, Doff JJ, Jayalakshmi Y, Hartung JP, Gao J, Sumer BD, Witjes MJH, van Dam GM, group Ss. Exploiting metabolic acidosis in solid cancers using a tumour-agnostic pH-activatable nanoprobe for fluorescence-guided surgery. *Nat Commun* 2020;11(1): 3257.

**18.** de Valk KS, Deken MM, Schaap DP, Meijer RP, Boogerd LS, Hoogstins CE, van der Valk MJ, Kamerling IM, Bhairosingh SS, Framery B, Hilling DE, Peeters KC, Holman FA, Kusters M, Rutten HJ, Cailler F, Burggraaf J, Vahrmeijer AL. Dose-Finding Study of a CEA-Targeting Agent, SGM-101, for Intraoperative Fluorescence Imaging of Colorectal Cancer. *Ann Surg Oncol* 2020.

**19.** Gutowski M, Framery B, Boonstra MC, Garambois V, Quenet F, Dumas K, Scherninski F, Cailler F, Vahrmeijer AL, Pèlegrin A. SGM-101: An innovative near-infrared dye-antibody conjugate that targets CEA for fluorescence-guided surgery. *Surg Oncol* 2017;26(2): 153-162.

**20.** Lv W, Gao T, Wang S, Hou J, Liu M, Yang J, Du T, Chen Z, Chen Z, Feng X, Zeng W. Long-term tracking of cancer cell nucleus and identification of colorectal cancer with an aggregation-induced emission-based fluorescent probe. *J Biomed Nanotechnol* 2019;15(5): 1033-1042.

**21.** Zhu B, Sevick-Muraca EM. A review of performance of near-infrared fluorescence imaging devices used in clinical studies. *Br J Radiol* 2015;88(1045): 20140547.

**22.** Whitley MJ, Cardona DM, Lazarides AL, Spasojevic I, Ferrer JM, Cahill J, Lee CL, Snuderl M, Blazer DG, 3rd, Hwang ES, Greenup RA, Mosca PJ, Mito JK, Cuneo KC, Larrier NA, O'Reilly EK, Riedel RF, Eward WC, Strasfeld DB, Fukumura D, Jain RK, Lee WD, Griffith LG, Bawendi MG, Kirsch DG, Brigman BE. A mouse-human phase 1 co-clinical trial of a protease-activated fluorescent probe for imaging cancer. *Sci Transl Med* 2016;8(320): 320ra324.

**23.** Figueredo A, Coombes ME, Mukherjee S. Adjuvant therapy for completely resected stage II colon cancer. *Cochrane Database Syst Rev* 2008(3): CD005390.

**24.** Yamamoto H, Murata K, Fukunaga M, Ohnishi T, Noura S, Miyake Y, Kato T, Ohtsuka M, Nakamura Y, Takemasa I, Mizushima T, Ikeda M, Ohue M, Sekimoto M, Nezu R, Matsuura N, Monden M, Doki Y, Mori M. Micrometastasis Volume in Lymph Nodes Determines Disease Recurrence Rate of Stage II Colorectal Cancer: A Prospective Multicenter Trial. *Clin Cancer Res* 2016;22(13): 3201-3208.

**25.** Cahill RA, Leroy J, Marescaux J. Localized resection for colon cancer. *Surg Oncol* 2009;18(4): 334-342.

**26.** Bao F, Zhao LY, Balde AI, Liu H, Yan J, Li TT, Chen H, Li GX. Prognostic impact of lymph node skip metastasis in Stage III colorectal cancer. *Colorectal Dis* 2016;18(9): O322-329.

**27.** Bembenek AE, Rosenberg R, Wagler E, Gretschel S, Sendler A, Siewert JR, Nahrig J, Witzigmann H, Hauss J, Knorr C, Dimmler A, Grone J, Buhr HJ, Haier J, Herbst H, Tepel J, Siphos B, Kleespies A, Koenigsrainer A, Stoecklein NH, Horstmann O, Grutzmann R, Imdahl A, Svoboda D, Wittekind C, Schneider W, Wernecke KD, Schlag PM. Sentinel lymph node biopsy in colon cancer: a prospective multicenter trial. *Ann Surg* 2007;245(6): 858-863.

**28.** Chand M, Keller DS, Joshi HM, Devoto L, Rodriguez-Justo M, Cohen R. Feasibility of fluorescence lymph node imaging in colon cancer: FLICC. *Tech Coloproctol* 2018;22(4): 271-277.

**29.** Nishigori N, Koyama F, Nakagawa T, Nakamura S, Ueda T, Inoue T, Kawasaki K, Obara S, Nakamoto T, Fujii H, Nakajima Y. Visualization of Lymph/Blood Flow in Laparoscopic Colorectal Cancer Surgery by ICG Fluorescence Imaging (Lap-IGFI). *Ann Surg Oncol* 2016;23 **Suppl** 2: S266-274.

**30.** Tuech JJ, Pessaux P, Regenet N, Bergamaschi R, Colson A. Sentinel lymph node mapping in colon cancer. *Surg Endosc* 2004;18(12): 1721-1729.

**31.** Ankersmit M, Bonjer HJ, Hannink G, Schoonmade LJ, van der Pas MHGM, Meijerink WJHJ. Near-infrared fluorescence imaging for sentinel lymph node identification in colon cancer: a prospective single-center study and systematic review with meta-analysis. *Tech Coloproctol* 2019;23(12): 1113-1126.

**32.** Andersen HS, Bennedsen ALB, Burgdorf SK, Eriksen JR, Eiholm S, Toxværd A, Riis LB, Rosenberg J, Gögenur I. In vivo and ex vivo sentinel node mapping does not identify the same lymph nodes in colon cancer. *Int J Colorectal Dis* 2017;32(7): 983-990.

**33.** Hirche C, Mohr Z, Kneif S, Doniga S, Murawa D, Strik M, Hünerbein M. Ultrastaging of colon cancer by sentinel node biopsy using fluorescence navigation with indocyanine green. *Int J Colorectal Dis* 2012;27(3): 319-324.

**34.** Nagata K, Endo S, Hidaka E, Tanaka JI, Kudo SE, Shiokawa A. Laparoscopic sentinel node mapping for colorectal cancer using infrared ray laparoscopy. *Anticancer Res* 2006;26(3 B): 2307-2311.

**35.** Cahill RA, Anderson M, Wang LM, Lindsey I, Cunningham C, Mortensen NJ. Near-infrared (NIR) laparoscopy for intraoperative lymphatic road-mapping and sentinel node identification during definitive surgical resection of early-stage colorectal neoplasia. *Surg Endosc Interv Tech* 2012;26(1): 197-204.

**36.** Burghgraef TA, Zweep AL, Sikkenk DJ, van der Pas M, Verheijen PM, Consten ECJ. In vivo sentinel lymph node identification using fluorescent tracer imaging in colon cancer: A systematic review and meta-analysis. *Crit Rev Oncol Hematol* 2021;158: 103149.

**37.** Ohnishi S, Lomnes SJ, Laurence RG, Gogbashian A, Mariani G, Frangioni JV. Organic alternatives to quantum dots for intraoperative near-infrared fluorescent sentinel lymph node mapping. *Mol Imaging* 2005;4(3): 172-181.

**38.** Schaafsma BE, Verbeek FPR, Van Der Vorst JR, Hutteman M, Kuppen PJK, Frangioni JV, Van De Velde CJH, Vahrmeijer AL. Ex vivo sentinel node mapping in colon cancer combining blue dye staining and fluorescence imaging. *J Surg Res* 2013;183(1): 253-257.

**39.** Hutteman M, Choi HS, Mieog JSD, Van Der Vorst JR, Ashitate Y, Kuppen PJK, Van Groningen MC, Löwik CWGM, Smit VTHBM, Van De Velde CJH, Frangioni JV, Vahrmeijer AL. Clinical translation of ex vivo sentinel lymph node mapping for colorectal cancer using invisible near-infrared fluorescence light. *Ann Surg Oncol* 2011;18(4): 1006-1014.

**40.** Weixler B, Rickenbacher A, Raptis DA, Viehl CT, Guller U, Rueff J, Zettl A, Zuber M. Sentinel Lymph Node Mapping with Isosulfan Blue or Indocyanine Green in Colon Cancer Shows Comparable Results and Identifies Patients with Decreased Survival: A Prospective Single-Center Trial. *World J Surg* 2017;41(9): 2378-2386.

**41.** Koppe MJ, Boerman OC, Oyen WJ, Bleichrodt RP. Peritoneal carcinomatosis of colorectal origin: incidence and current treatment strategies. *Ann Surg* 2006;243(2): 212-222.

**42.** Razenberg LG, Lemmens VE, Verwaal VJ, Punt CJ, Tanis PJ, Creemers GJ, de Hingh IH. Challenging the dogma of colorectal peritoneal metastases as an untreatable condition: Results of a population-based study. *Eur J Cancer* 2016;65: 113-120.

**43.** Simkens GA, van Oudheusden TR, Nieboer D, Steyerberg EW, Rutten HJ, Luyer MD, Nienhuijs SW, de Hingh IH. Development of a Prognostic Nomogram for Patients with Peritoneally Metastasized Colorectal Cancer Treated with Cytoreductive Surgery and HIPEC. *Ann Surg Oncol* 2016;23(13): 4214-4221.

**44.** Faron M, Macovei R, Goere D, Honore C, Benhaim L, Elias D. Linear Relationship of Peritoneal Cancer Index and Survival in Patients with Peritoneal Metastases from Colorectal Cancer. *Ann Surg Oncol* 2016;23(1): 114-119.

**45.** Maeda H. Tumour-selective delivery of macromolecular drugs via the EPR effect: background and future prospects. *Bioconjug Chem* 2010;21(5): 797-802.

**46.** Liberale G, Vankerckhove S, Gomez Caldon M, Ahmed B, Moreau M, El Nakadi I, Larsimont D, Donckier V, Bourgeois P. Fluorescence imaging after indocyanine green injection for detection of peritoneal metastases in patients undergoing cytoreductive surgery for peritoneal carcinomatosis from colorectal cancer: A pilot study. *Ann Surg* 2016;264(6): 1110-1115.

**47.** Filippello A, Porcheron J, Klein JP, Cottier M, Barabino G. Affinity of Indocyanine Green in the Detection of Colorectal Peritoneal Carcinomatosis. *Surg Innov* 2017;24(2): 103-108.

**48.** Harlaar NJ, Koller M, de Jongh SJ, van Leeuwen BL, Hemmer PH, Kruijff S, van Ginkel RJ, Been LB, de Jong JS, Kats-Ugurlu G, Linssen MD, Jorritsma-Smit A, van Oosten M, Nagengast WB, Ntziachristos V, van Dam GM. Molecular fluorescence-guided surgery of peritoneal carcinomatosis of colorectal origin: a single-centre feasibility study. *Lancet Gastroenterol Hepatol* 2016;1(4): 283-290.

**49.** Schaap DP, de Valk KS, Deken MM, Meijer RPJ, Burggraaf J, Vahrmeijer AL, Kusters M, Kusters M, Boogerd LSF, Schaap DP, Voogt ELK, Nieuwenhuijzen GAP, Rutten HJT, de Hingh IHJT, Burger JWA, Nienhuijs SW, de Valk KS, Meijer RPJ, Burggraaf J, Brandt-Kerkhof ARM, Verhoef C, Madsen EVE, van Kooten JP, Framery B, Gutowski M, A PM-h, Cailler F, van Lijnschoten I, Vahrmeijer AL, Hoogstins CES, Boogerd LSF, de Valk KS, Deken MM, Meijer RPJ. Carcinoembryonic antigen-specific, fluorescent image-guided cytoreductive surgery with hyperthermic intraperitoneal chemotherapy for metastatic colorectal cancer. *Br J Surg* 2020;107(4): 334-337.

**50.** Kobayashi H, Watanabe R, Choyke PL. Improving conventional enhanced permeability and retention (EPR) effects; what is the appropriate target? *Theranostics* 2013;4(1): 81-89.

**51.** Manfredi S, Lepage C, Hatem C, Coatmeur O, Faivre J, Bouvier AM. Epidemiology and management of liver metastases from colorectal cancer. *Ann Surg* 2006;244(2): 254-259.

**52.** Nierop PMH, Höppener DJ, van der Stok EP, Galjart B, Buisman FE, Balachandran VP, Jarnagin WR, Kingham TP, Allen PJ, Shia J, Vermeulen PB, Groot Koerkamp B, Grünhagen DJ, Verhoef C,

D'Angelica MI. Histopathological growth patterns and positive margins after resection of colorectal liver metastases. *HPB (Oxford)* 2020;22(6): 911-919.

**53.** Elfrink AKE, Pool M, van der Werf LR, Marra E, Burgmans MC, Meijerink MR, den Dulk M, van den Boezem PB, Te Riele WW, Patijn GA, Wouters M, Leclercq WKG, Liem MSL, Gobardhan PD, Buis CI, Kuhlmann KFD, Verhoef C, Besselink MG, Grünhagen DJ, Klaase JM, Kok NFM, the Dutch Hepato-Biliary Audit G. Preoperative imaging for colorectal liver metastases: a nationwide population-based study. *BJS Open* 2020;4(4): 605-621.

**54.** Liberale G, Bourgeois P, Larsimont D, Moreau M, Donckier V, Ishizawa T. Indocyanine green fluorescence-guided surgery after IV injection in metastatic colorectal cancer: A systematic review. *Eur J Surg Oncol* 2017;43(9): 1656-1667.

**55.** Van Der Vorst JR, Schaafsma BE, Hutteman M, Verbeek FPR, Liefers GJ, Hartgrink HH, Smit VTHBM, Löwik CWGM, Van De Velde CJH, Frangioni JV, Vahrmeijer AL. Near-infrared fluorescence-guided resection of colorectal liver metastases. *Cancer* 2013;119(18): 3411-3418.

**56.** Peloso A, Franchi E, Canepa MC, Barbieri L, Briani L, Ferrario J, Bianco C, Quaretti P, Brugnatelli S, Dionigi P, Maestri M. Combined use of intraoperative ultrasound and indocyanine green fluorescence imaging to detect liver metastases from colorectal cancer. *HPB* 2013;15(12): 928-934.

**57.** Aoki T, Murakami M, Koizumi T, Matsuda K, Fujimori A, Kusano T, Enami Y, Goto S, Watanabe M, Otsuka K. Determination of the surgical margin in laparoscopic liver resections using infrared indocyanine green fluorescence. *Langenbecks Arch Surg* 2018;403(5): 671-680.

**58.** Meijer RPJ, de Valk KS, Deken MM, Boogerd LSF, Hoogstins CES, Bhairosingh SS, Swijnenburg RJ, Bonsing BA, Framery B, Fariña Sarasqueta A, Putter H, Hilling DE, Burggraaf J, Cailler F, Mieog JSD, Vahrmeijer AL. Intraoperative detection of colorectal and pancreatic liver metastases using SGM-101, a fluorescent antibody targeting CEA. *Eur J Surg Oncol* 2020.

**59.** Handgraaf HJM, Boogerd LSF, Höppener DJ, Peloso A, Sibinga Mulder BG, Hoogstins CES, Hartgrink HH, van de Velde CJH, Mieog JSD, Swijnenburg RJ, Putter H, Maestri M, Braat AE, Frangioni JV, Vahrmeijer AL. Long-term follow-up after near-infrared fluorescence-guided resection of colorectal liver metastases: A retrospective multicenter analysis. *Eur J Surg Oncol* 2017;43(8): 1463-1471.

**60.** Achterberg FB, Sibinga Mulder BG, Meijer RPJ, Bonsing BA, Hartgrink HH, Mieog JSD, Zlitni A, Park SM, Farina Sarasqueta A, Vahrmeijer AL, Swijnenburg RJ. Real-time surgical margin assessment using ICG-fluorescence during laparoscopic and robot-assisted resections of colorectal liver metastases. *Ann Transl Med* 2020;8(21): 1448.

**61.** Gild P, Kluth LA, Vetterlein MW, Engel O, Chun FKH, Fisch M. Adult iatrogenic ureteral injury and stricture-incidence and treatment strategies. *Asian J Urol* 2018;5(2): 101-106.

**62.** Blackwell RH, Kirshenbaum EJ, Shah AS, Kuo PC, Gupta GN, Turk TMT. Complications of Recognized and Unrecognized Iatrogenic Ureteral Injury at Time of Hysterectomy: A Population Based Analysis. *J Urol* 2018;199(6): 1540-1545.

**63.** White LA, Joseph JP, Yang DY, Kelley SR, Mathis KL, Behm K, Viers BR. Intraureteral indocyanine green augments ureteral identification and avoidance during complex robotic-assisted colorectal surgery. *Colorectal Dis* 2020.

**64.** Mandovra P, Kalikar V, Patankar RV. Real-Time Visualization of Ureters Using Indocyanine Green During Laparoscopic Surgeries: Can We Make Surgery Safer? *Surg Innov* 2019;26(4): 464-468.

**65.** Cabanes M, Boria F, Hernández Gutiérrez A, Zapardiel I. Intra-operative identification of ureters using indocyanine green for gynecological oncology procedures. *Int J Gynecol Cancer* 2019.

**66.** Al-Taher M, Van Den Bos J, Schols RM, Bouvy ND, Stassen LPS. Fluorescence Ureteral Visualization in Human Laparoscopic Colorectal Surgery Using Methylene Blue. *J Laparoendosc Adv Surg Techn* 2016;26(11): 870-875.

**67.** Barnes TG, Hompes R, Birks J, Mortensen NJ, Jones O, Lindsey I, Guy R, George B, Cunningham C, Yeung TM. Methylene blue fluorescence of the ureter during colorectal surgery. 2018;32(9): 4036-4043.

**68.** Verbeek FPR, Van Der Vorst JR, Schaafsma BE, Swijnenburg RJ, Gaarenstroom KN, Elzevier HW, Van De Velde CJH, Frangioni JV, Vahrmeijer AL. Intraoperative near infrared fluorescence guided identification of the ureters using low dose methylene blue: A first in human experience. *J Urol* 2013;190(2): 574-579.

**69.** de Valk KS, Handgraaf HJ, Deken MM, Sibinga Mulder BG, Valentijn AR, Terwisscha van Scheltinga AG, Kuil J, van Esdonk MJ, Vuijk J, Bevers RF, Peeters KC, Holman FA, Frangioni JV, Burggraaf J, Vahrmeijer AL. A zwitterionic near-infrared fluorophore for real-time ureter identification during laparoscopic abdominopelvic surgery. *Nat Commun* 2019;10(1).

**70.** Farnam RW, Arms RG, Klaassen AH, Sorger JM. Intraoperative ureter visualization using a near-infrared imaging agent. *J Biomed Opt* 2019;24(6): 1-8.

**71.** Huh WK, Johnson JL, Elliott E, Boone JD, Leath CA, Kovar JL, Kim KH. Fluorescence Imaging of the Ureter in Minimally Invasive Pelvic Surgery. *J Minimally Invasive Gynecol* 2020.

**72.** Al-Taher M, van den Bos J, Schols RM, Kubat B, Bouvy ND, Stassen LPS. Evaluation of a novel dye for near-infrared fluorescence delineation of the ureters during laparoscopy. *BJS Open* 2018;2(4): 254-261.

**73.** Simone G, Misuraca L, Anceschi U, Minisola F, Ferriero M, Guaglianone S, Tuderti G, Gallucci M. Urethra and Ejaculation Preserving Robot-assisted Simple Prostatectomy: Near-infrared Fluorescence Imaging-guided Madigan Technique. *Eur Urol* 2019;75(3): 492-497.

**74.** Nitta T, Tanaka K, Kataoka J, Ohta M, Ishii M, Ishibashi T, Okuda J. Novel technique with the IRIS U kit to prevent urethral injury in patients undergoing transanal total mesorectal excision. *Ann Med Surg* 2019;46: 1-3.

**75.** Lange MM, Marijnen CA, Maas CP, Putter H, Rutten HJ, Stiggelbout AM, Meershoek-Klein Kranenbarg E, van de Velde CJ, Cooperative clinical investigators of the D. Risk factors for sexual dysfunction after rectal cancer treatment. *Eur J Cancer* 2009;45(9): 1578-1588.

**76.** Lange MM, van de Velde CJ. Urinary and sexual dysfunction after rectal cancer treatment. *Nat Rev Urol* 2011;8(1): 51-57.

**77.** Gonzales J, Pirovano G, Chow CY, de Souza Franca PD, Carter LM, Klint JK, Guru N, Lewis JS, King GF, Reiner T. Fluorescence labeling of a NaV1.7-targeted peptide for near-infrared nerve visualization. *EJNMMI Res* 2020;10(1).

**78.** Hingorani DV, Whitney MA, Friedman B, Kwon JK, Crisp JL, Xiong Q, Gross L, Kane CJ, Tsien RY, Nguyen QT. Nerve-targeted probes for fluorescence-guided intraoperative imaging. *Theranostics* 2018;8(15): 4226-4237.

**79.** Wang LG, Barth CW, Kitts CH, Mebrat MD, Montaño AR, House BJ, McCoy ME, Antaris AL, Galvis SN, McDowall I, Sorger JM, Gibbs SL. Near-infrared nerve-binding fluorophores for buried nerve tissue imaging. *Sci Transl Med* 2020;12(542).

**80.** Sparreboom CL, Komen N, Rizopoulos D, Verhaar AP, Dik WA, Wu Z, van Westreenen HL, Doornebosch PG, Dekker JWT, Menon AG, Daams F, Lips D, van Grevenstein WMU, Karsten TM, Bayon Y, Peppelenbosch MP, Wolthuis AM, D'Hoore A, Lange JF. A multicentre cohort study of serum and peritoneal biomarkers to predict anastomotic leakage after rectal cancer resection. *Colorectal Dis* 2020;22(1): 36-45.

**81.** Angeramo CA, Dreifuss NH, Schlottmann F, Bun ME, Rotholtz NA. Postoperative outcomes in patients undergoing colorectal surgery with anastomotic leak before and after hospital discharge. *Updates Surg* 2020;72(2): 463-468.

**82.** van Manen L, Handgraaf HJM, Diana M, Dijkstra J, Ishizawa T, Vahrmeijer AL, Mieog JSD. A practical guide for the use of indocyanine green and methylene blue in fluorescence-guided abdominal surgery. *J Surg Oncol* 2018;118(2): 283-300.

**83.** Watanabe J, Ishibe A, Suwa Y, Suwa H, Ota M, Kunisaki C, Endo I. Indocyanine green fluorescence imaging to reduce the risk of anastomotic leakage in laparoscopic low anterior resection for rectal cancer: a propensity score-matched cohort study. *Surg Endosc* 2020;34(1): 202-208.

**84.** Kin C, Vo H, Welton L, Welton M. Equivocal effect of intraoperative fluorescence angiography on colorectal anastomotic leaks. *Dis Colon Rectum* 2015;58(6): 582-587.

**85.** Kudszus S, Roesel C, Schachtrupp A, Höer JJ. Intraoperative laser fluorescence angiography in colorectal surgery: a noninvasive analysis to reduce the rate of anastomotic leakage. *Langenbeck's Arch Surg* 2010: 1-6.

**86.** Song M, Liu J, Xia D, Yao H, Tian G, Chen X, Liu Y, Jiang Y, Li Z. Assessment of intraoperative use of indocyanine green fluorescence imaging on the incidence of anastomotic leakage after rectal cancer surgery: a PRISMA-compliant systematic review and meta-analysis. *Tech Coloproctol* 2020.

**87.** De Nardi P, Elmore U, Maggi G, Maggiore R, Boni L, Cassinotti E, Fumagalli U, Gardani M, De Pascale S, Parise P, Vignali A, Rosati R. Intraoperative angiography with indocyanine green to assess anastomosis perfusion in patients undergoing laparoscopic colorectal resection: results of a multicenter randomized controlled trial. *Surg Endosc* 2020;34(1): 53-60.

**88.** Alekseev M, Rybakov E, Shelygin Y, Chernyshov S, Zarodnyuk I. A study investigating the perfusion of colorectal anastomoses using fluorescence angiography: results of the FLAG randomized trial. *Colorectal Dis* 2020.

**89.** Rahbari NN, Weitz J, Hohenberger W, Heald RJ, Moran B, Ulrich A, Holm T, Wong WD, Tiret E, Moriya Y, Laurberg S, den Dulk M, van de Velde C, Buchler MW. Definition and grading of anastomotic leakage following anterior resection of the rectum: a proposal by the International Study Group of Rectal Cancer. *Surgery* 2010;147(3): 339-351.

**90.** Jafari MD, Pigazzi A, McLemore EC, Mutch MG, Haas E, Rasheid S, Wait AD, Paquette IM, Bardakcioglu O, Safar B, Landmann RG, Varma M, Maron DJ, Martz J, Bauer J, George VV, Fleshman JW, Steele SR, Stamos MJ. Perfusion Assessment in Left-Sided/Low Anterior Resection (PILLAR III): A Randomized, Controlled, Parallel, Multicenter Study Assessing Perfusion Outcomes with PINPOINT Near-Infrared Fluorescence Imaging in Low Anterior Resection. *Dis Colon Rectum* 2021.

**91.** Musters GD, Klaver CEL, Bosker RJI, Burger JWA, van Duijvendijk P, van Etten B, van Geloven AAW, de Graaf EJR, Hoff C, Leijtens JWA, Rutten HJT, Singh B, Vuylsteke R, de Wilt JHW, Dijkgraaf

MGW, Bemelman WA, Tanis PJ. Biological Mesh Closure of the Pelvic Floor After Extralevator Abdominoperineal Resection for Rectal Cancer: A Multicenter Randomized Controlled Trial (the BIOPEX-study). *Ann Surg* 2017;265(6): 1074-1081.

**92.** Chandra A, Srivastava RK, Kashyap MP, Kumar R, Srivastava RN, Pant AB. The anti-inflammatory and antibacterial basis of human omental defense: selective expression of cytokines and antimicrobial peptides. *PLoS One* 2011;6(5): e20446.

**93.** Blok RD, Hagemans JAW, Klaver CEL, Hellinga J, van Etten B, Burger JWA, Verhoef C, Hompes R, Bemelman WA, Tanis PJ. A Systematic Review and Meta-analysis on Omentoplasty for the Management of Abdominoperineal Defects in Patients Treated for Cancer. *Ann Surg* 2020;271(4): 654-662.

**94.** Slooter MD, Blok RD, Wisselink DD, Buskens CJ, Bemelman WA, Tanis PJ, Hompes R. Near-infrared fluorescence angiography for intra-operative assessment of pedicled omentoplasty for filling of a pelvic cavity: a pilot study. *Tech Coloproctol* 2019;23(8): 723-728.

**95.** Slooter MD, Blok RD, de Krom MA, Buskens CJ, Bemelman WA, Tanis PJ, Hompes R. Optimizing omentoplasty for management of chronic pelvic sepsis by intra-operative fluorescence angiography: a comparative cohort study. *Colorectal Dis* 2020;22(12): 2252-2259.

**96.** Keereweer S, Van Driel PB, Snoeks TJ, Kerrebijn JD, Baatenburg de Jong RJ, Vahrmeijer AL, Sterenborg HJ, Löwik CW. Optical image-guided cancer surgery: challenges and limitations. *Clin Cancer Res* 2013;19(14): 3745-3754.

**97.** Lütken CD, Achiam MP, Svendsen MB, Boni L, Nerup N. Optimizing quantitative fluorescence angiography for visceral perfusion assessment. *Surg Endosc* 2020;34(12): 5223-5233.

**98.** Goncalves LN, van den Hoven P, van Schaik J, Leeuwenburgh L, Hendricks CHF, Verduijn PS, van der Bogt KEA, van Rijswijk CSP, Schepers A, Vahrmeijer AL, Hamming JF, van der Vorst JR. Perfusion Parameters in Near-Infrared Fluorescence Imaging with Indocyanine Green: A Systematic Review of the Literature. *Life* 2021;11(5): 433.

**99.** Lauwerends LJ, van Driel P, Baatenburg de Jong RJ, Hardillo JAU, Koljenovic S, Puppels G, Mezzanotte L, Löwik C, Rosenthal EL, Vahrmeijer AL, Keereweer S. Real-time fluorescence imaging in intraoperative decision making for cancer surgery. *Lancet Oncol* 2021.

## SUPPLEMENTARIES

**Supplement 1:** search strategies per database and the corresponding hits after removal of duplicates

| Database | Full search strategy |
|---|---|
| **Embase (1123 articles)** | ('fluorescence guided surgery'/de OR (('fluorescence angiography'/de OR 'fluorescence imaging system'/de OR 'indocyanine green angiography'/de OR 'indocyanine green'/de OR 'near infrared spectroscopy'/exp OR 'near infrared imaging system'/de OR 'fluorescence imaging'/de) AND ('surgery'/exp OR surgery:lnk OR 'laparoscope'/exp)) OR (((fluorescen* OR indocyanine-green* OR ICG OR near-infrared* OR near-infra-red*) NEAR/9 (surg* OR operat* OR intraoperat* OR resect* OR microsurg* OR laparoscop*))):ab,ti,kw) ***AND*** ('large intestine tumour'/exp OR 'large intestine cancer'/exp OR 'large intestine carcinoma'/exp OR 'colorectal surgery'/exp OR 'ureter'/de OR 'ureter injury'/de OR 'ureter surgery'/exp OR 'urethra'/exp OR 'urethra injury'/de OR 'urethra surgery'/exp OR 'peripheral nerve'/de OR (((rect* OR colorect* OR colon* OR appendi* OR anal* OR anus OR cecum OR caecum OR large-intestin* OR sigmoid* OR bowel*) NEAR/3 (carcinoma* OR neoplas* OR tumour* OR tumour* OR cancer* OR surger* OR resect*)) OR ureter* OR urethr* OR (nerve* NEAR/3 (imag* OR detect* OR locali*))):ab,ti,kw) *NOT (conference abstract)/lim AND (english)/lim* |
| **Medline (198 articles)** | (((Fluorescein Angiography/ OR Optical Imaging/ OR Indocyanine Green/ OR Spectroscopy, Near-Infrared/) AND (exp Surgical Procedures, Operative/ OR surgery.fs. OR Laparoscopy/)) OR (((fluorescen* OR indocyanine-green* OR ICG OR near-infrared* OR near-infra-red*) ADJ9 (surg* OR operat* OR intraoperat* OR resect* OR microsurg* OR laparoscop*))).ab,ti,kf.) ***AND*** (exp Colorectal Neoplasms/ OR Colorectal Surgery/ OR Urethra/ OR Ureter/ OR Peripheral Nerves/ OR (((rect* OR colorect* OR colon* OR appendi* OR anal* OR anus OR cecum OR caecum OR large-intestin* OR sigmoid* OR bowel*) ADJ3 (carcinoma* OR neoplas* OR tumour* OR tumour* OR cancer* OR surger* OR resect*)) OR ureter* OR urethr* OR (nerve* ADJ3 (imag* OR detect* OR locali*))).ab,ti,kf.) *NOT (letter* OR news OR comment* OR editorial* OR congres* OR abstract* OR book* OR chapter* OR dissertation abstract*).pt. AND english.lg.* |
| **Cochrane (73 articles)** | ((((fluorescen* OR indocyanine-green* OR ICG OR "near-infrared*" OR "near-infra-red*") NEAR/9 (surg* OR operat* OR intraoperat* OR resect* OR microsurg* OR laparoscop*))):ab,ti,kw) ***AND*** ((((rect* OR colorect* OR colon* OR appendi* OR anal* OR anus OR cecum OR caecum OR large-intestin* OR sigmoid* OR bowel*) NEAR/3 (carcinoma* OR neoplas* OR tumour* OR tumour* OR cancer* OR surger* OR resect*)) OR ureter* OR urethr* OR (nerve* NEAR/3 (imag* OR detect* OR locali*))):ab,ti,kw) |

**Supplement 2:** overview of all clinical studies on colorectal cancer surgery assessing experimental fluorescent agents.

**Primary tumour**

| First author | Tumour type | Year | Fluorescent agent | Study design | Fluorescence imaging application | Number of patients | (Optimal) dose | (Optimal) administration interval | Optimal TBR (mean) | Sensitivity | Specificity | Change in surgical management | Other outcomes |
|---|---|---|---|---|---|---|---|---|---|---|---|---|---|
| Boogerd (14) | CC + RC | 2018 | SGM-101 | Open-label, dose escalation | In vivo and PEARL MSI | 26* | 10 mg | 4 days | 1.64 (*in vivo*)<br>6.1 (*ex vivo*: PEARL MSI) | 98% | 62% | 35% | ppv: 81% \| npv: 94% \| acc: 84% |
| De Jongh (16) | RC | 2020 | Bevacizumab-800CW | Open-label, fixed dose, pilot study | 1 = Back table imaging for CRM evaluation<br>2 = Odyssey imaging to determine sens / spec for tumour detection | 1 = 8<br>2 = 17 | 4.5 mg | 2-3 days | 4.7 (*ex vivo*: Odyssey) | 96.19%** | 80.39%** | na | Tumour positive CRM correctly identified in 1 out of 2 patients (50%) |
| De Valk (15) | CC | 2020 | cRGD-ZW800-1 | Open-label, dose escalation | In vivo and PEARL MSI | 12 | 0.05 mg/kg | 18 hours | 1.6 (*in vivo*)<br>6.2 (*ex vivo*: PEARL MSI) | nr | nr | nr | Lymph nodes: sens 100% \| spec: 87% \| ppv: 33% \| npv: 100% \| acc: 88% |
| De Valk (18) | CC + RC | 2020 | SGM-101 | Open-label, dose escalation | In vivo and back table | 37* | 10 mg | 4 days | 1.9 (*in vivo*)<br>3.5 (*ex vivo*: back table) | 96% | 63% | 24% | ppv: 70% \| npv: 94% \| acc: 78% |
| Voskuil (17) | nr*** | 2020 | ONM-100 | Open-label, dose escalation | PEARL MSI | 3 | 1.2 mg/kg | 24 hours | nr*** | nr*** | nr*** | nr*** | - |

**Supplement 2:** overview of all clinical studies on colorectal cancer surgery assessing experimental fluorescent agents. (continued)

**Sentinel lymph node**

| First author | Year | Fluorescent agent | Study design | Fluorescence imaging application | Number of patients | (Optimal) dose | (Optimal) administration interval | SBR | Sensitivity | Specificity | Change in surgical management | Other outcomes |
|---|---|---|---|---|---|---|---|---|---|---|---|---|
| Hutteman (39) | 2011 | HSA800 | Pilot study | *Ex vivo* | 24 | 1cc 50 µM | post-operative in specimen | nr | nr | na | nr | SLN's detected: 100% \| avg SLN's: 3 |
| Schaafsma (38) | 2013 | HSA800 | Pilot study | *Ex vivo* | 22 | 1cc 50 µM | post-operative in specimen | nr | 80% | na | nr | SLN's detected: 95% \| avg SLN's: 3.5 |
| Weixler (40) | 2017 | HSA800 | Prospective single-centre | *Ex vivo* | 50 | 1cc 50 µM | post-operative in specimen | nr | 64% | na | 10% | SLN's detected: 100% \| avg SLN's: 4.4 |

**(C) Peritoneal metastases**

| First author | Year | Fluorescent agent | Study design | Fluorescence imaging application | Number of patients | (Optimal) dose | (Optimal) administration interval | Optimal TBR (mean) | Sensitivity | Specificity | Change in surgical management | Other outcomes |
|---|---|---|---|---|---|---|---|---|---|---|---|---|
| Harlaar (48) | 2016 | Bevacizumab-800CW | Open-label, feasibility study | In vivo and back table | 7 | 4.5 mg | 2 days | 6.92 (*ex vivo*: back table) | nr | nr | 29% | ppv: 53% \| npv: 100% |
| Schaap (49) | 2020 | SGM-101 | Open-label, pilot study | In vivo and back table | 14 | 10-15 mg | 4-6 days | nr | 98.5% | 62.2% | 50% | ppv: 82.3%\| npv: 95.8%\| acc: 85.4% |

**Supplement 2:** overview of all clinical studies on colorectal cancer surgery assessing experimental fluorescent agents. (continued)

**(D) Liver metastases**

| First author | Year | Fluorescent agent | Study design | Fluorescence imaging application | Number of patients | Optimal dose | (Optimal) administration interval | Optimal TBR (median) | Sensitivity | Specificity | Change in surgical management | Other outcomes |
|---|---|---|---|---|---|---|---|---|---|---|---|---|
| Meijer (58) | 2020 | SGM-101 | Open label, dose finding | In vivo (occult lesions and resection margin) | 8 | 10 mg | 4 days | 2.0 (in vivo) | nr | nr | 0% | ppv: 89%\| positive CRM: 9% |

**(E) Ureter**

| First author | Year | Fluorescent agent | Study design | Fluorescence imaging application | Number of patients | Optimal dose | Administration interval | Optimal SBR | Ureters identified | Duration of visualisation |
|---|---|---|---|---|---|---|---|---|---|---|
| De Valk (69) | 2019 | ZW800-1 | Open label, dose finding | In vivo | 12 | 2.5 mg | per-operative | 2.7 | 100% | 3.5 hours |
| Farnam (70) | 2019 | IS-001 | Open label, dose finding | In vivo | 24 | 20 - 40 mg | per-operative | 3.6 | 100% | nr |
| Huh (71) | 2020 | IRDye-800BK | Open label, dose finding | In vivo | 41 | 0.06 mg/kg | per-operative | nr | 100% | 1.5 hours |

* 21 out of 26 patients from Boogerd et al were also included in the study by de Valk et al
** Based on microscopy determined optimal mean fluorescence intensity cut off values for tumour detection
*** Results of interest not separately specified for colorectal cancer patients

**Supplement 3:** overview of all ongoing clinical trials on colorectal cancer surgery assessing experimental fluorescent agents

| Principal investigator | Fluorescent agent | Study phase | Imaging target | Tumour type | Planned inclusion FLI (n) | Control group (n) | Recruitment status | (Estimated) study completion date | NCT number |
|---|---|---|---|---|---|---|---|---|---|
| Barnes, T.G. | IRDYe-800BK | Phase I/II | Ureter | na | 40 | na | Completed | nov-18 | NCT03387410 |
| Chan, A.T. | LUM015 | Phase I | Primary tumour | All stage colorectal cancer | 11 | na | Recruiting | dec-20 | NCT02584244 |
| Cusack, J.C. | LUM015 | nr | Peritoneal metastases | Peritoneal metastases of CRC | nr* | na | Not yet recruiting | feb-21 | NCT03834272 |
| OncoNano Medicine, Inc. | ONM-100 | Phase II | Primary tumour | Colorectal cancer, not specified | nr* | na | Recruiting | dec-20 | NCT03735680 |
| Vahrmeijer, A.L. | SGM-101 | Phase III | Primary tumour and peritoneal metastases | LARC & LRRC, T4 colon cancer, locally recurrent colon cancer, and peritoneal metastases of CRC | 240 | 60 | Recruiting | dec-21 | NCT03659448 |
| Vahrmeijer, A.L | SGM-101 | Phase II | Extra abdominal metastases | Colorectal lung metastases | 10 | na | Recruiting | dec-21 | NCT04737213 |
| Vahrmeijer, A.L | SGM-101 | Phase II | Extra abdominal metastases | Colorectal brain metastases | 10 | na | Not yet recruiting | dec-22 | NCT04755920 |
| Vahrmeijer, A.L | SGM-101 | Phase III | Primary tumour | LARC & LRRC | 203 | na | Recruiting | oct-23 | NCT04642924 |

* Study assessing various tumour types, amount of patient undergoing surgery for colorectal cancer is not specified.

**Supplement 4:** MINORS score per study assessing experimental fluorescent agents

| First author | MINORS score | Maximum MINORS score | Clearly stated aim | Consecutive patients | Prospective data collection | Appropriate endpoint | Unbiased evaluation of endpoints | Appropriate follow-up | Loss to follow-up | Prospective calculation of sample size | Gold Standard control | Contemporary groups | Baseline equivalence of groups | Statistical analysis adapted to study design |
|---|---|---|---|---|---|---|---|---|---|---|---|---|---|---|
| Boogerd (14) | 14 | 16 | 2 | 2 | 2 | 2 | 0 | 2 | 2 | 2 | na | na | na | na |
| De Jongh (16) | 11 | 16 | 2 | 2 | 1 | 2 | 0 | 2 | 2 | 0 | na | na | na | na |
| De Valk (15) | 14 | 16 | 2 | 2 | 2 | 2 | 2 | 2 | 2 | 0 | na | na | na | na |
| De Valk (18) | 14 | 16 | 2 | 2 | 2 | 2 | 0 | 2 | 2 | 2 | na | na | na | na |
| Voskuil (17) | 14 | 16 | 2 | 2 | 2 | 2 | 2 | 2 | 2 | 0 | na | na | na | na |
| Hutteman (39) | 11 | 16 | 1 | 2 | 2 | 2 | 0 | 2 | 2 | 0 | na | na | na | na |
| Schaafsma (38) | 18 | 24 | 2 | 2 | 2 | 2 | 0 | 2 | 2 | 0 | 2 | 2 | 0 | 2 |
| Weixler (40) | 13 | 24 | 2 | 0 | 1 | 2 | 0 | 2 | 0 | 0 | 2 | 0 | 2 | 2 |
| Harlaar (48) | 14 | 16 | 2 | 2 | 2 | 2 | 2 | 2 | 2 | 0 | na | na | na | na |
| Schaap (49) | 12 | 16 | 2 | 2 | 2 | 2 | 0 | 2 | 2 | 0 | na | na | na | na |
| Meijer (58) | 12 | 16 | 2 | 2 | 2 | 2 | 0 | 2 | 2 | 0 | na | na | na | na |
| De Valk (69) | 14 | 16 | 2 | 2 | 2 | 2 | 2 | 2 | 2 | 0 | na | na | na | na |
| Farnam (70) | 14 | 16 | 2 | 2 | 2 | 2 | 0 | 2 | 2 | 2 | na | na | na | na |
| Huh (71) | 12 | 16 | 2 | 2 | 2 | 2 | 0 | 2 | 2 | 0 | na | na | na | na |

# Chapter 3

## Current intraoperative imaging techniques to improve surgical resection of laryngeal cancer: a systematic review

Hidde A. Galema*, Lorraine J. Lauwerends*, José A.U. Hardillo, Aniel Sewnaik, Dominiek Monserez, Pieter B.A.A. van Driel, Cornelis Verhoef, Robert J. Baatenburg de Jong, Denise E. Hilling‡, Stijn Keereweer‡

*Shared first authorship ‡ Shared senior authorship

Cancers (Basel). 2021 Apr 15;13(8):1895.

## ABSTRACT

Laryngeal cancer is a prevalent head and neck malignancy, with poor prognosis and low survival rates for patients with advanced disease. Treatment consists of unimodal therapy through surgery or radiotherapy in early staged tumours, while advanced stage tumours are generally treated with multimodal chemoradiotherapy or (total) laryngectomy followed by radiotherapy. Still, the recurrence rate for advanced laryngeal cancer is between 25 and 50%. In order to improve surgical resection of laryngeal cancer and reduce local recurrence rates, various intraoperative optical imaging techniques have been investigated. In this systematic review, we identify these technologies, evaluating the current state and future directions of optical imaging for this indication. Narrow-band imaging (NBI) and autofluorescence (AF) are established tools for early detection of laryngeal cancer. Nonetheless, their intraoperative utility is limited by an intrinsic inability to image beyond the (sub-)mucosa. Likewise, contact endoscopy (CE) and optical coherence tomography (OCT) are technically cumbersome and only useful for mucosal margin assessment. Research on fluorescence imaging (FLI) for this application is sparse, dealing solely with nonspecific fluorescent agents. Evidently, the imaging modalities that have been investigated thus far are generally unsuitable for deep margin assessment. We discuss two optical imaging techniques that can overcome these limitations and suggest how they can be used to achieve adequate margins in laryngeal cancer at all stages.

## INTRODUCTION

With almost 40,000 cases in Europe in 2018 (1), laryngeal cancer is the second most common malignancy of the head and neck region. Early diagnosis and adequate preoperative assessment increase the likelihood to cure disease while preserving functionality. Outcomes for patients with early stage (T1 and T2) tumours are favourable, with cure rates of 80–90% (2,3). More advanced staged laryngeal squamous cell carcinoma (SCC) have been reported to have recurrence rates ranging between 25 and 50% (4). These tumours are associated with loss of laryngeal function and poor prognosis, with 5-year survival rates dropping to 40% for patients with stage IV disease (2).

In head and neck cancer, margin status remains one of the most important factors for local recurrence and overall survival, demonstrating the need to improve surgical resection. In patients undergoing (total) laryng(-opharyng)ectomy, inadequate margins are clearly associated with poor survival (5,6). In patients that are treated with laser surgery (generally early stage laryngeal cancer), the relationship between resection margin and patient outcome is less evident. Numerous studies on laryngeal cancer produce inconsistent results with regards to margin status and local control or relapse rate (7–10). This is caused by both post-resection and fixation shrinkage of the tissue specimen and cauterization artefacts associated with laser carbonization, which hamper an adequate histological evaluation of the surgical margins in those cases (11). Consequently, a positive margin on the tissue specimen may not always indicate that there are residual tumour cells in the wound bed (12).

Importantly, it was clearly demonstrated that tumour-positive additional wound bed biopsies, taken after transoral CO2 laser microsurgery (TLM) of laryngeal cancer, significantly impacted local control (12). This finding illustrates that there is a clear clinical need for improved intraoperative margin assessment during laser surgery. Extensive wound bed sampling is no good alternative because this only allows analysis of a fraction of the wound bed, making it prone to sampling error. In addition, margin adequacy cannot be determined from sampling the wound bed. When a total laryng(-opharyng)ectomy is performed in advanced stage laryngeal cancer, a specimen-driven analysis of the surgical margins will likely be better, as has been shown in similar cases of oral cancer surgery (13, 14). Ideally, margin status would be assessed during surgery through less invasive and more thorough inspection measures. Improved intraoperative margin assessment may also facilitate more conservative resection during partial laryngectomies and prevent superfluous biopsies, which are important considerations in improving final functional outcome and organ preservation (11).

The surgeon's ability to distinguish between malignant and healthy tissue during laryngeal surgery remains suboptimal, elucidating the need for objective intraoperative tools for margin assessment that facilitate both specimen and wound bed evaluation. Optical imaging has

long been investigated and implemented for the early diagnosis of laryngeal cancer. Over the years, a number of these imaging modalities have been suggested as intraoperative tools to facilitate real-time enhanced visualization of resection margins (15, 16). This systematic review provides an overview of the intraoperative imaging modalities that have been studied to improve surgical resection of laryngeal tumours.

## MATERIALS AND METHODS

This systematic review is reported according to the Preferred Reporting Items for Systematic Reviews and Meta-Analyses (see PRISMA 2020 checklist, Supplementary Table S2), and was registered in the PROSPERO database for systematic reviews (CRD42020187479).

### Literature Search and Study Selection

A systematic search was conducted in the Embase, Medline, Web of Science Core Collection, Cochrane, and Google Scholar databases. A search strategy was constructed using the terms 'laryngeal cancer' and 'intraoperative imaging'. Supplementary File S1 shows the full search strings per database. The last search was conducted on October 26, 2020. Based on the title and abstract, all clinical studies concerning intraoperative imaging techniques in laryngeal cancer surgery and diagnosis were included. Only journal articles in English with the full text available were considered. Next, articles were screened on full text for final inclusion. Articles that did not explicitly describe imaging techniques for margin assessment during laryngeal cancer surgery were excluded. Screening on title and abstract and on full text was done by two independent authors (L.J.L. and H.A.G.). Disagreements were discussed with a third author (S.K.).

### Data Extraction

The following data were extracted from Tables and text: imaging technique, application of imaging technique (image guided resection and wound bed assessment), T-stage, surgical procedure, negative margin definition, negative margin rates, extra resection rate, patient-related outcomes (recurrence rate, disease specific survival, recurrence free survival), and diagnostic outcomes (sensitivity, specificity, positive predictive value, and negative predictive value).

### Quality Assessment

The 'methodological index for non-randomized studies' (MINORS) was applied to all studies in the final inclusion (17). The MINORS is a validated methodological index for non-randomized studies in which the included studies are rated on 8 (non-comparative studies) or 12 items (comparative studies). All items can obtain a score between 0 and 2 points. A 0 points score indicates that it was not reported in the article, 1 point if it was inadequately reported, and 2 points if it was adequately reported. Hence, a maximum score of 16 (non-comparative studies) or 24 points (comparative studies) could be obtained.

## RESULTS

Through the search strategies, 4128 articles were identified. A total of seven additional articles were found through snowballing. After removing duplicates, 2644 articles were screened on title and abstract. Then, 68 articles were screened on full text and 19 articles were included for qualitative assessment in the systematic review. After careful consideration, the contributions from articles with a MINORS score of 4 and lower were deemed of insufficient quality, and were excluded from the systematic review. This additional screening resulted in 18 studies for final inclusion. Supplementary 2 shows the PRISMA flow diagram. All studies were non-randomized studies. Study characteristics and main outcomes are shown in Table 1. These studies reported on the following imaging techniques: narrow-band imaging (10), autofluorescence (3), fluorescence (2), contact endoscopy (2), and optical coherence tomography (1). MINORS index from the included articles ranged from 5 to 19. The full MINORS of the included articles is shown in Supplementary 3.



### Intraoperative Narrow-Band Imaging

Narrow-band imaging (NBI) is an endoscopic technique that uses selective light wavelengths to visualize the abnormal vascular patterns of the mucosa associated with premalignant or neoplastic lesions. NBI uses optical filters to select blue and green light (wavelengths of 415 and 540 nm, respectively). Narrow-band blue light, because of its low penetration depth, highlights mainly the mucosal surface, making subjacent capillaries appear brown. At the same time, the narrow-band green light with its higher penetration depth, allows it to enhance visibility of vessels in the submucosa, making them appear dark green (Figure 1A, 2A–B).

The value of NBI during the diagnostic phase for early detection of laryngeal cancer and its precursor lesions is undisputed (35). Various studies have demonstrated that a combination of NBI and white light (WL) endoscopy is superior to WL alone for its diagnostic capability (35–39). Ni et al., for example, reported a diagnostic accuracy of 91% for NBI, compared with 71% for standard endoscopy (38). Detection sensitivity of laryngeal cancer and its precursor lesions in particular is increased in multiple studies, with values ranging between 95 and 100%, confirming its ability to easily distinguish (pre)malignant from benign lesions (22,35–40). NBI has been reported to identify malignant lesions that were missed by WL alone (26,39), and, conversely, has also been reported to reduce the amount of suspicious lesions compared to WL (36). NBI is redundant for diagnosing advanced tumours, as those can be adequately visualized with conventional WL endoscopy. Nevertheless, NBI can still define tumour borders with a diagnostic gain of 11% (37), which is an important quality when considering NBI for intraoperative margin assessment.

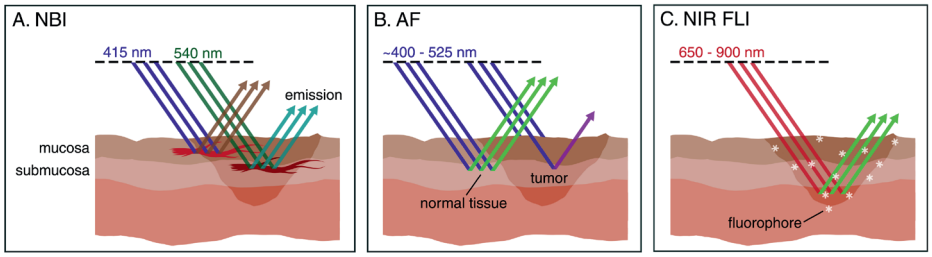


■ **Figure 1.** Schematic representation of fluorescence based imaging working principles.
*(A) Narrow-band imaging (NBI): NBI light consists of two wavelengths: 415 nm blue and 540 nm green light. The blue light penetrates the mucosa, increasing contrast in these capillaries (appearing brown), whereas the green light reaches the submucosa, visualizing the vasculature in these deeper layers (appearing dark green). (B) Autofluorescence (AF) imaging: When ex-posed to blue light, healthy laryngeal mucosa emits green fluorescence, whereas neoplastic mucosa emits both light of lower energy (red-violet) and heat. (C) Near-infrared (NIR) fluorescence imaging (FLI): When exposed to NIR light, previously administered fluorophores emit light of a wavelength, which is specific to the fluorophore (e.g., excitation and emission wavelengths for ICG: ~780 and 820 nm, respectively). Penetration depth of light in the NIR spectrum ranges from 0.5 to more than 10 mm, contingent to the wavelength.*

The value of NBI during the diagnostic phase for early detection of laryngeal cancer and its precursor lesions is undisputed (35). Various studies have demonstrated that a combination of NBI and white light (WL) endoscopy is superior to WL alone for its diagnostic capability (35–39). Ni et al., for example, reported a diagnostic accuracy of 91% for NBI, compared with 71% for standard endoscopy (38). Detection sensitivity of laryngeal cancer and its precursor lesions in particular is increased in multiple studies, with values ranging between 95 and 100%, confirming its ability to easily distinguish (pre)malignant from benign lesions (22,35–40). NBI has been reported to identify malignant lesions that were missed by WL alone (26,39), and, conversely, has also been reported to reduce the amount of suspicious lesions compared to WL (36). NBI is redundant for diagnosing advanced tumours, as those can be adequately visualized with conventional WL endoscopy. Nevertheless, NBI can still define tumour borders with a diagnostic gain of 11% (37), which is an important quality when considering NBI for intraoperative margin assessment.

■ **Table 1.** Included articles.

| First author | Year | Imaging technique | Control group | Study design | T-stage | n = (imaging) | n = (control) | Surgical procedure | Application of imaging | Negative margin definition |
|---|---|---|---|---|---|---|---|---|---|---|
| Fiz (3) | 2017 | NBI | WL[2] | Retrospective | Tis-T2 | 311 | 323 | TLM | Pre-resection | ≥ 1 mm |
| Garofolo (18) | 2014 | NBI | WL[2] | Prospective | Tis-T1a | 82 | 152 | TLM | Pre-resection | ≥ 1 mm |
| Hainarosie (19) | 2019 | NBI | WL[1] | nr | nr | 23 | 231 | TLM | Post-resection | nr |
| Klimza (20) | 2019 | NBI | na | Retrospective | T1-T2 | 44 | n/a | TLM | Pre-resection | ≥ 5 mm |
| Piersiala (21) | 2018 | NBI | na | Prospective | T2-T3 | 98 | n/a | TLM | Pre- and post-resection | ≥ 3 mm |
| Plaat (22) | 2017 | NBI | WL[2] | Retrospective | Tis-T2 | 42 | 51 | TLM | Pre- and post-resection | nr |
| Šifrer (23) | 2017 | NBI | WL[2] | Prospective | nr[3] | 14 | 8 | Laryngectomy | Pre- and post-resection | nr |
| Srivastava (24) | 2016 | NBI | na | Retrospective | Tis-T2 | 30 | n/a | TLM | Pre-resection | nr |
| Vicini (25) | 2015 | NBI | WL | Prospective | T1-T4 | 7 | 4 | Transoral surgery | Pre- and post-resection | ≥ 2 mm |
| Zwakenberg (26) | 2021 | NBI | WL[1] | Prospective | Tis-T4 | 89 | 891 | TLM, TLE | Pre-resection | nr |
| Fielding (27) | 2006 | AF | na | Prospective | nr | 48 | n/a | TLM | Pre-resection | nr |
| Paczona (28) | 2003 | AF | WL[1] | Prospective | nr | 10 | 101 | TLM | Pre- and post-resection | nr |
| Csanády (30) | 2004 | FLI (5-ALA) | na | nr | T1-T2 | 13 | n/a | TLM | Pre- and post-resection | nr |
| Digonnet (31) | 2016 | FLI (ICG) | na | Prospective | T1-T4 | 3 | n/a | Laryngectomy | Pre- and post-resection | nr |

**Table 1.** Included articles. (continued)

| First author | Year | Imaging technique | Control group | Study design | T-stage | n = (imaging) | n = (control) | Surgical procedure | Application of imaging | Negative margin definition |
|---|---|---|---|---|---|---|---|---|---|---|
| Dedivitis (32) | 2009 | CE | na | Prospective | T1b-T2 | 10 | n/a | Open surgery | Pre-resection | ≥ 2 mm |
| Stefanescu (33) | 2016 | CE | na | nr | T1-T2 | 43 | n/a | TLM | Pre-resection | nr |
| Shakhov (34) | 2001 | OCT | na | nr | Tis-T2 | 26 | n/a | TLM | Pre-resection | nr |

*NBI = narrow-band imaging; AF = autofluorescence; FLI = fluorescence imaging; 5-ALA = 5-aminolevulinic acid; ICG = indocyanine green; CE = contact endoscopy; OCT = optical coherence tomography; WL = white light; TLE = total laryngectomy; TLM = transoral laser microsurgery; na = not applicable; nr = not reported. 1 The patients served as their own controls: first the regular treatment was performed, followed by extra imaging. Based on extra imaging, extra resection was done. 2 Historical control group. 3 T-stage was not specified, but article text indicates that only patients with advanced cancer treated by laryngectomy were included. 4 For NBI, the separate outcomes are further described and compared in Table 2.*

Beyond the diagnostic phase, NBI holds a lot of promise for achieving more accurate margin delineation during TLM for early glottis cancer (Table 2, 3) (41). It has been re-ported that NBI was able to, statistically, significantly reduce (3,18,19,23,25), or completely prevent, the occurrence of positive superficial margins (20,21). Overall, two studies re-ported the detection of additional lesions that were not seen with WL alone (20,21). Additionally, four studies show significantly lower recurrence rates and better recurrence-free survival (RFS) with NBI as compared to WL alone (3,20–22). The majority of studies conclude superiority of NBI over WL endoscopy in patients with early laryngeal cancer, with Klimza et al. suggesting that the added value of NBI is higher in T2 tumours, as compared to T1 tumours (20). Then, one study included 3 patients with advanced (T3–T4) cancer, without differentiating the results according to tumour stage (25). Despite the anatomical restraints present in the resection of advanced laryngeal tumours, Šifrer et al. reported a significantly higher rate of resection margins that were initially tumour negative in patients treated with NBI compared to their historical control group, comprising all patients previously operated by the same surgeon, before availability of NBI instrumentation (23). The proportion of patients with T3 or T4 stage tumours, however, was not specified. Piersala et al. evaluated intraoperative NBI in patients with T2–T3 cancer, successfully achieving more accurate superficial resection margins (21). Finally, Zwakenberg et al. recently re-ported that they were able to identify tumour extent by an increase of 5.7% with NBI com-pared to WL (P = 0.02) (26). Nonetheless, these findings were not biopsy confirmed. Additionally, while this study reported inclusion of patients with Tcis-T4 tumours, the proportions were left unspecified and outcomes were not correlated with the tumour stage.

Overall, NBI was found to modify intraoperative decision-making in several ways: better visualization of tumour borders led to more secure resection margins, detection of additional lesions prompted additional biopsies, and NBI-led upstaging resulted in changes to the surgical plan (24). With its established position in current clinical practice for early diagnosis of laryngeal cancer, NBI is the most prominently featured modality in research of optical modalities for intraoperative margin detection. An important benefit of NBI is that it is not a labelling technique requiring exogenous agents, therefore side effects or complications are of no concern, nor does it require laborious agent development. Nevertheless, NBI is specifically suited to identification of superficial carcinomas due to their aberrant vascular pattern, thus limited to detection of mucosal margins (8, 42).

■ **Table 2.** Narrow-band imaging (NBI) trial data.

| Article | T-stage | n = (NBI/ WL ) | Negative margin rate[1] NBI (vs. WL) | Patient-related outcome NBI (vs. WL) | Diagnostic outcome NBI (vs. WL) | Other findings related to NBI |
|---|---|---|---|---|---|---|
| Fiz (3) | Tis-T2 | 311/323 | 50% (30%) | RFS: 83.9% (78.9%) DSS: 98.7% (98.8%) | nr | nr |
| Garofolo (18) | Tis-T1a | 82/152 | 96.4% (76.3%) | nr | nr | nr |
| Hainarosie (19) | nr | 23/23 | 98% (58.8%) | nr | nr | nr |
| Klimza (20) | T1-T2 | 44/na | 100% | Local recurrence: 3/44 (6.8%) | nr | Additional lesions not seen with WL |
| Piersiala (21) | T2-T3 | 98/na | 100% | Local recurrence: 5/98 (5%) | NBI+WL: Sens: 100% Spec: 98.88% PPV: 90% NPV: 100% Accuracy: 98.98% | Additional lesions not seen with WL in 10.2% of patients |
| Plaat (22) | Tis-T2 | 42/51 | nr | Local recurrence: 2% (24%) Two-year RFS: 98% (82%) | nr | nr |
| Šifrer (23) | T3-T4 | 14-aug | 88.9% (70.9%) | nr | NPV: 95.9% (88.4%) | nr |
| Srivastava (24) | Tis-T2 | 30/na | nr | nr | nr | Upstaging TNM class |
| Vicini (25) | T1-T4 | 7-apr | 87.9% (57.9%) | nr | Sens: 72.5% Spec: 66.7% NPV: 87.9% | nr |
| Zwakenberg (26) | Tis-T4 | 89/89 | nr | nr | Sens: 95% Spec: 82% PPV: 87% NPV: 92% Accuracy: 89% | 5.7% increase in identified tumour extent with NBI compared to WL (P = 0.02) |

[1] *Percentage of negative resection margins obtained with NBI (vs. with WL). Abbreviations: nr = not reported; na = not applicable; WL = white light; NBI = narrow-band imaging; RFS = recurrence-free survival; DSS = disease-specific survival; Sens = sensitivity; Spec = specificity; PPV = positive predictive value; NPV = negative predictive value.*

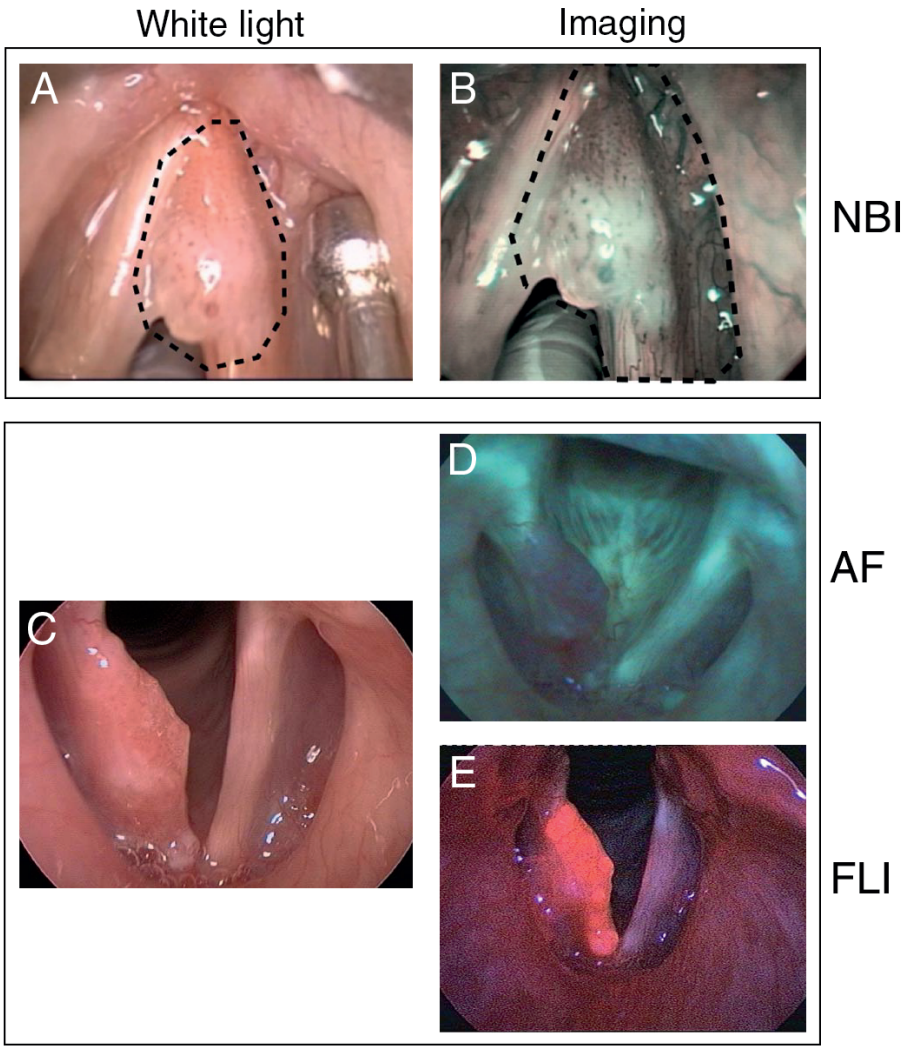


■ **Figure 2.** Clinical examples of fluorescence-based imaging modalities in laryngeal cancer.
*(A) White light image of cT1a laryngeal squamous cell carcinoma of the anterior third of the right vocal fold and its presumptive resection margins (dotted line) compared to (B) Narrow-Band Imaging (NBI), showing thick dark spots typically associated with carcinoma in situ. The planned superficial resection margins of type II cordectomy (A) were extended on the basis thereof (B). (C) White-light laryngoscopy demonstrating a bulging small squamous cell carcinoma of the right vocal fold with extension from the anterior commissure to the vocal process. (D) Autofluorescence (AF) laryngoscopy shows a reddish-violet fluorescence of the cancerous right vocal fold and green fluorescence of the normal mucosa. (E) Protoporphyrin IX accumulates in the cancerous tissue demonstrating a bright orange-red fluorescence signal during indirect laryngoscopy. A and B are adapted and reproduced from Garofolo et al. (18), by permission of SAGE Publications, Inc. C–E are adapted and reproduced from Arens et al. (43), by permission of Springer Nature.*

## INTRAOPERATIVE AUTOFLUORESCENCE IMAGING

Autofluorescence (AF) is the natural fluorescence emission of tissue when exposed to light of a suitable wavelength (Table 3). AF is based on the common presence of intrinsic biomolecules acting as endogenous fluorophores (44). Upon illumination, the electrons of a fluorophore are elevated to a higher energy level. The fluorophore is unstable in this ex-cited state, and will rapidly revert to a slightly lower, more stable energy level by expelling heat. With some of the energy already released, the emitted light has a longer wavelength and is of lower energy than that of the illuminating light (15).

The fundamental principle of AF is related to changes in tissue morphology, optical properties, and the concentration of endogenous fluorophores in tissue as a result of neoplasia. When exposed to blue light, healthy laryngeal mucosa emits green fluorescence, whereas neoplastic mucosa fluoresces red-violet (Figure 1B, 2C–D). The advantage of AF over conventional WL endoscopy stems from the fact that (pre)malignant lesions can be differentiated from normal tissue because of decreased AF (15,16,45). AF has previously been widely evaluated for the early diagnosis of laryngeal cancer (46), demonstrating demarcation of tumour borders and high sensitivity compared to standard technique (97.5 vs. 82.5%) (47).

In total, three clinical studies evaluate the intraoperative benefit of AF for margin assessment. Succo et al. reported high sensitivity and specificity (96.8 and 98.5%), stating an improvement in diagnostic accuracy over WL alone in 12 out of 73 cases (16.4%) (29). Paczona et al. performed a more extensive excision based on AF in 2 of 10 cases, and re-ported a sensitivity and specificity of 97.4 and 60%, respectively (28). In 2006, Fielding et al. reported the finding of additional malignant lesions in 5 out of 48 patients with laryngeal cancer, noting that AF may have potential for detecting unknown primaries and limiting the amount of sites requiring biopsies (27).

These studies suggest that direct AF can have a positive impact on disease-free survival and local control. However, more substantive studies are warranted to examine the added benefit of AF for more discrete identification of tumour presence, or positive margin reduction. AF is limited to examination of surface tissues. The illuminating light does not penetrate diseased epithelium, so that neoplastic changes within the basal mucosal layer may be hidden by epithelial hyperkeratosis. The presence of necrosis, scar tissue, bleeding, and inflammation can alter mucosal fluorescence in an unpredictable manner (15).

### Intraoperative Fluorescence Imaging

Fluorescence Imaging (FLI) is an emerging optical modality that facilitates intraoperative guidance aimed at complete resection of tumour tissue (48). After systemic administration of

a fluorescent agent and an appropriate dispersion time interval, FLI is per-formed real-time using an intraoperative camera system (Figure 1C, 2C, E).

The application of FLI for intraoperative margin detection in laryngeal cancers is thus far underexplored. A 2004 trial reported a sensitivity of 96% for 5-aminolevulinic ac-id-induced protoporphyrin-IX (5-ALA Pp-IX) fluorescence in the control of pharyngo-laryngeal cancer (30). In this study including 13 patients with T1–T2 laryngeal cancer, Pp-IX fluorescence better visualized the borderline of superficial neoplastic tissue, facilitating more precise diagnosis and excision.



The attenuating effects of light scattering, non-specific autofluorescence and absorption are relatively low for fluorescence in the near-infrared (NIR) range (49). In a study on the use of intravenous administration of NIR agent indocyanine green (ICG) for therapeutic lymph node dissection, Digonnet et al. briefly described primary tumour examination 3 patients with laryngeal cancer, reporting a fluorescent signal in 2 patients (31). FLI with tumour-specific NIR fluorescent agents has not yet been investigated in laryngeal cancer (Table 3).

### Contact Endoscopy

Contact endoscopy (CE) is a technique that allows for in vivo visualization in cellular detail. After staining superficial cells of the mucosa with methylene blue, a microscopic endoscope is placed in direct contact with the surface, providing images of the suspected area at x60 or x150 magnification (Figure 3A–B, Table 3). Contact laryngomicroscopy is a non-invasive method capable of obtaining detailed information of cells and blood vessels in the live epithelium without biopsy, distinguishing malignant from benign tissue. CE has been shown to detect post-radiotherapy residual and recurrent cancer in the upper aerodigestive tract with similar sensitivity and specificity compared to in non-irradiated tissues (50).

CE has been studied for the detection of microscopic margins during surgery in 10 patients with early glottic SCC, yielding histopathologically confirmed complete excision (negative margins defined as ≥ 2 mm) by Dedivitis et al., without local recurrence after a minimum follow-up period of 5 years (32). This survival benefit in early laryngeal cancer patients is promising, but needs confirmation from larger scale, adequately powered studies. A more recent study in 43 patients with T1–T2 vocal fold carcinoma finds a similar, if slightly lower, negative resection rate for CE compared to frozen sections after histopathological examination of paraffin sections: 92 vs. 98.3% (33). While these results are indicative of its reliability for early laryngeal cancer, studies including patients with advanced laryngeal lesions are absent. Additionally, CE requires topical staining and is associated with considerable instrumentation costs, requires a steep learning curve for the interpretation of the vascular network, and is solely capable of characterizing the superficial layers of the mucosa (51).

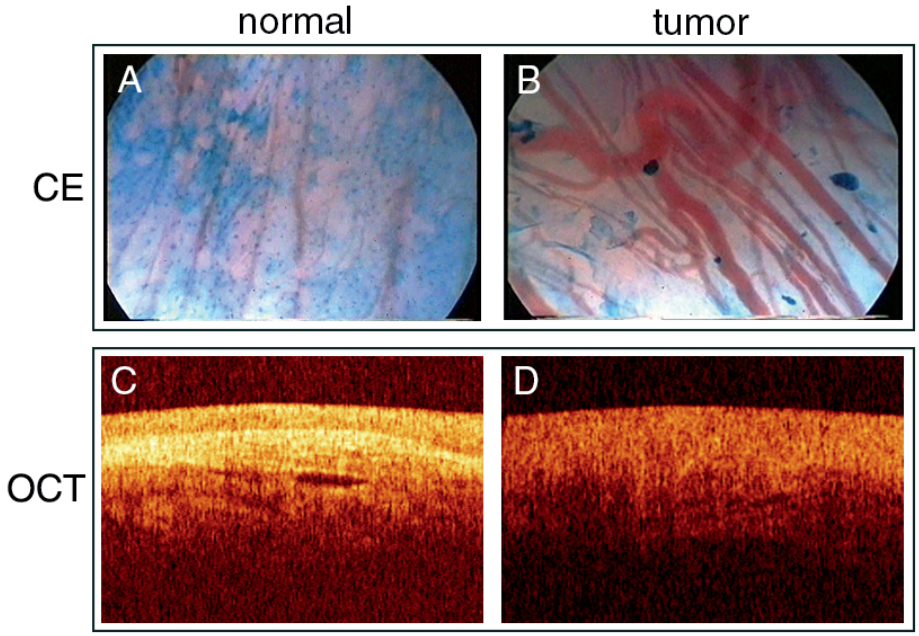


■ **Figure 3.** Clinical examples of contact endoscopy (CE) and optical coherence tomography (OCT) in laryngeal cancer.
*(A) Normal vascular network of the vocal fold in CE. (B) Vascular network of the vocal fold carcinoma in CE. (C) OCT image of healthy portion of larynx. (D) OCT image of exophytic tumour of larynx. A and B were adapted and reproduced from Stefanescu et al. (CC BY 4.0) (33). C and D were adapted and reproduced from Sergeev et al. (CC BY 4.0) (52).*

■ **Table 3.** Working principles and clinical usability of all imaging techniques for intraoperative margin assessment in laryngeal cancer.

| Imaging Technique | Working principle | Clinical usability for intraoperative margin assessment: pros (+) and cons (-) |
|---|---|---|
| **Narrow-band Imaging (NBI)** | NBI uses blue (415 nm) and green (540 nm) light corresponding with the main peak absorbance of hemoglobin, to enhance visibility of mucosal and submucosal capillaries, respectively. | + widely studied + provides real-time information<br>+ does not require exogenous agents<br>+ can be used to scan large surfaces for occult tumours<br>+ suitable for mucosal margin delineation (pre-resection)<br><br>- not suitable for deep margin assessment |

| Imaging Technique | Working principle | Clinical usability for intraoperative margin assessment: pros (+) and cons (-) |
|---|---|---|
| **Autofluorescence (AF)** | AF detects changes in tissue morphology and optical properties as a result of neoplasia. Using blue light, AF can differentiate between healthy and neoplastic laryngeal mucosa. | + provides real-time information<br>+ does not require exogenous agents<br>+ can be used to scan large surfaces for occult tumours<br><br>- not suitable for deep margin assessment |
| **Fluorescence Imaging (FLI)** | FLI uses a systemically administered fluorescent agent that 'targets' tumour cells over healthy cells. A dedicated camera system is required to detect these fluorescent agents, facilitating real-time image-guided surgery. | + suitable for deep margin assessment (i.e., wound bed inspection)<br>+ provides real-time information<br>+ can be used to scan large surfaces for occult tumours<br>+ Near-infrared (NIR) FLI has high penetration depth (up to 10 mm)<br><br>- requires administration of fluorescent agents<br>- tumour-specific fluorescent agents have not been studied in laryngeal cancer yet |
| **Contact Endoscopy (CE)** | After staining of superficial mucosal cells with methylene blue, a microscopic endoscope is placed in direct contact with the surface, distinguishing tumour from healthy cells in vivo. | + suitable to detect residual or recurrent cancer after radiotherapy<br><br>- not suitable for deep margin assessment<br>- requires topical staining<br>- requires direct tissue contact<br>- steep learning curve for image interpretation |
| **Optical Coherence Tomography (OCT)** | OCT is based on changes in refractive index of tumour cells, by detecting light that is backscattered off tissue boundaries. It is thus capable of imaging cross-sectional anatomy at high resolution in living tissue. | + provides real-time information<br>+ does not require exogenous agents<br><br>- maximum penetration depth of ~2 mm<br>- requires direct tissue contact |
| **Raman Spectroscopy (RS)** | RS uses spectral differences between normal and malignant tissue, and is capable of near-instant, accurate and non-invasive analysis of a tissue's molecular composition. | + able to characterize tissues other than mucosa<br>+ suitable for deep margin assessment<br>+ high specificity<br>+ does not require exogenous agents<br><br>- limited to point measurements<br>- requires direct tissue contact<br>- does not provide real-time information (although near-instant)<br>- Intraoperative RS for margin assessment in laryngeal cancer has not been studied yet |

### Optical Coherence Tomography

Optical coherence tomography (OCT) is the optical counterpart of ultrasound, and is capable of imaging cross-sectional anatomy at high resolutions in living tissue (Figure 3C–D, Table 3). OCT is based on changes in refractive index, by detecting light that is backscattered off tissue boundaries (15). It is a noninvasive imaging method that allows in vivo use, provides real time information, and does not cause any side effects.

OCT has only been studied for intraoperative margin assessment during TLM by Shakhov et al. in 26 patients with early laryngeal carcinoma (34). While they reported tumour margins extending beyond those seen with WL alone, no data were provided on diagnostic accuracy.

## DISCUSSION

There is a paucity of trials that analyze intraoperative imaging as a surgical adjunct during procedures for laryngeal cancer. The diagnostic value of NBI and AF in early laryngeal cancer is known. Their intraoperative application as an aid in defining surgical margins has not yet been studied as extensively, with most data available on NBI in this setting. As NBI visualization is limited to microvascular changes of the (sub)mucosa, evaluation of deep margin infiltration is impossible. Nevertheless, some recent studies report encouraging results of intraoperative NBI in patients with moderate-advanced laryngeal tumours. Distinct from intraoperative margin assessment, an interesting application for NBI is the follow-up of patients with early to moderate stage glottic cancer after curative treatment. Witkiewicz et al. recently reported that NBI after TLM is a good predictor of margin positivity, supporting clinical decision-making regarding the need for second-look surgery (53). NBI during outpatient transnasal endoscopy was found to be an excellent follow-up tool of laryngeal cancer patients after radiotherapy to screen for recurrent dis-ease (54). Still, caution is warranted in the interpretation of NBI images. Post-radiotherapy nonspecific inflammation often presents as brownish spots similar to those that are typical for early cancer, and may thus be mistaken for recurrence (39,55). More clinical studies are required to make conclusive statements about NBI for TLM of moderate-advanced laryngeal tumours. AF has been demonstrated to be useful in early laryngeal cancer detection, although intrinsic mucosal fluorescence can unpredictably be altered by numerous tissue properties (15).

Both OCT and CE are associated with various technical impracticalities. CE requires topical staining and is only able to clearly image the superficial layers of the epithelium (45). Previous *ex vivo* and probe-based in vivo diagnostic efforts using OCT for laryngeal cancer have demonstrated the technique's performance in distinguishing normal from cancerous tissue (52,56–59). Nevertheless, its maximum penetration depth of ~2 mm restricts its use to peripheral margin assessment. This inherent limited applicability likely explains the apparent

shortage of studies using AF, OCT, and CE for intraoperative mar-gin assessment in the larynx. This systematic evaluation of imaging techniques for intraoperative margin assessment reveals a prevailing incompatibility of the studied modalities in their utility for advanced stage laryngeal cancer, primarily attributable to imaging depth limitations. Furthermore, our assessment based on the MINORS criteria has revealed that the methodology and scientific evidence of a sizable portion of included studies are of suboptimal quality (Table S1). In view of this apparent research gap, it may be useful to investigate other, more widely applicable imaging techniques to improve surgical resection of both early and advanced laryngeal cancer.



Although only 2 studies employing FLI for margin assessment were identified, laryngeal cancer surgery might be amenable to the more prevailing developments in FLI. An important advantage of FLI is that it can be used to scan large surfaces. In addition to the possibility to image fluorescence at considerable depths and tissues other than the mucosa, FLI is thus ideally suited for wound bed inspection and detection of clinically occult lesions. An interesting area to explore for FLI would be to identify suitable tumour-specific tracers for intraoperative imaging of early to advanced laryngeal cancer (60). Previous re-search on the diagnostic value of FLI for laryngeal cancer is scarce, and, thus far, only features 5-ALA and ICG (46,61,62). While these agents are easily available and approved by the U.S. Food and Drug Administration (FDA), they are both nonspecific. Furthermore, 5-ALA-induced Pp-IX fluorescence is outside the NIR-range, such that the signal is prone to significant interference due to the tissue's optical characteristics (30). The compatibility of FLI with CO2 laser surgery in head and neck cancer was recently validated by Odenthal and colleagues (63). In vitro and preclinical results from this study suggest the effective-ness of fluorescence-guided surgery (FGS) using NIR dyes. Moreover, they demonstrated that laser cauterization and its associated autofluorescence are unlikely to interfere with the fluorescence signal of the injected tumour-specific tracer. Additionally, FLI for intraoperative margin assessment in head and neck cancers is currently a prolific field of research, with numerous phase I/II trials on oral cancer completed and ongoing (Figure 4) (64–67). Oral cancer is well-suited to FGS, as the oral cavity is easily accessible to the NIR camera. However, with the rapidly evolving FLI cameras it is only a matter of time before FGS can be adopted to treat a wider variety of cancers. This notwithstanding, tumour-specific FLI is still under development and not without pitfalls. Signal processing for FLI is complex, and objective evaluation and quantification of both fluorescence and its influencing factors is challenging (49). Development of suitable fluorescent agents is costly and time-consuming, with a lot of work left before regulatory approval and clinical implementation can be realized. Altogether, yet undiscovered potential for FLI in laryngeal cancer surgery at all stages is strongly hinted at, encouraging dedicated research for this indication.

As per the confines of this systematic review, there currently is no real-time application for Raman spectroscopy (RS) in margin assessment of laryngeal cancer. However, its demonstrated potential for both in and *ex vivo* tissue discrimination is worth noting. RS is a technique based on spectral differences between normal and malignant tissue, and is capable of near-instant, accurate, and non-invasive analysis of a tissue's molecular com-position (Table 3). In oral cancer specimen, water concentration analysis with RS has been demonstrated to objectively localize tumour borders (68). The capacity of RS to differentiate tumour from healthy cells has been thoroughly demonstrated using laryngeal tissue samples, producing significant differences in Raman spectra between malignant and normal tissue (69–72). Bergholt et al. were the first to demonstrate the feasibility of RS in transnasal endoscopic applications (73). In their 2012 study, they acquired near-instant information of the endogenous biomolecular tissue composition from the larynx in healthy subjects, using a fiber-optic Raman probe. In 2016, Lin et al. conducted a similar study for in vivo probe-based RS during endoscopic examination, reporting improved diagnosis (74). In a recent study of Stimulated Raman Scattering (SRS), Zhang et al. demonstrate the efficacy of deep-learning based SRS microscopy for margin assessment through simulated resection margins on completely removed larynx specimen (75). Contrary to NBI and AF, RS is able to characterize tissue other than the mucosa. This is an important advantage allowing for post-resection assessment of tumour extension in the deep plane (8). Nonetheless, RS is limited to point measurements, requiring direct tissue contact. As wide-field imaging is impossible, RS cannot be employed to screen for occult lesions and second primary tumours, and resection guidance and complete wound bed inspection are not currently feasible. The strength of RS lies in its application for specimen-driven margin assessment, at uniquely high specificity.

## Conclusions

The demonstrated effectiveness of NBI in the early diagnosis has led to reasonable evidence for its application in intraoperative margin detection, although inclusion of patients with T3–T4 laryngeal cancer is rare. An important disadvantage remains the technique's intrinsic inability to image structures other than the (sub-)mucosa. Similar limitations hold for AF, OCT, and CE. Finally, FLI has scarcely been studied for intraoperative margin assessment in laryngeal cancer. Indeed, one might need to consider optical imaging advancements in adjacent anatomical regions and similar applications to gain insight into which modalities warrant further exploration in achieving adequate margins. NIR FLI with tumour-specific fluorescent agents and RS are emerging technologies that overcome many of the limitations associated with NBI, AF, CE, and OCT. With evidence supporting their value in assessing tumour depth infiltration, we believe it is worthwhile to pursue their clinical development for margin assessment in laryngeal cancer.

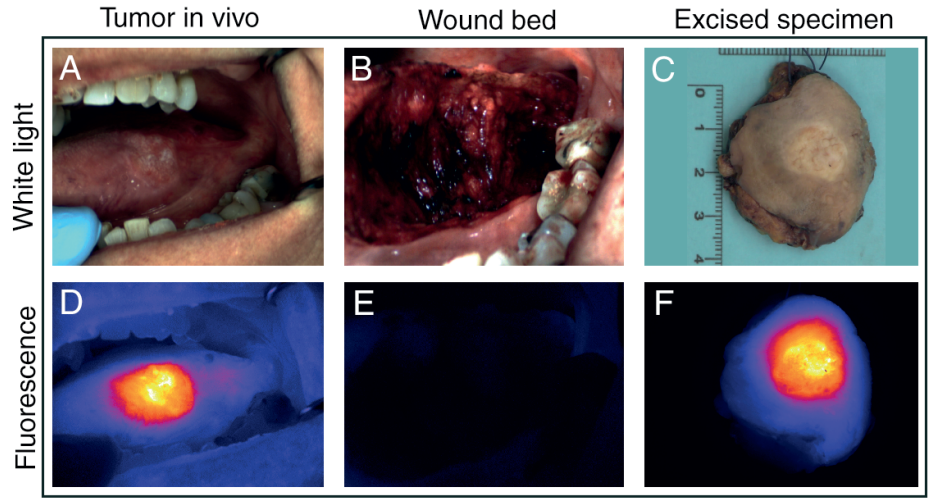


■ **Figure 4.** Fluorescence imaging using pH-activatable nanoprobe ONM-100 in head and neck squamous cell carcinoma of the tongue.
*In vivo (A,B,D,E) and ex vivo (C,F) visualization of high fluorescence signal in the tumour and low fluorescence signal in tumour-free margin and wound bed. Adapted and reproduced from Voskuil et al. (CC BY 4.0) (67).*

## Acknowledgments

The authors wish to thank S. Meertens-Gunput from the Medical Library of the Erasmus Medical Center for developing and updating the search strategies.

## REFERENCES


1. Bray, F.; Ferlay, J.; Soerjomataram, I.; Siegel, R.L.; Torre, L.A.; Jemal, A. Global cancer statistics 2018: GLOBOCAN estimates of incidence and mortality worldwide for 36 cancers in 185 countries. CA Cancer J. Clin. 2018, 68, 394–424.
2. Obid, R.; Redlich, M.; Tomeh, C. The Treatment of Laryngeal Cancer. Oral Maxillofac. Surg. Clin. North Am. 2019, 31, 1–11, doi:10.1016/j.coms.2018.09.001.
3. Fiz, I.; Mazzola, F.; Fiz, F.; Marchi, F.; Filauro, M.; Paderno, A.; Parrinello, G.; Piazza, C.; Peretti, G. Impact of Close and Positive Margins in Transoral Laser Microsurgery for Tis–T2 Glottic Cancer. Front. Oncol. 2017, 7, 245, doi:10.3389/fonc.2017.00245.
4. Brandstorp-Boesen, J.; Falk, R.S.; Evensen, J.F.; Boysen, M.; Brøndbo, K. Risk of Recurrence in Laryngeal Cancer. PLOS ONE 2016, 11, e0164068, doi:10.1371/journal.pone.0164068.
5. Tassone, P.; Savard, C.; Topf, M.C.; Keane, W.; Luginbuhl, A.; Curry, J.; Cognetti, D. Association of Positive Initial Margins With Survival Among Patients With Squamous Cell Carcinoma Treated With Total Laryngectomy. JAMA Otolaryngol. Neck Surg. 2018, 144, 1030, doi:10.1001/jamaoto.2018.1095.
6. Zhu, X.; Heng, Y.; Zhou, L.; Tao, L.; Zhang, M. A prognostic nomogram for predicting risk of recurrence in laryngeal squa-mous cell carcinoma patients after tumour resection to assist decision making for postoperative adjuvant treatment. J. Surg. Oncol. 2019, 120, 698–706, doi:10.1002/jso.25614.
7. Saraniti, C.; Speciale, R.; Gallina, S.; Salvago, P. Prognostic role of resection margin in open oncologic laryngeal surgery: survival analysis of a cohort of 139 patients affected by squamous cell carcinoma. Braz. J. Otorhinolaryngol. 2019, 85, 603–610, doi:10.1016/j.bjorl.2018.04.012.
8. Sjögren, E. Transoral Laser Microsurgery in Early Glottic Lesions. Curr. Otorhinolaryngol. Rep. 2017, 5, 56-68, doi:10.1007/s40136-017-0148-2.
9. Chiesa-Estomba, C.M.; González-García, J.A.; Larruscain, E.; Calvo-Henríquez, C.; Mayo-Yáñez, M.; A Sistiaga-Suarez, J.; Sistiaga-Suarez, J. CO2 Transoral Laser Microsurgery in Benign, Premalignant and Malignant (Tis, T1, T2) Lesion of the Glottis. A Literature Review. Med. 2019, 6, 77, doi:10.3390/medicines6030077.
10. Michel, J.; Fakhry, N.; Duflo, S.; Lagier, A.; Mancini, J.; Dessi, P.; Giovanni, A. Prognostic value of the status of resection margins after endoscopic laser cordectomy for T1a glottic carcinoma. Eur. Ann. Otorhinolaryngol. Head Neck Dis. 2011, 128, 297–300, doi:10.1016/j.anorl.2011.05.006.
11. Fiz, I.; Koelmel, J.C.; Sittel, C. Nature and role of surgical margins in transoral laser microsurgery for early and intermedi-ate glottic cancer. Curr. Opin. Otolaryngol. Head Neck Surg. 2018, 26, 78–83, doi:10.1097/moo.0000000000000446.
12. Hendriksma, M.; Montagne, M.W.; Langeveld, T.P.M.; Veselic, M.; Van Benthem, P.P.G.; Sjögren, E.V. Evaluation of surgical margin status in patients with early glottic cancer (Tis-T2) treated with transoral CO2 laser microsurgery, on local control. Eur. Arch. Oto-Rhino-Laryngology 2018, 275, 2333-2340, doi:10.1007/s00405-018-5070-9.
13. Amit, M.; Na'Ara, S.; Leider-Trejo, L.; Akrish, S.; Cohen, J.T.; Billan, S.; Gil, Z. Improving the rate of negative margins after surgery for oral cavity squamous cell carcinoma: A prospective randomized controlled study. Head Neck 2016, 38, E1803–E1809, doi:10.1002/hed.24320.

**14.** Van Lanschot, C.G.; Mast, H.; Hardillo, J.A.; Monserez, D.; Hove, I.T.; Barroso, E.M.; Cals, F.L.; Smits, R.W.; Van Der Kamp, M.F.; Meeuwis, C.A.; et al. Relocation of inadequate resection margins in the wound bed during oral cavity oncological surgery: A feasibility study. Head Neck 2019, 41, 2159–2166, doi:10.1002/hed.25690.

**15.** Hughes, O.R.; Stone, N.; Kraft, M.; Arens, C.; Birchall, M.A.; Stone, N. Optical and molecular techniques to identify tumour margins within the larynx. Head Neck 2010, 32, 1544–1553, doi:10.1002/hed.21321.

**16.** Mannelli, G.; Cecconi, L.; Gallo, O. Laryngeal preneoplastic lesions and cancer: challenging diagnosis. Qualitative literature review and meta-analysis. Crit. Rev. Oncol. 2016, 106, 64–90, doi:10.1016/j.critrevonc.2016.07.004.

**17.** Slim, K.; Nini, E.; Forestier, D.; Kwiatkowski, F.; Panis, Y.; Chipponi, J. Methodological index for non-randomized studies (MINORS ): development and validation of a new instrument. ANZ J. Surg. 2003, 73, 712–716, doi:10.1046/j.1445-2197.2003.02748.x.

**18.** Garofolo, S.; Piazza, C.; Del Bon, F.; Mangili, S.; Guastini, L.; Mora, F.; Nicolai, P.; Peretti, G. Intraoperative Narrow Band Imaging Better Delineates Superficial Resection Margins During Transoral Laser Microsurgery for Early Glottic Cancer. Ann. Otol. Rhinol. Laryngol. 2014, 124, 294–298, doi:10.1177/0003489414556082.

**19.** Hainăroșie, R.; Anghelina, F.; Hainăroșie, M.; Pietroșanu, C.; Ioniță, I.; Rusescu, A.; Paduraru, D.N.; Ene, B.; Badiu, D.C.; Zainea, V. The utility of Narrow Band Imaging in obtaining disease free resection margins during endo-scopic surgery of the larynx. Romanian Biotechnol. Lett. 2019, 24, 360–365, doi:10.25083/rbl/24.2/360.365.

**20.** Klimza, H.; Jackowska, J.; Piazza, C.; Banaszewski, J.; Wierzbicka, M. The role of intraoperative narrow-band imaging in transoral laser microsurgery for early and moderately advanced glottic cancer. Braz. J. Otorhinolaryngol. 2019, 85, 228–236, doi:10.1016/j.bjorl.2018.01.004.

**21.** Piersiala, K.; Klimza, H.; Jackowska, J.; Majewska, A.; Wierzbicka, M. Narrow band imaging in transoral laser microsurgery (TLM) in moderately advanced (T2, T3) glottic cancer. Otolaryngol. Polska 2018, 72, 17–23, doi:10.5604/01.3001.0012.0486.

**22.** Plaat, B.E.C.; Zwakenberg, M.A.; Van Zwol, J.G.; Wedman, J.; Van Der Laan, B.F.A.M.; Halmos, G.B.; Dikkers, F.G. Nar-row-band imaging in transoral laser surgery for early glottic cancer in relation to clinical outcome. Head Neck 2017, 39, 1343–1348, doi:10.1002/hed.24773.

**23.** Šifrer, R.; Urbančič, J.; Strojan, P.; Aničin, A.; Žargi, M. The assessment of mucosal surgical margins in head and neck cancer surgery with narrow band imaging. Laryngoscope 2017, 127, 1577–1582, doi:10.1002/lary.26405.

**24.** Srivastava, R. Narrow band imaging during transoral laser surgery for premalignant and early malignant glottic lesions. J. Head Neck Physicians Surg. 2016, 4, 35, doi:10.4103/2347-8128.182849.

**25.** Vicini, C.; Montevecchi, F.; D'Agostino, G.; De Vito, A.; Meccariello, G. A novel approach emphasising intra-operative su-perficial margin enhancement of head-neck tumours with narrow-band imaging in transoral robotic surgery. Acta Otorhi-nolaryngol. Ital. 2015, 35, 157–161.

**26.** Zwakenberg, M.A.; Halmos, G.B.; Wedman, J.; Laan, B.F.A.M.V.D.; Plaat, B.E.C. Evaluating Laryngopharyngeal Tumour Ex-tension Using Narrow Band Imaging Versus Conventional White Light Imaging. Laryngoscope 2021, doi:10.1002/lary.29361.

**27.** Fielding, D.; Agnew, J.; Wright, D.; Hodge, R. DAFE autofluorescence assessment of oral cavity, larynx and bronchus in head and neck cancer patients. Photodiagnosis Photodyn. Ther. 2006, 3, 259–265, doi:10.1016/j.pdpdt.2006.07.004.

**28.** Paczona, R.; Marandas, P.; Luboinski, B. Autofluorescence videoendoscopy for photodiagnosis of head and neck squamous cell carcinoma. Eur. Arch. Oto-Rhino-Laryngology 2003, 260, 544–548, doi:10.1007/s00405-003-0635-6.

**29.** Succo, G.; Garofalo, P.; Fantini, M.; Monticone, V.; Abbona, G.; Crosetti, E. Direct autofluorescence during CO2 laser surgery of the larynx: can it really help the surgeon? Acta Otorhinolaryngol. Ital. 2014, 34, 174–183.

**30.** Czigner, J.; Csanády, M.; Kiss, J.G.; Ivan, L.; Jori, J. ALA (5-aminolevulinic acid)-induced protoporphyrin IX fluorescence in the endoscopic diagnostic and control of pharyngo-laryngeal cancer. Eur. Arch. Oto-Rhino-Laryngology 2003, 261, 262-266, doi:10.1007/s00405-003-0660-5.

**31.** Digonnet, A.; Van Kerckhove, S.; Moreau, M.; Willemse, E.; Quiriny, M.; Ahmed, B.; Aubain, N.D.S.; Andry, G.; Bourgeois, P. Near infrared fluorescent imaging after intravenous injection of indocyanine green during neck dissection in patients with head and neck cancer: A feasibility study. Head Neck 2015, 38, E1833–E1837, doi:10.1002/hed.24331.

**32.** Dedivitis, R.A.; Pfuetzenreiter Jr, E.G.; Guimaraes, A.V. Contact endoscopy of the larynx as an auxiliary method to the sur-gical margins in frontolateral laryngectomy. Acta Otorhinolaryngol Ital 2009, 29, 16–20.

**33.** Stefanescu, D.C.; Ceachir, O.; Zainea, V.; Hainarosie, M.; Pietrosanu, C.; Ionita, I.G.; Hainarosie, R. The Use of Methylene Blue in Assessing Disease Free Margins During CO2 LASER Assisted Direct Laryngoscopy for Glottis Cancer. Revista De Chimie 2016, 67, 1327-1328.

**34.** Shakhov, A.V.; Terentjeva, A.B.; Kamensky, V.A.; Snopova, L.B.; Gelikonov, V.M.; Feldchtein, F.I.; Sergeev, A.M. Optical coherence tomography monitoring for laser surgery of laryngeal carcinoma. J. Surg. Oncol. 2001, 77, 253–258, doi:10.1002/jso.1105.

**35.** Kraft, M.; Fostiropoulos, K.; Gürtler, N.; Arnoux, A.; Davaris, N.; Arens, C. Value of narrow band imaging in the early di-agnosis of laryngeal cancer. Head Neck 2015, 38, 15–20, doi:10.1002/hed.23838.

**36.** Popek, B.; Bojanowska-Poźniak, K.; Tomasik, B.; Fendler, W.; Jeruzal-Świątecka, J.; Pietruszewska, W. Clinical experience of narrow band imaging (NBI) usage in diagnosis of laryngeal lesions. Otolaryngol. Polska 2019, 73, 18–23, doi:10.5604/01.3001.0013.3401.

**37.** Bertino, G.; Cacciola, S.; Fernandes, W.B.; Fernandes, C.M.; Occhini, A.; Tinelli, C.; Benazzo, M. Effectiveness of narrow band imaging in the detection of premalignant and malignant lesions of the larynx: Validation of a new endoscopic clinical clas-sification. Head Neck 2014, 37, 215–222, doi:10.1002/hed.23582.

**38.** Ni, X.-G.; Zhang, Q.-Q.; Wang, G.-Q. Narrow band imaging versus autofluorescence imaging for head and neck squamous cell carcinoma detection: a prospective study. J. Laryngol. Otol. 2016, 130, 1001–1006, doi:10.1017/s0022215116009002.

**39.** Sikka, K.; Sakthivel, P.; Thakar, A.; A Singh, C.; Sharma, S.C.; Rajeshwari, M.; Kakkar, A. Role of narrow band imaging in the diagnosis of laryngeal lesions: Pilot study from India. Indian J. Cancer 2018, 55, 242–247, doi:10.4103/ijc.ijc_590_17.

**40.** Klimza, H.; Jackowska, J.; Wierzbicka, M. The usefulness of the NBI – narrow band imaging for the larynx assessment. Oto-laryngol. Polska 2018, 72, 1–5, doi:10.5604/01.3001.0011.7253.

**41.** Campo, F.; D'Aguanno, V.; Greco, A.; Ralli, M.; De Vincentiis, M. The Prognostic Value of Adding Narrow-Band Imaging in Transoral Laser Microsurgery for Early Glottic Cancer: A Review. Lasers Surg. Med. 2020, 52, 301–306, doi:10.1002/lsm.23142.

**42.** Robbins, K.T.; Triantafyllou, A.; Suárez, C.; López, F.; Hunt, J.L.; Strojan, P.; Williams, M.D.; Braakhuis, B.J.; De Bree, R.; Hinni, M.L.; et al. Surgical margins in head and neck cancer: Intra- and postoperative considerations. Auris Nasus Larynx 2019, 46, 10-17, doi:10.1016/j.anl.2018.08.011.

**43.** Arens, C.; Reußner, D.; Woenkhaus, J.; Leunig, A.; Betz, C.S.; Glanz, H. Indirect fluorescence laryngoscopy in the diagnosis of precancerous and cancerous laryngeal lesions. Eur. Arch. Oto-Rhino-Laryngology 2007, 264, 621-626, doi:10.1007/s00405-007-0251-y.

**44.** Croce, A.; Bottiroli, G. Autofluorescence spectroscopy and imaging: a tool for biomedical research and diagnosis. Eur. J. Histochem. 2014, 58, 2461, doi:10.4081/ejh.2014.2461.

**45.** Tibbetts, K.M.; Tan, M. Role of Advanced Laryngeal Imaging in Glottic Cancer. Otolaryngol. Clin. North Am. 2015, 48, 565–584, doi:10.1016/j.otc.2015.04.004.

**46.** Kraft, M.; Betz, C.S.; Leunig, A.; Arens, C. Value of fluorescence endoscopy for the early diagnosis of laryngeal cancer and its precursor lesions. Head Neck 2010, 33, 941–948, doi:10.1002/hed.21565.

**47.** Saetti, R.; Derosas, F.; Silvestrini, M.; Narne, S. Efficacy of autofluoroscence videoendoscopy in the diagnosis of laryngeal lesions. Acta Otorhinolaryngol. Ital. 2007, 27, 181–185.

**48.** Vahrmeijer, A.L.; Hutteman, M.; Van Der Vorst, J.R.; Van De Velde, C.J.H.; Frangioni, J.V. Image-guided cancer surgery using near-infrared fluorescence. Nat. Rev. Clin. Oncol. 2013, 10, 507–518, doi:10.1038/nrclinonc.2013.123.

**49.** Keereweer, S. (Stijn); Van Driel, P. (Pieter); Snoeks, T. (Thomas); Kerrebijn, J. (Jeroen); De Jong, R. (Robert J.B.; Vahrmeijer, A. (Alexander); Sterenborg, H.J.; Löwik, C. (Clemens) Optical Image-Guided Cancer Surgery: Challenges and Limitations. Clin. Cancer Res. 2013, 19, 3745-3754, doi:10.1158/1078-0432.ccr-12-3598.

**50.** Kumar, S.; Mishra, A.K.; Galagali, J.R.; Sethi, A.; Malik, A. Contact endoscopy for detection of residual or recurrent disease after radiotherapy for squamous cell carcinoma of the upper aerodigestive tract. J. Laryngol. Otol. 2020, 134, 344–349, doi:10.1017/s0022215120000651.

**51.** Mishra, A.; Sahai, K.; Singh, S.; Datta, R.; Nilakantan, A.; Sethi, A. Contact Endoscopy - A promising tool for evaluation of laryngeal mucosal lesions. J. Laryngol. Voice 2012, 2, 53, doi:10.4103/2230-9748.106978.

**52.** Sergeev, A.M.; Gelikonov, V.M.; Gelikonov, G.V.; I Feldchtein, F.; Kuranov, R.V.; Gladkova, N.D.; Shakhova, N.M.; Snopova, L.B.; Shakhov, A.V.; Kuznetzova, I.N.; et al. In vivo endoscopic OCT imaging of precancer and cancer states of human mu-cosa. Opt. Express 1997, 1, 432–440, doi:10.1364/oe.1.000432.

**53.** Witkiewicz, J.; Klimza, H.; Piersiala, K.; Jackowska, J.; Wierzbicka, M. The usefulness of the narrow band imaging (NBI) in decision-making process regarding second look procedure (SL) in laryngeal cancer follow-up after transoral laser micro-surgery. PLOS ONE 2020, 15, e0236623, doi:10.1371/journal.pone.0236623.

**54.** Zabrodsky, M.; Luke, P.; Lukesova, E.; Boucek, J.; Plzák, J. The Role of Narrow Band Imaging in the Detection of Recurrent Laryngeal and Hypopharyngeal Cancer after Curative Radiotherapy. BioMed Res. Int. 2014, 2014, 1–9, doi:10.1155/2014/175398.

**55.** Wang, W.-H.; Lin, Y.-C.; Chen, W.-C.; Chen, M.-F.; Chen, C.-C.; Lee, K.-F. Detection of Mucosal Recurrent Nasopharyngeal Carcinomas After Radiotherapy With Narrow-Band Imaging Endoscopy. Int. J. Radiat. Oncol. 2012, 83, 1213–1219, doi:10.1016/j.ijrobp.2011.09.034.

**56.** Bibas, A.; Podoleanu, A.; Cucu, R.; Bonmarin, M.; Dobre, G.; Ward, V.; Odell, E.; Boxer, A.; Gleeson, M.; Jackson, D. 3-D opti-cal coherence tomography of the laryngeal mucosa*. Clin. Otolaryngol. 2004, 29, 713–720, doi:10.1111/j.1365-2273.2004.00902.x.

**57.** Kraft, M.; Lüerssen, K.; Lubatschowski, H.; Glanz, H.; Arens, C. Technique of Optical Coherence Tomography of the Larynx During Microlaryngoscopy. Laryngoscope 2007, 117, 950-952, doi:10.1097/mlg.0b013e318038166d.

**58.** Burns, J.A. Optical coherence tomography. Curr. Opin. Otolaryngol. Head Neck Surg. 2012, 20, 477–481, doi:10.1097/moo.0b013e3283582d7d.

**59.** Englhard, A.S.; Betz, T.; Volgger, V.; Lankenau, E.; Ledderose, G.J.; Stepp, H.; Homann, C.; Betz, C.S. Intraoperative assess-ment of laryngeal pathologies with optical coherence tomography integrated into a surgical microscope. Lasers Surg. Med. 2017, 49, 490–497, doi:10.1002/lsm.22632.

**60.** Odenthal, J.; Rijpkema, M.; Bos, D.; Wagena, E.; Croes, H.; Grenman, R.; Boerman, O.; Takes, R.; Friedl, P. Targeting CD44v6 for fluorescence-guided surgery in head and neck squamous cell carcinoma. Sci. Rep. 2018, 8, 1–11, doi:10.1038/s41598-018-28059-9.

**61.** Schmidt, F.; Dittberner, A.; Koscielny, S.; Petersen, I.; Guntinas-Lichius, O. Feasibility of real-time near-infrared indocyanine green fluorescence endoscopy for the evaluation of mucosal head and neck lesions. Head Neck 2016, 39, 234–240, doi:10.1002/hed.24570.

**62.** Mehlmann, M.; Stepp, H.; Baumgartner, R.; Betz, C.; Grevers, G.; Leunig, A.; Arbogast, S. Fluorescence staining of laryngeal neoplasms following topical application of 5-aminolevulinic acid: preliminary results#. Biomedical Optics 1999, 25, 414–420,, doi:10.1364/bio.1999.ctue1.

**63.** Odenthal, J.; Friedl, P.; Takes, R.P. Compatibility of CO 2 laser surgery and fluorescence detection in head and neck cancer cells. Head Neck 2019, 41, 1253–1259, doi:10.1002/hed.25547.

**64.** Moore, L.S.; Rosenthal, E.L.; Chung, T.K.; De Boer, E.; Patel, N.; Prince, A.C.; Korb, M.L.; Walsh, E.M.; Young, E.S.; Stevens, T.M.; et al. Characterizing the Utility and Limitations of Repurposing an Open-Field Optical Imaging Device for Fluores-cence-Guided Surgery in Head and Neck Cancer Patients. J. Nucl. Med. 2016, 58, 246–251, doi:10.2967/jnumed.115.171413.

**65.** Nishio, N.; Berg, N.S.V.D.; van Keulen, S.; Martin, B.A.; Fakurnejad, S.; Zhou, Q.; Lu, G.; Chirita, S.U.; Kaplan, M.J.; Divi, V.; et al. Optimal Dosing Strategy for Fluorescence-Guided Surgery with Panitumumab-IRDye800CW in Head and Neck Can-cer. Mol. Imaging Biol. 2020, 22, 156–164, doi:10.1007/s11307-019-01358-x.

**66.** Rosenthal, E.L.; Warram, J.M.; De Boer, E.; Chung, T.K.; Korb, M.L.; Brandwein-Gensler, M.; Strong, T.V.; Schmalbach, C.E.; Morlandt, A.B.; Agarwal, G.; et al. Safety and Tumour Specificity of Cetuximab-IRDye800 for Surgical Navigation in Head and Neck Cancer. Clin. Cancer Res. 2015, 21, 3658–3666, doi:10.1158/1078-0432.ccr-14-3284.

**67.** Voskuil, F.J.; De Jongh, S.J.; Hooghiemstra, W.T.R.; Linssen, M.D.; Steinkamp, P.J.; De Visscher, S.A.H.J.; Schepman, K.-P.; Elias, S.G.; Meersma, G.-J.; Jonker, P.K.C.; et al. Fluorescence-guided

imaging for resection margin evaluation in head and neck cancer patients using cetuximab-800CW: A quantitative dose-escalation study. Theranostics 2020, 10, 3994–4005, doi:10.7150/thno.43227.

**68.** Barroso, E.M.; Smits, R.W.; Van Lanschot, C.G.; Caspers, P.J.; Hove, I.T.; Mast, H.; Sewnaik, A.; Hardillo, J.A.; Meeuwis, C.A.; Verdijk, R.; et al. Water Concentration Analysis by Raman Spectroscopy to Determine the Location of the Tumour Border in Oral Cancer Surgery. Cancer Res. 2016, 76, 5945–5953, doi:10.1158/0008-5472.can-16-1227.

**69.** Lau, D.P.; Huang, Z.; Lui, H.; Anderson, D.W.; Berean, K.; Morrison, M.D.; Shen, L.; Zeng, H. Raman spectroscopy for optical diagnosis in the larynx: Preliminary findings. Lasers Surg. Med. 2005, 37, 192–200, doi:10.1002/lsm.20226.

**70.** Pujary, P.; Maheedhar, K.; C, M.K.; Pujary, K. Raman Spectroscopic Methods for Classification of Normal and Malignant Hypopharyngeal Tissues: An Exploratory Study. Pathol. Res. Int. 2011, 2011, 1–9, doi:10.4061/2011/632493.

**71.** Teh, S.K.; Zheng, W.; Lau, D.P.; Huang, Z. Spectroscopic diagnosis of laryngeal carcinoma using near-infrared Raman spec-troscopy and random recursive partitioning ensemble techniques. Anal. 2009, 134, 1232–1239, doi:10.1039/b811008e.

**72.** Stone, N.; Stavroulaki, P.; Kendall, C.; Birchall, M.; Barr, H. Raman Spectroscopy for Early Detection of Laryngeal Malignancy: Preliminary Results. Laryngoscope 2000, 110, 1756–1763, doi:10.1097/00005537-200010000-00037.

**73.** Bergholt, M.S.; Lin, K.; Zheng, W.; Lau, D.P.; Huang, Z. In vivo, real-time, transnasal, image-guided Raman endoscopy: defining spectral properties in the nasopharynx and larynx. J. Biomed. Opt. 2012, 17, 077002, doi: 10.1117/1.JBO.17.7.077002.

**74.** Lin, K.; Zheng, W.; Lim, C.M.; Huang, Z. Real-time in vivo diagnosis of laryngeal carcinoma with rapid fiber-optic Raman spectroscopy. Biomed. Opt. Express 2016, 7, 3705–3715, doi:10.1364/boe.7.003705.

**75.** Zhang, L.; Wu, Y.; Zheng, B.; Su, L.; Chen, Y.; Ma, S.; Hu, Q.; Zou, X.; Yao, L.; Yang, Y.; et al. Rapid histology of laryngeal squamous cell carcinoma with deep-learning based stimulated Raman scattering microscopy. Theranostics 2019, 9, 2541–2554, doi:10.7150/thno.32655.

## SUPPLEMENTARIES

**Supplementary 1** - Search Strategy

| Database | Full search strategy |
|---|---|
| **Embase (2146 references)** | ('epiglottis tumour'/exp OR 'larynx tumour'/exp OR 'larynx'/exp OR (((epiglott* OR larynx* OR microlaryng* OR laryng* OR glott* OR postcricoid* OR subglot* OR supraglot* OR vocal-cord*) NEAR/6 (cancer* OR carcinoma* OR tumour* OR tumour* OR neoplas* OR papilloma* OR granuloma* OR lesion* OR malignan* OR premalignan* OR leukoplak* OR dysplas* OR surg* OR operat*))):ab,ti,kw) AND ('narrow band imaging'/de OR 'autofluorescence'/de OR 'Raman spectrometry'/de OR 'coherent anti Stokes Raman spectroscopy'/de OR 'fluorescence'/de OR 'confocal microscopy'/exp OR 'fluorescent dye'/de OR 'white light'/de OR (((narrowband* OR narrow-band*) NEAR/3 (imag*)) OR autofluorescence* OR auto-fluorescence* OR intrinsic-fluorescence* OR native-fluorescence* OR ((fluorescen* OR imag*) NEAR/3 guided) OR ((light* OR optical* OR molecular*) NEAR/3 (imag*)) OR near-infrared OR tracer* OR target* OR dye* OR probe* OR raman* OR confocal* OR ((contact*) NEAR/3 (endomicroscop* OR microscop* OR endoscop*))):ab,ti,kw) AND ('intraoperative period'/de OR 'intraoperative monitoring'/de OR 'surgery'/exp OR 'surgery':lnk OR 'laryngoscopy'/exp OR (intraoperativ* OR intra-operativ* OR intrasurg* OR surg* OR real-time* OR margin* OR microsurg* OR laryngoscop* OR microlaryngoscop*):ab,ti,kw) |
| **Medline (140 references)** | (Laryngeal Neoplasms/ OR Granuloma, Laryngeal/ OR (((epiglott* OR larynx* OR microlaryng* OR laryng* OR glott* OR postcricoid* OR subglot* OR supraglot* OR vocal-cord*) ADJ6 (cancer* OR carcinoma* OR tumour* OR tumour* OR neoplas* OR papilloma* OR granuloma* OR lesion* OR malignan* OR premalignan* OR leukoplak* OR dysplas* OR surg* OR operat*))).ab,ti,kf.) AND (Optical Imaging/ OR Narrow Band Imaging/ OR autofluorescence/ OR Fluorescence/ OR Microscopy, Confocal/ OR Fluorescent Dyes/ OR (((narrowband* OR narrow-band*) ADJ3 (imag*)) OR autofluorescence* OR auto-fluorescence* OR intrinsic-fluorescence* OR native-fluorescence* OR ((fluorescen* OR imag*) ADJ3 guided) OR ((light* OR optical* OR molecular*) ADJ3 (imag*)) OR near-infrared OR tracer* OR target* OR dye* OR probe* OR raman* OR confocal* OR ((contact*) ADJ3 (endomicroscop* OR microscop* OR endoscop*))).ab,ti,kf.) AND (exp Intraoperative Period/ OR Monitoring, Intraoperative/ OR exp Surgical Procedures, Operative/ OR surgery.fs. OR Laryngoscopy/ OR (intraoperativ* OR intra-operativ* OR intrasurg* OR surg* OR real-time* OR margin* OR microsurg* OR laryngoscop* OR microlaryngoscop*).ab,ti,kf.) |
| **Web of Science Core Collection (156 references)** | TS=(((((epiglott* OR larynx* OR microlaryng* OR laryng* OR glott* OR postcricoid* OR subglot* OR supraglot* OR vocal-cord*) NEAR/5 (cancer* OR carcinoma* OR tumour* OR tumour* OR neoplas* OR papilloma* OR granuloma* OR lesion* OR malignan* OR premalignan* OR leukoplak* OR dysplas* OR surg* OR operat*)))) AND ((((narrowband* OR narrow-band*) NEAR/2 (imag*)) OR autofluorescence* OR auto-fluorescence* OR intrinsic-fluorescence* OR native-fluorescence* OR ((fluorescen* OR imag*) NEAR/2 guided) OR ((light* OR optical* OR molecular*) NEAR/2 (imag*)) OR near-infrared OR tracer* OR target* OR dye* OR probe* OR raman* OR confocal* OR ((contact*) NEAR/2 (endomicroscop* OR microscop* OR endoscop*)))) AND ((intraoperativ* OR intra-operativ* OR intrasurg* OR surg* OR real-time* OR margin* OR microsurg* OR laryngoscop* OR microlaryngoscop*))) |

**Supplementary 1** - Search Strategy (continued)

| Database | Full search strategy |
|---|---|
| **Cochrane Central Register of Controlled Trials (54 references)** | ((((epiglott* OR larynx* OR microlaryng* OR laryng* OR glott* OR postcricoid* OR subglot* OR supraglot* OR vocal NEXT cord*) NEAR/6 (cancer* OR carcinoma* OR tumour* OR tumour* OR neoplas* OR papilloma* OR granuloma* OR lesion* OR malignan* OR premalignan* OR leukoplak* OR dysplas* OR surg* OR operat*)):ab,ti,kw) AND ((((narrowband* OR narrow NEXT band*) NEAR/3 (imag*)) OR autofluorescence* OR auto NEXT fluorescence* OR intrinsic NEXT fluorescence* OR native NEXT fluorescence* OR ((fluorescen* OR imag*) NEAR/3 guided) OR ((light* OR optical* OR molecular*) NEAR/3 (imag*)) OR "near infrared" OR tracer* OR target* OR dye* OR probe* OR raman* OR confocal* OR ((contact*) NEAR/3 (endomicroscop* OR microscop* OR endoscop*))):ab,ti,kw) AND ((intraoperativ* OR intra NEXT operativ* OR intrasurg* OR surg* OR real NEXT time* OR margin* OR microsurg* OR laryngoscop* OR microlaryngoscop*):ab,ti,kw) |
| **Other sources** | "epiglottis\|larynx\|laryngeal cancer\|carcinoma\|tumour\|tumour\|neoplasm" "narrow band imaging" \|"optical\|molecular imaging"\|autofluorescence\|"auto\|intrinsic\|native fluorescence" \|tracer\|target\| dye\|probe\|raman\|confocal intraoperative |

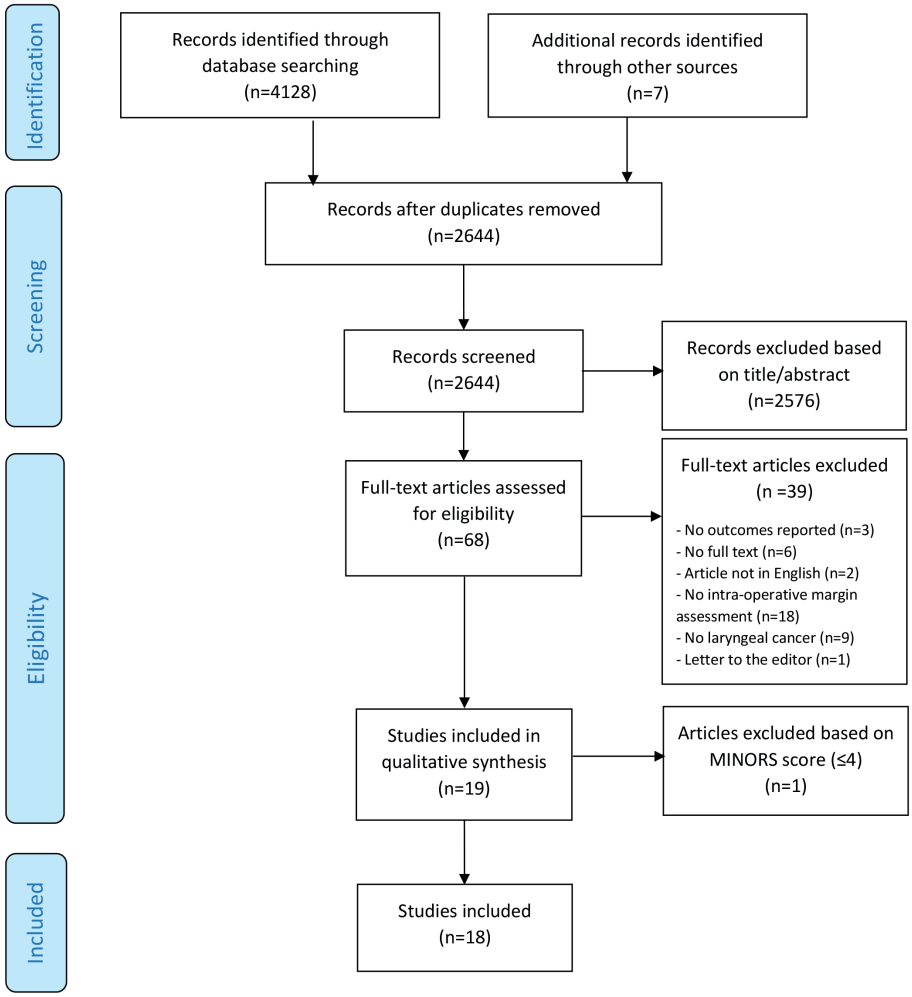


**Supplementary 2** –PRISMA flow diagram

**Supplementary 3** – MINORS scores

| Study | Cumulative MINORS score | Maximum MINORS score | Clearly stated aim | Consecutive patients | Prospective data collection | Appropriate endpoint | Unbiased evaluation of endpoints | Appropriate follow-up | Loss to follow-up | Prospective calculation of sample size | Gold Standard control | Contemporary groups | Baseline equivalence of groups | Statistical analysis adapted to study design |
|---|---|---|---|---|---|---|---|---|---|---|---|---|---|---|
| **Fiz (3)** | 17 | 24 | 2 | 2 | 1 | 2 | 0 | 2 | 1 | 0 | 2 | 1 | 2 | 2 |
| **Garofolo (18)** | 18 | 24 | 2 | 2 | 1 | 2 | 0 | 2 | 2 | 0 | 2 | 1 | 2 | 2 |
| **Hainarosie (19)** | 9 | 24 | 0 | 0 | 0 | 1 | 0 | 2 | 2 | 0 | 2 | 1 | 1 | 0 |
| **Klimza (20)** | 11 | 16 | 2 | 2 | 1 | 2 | 0 | 2 | 2 | 0 | na | na | na | na |
| **Piersiala (21)** | 12 | 16 | 2 | 2 | 2 | 2 | 0 | 2 | 2 | 0 | na | na | na | na |
| **Plaat (22)** | 17 | 24 | 2 | 2 | 1 | 1 | 0 | 2 | 2 | 0 | 2 | 1 | 2 | 2 |
| **Šifrer (23)** | 18 | 24 | 2 | 2 | 2 | 0 | 2 | 2 | 2 | 0 | 2 | 1 | 2 | 1 |
| **Srivastava (24)** | 7 | 16 | 0 | 2 | 1 | 0 | 0 | 2 | 2 | 0 | na | na | na | na |
| **Vicini (25)** | 17 | 24 | 2 | 1 | 1 | 2 | 0 | 2 | 2 | 0 | 2 | 2 | 2 | 1 |
| **Zwakenberg (26)** | 20 | 24 | 2 | 0 | 2 | 2 | 2 | 2 | 2 | 0 | 2 | 2 | 2 | 2 |
| **Fielding (27)** | 10 | 16 | 2 | 1 | 2 | 1 | 0 | 2 | 2 | 0 | na | na | na | na |
| **Paczona (28)** | 10 | 24 | 2 | 0 | 2 | 0 | 0 | 0 | 2 | 0 | 2 | 1 | 1 | 0 |
| **Succo (29)** | 15 | 24 | 2 | 1 | 2 | 2 | 0 | 2 | 2 | 0 | 2 | 1 | 1 | 0 |
| **Csanády (30)** | 6 | 16 | 1 | 0 | 0 | 1 | 0 | 2 | 2 | 0 | na | na | na | na |
| **Digonnet (31)** | 10 | 16 | 1 | 2 | 2 | 1 | 0 | 2 | 2 | 0 | na | na | na | na |
| **Dedivitis (32)** | 9 | 16 | 2 | 0 | 2 | 1 | 0 | 2 | 2 | 0 | na | na | na | na |
| **Stefanescu (33)** | 7 | 16 | 2 | 0 | 0 | 1 | 0 | 2 | 2 | 0 | na | na | na | na |
| **Shakhov (34)** | 5 | 16 | 1 | 0 | 0 | 0 | 0 | 2 | 2 | 0 | na | na | na | na |

*Abbreviations: na = not applicable*

# Chapter 4

## Fluorescence-guided sentinel lymph node detection in colorectal cancer

Ruben P.J. Meijer, Hidde A. Galema, Lorraine J. Lauwerends, Cornelis Verhoef, Jacobus Burggraaf, Stijn Keereweer, Merlijn Hutteman, Alexander L. Vahrmeijer, Denise E. Hilling

The Lymphatic System in Colorectal Cancer. Basic Concepts, Pathology, Imaging and Treatment Perspectives. 2022, Pages 245-255

## ABSTRACT

Sentinel lymph node (SLN) mapping can be a valuable addition to the treatment of colorectal cancer patients. Nevertheless, conventional lymph node mapping methods using blue dye are limited due to inadequate depth penetration, and the use of a radiocolloid tracer has its logistic hurdles. With near-infrared (NIR) fluorescence imaging, the SLN can be accurately identified in most patients resulting in more accurate lymph node staging. Current technical challenges and the low negative predictive value of the SLN withhold surgeons from its use in daily practice.

## CONCEPT OF SENTINEL LYMPH NODE MAPPING

Adequate lymph node staging is important in colorectal cancer (CRC) treatment, as lymph node metastases are an important determinant for patient prognosis and an indication for adjuvant systemic treatment. The sentinel lymph node (SLN) is defined as the first group of lymph node(s) draining a tumour. The identification, removal, and analysis of these SLNs (SLN mapping) can therefore be of added value for the staging of CRC patients, and subsequent treatment. SLN mapping was first described in 1960 for parotid cancer and is nowadays standard of care in breast cancer and melanoma patients (1-3).



The SLN concept could also be of added value in CRC patients. Patients with stage I and II diseases (with no lymph node involvement) still develop distant metastases in up to 30% of cases (4). This could be the result of, among others, understaging of these patients due to missed lymph nodes with occult tumour cells and micrometastases during routine histopathological examination, or inadequate lymph node harvesting at the time of primary treatment. Routine histopathological examination currently exists of reviewing a single paraffin-embedded slide per lymph node, with the chance of missing tumour cells away from the slide's cutting edge. Extensive histopathological analysis of all lymph nodes using serial sectioning or reverse transcriptase polymerase chain reaction could result in more accurate lymph node staging. However, both methods are expensive and time consuming (5-7). As the SLN procedure identifies the lymph node(s) with the highest chance of containing metastases, more extensive histopathological analysis of only these lymph nodes is feasible. Furthermore, tumour-negative SLNs create an opportunity for local or endoscopic resection of CRC, especially in early-stage tumours (8).

Conventional methods for SLN mapping include the use of either blue dye, a radiocolloid tracer, or the combination of both (2, 3). The use of blue dye for SLN mapping in CRC is limited due to inadequate depth penetration and the utilization of radiocolloid tracers has some logistic hurdles (9). A nuclear medicine physician and an endoscopist are required for tracer injection. Moreover, the gamma probe used for localization does not enable real-time visualization. These shortcomings have increased the interest in novel techniques, such as near-infrared (NIR) fluorescence imaging.

## FLUORESCENCE-GUIDED SURGERY

NIR fluorescence imaging provides the surgeon with real-time information of the surgical field and can aid in differentiation between malignant and healthy tissue during surgery (10). NIR light (700-900 nm) is not visible to the human eye and has relatively deep (up to 10 mm) tissue penetration. Human tissue itself has low autofluorescence in the NIR light spectrum, resulting in a high signal-to-background ratio (11). NIR fluorescence-guided surgery requires

two components: an NIR camera system and a fluorescent agent (Fig. 1). These NIR camera systems are composed of an NIR excitation light source, collection optics (including optical filtration), and a camera that can detect emitted NIR light. These systems emit photons with a specific wavelength, which are absorbed by the fluorescent agent. Electrons within these agent's molecules transit to an excited state and fall back to their ground state (Fig. 2). This will release the stored energy in an emitted photon with a longer wavelength than the exciting light of the NIR camera system, the so-called Stokes shift. This emitted photon is subsequently captured by the camera system. The camera output is usually displayed on a monitor including a merged image of the fluorescence signal and the white light image. Both the camera systems and fluorescent agents have shown great improvements in the last decades and have resulted in the clinical use of NIR fluorescence for different purposes during surgery (e.g., bile duct detection, tissue perfusion) (12-14).

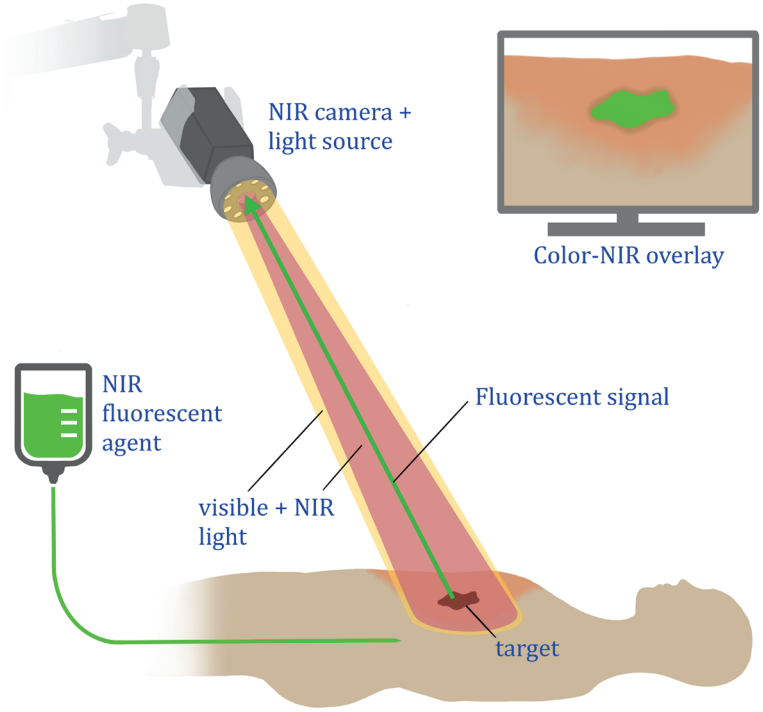


■ **Figure 1.** Fluorescence-guided surgery.
*NIR fluorescent agents are administered intravenously or locally. NIR fluorescence is visualized using a specialized imaging system for intraoperative imaging. The imaging system uses dedicated NIR excitation light to excite the fluorophore. Collection optics, emission filters, and an image sensor capable of detecting NIR fluorescence emission light. The NIR fluorescence signal is displayed on a monitor in the surgical theater. A simultaneous white light image, which can be merged with the NIR fluorescence image, is desirable.*

Several dedicated NIR fluorescence imaging systems are clinically used for open, laparoscopic, and robotic surgery. On the other hand, only two fluorescent agents, indocyanine green (ICG) and methylene blue, have been approved for clinical use by the US Food and Drug Administration (FDA) and European Medicines Agency (EMA). Both are nontargeted fluorescent agents, meaning these agents do not bind to a specific target. ICG, first described in 1957 for the determination of cardiac output, is the most used agent for fluorescence-guided SLN mapping in various cancer types and can also be used for the visualization of vital structures (e.g., bile ducts), liver tumours, and assessment of tissue perfusion (14, 15).



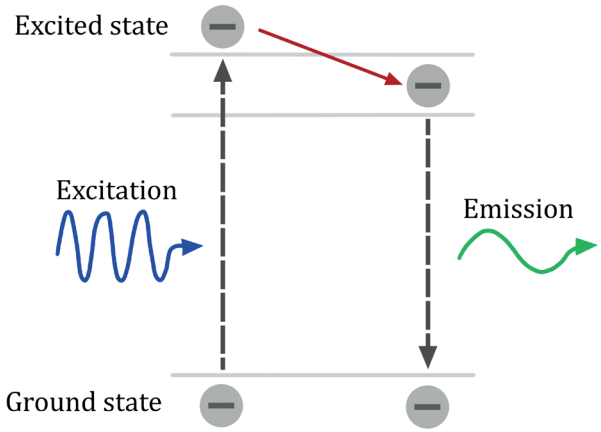


**Figure 2.** Schematic overview of the principle of fluorescence.
*A photon in the appropriate wavelength (excitation light) is absorbed by the fluorophore, elevating an electron to an excited state. When the electron transitions back to its ground state, a photon is emitted. This emitted photon is of a longer wavelength and lower energy.*

## FLUORESCENCE-GUIDED SENTINEL LYMPH NODE DETECTION IN COLORECTAL CANCER

While peritumoural injection of ICG is the most used technique for NIR fluorescence guided SLN mapping, alternative fluorescent dyes have also been assessed (Fig. 3). In addition, different injection sites and variable timing of the injection have been investigated.

The injection site of ICG can be either subserosal or submucosal, with a slight preference for the latter (16-18). The submucosa houses an important part of the intestinal lymphatic system, which might improve the lymphatic uptake of the fluorescent agent from the tumour surrounding tissue (19). Submucosal injection is performed prior to or during surgery, via endoscopy. Subserosal injection, on the other hand, is performed intraoperatively by the surgeon. In minimally invasive surgery, this requires transcutaneous injection of the fluorescent agent. Correct positioning of the needle and maintaining this position during injection of

the fluorescent agent is easier with the submucosal technique and therefore leads to less spillage of ICG (16, 17).

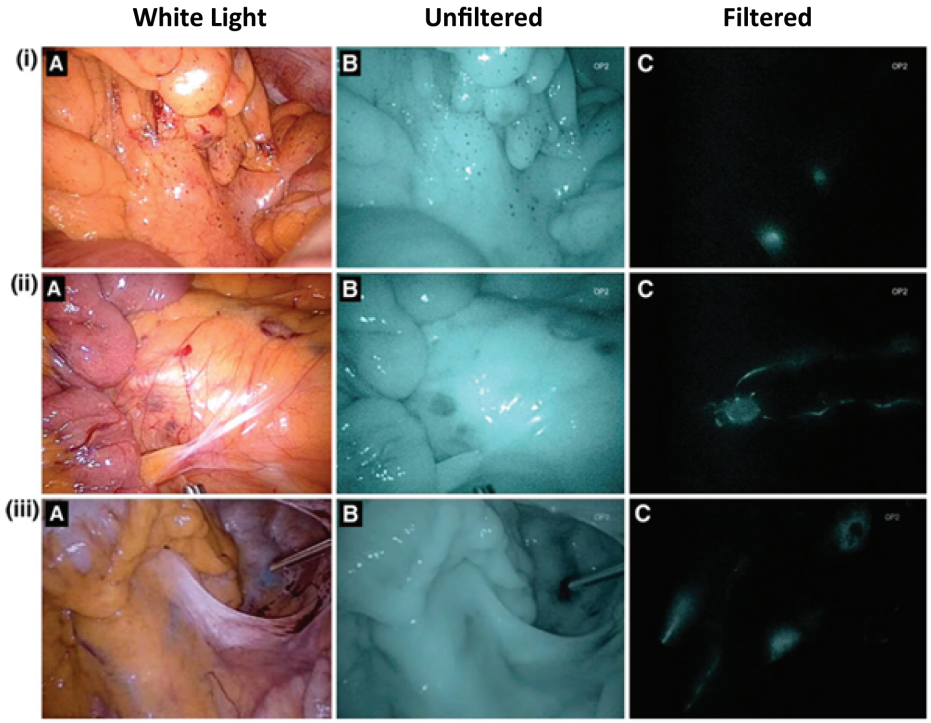


**Figure 3.** Intraoperative results of sentinel lymph node mapping using with indocyanine green.
*Three patients (i - iii) demonstrating NIR fluorescence-guided sentinel lymph node mapping with indocyanine green (A, a white light image; B, an NIR image without filter; and C, a filtered NIR image). (i) Two bright spots in the mesocolon were identified in the filtered view, consistent with sentinel lymph nodes. (ii) A bright spot is seen in the filtered view, consistent with a paraaortic sentinel lymph node. (iii) A bright spot is seen in the filtered view, alongside the right iliac artery, consistent with a sentinel lymph node. The injection site of the rectal tumour is clearly visible, as well as an efferent channel in the sigmoid mesentery which was found to lead to another sentinel lymph node. Source: Reproduced by permission from Cahill, R. A., Anderson, M., Wang, L. M., Lindsey, I., Cunningham, C., Mortensen, N. J. (2012) (40). Near-infrared (NIR) laparoscopy for intraoperative lymphatic road-mapping and sentinel node identification during definitive surgical resection of early-stage colorectal neoplasia. Surgical Endoscopy, 26(1), 197 - 204.*

Timing of fluorescent dye administration and assessment has been assessed directly pre- or intraoperatively (both referred to as in vivo), and postoperatively (*ex vivo*). In vivo administration has some practical drawbacks, particularly for the preferred submucosal injection. For in vivo submucosal injection, an endoscopy in the operating room is required directly before or during surgery, which poses a logistical challenge. Furthermore, bowel insufflation might alter the surgical field and therefore hamper the surgical procedure. The alternative, *ex vivo* imaging, is logistically simpler and enables the use of experimental agents. *Ex vivo* imaging also has some disadvantages. Lymphatic flow may be disrupted after resection, and altering

the surgical plan (i.e., perform a more limited resection) based on histopathological analysis of the harvested lymph nodes is not possible. Moreover, *ex vivo* fluorescent agent injection and lymph node identification does not facilitate identifying SLNs in patients with aberrant lymph node drainage patterns (20).

Table 1 summarizes studies that describe fluorescence-guided SLN mapping in CRC patients. A procedure is defined as successful if one or more lymph nodes were identified by fluorescence (the SLN). An upstaged patient is defined as a patient who was staged as N0 (all lymph nodes being tumour-negative) using conventional histopathology but showed tumour-positive SLNs after additional extensive histopathological assessment of the SLNs. These patients can consequently change from stage I or II CRC to stage III. The percentage of upstaged patients was calculated by dividing the number of upstaged patients by all lymph node-negative patients before extensive histopathological assessment of the SLN.



In all studies, intraoperative identification of the SLNs was performed using ICG and this was successful in most cases. Andersen et al. had a remarkably lower success rate of 65.5% in their multicenter trial, with all other studies being single center (16). This could be explained by a learning curve, which is suggested by Bembenek et al. to be more than 22 cases per center, a number none of their centers had reached (9). The sensitivity of SLN identification with ICG ranged from 0.33 to 1, and the negative predictive value was relatively low, with only three (33%) studies reporting an NPV above 0.9.

■ *Table 1. Results of clinical trials assessing fluorescence-guided SLN mapping for CRC*

| | Agent | Patients | Diagnosis | Procedure | Injection site | Number SLNs | Success rate | Sensitivity | NPV | Upstaged patients* (%) |
|---|---|---|---|---|---|---|---|---|---|---|
| **Intraoperative** | | | | | | | | | | |
| **Andersen (18)** | ICG:HA | 29 | CC | L | SS | 1 (0-3)* | 65.50% | 0.33 | 0.76 | 1 (12%) |
| **Ankersmit (17)** | ICG:HA | 29 | CC | L | 14 SS; 15 SM | 2 (0-6)* | 89.70% | 0.44 | 0.8 | 3 (13%) |
| **Cahill (35)** | ICG | 18 | CRC | L | SM | 3.6 (1-5)** | 100% | 1 | 1 | 0 (0%) |
| **Carrara (36)** | ICG | 95 | CRC | L | SS | 1.5 (1-5)** | 96.8 | 0.73 | 0.96 | 1 (1%) |
| **Currie (37)** | ICG | 30 | CC | L | SM | 3 (1-4)*** | 90% | 0.33 | 0.75 | 1 (5%) |
| **Hirche (38)** | ICG | 26 | CC | O | SS | 1.7 (0-5)** | 96% | 0.82 | 0.87 | 3 (21%) |
| **Kusano (39)** | ICG | 26 | CRC | O | SS | 2.6 (± 2.4)**** | 88.50% | 0.5 | 0.81 | nr |
| **Nagata (40)** | ICG | 48 | CRC | L | SS | 3.5 (± 1.7) **** | 97.90% | 0.44 | 0.89 | nr |
| **Noura (41)** | ICG | 25 | RC | O | SM | 2.1 (± 0.8)**** | 92% | 1 | 1 | nr |
| **Watanabe (42)** | ICG | 31 | CC | L | SS | 10.4 (± 4.73)**** | 100% | 0.67 | 0.93 | nr |
| **Postoperative** | | | | | | | | | | |
| **Hutteman (16)** | HSA800 | 24 | CRC | na | SM | 3 (1-5)* | 100% | 0.89 | 0.94 | nr |
| **Liberale (43)** | ICG | 20 | CC | na | SS | 1 (0-4)* | 95% | 0.57 | 0.81 | 3 (23%) |
| **Schaafsma (44)** | HSA800 | 22 | CC | na | SM | 3.5 (± 1.9)**** | 95% | 0.8 | 0.94 | nr |
| **Weixler (45)** | HSA800 | 50 | CC | na | SS | 4.4 (± 2.2)**** | 98% | 0.64 | 0.74 | 5 (17%) |

*The number of detected SLNs are presented as: *median with range, **mean with range, ***median with interquartile range, ****mean with standard deviation*
*The sensitivity is calculated by dividing the number of procedures with a tumour-positive SLN (true positives) by the sum of true positive and false negative procedures. The negative predictive value is determined by dividing the amount of true negative procedures by the sum of true negative and false negative procedures. Upstaged patients are defined as patients with no tumour involvement on conventional histopathology of all lymph nodes, but a tumour-positive SLN at advanced histopathology. The percentage of upstaged patients is calculated as: upstaged patients/upstaged patients + true negatives. Abbreviations: CC = Colon cancer; CRC = colorectal cancer; HA = human albumin; ICG = indocyanine green; L = laparoscopic; na = not applicable; NPV = negative predictive value; nr = not reported; O = open; RC = rectal cancer; SLN = sentinel lymph nodes; SM = submucosal; SS = subserosal*

HSA800 (IRDye 800CW conjugated to human serum albumin) is another fluorescent agent used for *ex vivo* SLN mapping in CRC patients, which has not been approved by the FDA or EMA yet. Preclinical studies have shown an advantage of HSA800 over ICG regarding lymphatic entry, flow, fluorescence yield, and reproducibility. This is most likely a result of its bigger hydrodynamic diameter, resulting in improved retention in the SLN (21). Clinical *ex vivo* studies with HSA800 have shown comparable results to in vivo assessment with ICG with a wide range in sensitivity (0.64 - 0.89) and negative predictive value (0.74 - 0.94).

## FUTURE PERSPECTIVES



Fluorescence-guided SLN mapping has the potential to improve adequate staging in CRC patients. Despite its advantages and several published clinical studies, it is not used in common day practice. This might be the result of technical and logistic hurdles. Moreover, it is unknown if the upstaging of patients with micrometastatic lymph nodes and subsequent adjuvant treatment will lead to improved patient outcomes.

The number of early-stage CRC patients is expected to increase in the coming years, due to the introduction of nationwide screening programs (22, 23). With this increasing number of early-stage CRC patients, the number of lymph node-negative patients is also expected to rise, since 90% of the T1 tumours are N0 (24, 25). Especially in these patients SLN mapping might be valuable. Because of the low incidence of lymph node metastases in these patients, a reliable SLN procedure showing a tumour-negative SLN enables the possibility for local excision without an extensive lymphadenectomy, thereby potentially lowering perioperative morbidity (8).

The relatively low negative predictive value of the SLNs (the probability that in case of a tumour-negative SLN, all other regional lymph nodes are tumour negative) is an important reason that this procedure is not yet implemented in daily practice. It withholds surgeons from performing a local excision and omitting an oncological resection based on a tumour-negative SLN. The low NPV is mainly a consequence of a high false negative rate (tumour-negative SLNs in the presence of a tumour-positive regional lymph node). One explanation for this high false negative rate is the occurrence of the so-called skip metastases, which are reported in 10 – 22% of the cases (26, 27). Tumour size could be another reason for this high false negative rate. T3 – T4 tumours showed false negative results in 23% of the cases compared to 2% of the T1 – T2 tumours (28). It is suggested that these more invasive tumours (T3 – T4) alter the lymphatic flow, resulting in skip metastases.

Based on the promising preliminary results, the interest in neoadjuvant treatment for colon cancer has increased in recent years (29, 30). This novel treatment strategy could influence

the success rate of SLN mapping, as research in other tumour types suggest altered lymphatic flow after neoadjuvant treatment (31). As a result, it could be preferable to perform SLN mapping prior to neoadjuvant therapy.

A meta-analysis by Ankersmit et al. showed a pooled upstaging (no tumour involvement on conventional histopathology, but a tumour-positive SLN at advanced histopathology) in 15% of the patients (17). This means that roughly one out of seven patients is wrongly classified as N0 without the use of fluorescence imaging and extensive histopathological assessment of the SLN. These patients would not have been upstaged to stage III and wrongfully been withheld adjuvant therapy, which theoretically leads to worse survival.

As emphasized, the use of fluorescence-guided SLN mapping with ICG increases the detection rate of SLNs in CRC patients and can result in upstaging in a substantial number of patients. Nevertheless, this concept still requires postoperative histopathological analysis. Direct intraoperative feedback regarding the malignancy status of any lymph node could be provided with the use of tumour-targeted fluorescence-guided surgery. Tumour-targeted agents consist of a fluorophore conjugated to a targeting component and therefore possess strong binding affinity for a specific cancer-associated molecular target or biomarker (32). Unfortunately, tumour-targeted tracers tend to show a relatively high false positive rate (fluorescent lymph node without tumour localization) of 7% - 33% for lymph node imaging, due to aspecific tracer localization (33-35). On the other hand, it is still debated whether a small tumour load (micrometastases and lymph nodes with isolated tumour cells) accumulate enough volume of the tracer to produce a sufficiently enhanced fluorescent signal. Nevertheless, tumour-targeted agents do not only allow for the identification of lymph node metastases but also other metastases, the primary tumour and tumour-positive resection margins (36). Several tumour-targeted agents are currently studied in phase II and III trials (SGM-101 in Locally Advanced and Recurrent Rectal Cancer (37, 38).

## CONCLUSIONS

Fluorescence-guided SLN mapping in CRC can be a valuable addition to detect micrometastases and occult metastases in locoregional lymph nodes. It can result in upstaging in a significant part of the patients, whom otherwise would not have received adjuvant therapy. The low negative predictive value appears to be an important reason for the delayed introduction to current standard of care. Tumour-targeted fluorescent agents might overcome these shortcomings in the future.

## REFERENCES


1. Gould EA, Winship T, Philbin PH, Kerr HH. Observations on a "sentinel node" in cancer of the parotid. Cancer. 1960;13:77-8.
2. He PS, Li F, Li GH, Guo C, Chen TJ. The combination of blue dye and radioisotope versus radioisotope alone during sentinel lymph node biopsy for breast cancer: a systematic review. BMC Cancer. 2016;16:107.
3. Valsecchi ME, Silbermins D, de Rosa N, Wong SL, Lyman GH. Lymphatic mapping and sentinel lymph node biopsy in patients with melanoma: a meta-analysis. J Clin Oncol. 2011;29(11):1479-87.
4. Figueredo A, Coombes ME, Mukherjee S. Adjuvant therapy for completely resected stage II colon cancer. Cochrane Database Syst Rev. 2008;2008(3):CD005390.
5. Doekhie FS, Mesker WE, Kuppen PJ, van Leeuwen GA, Morreau H, de Bock GH, et al. Detailed examination of lymph nodes improves prognostication in colorectal cancer. Int J Cancer. 2010;126(11):2644-52.
6. Liefers GJ, Cleton-Jansen AM, van de Velde CJ, Hermans J, van Krieken JH, Cornelisse CJ, et al. Micrometastases and survival in stage II colorectal cancer. N Engl J Med. 1998;339(4):223-8.
7. Yamamoto H, Murata K, Fukunaga M, Ohnishi T, Noura S, Miyake Y, et al. Micrometastasis Volume in Lymph Nodes Determines Disease Recurrence Rate of Stage II Colorectal Cancer: A Prospective Multicenter Trial. Clin Cancer Res. 2016;22(13):3201-8.
8. Cahill RA, Leroy J, Marescaux J. Localized resection for colon cancer. Surg Oncol. 2009;18(4):334-42.
9. Bembenek AE, Rosenberg R, Wagler E, Gretschel S, Sendler A, Siewert JR, et al. Sentinel lymph node biopsy in colon cancer: a prospective multicenter trial. Ann Surg. 2007;245(6):858-63.
10. Vahrmeijer AL, Hutteman M, van der Vorst JR, van de Velde CJ, Frangioni JV. Image-guided cancer surgery using near-infrared fluorescence. Nat Rev Clin Oncol. 2013;10(9):507-18.
11. Frangioni JV. New technologies for human cancer imaging. J Clin Oncol. 2008;26(24):4012-21.
12. Griffiths M, Chae MP, Rozen WM. Indocyanine green-based fluorescent angiography in breast reconstruction. Gland Surg. 2016;5(2):133-49.
13. van den Hoven P, Ooms S, van Manen L, van der Bogt KEA, van Schaik J, Hamming JF, et al. A systematic review of the use of near-infrared fluorescence imaging in patients with peripheral artery disease. J Vasc Surg. 2019;70(1):286-97 e1.
14. van Manen L, Handgraaf HJM, Diana M, Dijkstra J, Ishizawa T, Vahrmeijer AL, et al. A practical guide for the use of indocyanine green and methylene blue in fluorescence-guided abdominal surgery. J Surg Oncol. 2018;118(2):283-300.
15. Fox IJ, Brooker LG, Heseltine DW, Essex HE, Wood EH. A tricarbocyanine dye for continuous recording of dilution curves in whole blood independent of variations in blood oxygen saturation. Proc Staff Meet Mayo Clin. 1957;32(18):478-84.
16. Andersen HS, Bennedsen ALB, Burgdorf SK, Eriksen JR, Eiholm S, Toxværd A, et al. In vivo and ex vivo sentinel node mapping does not identify the same lymph nodes in colon cancer. Int J Colorectal Dis. 2017;32(7):983-90.

**17.** Ankersmit M, Bonjer HJ, Hannink G, Schoonmade LJ, van der Pas M, Meijerink W. Near-infrared fluorescence imaging for sentinel lymph node identification in colon cancer: a prospective single-center study and systematic review with meta-analysis. Tech Coloproctol. 2019;23(12):1113-26.

**18.** Hutteman M, Choi HS, Mieog JS, van der Vorst JR, Ashitate Y, Kuppen PJ, et al. Clinical translation of ex vivo sentinel lymph node mapping for colorectal cancer using invisible near-infrared fluorescence light. Ann Surg Oncol. 2011;18(4):1006-14.

**19.** Miller MJ, McDole JR, Newberry RD. Microanatomy of the intestinal lymphatic system. Ann N Y Acad Sci. 2010;1207 Suppl 1(Suppl 1):E21-8.

**20.** Tuech JJ, Pessaux P, Regenet N, Bergamaschi R, Colson A. Sentinel lymph node mapping in colon cancer. Surg Endosc. 2004;18(12):1721-9.

**21.** Ohnishi S, Lomnes SJ, Laurence RG, Gogbashian A, Mariani G, Frangioni JV. Organic alternatives to quantum dots for intraoperative near-infrared fluorescent sentinel lymph node mapping. Mol Imaging. 2005;4(3):172-81.

**22.** Cardoso R, Guo F, Heisser T, Hackl M, Ihle P, De Schutter H, et al. Colorectal cancer incidence, mortality, and stage distribution in European countries in the colorectal cancer screening era: an international population-based study. Lancet Oncol. 2021;22(7):1002-13.

**23.** Navarro M, Nicolas A, Ferrandez A, Lanas A. Colorectal cancer population screening programs worldwide in 2016: An update. World J Gastroenterol. 2017;23(20):3632-42.

**24.** Fields AC, Lu P, Hu F, Hirji S, Irani J, Bleday R, et al. Lymph Node Positivity in T1/T2 Rectal Cancer: a Word of Caution in an Era of Increased Incidence and Changing Biology for Rectal Cancer. J Gastrointest Surg. 2021;25(4):1029-35.

**25.** Ricciardi R, Madoff RD, Rothenberger DA, Baxter NN. Population-based analyses of lymph node metastases in colorectal cancer. Clin Gastroenterol Hepatol. 2006;4(12):1522-7.

**26.** Bao F, Zhao LY, Balde AI, Liu H, Yan J, Li TT, et al. Prognostic impact of lymph node skip metastasis in Stage III colorectal cancer. Colorectal Dis. 2016;18(9):O322-9.

**27.** Saha S, Sehgal R, Patel M, Doan K, Dan A, Bilchik A, et al. A multicenter trial of sentinel lymph node mapping in colorectal cancer: prognostic implications for nodal staging and recurrence. Am J Surg. 2006;191(3):305-10.

**28.** Burghgraef TA, Zweep AL, Sikkenk DJ, van der Pas M, Verheijen PM, Consten ECJ. In vivo sentinel lymph node identification using fluorescent tracer imaging in colon cancer: A systematic review and meta-analysis. Crit Rev Oncol Hematol. 2021;158:103149.

**29.** Karoui M, Rullier A, Piessen G, Legoux JL, Barbier E, De Chaisemartin C, et al. Perioperative FOLFOX 4 Versus FOLFOX 4 Plus Cetuximab Versus Immediate Surgery for High-Risk Stage II and III Colon Cancers: A Phase II Multicenter Randomized Controlled Trial (PRODIGE 22). Ann Surg. 2020;271(4):637-45.

**30.** Seymour MT, Morton, D. FOxTROT: an international randomised controlled trial in 1052 patients (pts) evaluating neoadjuvant chemotherapy (NAC) for colon cancer. Journal of Clinical Oncology. 2019;37(15).

**31.** Kuehn T, Bauerfeind I, Fehm T, Fleige B, Hausschild M, Helms G, et al. Sentinel-lymph-node biopsy in patients with breast cancer before and after neoadjuvant chemotherapy (SENTINA): a prospective, multicentre cohort study. Lancet Oncol. 2013;14(7):609-18.

**32.** Hernot S, van Manen L, Debie P, Mieog JSD, Vahrmeijer AL. Latest developments in molecular tracers for fluorescence image-guided cancer surgery. Lancet Oncol. 2019;20(7):e354-e67.

**33.** de Valk KS, Deken MM, Handgraaf HJM, Bhairosingh SS, Bijlstra OD, van Esdonk MJ, et al. First-in-Human Assessment of cRGD-ZW800-1, a Zwitterionic, Integrin-Targeted, Near-Infrared Fluorescent Peptide in Colon Carcinoma. Clin Cancer Res. 2020;26(15):3990-8.

**34.** Lu G, van den Berg NS, Martin BA, Nishio N, Hart ZP, van Keulen S, et al. Tumour-specific fluorescence-guided surgery for pancreatic cancer using panitumumab-IRDye800CW: a phase 1 single-centre, open-label, single-arm, dose-escalation study. Lancet Gastroenterol Hepatol. 2020;5(8):753-64.

**35.** Rosenthal EL, Moore LS, Tipirneni K, de Boer E, Stevens TM, Hartman YE, et al. Sensitivity and Specificity of Cetuximab-IRDye800CW to Identify Regional Metastatic Disease in Head and Neck Cancer. Clin Cancer Res. 2017;23(16):4744-52.

**36.** de Valk KS, Deken MM, Schaap DP, Meijer RP, Boogerd LS, Hoogstins CE, et al. Dose-Finding Study of a CEA-Targeting Agent, SGM-101, for Intraoperative Fluorescence Imaging of Colorectal Cancer. Ann Surg Oncol. 2021;28(3):1832-44.

**37.** SGM-101 in Locally Advanced and Recurrent Rectal Cancer (SGM-LARRC) [Internet]. clinicaltrials.gov. 2020. Available from: https://clinicaltrials.gov/ct2/show/NCT04642924.

**38.** Performance of SGM-101 for the Delineation of Primary and Recurrent Tumour and Metastases in Patients Undergoing Surgery for Colorectal Cancer [Internet]. Clinicaltrials.gov. 2018. Available from: https://clinicaltrials.gov/ct2/show/NCT03659448.

**39.** Ankersmit M, Bonjer HJ, Hannink G, Schoonmade LJ, van der Pas MHGM, Meijerink WJHJ. Near-infrared fluorescence imaging for sentinel lymph node identification in colon cancer: a prospective single-center study and systematic review with meta-analysis. Tech Coloproctol. 2019;23(12):1113-26.

**40.** Cahill RA, Anderson M, Wang LM, Lindsey I, Cunningham C, Mortensen NJ. Near-infrared (NIR) laparoscopy for intraoperative lymphatic road-mapping and sentinel node identification during definitive surgical resection of early-stage colorectal neoplasia. Surg Endosc. 2012;26(1):197-204.

**41.** Carrara A, Motter M, Amabile D, Pellecchia L, Moscatelli P, Pertile R, et al. Predictive value of the sentinel lymph node procedure in the staging of non-metastatic colorectal cancer. Int J Colorectal Dis. 2020;35(10):1921-8.

**42.** Currie AC, Brigic A, Thomas-Gibson S, Suzuki N, Moorghen M, Jenkins JT, et al. A pilot study to assess near infrared laparoscopy with indocyanine green (ICG) for intraoperative sentinel lymph node mapping in early colon cancer. Eur J Surg Oncol. 2017;43(11):2044-51.

**43.** Hirche C, Mohr Z, Kneif S, Doniga S, Murawa D, Strik M, et al. Ultrastaging of colon cancer by sentinel node biopsy using fluorescence navigation with indocyanine green. Int J Colorectal Dis. 2012;27(3):319-24.

**44.** Kusano M, Tajima Y, Yamazaki K, Kato M, Watanabe M, Miwa M. Sentinel node mapping guided by indocyanine green fluorescence imaging: a new method for sentinel node navigation surgery in gastrointestinal cancer. Dig Surg. 2008;25(2):103-8.

**45.** Nagata K, Endo S, Hidaka E, Tanaka J, Kudo SE, Shiokawa A. Laparoscopic sentinel node mapping for colorectal cancer using infrared ray laparoscopy. Anticancer Res. 2006;26(3B):2307-11.

**46.** Noura S, Ohue M, Seki Y, Tanaka K, Motoori M, Kishi K, et al. Feasibility of a lateral region sentinel node biopsy of lower rectal cancer guided by indocyanine green using a near-infrared camera system. Ann Surg Oncol. 2010;17(1):144-51.

**47.** Watanabe J, Ota M, Suwa Y, Ishibe A, Masui H, Nagahori K. Evaluation of lymph flow patterns in splenic flexural colon cancers using laparoscopic real-time indocyanine green fluorescence imaging. Int J Colorectal Dis. 2017;32(2):201-7.

**48.** Liberale G, Vankerckhove S, Galdon MG, Larsimont D, Ahmed B, Bouazza F, et al. Sentinel Lymph Node Detection by Blue Dye Versus Indocyanine Green Fluorescence Imaging in Colon Cancer. Anticancer Res. 2016;36(9):4853-8.

**49.** Schaafsma BE, Verbeek FP, van der Vorst JR, Hutteman M, Kuppen PJ, Frangioni JV, et al. Ex vivo sentinel node mapping in colon cancer combining blue dye staining and fluorescence imaging. J Surg Res. 2013;183(1):253-7.

**50.** Weixler B, Rickenbacher A, Raptis DA, Viehl CT, Guller U, Rueff J, et al. Sentinel Lymph Node Mapping with Isosulfan Blue or Indocyanine Green in Colon Cancer Shows Comparable Results and Identifies Patients with Decreased Survival: A Prospective Single-Center Trial. World J Surg. 2017;41(9):2378-86.

# Part II

## Tumour target expression in tumour tissue samples for targeted NIR fluorescence imaging

# Chapter 5

## Effects of neoadjuvant therapy on tumour target expression of oesophageal cancer tissue for NIR fluorescence imaging

Hidde A. Galema*, Lisanne K.A. Neijenhuis*, Lorraine J. Lauwerends, N. Geeske Dekker-Ensink, Cornelis Verhoef, Alexander L. Vahrmeijer, Shadhvi Bhairosingh, Peter J.K. Kuppen, Stephan Rogalla, Jacobus Burggraaf, Sjoerd M. Lagarde, Bas P.L. Wijnhoven, Merlijn Hutteman, Michail Doukas, Stijn Keereweer, Denise E. Hilling

* Shared first authorship

Submitted

## ABSTRACT

### Introduction

Oesophageal cancer patients with a clinical complete response (CR) after neoadjuvant chemoradiotherapy (nCRT) may be offered an active surveillance strategy. Regrowth rates of 40% after initial clinical CR indicate that identification of a true complete response to nCRT remains challenging. Near-infrared tumour-specific fluorescence endoscopic imaging might help to discriminate patients with an true complete response from those with residual disease. This study aims to find potential markers for molecular imaging and to assess the effect of nCRT on this marker expression.

### Methods

Oesophageal cancer tissue slides of diagnostic biopsies (n=41) (pre-treatment) and paired surgical specimens (n=31) (post-treatment) were collected. Immunohistochemistry was performed to assess expression of the tumour markers CEA, EpCAM, VEGF-α, EGFR, and c-MET on adenocarcinoma and squamous cell carcinoma (SCC).

### Results

The median total immunostaining score (TIS) of EpCAM in adenocarcinomas was 10, vs. 0 in healthy mucosa ($p < 0.001$). The median TIS of EGFR in SCC was 12, vs. 4 in healthy mucosa ($p < 0.001$). VEGF-α was highly expressed in adenocarcinoma and SCC (median TIS: 8), but this was also the case in healthy adjacent mucosa (median TIS: 8). Neoadjuvant therapy did not affect the expression of any of the promising markers.

### Discussion

EpCAM and EGFR appear to be the most suitable targets for tumour-specific NIR fluorescence imaging of oesophageal adenocarcinoma and SCC respectively. Unaffected expression of all suitable markers by neoadjuvant therapy implies that the diagnostic biopsy can be used to select a patient-specific target for response evaluation by molecular imaging.

## INTRODUCTION

Oesophageal cancer is the eight most common cancer worldwide, with over 500,000 patients diagnosed annually (1). With the introduction of neoadjuvant chemoradiotherapy (nCRT), cure rates and overall survival have drastically improved over the last two decades. Approximately 30% of all oesophageal cancer patients achieve a pathologically complete response in the resection specimen after neoadjuvant therapy (2, 3). When a complete response is suspected based on imaging modalities including PET-CT and white light endoscopy (i.e., a clinical complete response), patients may be offered an organ preserving treatment strategy (active surveillance) (4). However, discriminating treatment related fibrosis from residual tumour remains challenging. Regrowth rates of 40% after a clinical complete response underline the fact that small residual tumour can be missed with conventional diagnostic tools (5, 6). New imaging modalities may improve tumour identification after nCRT for oesophageal cancer, either during endoscopic response evaluation, or during surgery.



Tumour-specific fluorescence imaging (FLI) is a modality that can be used to perform real-time imaging of tumour cells. To perform FLI, a tumour-specific tracer comprising a fluorophore and a targeting agent which binds to a specific ligand or is activated by the tumour-specific environment, is required . The fluorophore can be excited by a specific light source, emitting photons that are detected by a fluorescence camera. In the near-infrared (NIR) spectrum (700 – 900 nm), optical tissue properties (absorption, scattering, and tissue autofluorescence) are limited, resulting in a higher light penetration depth and enhanced contrast compared to visible light (7, 8).

For a tumour-targeted fluorescence tracer to adequately delineate a tumour, overexpression of a specific tumour marker in cancer cells is vital. Likewise, these biomarkers must be absent or underexpressed in the healthy cells and fibrosis. A recent study showed that carcinoembryonic antigen-related cell adhesion molecule 5 (CECAM5, from here on to be referred to as CEA), epithelial cell adhesion molecule (EpCAM), vascular endothelial growth factor α (VEGF-α), and epithelial membrane antigen (EMA) were all overexpressed in oesophageal adenocarcinoma tissue, with only minimal overexpression in healthy tissue (9). However, effects of neoadjuvant treatment on the expression of these markers, as well as marker expression in oesophageal squamous cell carcinoma (SCC) is currently unknown. Oesophageal SCC is particularly interesting as these tumours tend to show higher rates of pathologically complete responses (approximately 40% vs. 20% in adenocarcinomas (10)). This study aims to find new molecular markers for tumour-specific imaging of oesophageal adenocarcinoma and SCC, and to explore the effect of neoadjuvant treatment on expression of these markers. These tumour markers may be suitable targets for NIR fluorescence imaging during endoscopic response evaluation.

## METHODS

This study was reviewed and approved by the Medical Ethical Committee of the Erasmus Medical Centre (METC Erasmus MC, MEC-2021-0339) and was conducted according to the Declaration of Helsinki (10th version, Fortaleza, 2013).

### Tissue selection

Formalin-fixed paraffin-embedded (FFPE) tissue blocks of oesophageal cancer patients that underwent surgery were collected and reviewed by a dedicated pathologist (MD). Tissue blocks containing both tumour and healthy tissue were selected. Pre-neoadjuvant treatment tissue (diagnostic biopsies) were paired with post-neoadjuvant treatment tissue blocks (resection specimens). Tissue slides from patients with a pathological complete response (i.e. Mandard 1), a near-complete response (i.e. Mandard 2) and minimal response (i.e. Mandard 4 – 5) were selected. Tissue slides from patients with a pathological complete response were selected based on reactive changes such as fibrosis. All tissue blocks were collected from the tissue bank from the Erasmus Medical Centre from patients that underwent surgery between 2010 and 2020. Tissue slices of 4 µm were cut and further processed for immunohistochemistry (IHC) staining.

### Marker selection

The following markers were selected for IHC staining: CEA, EpCAM, VEGF-α, epithelial growth factor receptor (EGFR), and c-mesenchymal-epithelial transition factor (c-MET). These markers were selected based on the (pre-)clinical availability of a fluorescent agent.

### Immunohistochemistry staining

Tissue slides were deparaffinized in xylene, and then rehydrated in a series of decreasing concentrations of diluted ethanol (100%, 70%, and 50%). The slides were rinsed with demineralized water and treated with 0.3% hydrogen peroxide (from Merck Millipore, Darmstadt, Germany) for 20 minutes at room temperature to block endogenous peroxidase. The used method for Antigen Retrieval was dependent on the protocol of the antibody (Supplementary table 1). Antigen retrieval for CEA, EpCAM was performed by heat induction at 95°C for 10 minutes using PT Link (Dako) with low-pH (pH 6.0). For c-MET and EGFR, PT Link with high-pH (pH 9.0) was used. No antigen retrieval was used for VEGF-α. The slides were incubated overnight at room temperature with the primary antibody (diluted in 1% BSA/PBS). A negative control was also incubated with 1% BSA/PBS, and tissue sections known to express the marker(s) were used as positive controls. The following day, slides were washed with PBS and then incubated with HRP-labelled secondary antibodies (either anti-mouse or anti-rabbit, both from Dako) for 30 minutes at room temperature. For staining, DAB substrate was applied for 10 minutes, and for counterstaining hematoxylin (VWR international, Amsterdam,

the Netherlands) was applied for 15 seconds. Finally, the tissue sections were dehydrated at 37°C for 60 minutes and mounted in Pertex (Histolab, Askim, Sweden).

### Scoring methods

All biopsies and surgical specimen were scored for all five tumour markers. In tissue from patients with a pathological complete response, the tumour area was selected as the tissue with therapy effect. Scoring was done according to the total immunostaining score (TIS), which consists of the intensity score (IS) and the proportion score (PS) (11). The IS represents the intensity of staining of the cells and ranges between 0 and 3 (0 = no staining; 1 = weak; 2 = moderate; 3 = strong). The PS represents the proportion of cells that is stained and ranges between 0 and 4 (0 = none; 1 = 1 – 10%; 2 = 11 – 50%; 3 = 51 – 80%; 4 = 81 – 100%). The TIS is calculated by multiplying the IS and the PS. Marker expression was categorized in low expression (TIS 0-5) and high expression (TIS 6-12). Both tumour and adjacent mucosa was scored and a tumour-to-mucosa ratio was calculated for each tissue slide. A ratio of ≥ 2 was deemed as adequate contrast.



### Statistical analysis

Statistical analysis was performed with R-studio software (version 4.1.0, R Foundation for statistical computing, Vienna, Austria). Patient characteristics were presented with descriptive statistics. Marker expression was based on the pre-treatment biopsies. Effects of nCRT was assessed by comparing TIS of pre- and post-treatment tissue samples of the same patient (i.e. paired samples). Differences in marker expression between tumour and adjacent mucosa was assessed with the Mann-Whitney U test. Differences in marker expression between the paired pre- and post-treatment tissue samples was assessed with the Wilcoxon signed rank test. A p-value < 0.05 was considered significant.

## RESULTS

Tissues of 41 patients, acquired between 2010 and 2019, were included with a total of 70 FFPE tissue blocks. In total, 31 paired pre- and post-treatment tissue samples were included and for ten patients, only the pre-treatment biopsies were available. Patient- and tumour characteristics are presented in Table 1.

**Table 1:** Patient and tissue baseline characteristics

| | | n (%) |
|---|---|---|
| **Patients** | | 41 (100) |
| **Age, years (mean (sd))** | | 67.1 (8) |
| **Gender** | *Male* | 33 (80) |
| | *Female* | 8 (20) |
| **Tumour histology** | *Adenocarcinoma* | 29 (71) |
| | *Squamous cell carcinoma* | 12 (29) |
| **Tissue available** | *Pair* | 31 (76) |
| | *Biopsy only* | 10 (24) |
| **Differentiation grade** | *Good* | 2 (5) |
| | *Good / moderate* | 5 (12) |
| | *Moderate* | 17 (42) |
| | *Moderate / poor* | 5 (12) |
| | *Poor* | 12 (29) |
| **Neoadjuvant regimen** | *CROSS* | 40 (98) |
| | *MAGIC* | 1 (2) |
| **Response** | Complete response | 14 (34) |
| | Near-complete response | 17 (42) |
| | Minimal response | 10 (24) |
| **ypT-stage** | *ypT-0* | 14 (34) |
| | *ypT-1* | 8 (19) |
| | *ypT-2* | 6 (15) |
| | *ypT-3* | 13 (32) |

## Marker expression in oesophageal adenocarcinoma biopsies and healthy mucosa

In adenocarcinoma, overexpression in tumour compared to healthy mucosa was observed for CEA (median TIS: 6 vs. 2, $p < 0.001$), EpCAM (median TIS: 8 vs. 0, $p < 0.001$), and VEGF-α (median TIS: 8 vs. 8, $p < 0.01$) (Figure 1). Out of these three markers, EpCAM had the highest tumour-to-mucosa ratio (median: 10) and the highest proportion of samples with a ratio ≥ 2 (97%) (figure 2a). Figure 3a presents representative stained tissue slide for each tumour marker on adenocarcinoma. Supplementary table 2 presents a more detailed overview of the TIS in adenocarcinomas for each tumour marker.

## Marker expression in oesophageal SCC biopsies and healthy mucosa

In SCC, overexpression in tumour compared to healthy mucosa was observed for EGFR (median TIS: 12 vs. 4, < 0.001), EpCAM (median TIS: 4 vs. 0, $p < 0.001$), and VEGF-α (median TIS: 8 vs. 8, $p < 0.01$) (Figure 1). Out of these markers, EGFR had a median tumour-to-mucosa ratio of 3, with 100% of the samples having a ratio of ≥ 2 and EpCAM had a median tumour-to-mucosa ratio of 4, with 82% of the samples having a ratio of a ratio ≥ 2 (figure 2b). c-MET and CEA were not overexpressed in oesophageal SCC compared to healthy mucosa. Figure 3b presents a representative stained tissue slide for each tumour marker. Supplementary table 2 presents a more detailed overview of the TIS in oesophageal SCC for each tumour marker.

## Marker expression in healthy tissue

Marker expression in healthy mucosa is scored and presented for adenocarcinoma and SCC combined (figure 1). VEGF-α expression was high in healthy mucosa in 73% (median TIS: 8) of the samples and EGFR expression was high in healthy mucosa in 36% (median TIS: 4) of the samples. c-MET, CEA, and EpCAM had no samples with 'high expression' in the healthy mucosa (Figure 1, Supplementary Table 2). The location of staining in the healthy tissue samples per tumour marker is summarised in Table 2.

**Table 2:** Location of staining on tumour tissue and adjacent healthy mucosa

| Tumour marker | Localisation expression in tumour | Localisation expression in healthy adjacent mucosa | Expression in other healthy tissue |
|---|---|---|---|
| **c-MET** | Membranous staining with cytoplasmic background staining | No / Minimal expression | No expression |
| **CEA** | Membranous staining with cytoplasmic background staining | Weak – moderate expression in the upper 33% of the luminal side of the epithelial cell layer. | No expression |
| **EGFR** | Membranous and cytoplasmic | Moderate expression in the first 33% – 67% of the basal and para-basal cell layer of the squamous cell epithelium. | Weak expression of 100% of the muscular layers |
| **EpCAM** | Membranous and cytoplasmic | No / Minimal expression | No expression |
| **VEGF-α** | Membranous and cytoplasmic | Moderate – strong expression in the basal cell layer, gradient weakening towards luminal side | Weak – moderate expression in 100% of the muscular layers<br><br>Weak – moderate expression in 100% of the stromal cells |

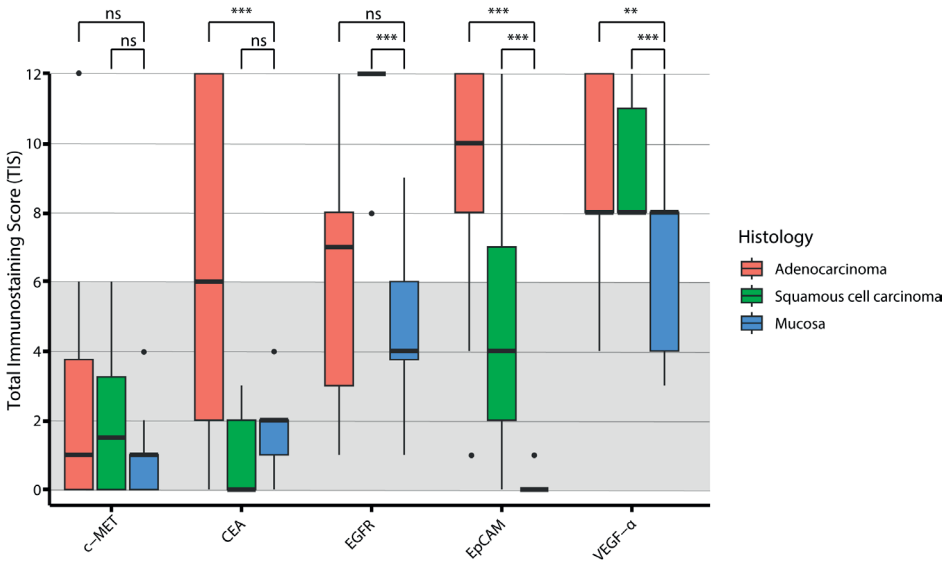


■ **Figure 1:** Total immunostaining score (TIS) per tumour marker in EAC, ESSC, and adjacent mucosa in pre-treated biopsies.
*The boxplots represent the medians with q1 and q3 with the error bars representing the range and the dots for outliers. The grey shaded box displays all the TIS < 6, indicating 'low expression'.*
*Abbreviations: ns = not significant; * = p < 0.05; ** = p < 0.01; *** = p < 0.001*

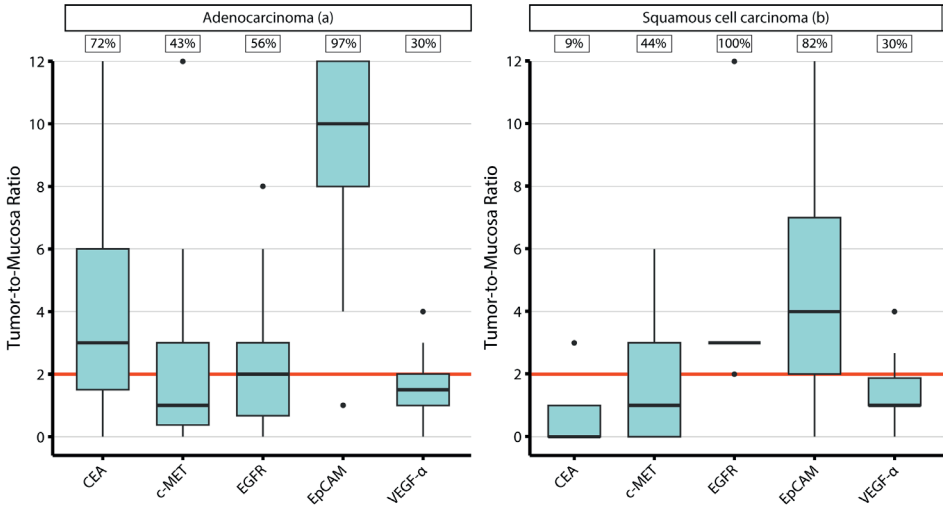


■ **Figure 2:** Median tumour-to-mucosa ratios per tumour marker oesophageal adenocarcinoma (a) squamous cell carcinoma (b).
*The boxplots represent the medians with q1 and q3 with the error bars representing the range and the dots for outliers. The percentages in the boxes present the proportion of tissue samples with a tumour-to-mucosa ratio of ≥ 2.0. The red line displays a tumour-to-mucosa ratio of 2 or higher, indicating adequate contrast.*

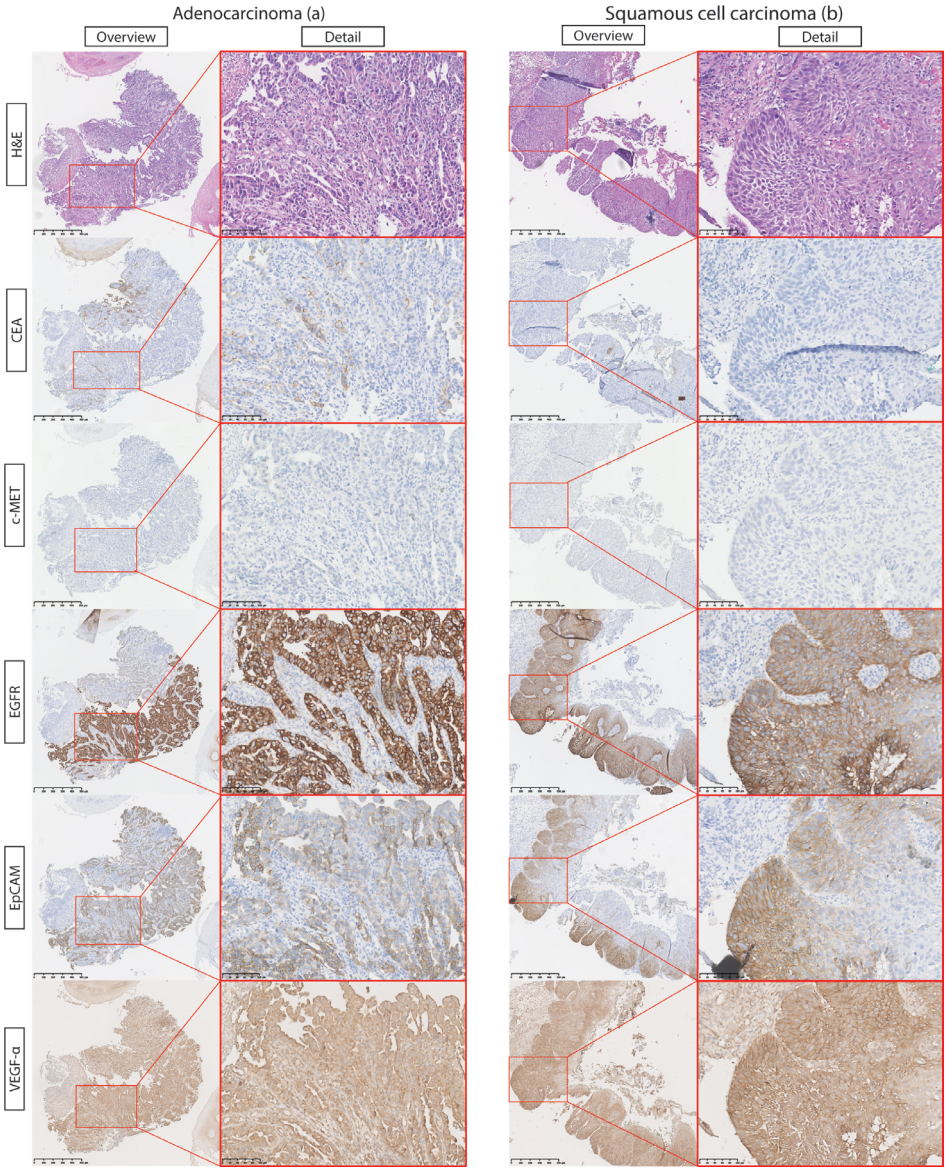


■ **Figure 3:** A representative tissue slide of an adenocarcinoma and a squamous cell carcinoma with the H&E slide and the five tumour markers

### Effects of neoadjuvant therapy on marker expression

Differences in marker expression between pre- and post-treatment samples were scored for adenocarcinoma and SCC combined. Neoadjuvant therapy did not affect expression of any of the markers. Only VEGF-α expression was observed in scar tissue of post-treatment tissue samples of patients with a pathological complete response (median TIS: 3). All other markers had no expression in the scar tissue of post-treatment tissue samples (mean TIS: 0). Supplementary Figure 1 presents an overview of tumour marker expression in paired pre- and post-treatment samples for all five tumour markers, stratified for response stage. α

## DISCUSSION

Based on IHC on tissue samples to assess tumour marker expression in oesophageal adenocarcinoma, EpCAM appears the most suitable target for tumour-specific NIR fluorescence imaging. The median TIS of 10, median tumour-to-mucosa ratio of 10, and 97% of the samples having a tumour-to-mucosa ratio ≥ 2.0 al indicate that EpCAM may be a suitable tumour marker. CEA and VEGF-α were also overexpressed in tumour compared to healthy mucosa. However, absolute CEA expression was low, with only 46% of the samples having 'high expression'. With regard to EGFR, only 56% of the samples had a tumour-to-mucosa ratio higher than 2. As such, both of these targets appear less useful for tumour-specific imaging. For oesophageal squamous cell carcinoma, EGFR appears most suitable for tumour-specific imaging as the median TIS was 12, all samples had a tumour-to-mucosa ratio higher than 2 (median 3), and all samples having 'high expression'. Despite that EGFR expression was high in 36% of the healthy tissue samples, the tumour-to-mucosa ratio indicate sufficient contrast. EpCAM expression was also significantly higher in tumour tissue than in healthy mucosa, but only 45% of the samples showed high expression. With regard to VEGF-α, high expression was observed in 96% (adenocarcinoma) and 100% (SSC) of the samples. However, this was also the case for the healthy mucosa, as 73% had high expression. This was also reflected in the median tumour-to-mucosa ratios of VEGF-α of 1.5 for adenocarcinoma and 1.0 for SCC. Moreover, stromal cells, scar tissue, and the muscle layers also had significant expression of VEGF-α. This combination makes VEGF-α a suboptimal tumour marker for tumour-specific endoscopic fluorescence imaging of oesophageal cancer.

Importantly, expression of all relevant tumour markers was not affected by neoadjuvant therapy. A patient-specific approach may therefore be feasible in which the optimal marker could be selected based on the diagnostic (i.e. pre-treatment) biopsy. In resection specimen with a pathologically complete response, no expression of the most promising tumour markers (EpCAM, EGFR, CEA) was observed in the areas with therapy effect or tumour scar tissue. Overall, these results provide promising results regarding *in vivo* NIR fluorescence imaging of oesophageal adenocarcinoma and SCC in future studies.

The immunohistochemistry results for adenocarcinoma were comparable to the results of de Gouw et al. (9), who also found overexpression of EpCAM and CEA, while only minimal expression of these markers in healthy tissue samples was observed. Although no clinical trials with endoscopic NIR fluorescence imaging for oesophageal cancer have been performed, several were performed assessing the ability to identify Barrett's segments (12-14). In all three studies, additional to conventional white light imaging, occult lesions were identified using this technique, underlining its potential. For oesophageal cancer, endoscopic NIR fluorescence imaging may be used during clinical response evaluation after neoadjuvant therapy. As approximately two thirds of the missed residual tumour lesions are located in the mucosa, endoscopic NIR fluorescence imaging may be a good candidate to improve detection of these currently missed lesions (15). The other one third of the currently missed residual tumour lesions are located in the submucosa. Depending on the depth of these lesions, they could be detected with NIR fluorescence imaging, possibly improving clinical response evaluation (7). Despite earlier detection and resection of residual disease does not appear to improve overall survival, it will result in less invasive response evaluations for these patients (16).



Besides its use during endoscopic response evaluation, tumour-specific NIR fluorescence imaging can also be performed during oesophagectomy. In general, intraoperative NIR fluorescence imaging can be used for detection of occult metastases and resection margin assessment. One such application may be to identify peritoneal metastases, in which case resection should be avoided. NIR fluorescence imaging may also aid in detection of tumour positive lymph nodes. For instance, the identification of enlarged (metastatic) lymph nodes seen on preoperative FDG-PET/CT-scan. Although we did not assess tumour marker expression in metastatic lymph nodes, a previous study showed that expression of tumour markers was highly correlated between the primary tumour and metastatic lymph nodes (9). The application of intraoperative NIR fluorescence imaging for margin assessment appears limited after oesophagectomy, as tumour positive resection margins are only reported in 5 – 7.5% of the cases (17). Besides NIR fluorescence imaging, these identified tumour markers may also be suitable for other purposes such as targeted PET-imaging or targeted therapy.

Performing IHC assessment to assess overexpression of tumour markers is an important first step in studying tumour-specific NIR fluorescence imaging of oesophageal cancer. Despite that our results providing promising targets, a good correlation between the tumour marker expression and the observed in vivo contrast of specific fluorescent tracers is not guaranteed. A variety of pharmacokinetic variables can lead to insufficient binding of the tracer to the target. Moreover, performance of a tumour-specific tracer depends on the dose and the interval between administration and imaging. Finally, clinical tracers may bind to different epitopes than the antibodies that were used for the immunohistochemistry staining. As such, the next step consists of validating these results by performing feasibility studies in vivo.

In conclusion, our results demonstrate that EpCAM and EGFR are the most promising targets for NIR fluorescence imaging of oesophageal adenocarcinoma and SCC, respectively. Neoadjuvant therapy does not negatively affect expression of the assessed markers and no expression of the most promising was observed in the tumour scar tissue. These results form an important foundation for subsequent clinical trials with tumour-specific NIR fluorescence imaging to improve tumour detection of residual oesophageal cancer after neoadjuvant therapy.

## REFERENCES


1. Bray F, Ferlay J, Soerjomataram I, Siegel RL, Torre LA, Jemal A. Global cancer statistics 2018: GLOBOCAN estimates of incidence and mortality worldwide for 36 cancers in 185 countries. CA Cancer J Clin. 2018;68(6):394-424.
2. Eyck BM, van Lanschot JJB, Hulshof M, van der Wilk BJ, Shapiro J, van Hagen P, et al. Ten-Year Outcome of Neoadjuvant Chemoradiotherapy Plus Surgery for Esophageal Cancer: The Randomized Controlled CROSS Trial. J Clin Oncol. 2021;39(18):1995-2004.
3. van Hagen P, Hulshof MC, van Lanschot JJ, Steyerberg EW, van Berge Henegouwen MI, Wijnhoven BP, et al. Preoperative chemoradiotherapy for esophageal or junctional cancer. N Engl J Med. 2012;366(22):2074-84.
4. Eyck BM, van der Wilk BJ, Noordman BJ, Wijnhoven BPL, Lagarde SM, Hartgrink HH, et al. Updated protocol of the SANO trial: a stepped-wedge cluster randomised trial comparing surgery with active surveillance after neoadjuvant chemoradiotherapy for oesophageal cancer. Trials. 2021;22(1):345.
5. van der Wilk BJ, Eyck BM, Hofstetter WL, Ajani JA, Piessen G, Castoro C, et al. Chemoradiotherapy followed by Active Surveillance Versus Standard Esophagectomy for Esophageal Cancer: A Systematic Review and Individual Patient Data Meta-Analysis. Ann Surg. 2021.
6. Eyck BM, Onstenk BD, Noordman BJ, Nieboer D, Spaander MCW, Valkema R, et al. Accuracy of Detecting Residual Disease After Neoadjuvant Chemoradiotherapy for Esophageal Cancer: A Systematic Review and Meta-analysis. Ann Surg. 2020;271(2):245-56.
7. Keereweer S, Van Driel PB, Snoeks TJ, Kerrebijn JD, Baatenburg de Jong RJ, Vahrmeijer AL, et al. Optical image-guided cancer surgery: challenges and limitations. Clin Cancer Res. 2013;19(14):3745-54.
8. Vahrmeijer AL, Hutteman M, van der Vorst JR, van de Velde CJ, Frangioni JV. Image-guided cancer surgery using near-infrared fluorescence. Nat Rev Clin Oncol. 2013;10(9):507-18.
9. de Gouw D, Rijpkema M, de Bitter TJJ, Baart VM, Sier CFM, Hernot S, et al. Identifying Biomarkers in Lymph Node Metastases of Esophageal Adenocarcinoma for Tumor-Targeted Imaging. Mol Diagn Ther. 2020;24(2):191-200.
10. Al-Kaabi A, van der Post RS, van der Werf LR, Wijnhoven BPL, Rosman C, Hulshof M, et al. Impact of pathological tumor response after CROSS neoadjuvant chemoradiotherapy followed by surgery on long-term outcome of esophageal cancer: a population-based study. Acta Oncol. 2021;60(4):497-504.
11. Spizzo G, Fong D, Wurm M, Ensinger C, Obrist P, Hofer C, et al. EpCAM expression in primary tumour tissues and metastases: an immunohistochemical analysis. J Clin Pathol. 2011;64(5):415-20.
12. Nagengast WB, Hartmans E, Garcia-Allende PB, Peters FTM, Linssen MD, Koch M, et al. Near-infrared fluorescence molecular endoscopy detects dysplastic oesophageal lesions using topical and systemic tracer of vascular endothelial growth factor A. Gut. 2019;68(1):7-10.
13. Gabriels RY, van Heijst LE, Hooghiemstra WTR, van der Waaij AM, Kats-Ugurlu G, Karrenbeld A, et al. Detection of early esophageal neoplastic Barrett lesions with quantified fluorescence molecular endoscopy using cetuximab-800CW. J Nucl Med. 2023.

**14.** de Jongh SJ, Voskuil FJ, Schmidt I, Karrenbeld A, Kats-Ugurlu G, Meersma GJ, et al. C-Met targeted fluorescence molecular endoscopy in Barrett's esophagus patients and identification of outcome parameters for phase-I studies. Theranostics. 2020;10(12):5357-67.

**15.** van der Wilk BJ, Eyck BM, Doukas M, Spaander MCW, Schoon EJ, Krishnadath KK, et al. Residual disease after neoadjuvant chemoradiotherapy for oesophageal cancer: locations undetected by endoscopic biopsies in the preSANO trial. Br J Surg. 2020;107(13):1791-800.

**16.** B.M. Eyck HCGO, B.J. van der Wilk, B.J. Noordman, B.P.L. Wijnhoven, J.J.B. van Lanschot, S.M. Lagarde. Prolonged time to surgery in patients with resdiual disease after neodjuvant chemoradiotherapy for oesophageal cancer (article in preparation). 2023.

**17.** Eyck BM, Gao X, Yang Y, van der Wilk BJ, Wong I, Wijnhoven BPL, et al. Pathological response to neoadjuvant chemoradiotherapy for oesophageal squamous cell carcinoma: multicentre East Asian and Dutch database comparison. Br J Surg. 2022;109(12):1312-8.

## SUPPLEMENTARIES

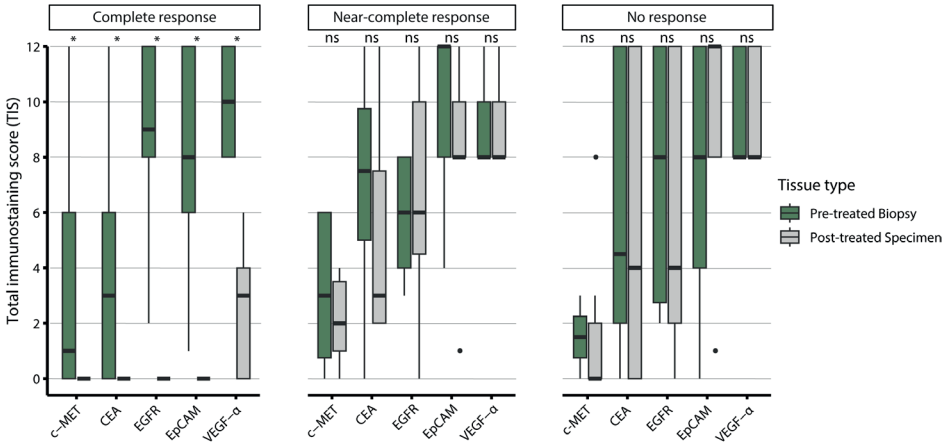


**Supplementary Figure 1:** Comparison of total immunostaining score (TIS) per tumour marker between paired pre-treated biopsies and post-treated specimen (adenocarcinoma and squamous cell carcinoma combined).
*The boxplots represent the median with q1 and q3 with the error bars representing the range and the dots for outliers. Abbreviations: ns = not significant; * = p < 0.05*

**Supplementary table 1:** An overview of the immunohistochemistry methods

| Protein abbreviation | Antibody | Company | Dilution | Antigen retrieval | Secondary antibody | Stock concentration |
|---|---|---|---|---|---|---|
| **CEA** | CI-P83-1 | Santa Cruz | 1/1000 | Dako PT link Target Retrieval Solution, pH 6.0 | Anti-mouse | 0.2 mg/ml |
| **c-MET** | EP1454Y | Abcam | 27395 | Dako PT link Target Retrieval Solution, pH 9.0 | Anti-rabbit | 0.479 mg/ml |
| **EGFR** | D38B1XP | Cell signaling technology | 1/100 | Dako PT link Target Retrieval Solution, pH 9.0 | Anti-rabbit | 0.1 mg/ml |
| **EpCAM** | MOC31 | Acris antibodies | 1/10000 | Dako PT link Target Retrieval Solution, pH 6.0 | Anti-mouse | 0.64 mg/ml |
| **VEGF-α** | G153-694 | BD Pharmingen | 18264 | No antigen retrieval | Anti-mouse | 0.5 mg/ml |

**Supplementary table 2:** A detailed overview of the TIS scores per tumour marker in pre-treated tissues, stratified for tissue histology.

| | | Low expression | | High expression | |
|---|---|---|---|---|---|
| **Tumour marker** | **Histology** | **% TIS 0 (n)** | **% TIS 1 - 5 (n)** | **% TIS 6 - 8 (n)** | **% TIS 9 - 12 (n)** |
| **c-MET** | *Adenocarcinoma* | 43% (12) | 32% (9) | 18% (5) | 7% (2) |
| | *SSC* | 38% (3) | 50% (4) | 13% (1) | 0% (0) |
| | *Mucosa* | 38% (15) | 63% (25) | 0% (0) | 0% (0) |
| **CEA** | *Adenocarcinoma* | 7% (2) | 32% (9) | 21% (6) | 39% (11) |
| | *SSC* | 64% (7) | 36% (4) | 0% (0) | 0% (0) |
| | *Mucosa* | 16% (6) | 84% (31) | 0% (0) | 0% (0) |
| **EGFR** | *Adenocarcinoma* | 0% (0) | 38% (10) | 42% (11) | 19% (5) |
| | *SSC* | 0% (0) | 0% (0) | 11% (1) | 89% (8) |
| | *Mucosa* | 8% (3) | 56% (20) | 25% (9) | 11% (4) |
| **EpCAM** | *Adenocarcinoma* | 0% (0) | 10% (3) | 40% (12) | 50% (15) |
| | *SSC* | 9% (1) | 45% (5) | 27% (3) | 18% (2) |
| | *Mucosa* | 95% (35) | 5% (2) | 0% (0) | 0% (0) |
| **VEGF-α** | *Adenocarcinoma* | 0% (0) | 4% (1) | 52% (14) | 44% (12) |
| | *SSC* | 0% (0) | 0% (0) | 70% (7) | 30% (3) |
| | *Mucosa* | 0% (0) | 27% (10) | 68% (25) | 5% (2) |

*SCC = Squamous cell carcinoma*

# Part III

## Clinical studies on intraoperative NIR fluorescence imaging in surgical oncology

# Chapter 6

## ICG-fluorescence angiography assessment of colon interposition for oesophageal cancer – a video vignette

Hidde A. Galema, Jan M. van Rees, Robert A. Matthijsen, Denise E. Hilling, Bas P.L. Wijnhoven, Sjoerd M. Lagarde

Colorectal Disease. 2022 May;24(5):665.

## ABSTRACT

Oesophageal cancer surgery is complex and carries a high risk of complications. Nowadays, a gastric conduit is the reconstruction of choice after oesophageal resection. In a limited percentage of cases a gastric conduit is not possible. Previous gastric surgery, tumour location, or iatrogenic injury to the gastroepiploic artery can all be reasons to choose a different interposition. In these cases, a colonic interposition is the best alternative for continuity restoration. This video vignette demonstrates how indocyanine green (ICG) fluorescence angiography can be used to assess perfusion of the colon interposition.

The case reported here is of a 63-year old woman who was diagnosed with oesophageal cancer for which she received neoadjuvant chemoradiotherapy followed by Ivor Lewis oesophagectomy with gastric conduit reconstruction. The procedure was complicated by a diaphragmatic hernia and an intrathoracic colon. During repair of this diaphragmatic hernia, the gastroepiploic artery was injured, leaving the gastric conduit without sufficient blood supply and necrosis as a consequence. The gastric conduit was resected, and a temporary oesophageal fistula was performed. The patient was referred to an academic medical centre for delayed restoration of continuity with a colon interposition. During surgery, 10 mg ICG was intravenously injected and an intense fluorescence signal over the whole left colon was observed. After transection of the colon, another 10 mg ICG was administered to assess perfusion of the colon interposition. Perfusion was judged as sufficient and adequate anastomoses were created. Postoperatively the patient recovered well and was able to take full oral intake after 7 weeks.

## Acknowledgements

The authors wish to thank L.J. Lauwerends for supplying the schematic figures presented in the video.

The video can be accesed through: https://bit.ly/430eSmk
or by scanning the following QR-code

(scroll down to ‘supporting information’ for the video)

# Chapter 7

# Fluorescence-guided surgery using methylene blue to improve identification of metastatic small intestinal neuroendocrine tumours

Hidde A. Galema, Tessa M. van Ginhoven, Gaston J.H. Franssen, Johannes Hofland, Claire G.O.T. Bouman, Cornelis Verhoef, Alexander L. Vahrmeijer, Merlijn Hutteman, Denise E. Hilling‡, Stijn Keereweer‡

‡Shared senior authorship

British Journal of Surgery. 2023 Apr 12;110(5):541-544. doi: 10.1093/bjs/znad043.

## ABSTRACT

### Introduction

Small intestinal neuroendocrine tumours (SI-NETs) often present with multiple primaries and metastatic disease. Detection of multiple primaries and metastases is important, as complete resection of all tumours is the only curative treatment. Resection in asymptomatic patients with irresectable disease should be refrained from. Intraoperative near-infrared (NIR) fluorescence imaging might improve visualisation of SI-NETs and thereby improve patient selection for surgery. The aim of this prospective clinical trial was to investigate if SI-NETs and metastatic lesions could be detected by intraoperative fluorescence imaging using methylene blue as a contrast agent.

### Methods

Seventeen patients undergoing open resection of SI-NETs were included in this prospective clinical trial. Intravenous methylene blue was intraoperatively administered followed by NIR fluorescence imaging. The primary endpoint was tumour-to-background ratio (TBR) of the primary tumour. Among the secondary endpoints were the TBR of metastatic lesions (lymph node, peritoneal, and liver metastases), and the number of extra lesions found.

### Results

Seventeen primary tumour lesions, with a median TBR of 1.10 (IQR: 1.00–1.17), were identified. None of the primary tumours or the multiple primaries had a TBR ≥ 1.5. A total of 109 metastatic lesions were identified, of which 101 (93%) had a TBR ≥ 1.5 (median TBR: 1.90 (IQR: 1.71–2.01)). Based on NIR fluorescence imaging, additional peritoneal metastases were found in three patients.

### Discussion

NIR fluorescence imaging after methylene blue administration can be used to improve visualisation of peritoneal metastases, liver metastases, and mesenteric masses of SI-NETs. Methylene blue does not appear to be useful for detection of the primary tumour or occult multiple primaries.

## INTRODUCTION

Small intestinal neuroendocrine tumours (SI-NETs) are rare tumours with a prevalence of 1 per 100 000 patients per year (1). SI-NETs typically grow slowly, resulting in the majority of patients presenting with advanced local disease and distant metastases (2, 3). Multiple primary tumours are common in SI-NETs and are present in up to 50% of the patients (4). Staging of SI-NETs is of paramount importance, as surgery is only indicated for patients with resectable disease (curative), or for patients with irresectable disease and symptoms caused by local tumour growth or hormone production (palliative). In general, resection of any tumour lesion in asymptomatic patients with irresectable disease should not be performed (5).

Current preoperative staging usually includes nuclear imaging with a $^{68}$Gallium-labelled somatostatin analogue (SSA) PET/CT scan. However, minor peritoneal- or lymph node metastases or multiple primaries can be too small to be detected with preoperative imaging and can therefore be missed. Therefore, the international guideline states that curative surgery should be performed via laparotomy in order to perform palpation of the whole abdominal cavity for intraoperative staging, prior to proceeding with curative resection (5, 6). Despite this extensive procedure to optimally select patients for curative surgery, recurrence is common. Recurrence rates of 9% after 1 year and over 50% after 10 years are reported (7). Most disease recurrence occurs in the liver or the peritoneum, with a small proportion of patients developing recurrence in the small bowel (8).This may indicate that with the current staging protocol, small tumour deposits are still being missed. Better pre- and intraoperative visualization of SI-NETs could possibly improve detection of clinically occult lesions and increase complete resection rates. Improved intraoperative visualisation prior to resection could lead to better patient selection for curative-intended surgery, as surgical resection in asymptomatic patients who have irresectable disease can be avoided.



Near-infrared (NIR) fluorescence imaging is an imaging modality that can be used to improve visualisation of tumours and vital structures during surgery (9). It can be used in both an open and a laparoscopic setting. A fluorescent contrast agent is required to image the structures of interest, which is generally administered systemically (10). Methylene blue is a blue dye that has been used off-label for fluorescence imaging purposes. Although methylene blue is primarily used as a blue dye, with no completely understood targeting properties, specific imaging of occult pancreatic NETs (PNETs) has been described in a case report and a preclinical study (11, 12). The aim of this study is to investigate if SI-NETs can be detected with intraoperative fluorescence imaging using methylene blue as a fluorescent contrast agent.

## METHODS

This study was reviewed and approved by the medical ethical committee of the Erasmus medical centre (MEC-2021-0021, METC Erasmus MC) and was conducted according to the declaration of Helsinki (10th version, Fortaleza, 2013). The trial was registered in the International Clinical Trials Registry Platform (ICTRP, https://trialsearch.who.int) under registration code 'NL9305'.

Seventeen consecutive patients with SI-NETs eligible for surgery were included and chronologically assigned to one of the two dosing groups. The first five patients received a dose of 0.5 mg/kg methylene blue, after which another five patients received a dose of 1.0 mg/kg methylene blue. Doses were selected based on earlier studies with methylene blue (12, 13). Next, an interim analysis was performed to decide the optimal dose based on the tumour-to-background ratio (TBR) of the primary tumour and metastatic lesions. Patients 11 to 17 were assigned to the extension cohort with the optimal dose.

### Patient selection

All patients with a radiologically ($^{68}$Ga-DOTATATE-PET-CT positive lesions) or a biopsy proven SI-NET, with the primary tumour in situ, scheduled for either curative or palliative surgery via laparotomy, were eligible for inclusion. Exclusion criteria were the use of selective serotonin reuptake inhibitors (SSRIs), serotonin noradrenalin reuptake inhibitors (SNRIs), tricyclic antidepressants (TCAs), Bupropion, Buspiron, serotonergic party drugs, Glucose-6-Phosphate Dehydrogenase (G6DP) deficiency, a clinically overt carcinoid syndrome, a clinically significant history of allergic reaction to methylene blue, and females who were pregnant, breastfeeding, or of childbearing potential without adequate contraceptives.

### Endpoints

The primary endpoint of this study was the *in vivo* TBR of the primary tumour. A TBR of ≥ 1.5 was defined as fluorescence positive (14). Secondary endpoints were the TBR of occult multiple primaries, the TBR of metastatic lesions, the optimal dose of methylene blue, and the optimal time frame in which the tumour could be visualised. Occult primaries were defined as preoperatively undetected tumours in the small bowel, detected during surgery (visualisation, palpation, and/or fluorescence imaging) or postoperatively by the pathologist.

### Surgical protocol

All patients received a standard midline laparotomy, followed by inspection of the abdominal cavity and identification of the primary tumour. Thereafter, manual and visual assessment of lymph node, liver, peritoneal, and small bowel status was performed. The surgical approach (i.e. curative vs palliative intent) was defined prior to fluorescence measurements.

### Near-infrared fluorescence imaging protocol

After completing the standard surgical assessment and locating the primary tumour, the fluorescence camera was installed on the stabilized arm with optimal view of the primary tumour at a standardized 20 – 30 cm distance of the surgical field. Then, undiluted (10 mg/ml) methylene blue was intravenously administered in three to five minutes and for the following ten minutes a snapshot of the primary SI-NET was taken every minute. Between these snapshots, single snapshots were taken of the clinically suspected metastatic lesions and/or multiple primaries. Finally, the abdominal cavity was screened for clinically occult metastases with the fluorescence camera. Biopsies were taken from occult lesions to correlate with histopathology as long as the biopsy did not pose any risk to the patient. *In vivo* and *ex vivo* back-table imaging fluorescence imaging was performed with the Quest Spectrum V2 fluorescence camera (Quest Medical Imaging, Middenmeer, The Netherlands). Closed-field imaging was performed with the Pearl trilogy imaging system or the Odyssey CLx (Li-Cor, Lincoln, Nebraska, USA). TBRs were calculated with Quest software.

### Statistics

Statistical analyses were performed with R-studio software (version 4.1.0, R Foundation for statistical computing, Vienna Austria). Patient demographics, TBRs, and mean fluorescence intensity (MFI) were reported in median with interquartile range (IQR). A Wilcoxon rank test was done to assess statistical difference between dosing groups and a one-way ANOVA test was performed for difference in timing intervals.



## RESULTS

The study comprised 12 males and 5 females with a median age of 60 years (IQR: 50 – 72). Ten patients underwent surgery with curative intent and seven patients underwent palliative surgery. A small bowel resection was performed in 12 patients and a right hemicolectomy was performed in five patients. All patient characteristics are presented in Table 1.

**Table 1:** Patient characteristics

| | | N (%) |
|---|---|---|
| **Gender** | *Female* | 5 (29) |
| | *Male* | 12 (71) |
| **Age (median [IQR])** | | 60 [50 - 72] |
| **Surgery performed*** | *Small bowel resection* | 12 |
| | *Right hemicolectomy* | 5 |
| | *Jejuno-jejunostomy bypass* | 1 |
| **Indication for surgery** | *Curative* | 10 (59) |
| | *Palliative* | 7 (41) |
| **pT stage** | *1* | 0 (0) |
| | *2* | 3 (18) |
| | *3* | 5 (29) |
| | *4* | 9 (53) |
| **pN stage** | *0* | 1 (6) |
| | *1* | 7 (41) |
| | *2* | 9 (53) |
| **M stage** | *0* | 9 (53) |
| | *1* | 8 (47) |
| **WHO classification** | *1* | 7 (41) |
| | *2* | 9 (53) |
| | *3* | 1 (6) |

**One patient underwent a combined small bowel resection and right hemicolectomy*
*Abbreviations: NEC: neuroendocrine carcinoma*

## Primary SI-NETs

Seventeen primary tumour lesions were detected with pre-operative imaging. All primary tumours were histopathological confirmed SI-NETs. Median TBR of the primary tumours was 1.10 (IQR: 1.00 – 1.13, Figure 1). None of the primary tumour lesions met the predetermined criterion (TBR ≥ 1.5) for fluorescence positive.

## Multiple primaries

Six multiple primary lesions were intraoperatively identified after inspection and palpation of the abdominal cavity. Median TBR was 1.16 (IQR: 1.04 – 1.18) and none had a TBR of ≥ 1.5. No occult multiple primaries were detected with fluorescence imaging. After histopathological assessment of the resected bowel specimens, 37 occult primaries (median 4, range: 2 – 20) were detected by the pathologist in five patients. These tumours were not identified

with regular intraoperative white light inspection, nor with fluorescence imaging. In two of those five patients a curative intended resection was performed. Altogether, eight patients had multiple primaries.

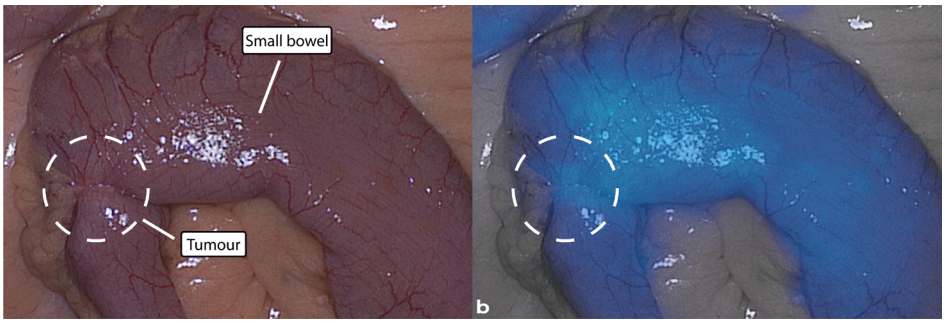


**Figure 1:** A representative image of a primary tumour
*White light (left panels) and gradient fluorescence overlay (right panels) images*

**Table 2:** Characteristics of all metastatic lesions, stratified by lesion type

| Lesion type | N (patients, (%)) | N (lesions) | TP (%) | FN (%) | FP (%) | TBR (median (IQR))* | Occult lesions identified with FLI (% of patients) | Figure |
|---|---|---|---|---|---|---|---|---|
| **Primary tumours** | 16 (94) | 17 | 0 (0) | 17 (100) | 0 (0) | 1.10 (0.99 - 1.17) | 0 (0) | S1 |
| **Multiple primaries** | 8 (47) | 43 | 0 (0) | 43 (100) | 0 (0) | 1.16 (1.04 - 1.18) | 0 (0) | - |
| **Peritoneal metastases** | 4 (24) | 82 | 76 (94) | 5 (6) | 0 (0) | 1.88 (1.70 - 2.05) | 3 (18) | 1 |
| **Liver metastases** | 2 (12) | 14 | 13 (93) | 1 (7) | 0 (0) | 2.13 (1.89 - 2.46) | 0 (0) | 1 |
| **Mesenteric masses** | 13 (76) | 13 | 11 (85) | 2 (15) | 0 (0) | 1.91 (1.60 - 2.12) | 0 (0) | S3 |
| **Lymph nodes** | 4 (24) | 6 | 1 (17) | 0 (0) | 5 (83) | 1.78 | 1 (6) | S5 |

*Abbreviations: TP: true positives | FP: false positives | FN: false negatives | FLI: fluorescence imaging |S: Supplementary figure*
** benign lesions (i.e. false positives) were excluded from TBR analysis.*

## Metastatic lesions

In total, 125 lesions suspect for metastases were identified during surgery with white light inspection or fluorescence imaging. One hundred and fifteen lesions were resected or biopsied, of which 109 were histopathological proven SI-NET and six lesions were benign. Ten lesions were not biopsied and could therefore not be correlated with histopathology. Out of the 109 confirmed SI-NETs metastases, 101 lesions (93%) were detected with fluorescence imaging with a TBR >1.5 (true positives). Median TBR for all metastatic SI-NET lesions was 1.90 (IQR: 1.71 – 2.01, Figure 2, Figure 3). In the eight metastatic lesions with a TBR <1.5 (false

negatives), the median TBR was 1.36 (IQR: 1.31 – 1.47). In three patients with overt peritoneal metastasis, fluorescence imaging showed additional peritoneal lesions, not affecting the surgical strategy (Figure 2a, b, e, f). Six benign lesions were biopsied or resected. Five of these were lymph nodes and were resected based on positive fluorescence signal, but were benign (false positives) and one was malignant (true positive, Supplementary Figure 1). These lymph nodes were not identified with regular white light inspection and were not suspect for metastatic lymph nodes. Ten similar, potential false positive lymph nodes were identified but not biopsied due to low clinical suspicion and the explorative design of the study. One benign peritoneal lesion was clinically suspect to be a peritoneal metastasis, but fluorescence negative (true negative, Figure 4). Table 2 presents a specified overview of the metastatic lesions and the characteristics, stratified by lesion type.

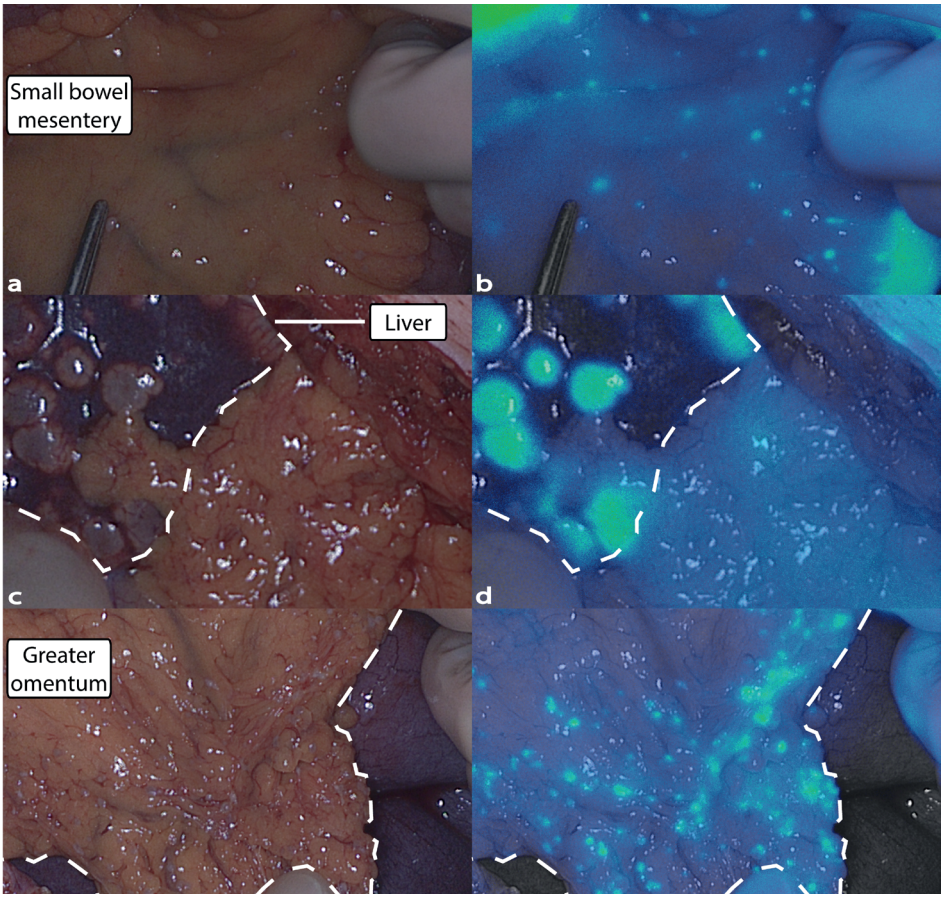


■ **Figure 2:** Representative images of metastases
*Images of metastases in a small bowel, b liver, and c greater omentum shown in white light (left panels) and gradient fluorescence overlay (right panels)*

## Methylene blue dose

After ten patients, an interim analysis was performed to determine the optimal dose of methylene blue (0.5 mg/kg vs 1.0 mg/kg). Median TBRs of the primary tumours were 1.00 and 1.15 respectively (p=0.22). For metastatic lesions, median TBRs were 1.54 and 2.11 respectively ($p < 0.01$). Based on the TBR for metastatic lesions, the 1.0 mg/kg cohort was expanded with seven more patients.

After final analysis of all patients, there was no difference in median TBR of the primary tumours between the 0.5 mg/kg and 1.0 mg/kg group (1.00 vs. 1.11, p=0.55). For metastatic lesions, a higher median TBR was found in patients that received 1.0 mg/kg of methylene blue (1.54 vs. 1.91, p=0.02). Supplementary Figure 2 presents median TBRs with (interquartile) range stratified for methylene blue dose and lesion type.

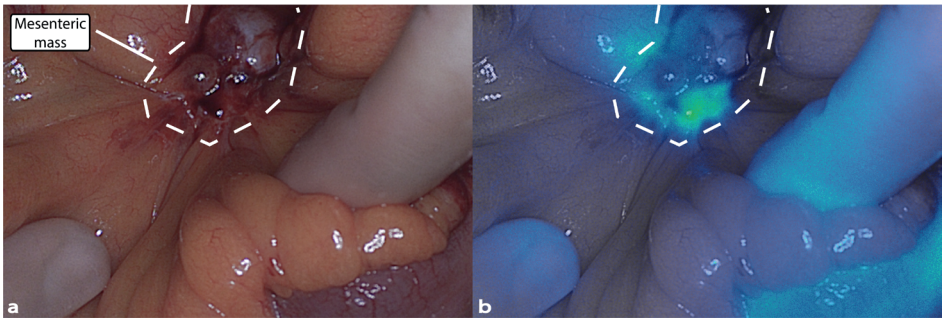


**Figure 3:** Representative image of a mesenteric mass
*White light (left panels) and gradient fluorescence overlay (right panels) images*

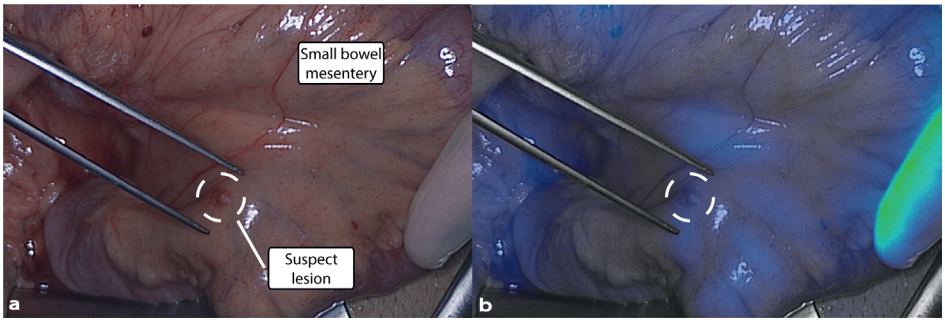


**Figure 4:** A clinically suspect, non-fluorescent peritoneal lesion that was proven benign by frozen section (true negative)
*White light (left panels) and gradient fluorescence overlay (right panels) images*

### Time frame for imaging

The median TBR of primary tumours did not significantly peak within the first ten minutes (p=0.968). Median time between methylene blue administration and imaging of metastatic lesions was 8 minutes (IQR: 4.5 – 11 minutes). To assess whether the optimal time frame for imaging was beyond 10 minutes after injection, delayed imaging of primary tumours and metastases was performed in five patients. Imaging between 20 and 34 minutes after injection resulted in absence of fluorescence signal of both tumour and background, indicating clearance of the fluorophore in both the tumour and the surrounding healthy tissue. Back-table imaging and closed-field imaging of the specimen and tissue slides confirmed these results.

### Absolute fluorescence intensity

The median MFI for tumour of primary tumour lesions and metastatic lesions were 58.06 (IQR: 47.80 – 102.55) and 78.93 (IQR: 63.84 – 91.08) respectively (p = 0.32). Median MFI for background of primary tumour lesions and metastatic lesions were 59.17 (IQR: 46.58 – 102.21) and 45.71 (IQR: 37.10 – 45.71) respectively (p > 0.001).

## DISCUSSION

The aim of this study was to investigate if primary SI-NETs could be detected with intraoperative NIR fluorescence imaging using methylene blue as a contrast agent. Results showed that primary tumours and multiple primaries could not be detected with NIR fluorescence imaging. Small lymph nodes in the mesentery were fluorescent, but this seemed not to be specific for metastasis as five out of six biopsied lymph nodes were tumour negative. On the contrary, peritoneal metastases, liver metastases, and mesenteric masses showed excellent fluorescence signal. Out of all metastatic lesions, 93% had a positive fluorescent signal (TBR ≥ 1.5) and in three patients additional metastases were found. Interestingly, one clinically suspect peritoneal lesion that was fluorescence negative was proven benign by frozen section analysis. Although this was only one lesion, it suggests that methylene blue selectively stains malignant lesions and not benign peritoneal lesions. Altogether, there seems to be a role for NIR fluorescence imaging with methylene blue for improved staging of SI-NET distant metastases. Especially when considering that, according to current literature, the majority of disease recurrences present in the liver or the peritoneum. By using this technique, small occult metastases could potentially be detected intraoperatively to guide the surgeon in determining the operative strategy. A laparoscopic approach with NIR fluorescence imaging and methylene blue cannot be advised as primary tumours and multiple primaries will be missed. Our results confirm that multiple primaries are common, and even after extensive inspection and palpation of the complete small bowel, these lesions are challenging to identify. In this study, eight patients (47%) had multiple primaries and in five of those patients these were not detected pre- or intraoperatively. Importantly, in two of ten patients in whom

surgery with curative intent was performed, occult multiple primaries were detected during histopathology assessment.

We found that imaging of metastatic lesions with methylene blue was dose-dependent: a dosage of 1.0 mg/kg resulted in a higher median TBR of 1.91. Time window to image metastatic lesions was mostly between four and eleven minutes after administration of methylene blue. Since our study protocol was designed to find to optimal time window of imaging of the primary tumour, the exact optimal time window for imaging of metastases could not be determined. Therefore, we hypothesise that TBRs and fluorescence positive rates of metastases would be higher if imaging of all lesions was performed within an optimal and standardized time window.

As the methylene blue compound could not be traced anymore in the *ex vivo* specimens, mechanism behind the tumour-specific imaging of methylene blue in SI-NET metastases remains unclear. We hypothesize that the enhanced permeability and retention (EPR) effect could be responsible for the targeting mechanism (15). Because of a lack of specific binding, a common issue of the EPR effect is that no residual tracer can be detected after *ex vivo* tissue processing. Next, the observed difference in TBR between primary tumour lesions and metastatic lesions could have been caused by a 'background problem' instead of a lack of uptake by tumour tissues. Since healthy bowel tissue is well perfused, high fluorescence intensities of the healthy bowel (background) were observed with subsequent low contrast ratios. Absolute fluorescence intensity of metastatic lesions was not higher compared to primary tumour lesions, but background intensity of metastatic lesions was significantly lower. Although a longer washout period might theoretically overcome this problem, our results demonstrated that all fluorescence signals (i.e. both tumour and background) had been washed out after approximately 30 minutes.



In current literature, there are no studies regarding NIR fluorescence imaging with methylene blue for detection of SI-NET. One case report described the use of methylene blue for detection of multiple pancreatic NETs, as well as a pre-clinical study in ten mice (11, 12). Handgraaf *et al*. reported on a patient with a pancreatic NET who was injected with 0.5 mg/kg methylene blue. After several minutes, multiple additional primary NETs were observed with fluorescence imaging, and the procedure was aborted because of this finding. In contrast to the small bowel, primary tumours of the pancreas appear to be well detected by this technique. Possibly, perfusion status, and thus background staining of the pancreas is more similar to the peritoneum or liver than the small bowel.

Tumour-specific tracers are currently being developed for multiple solid cancers to improve intraoperative detection, but no tumour-specific tracers have yet been studied for SI-NETs

(9). Interestingly, Dijkstra *et al.* recently published their pre-clinical results of a somatostatin receptor 2 ($SSTR_2$) targeted molecular fluorescence tracer for the detection of meningioma. This tracer might also be suitable for detection of SI-NETs, as the $SSTR_2$ is also the target of choice for current pre-operative staging with $^{68}$Ga-DOTA-SSA PET/CT scan (16). The majority of SI-NETs express $SSRT_2$, but approximately 17% of the tumours have no or low expression (17). Since the tracer is labelled with an 800nm fluorophore (IRDye800CW), dual-wavelength imaging with methylene blue (~700 nm) may be feasible, which could yield complementary information (18). Future studies should demonstrate if such tracers can detect (multiple) primaries and metastases of SI-NETs.

A limitation of the use of methylene blue is that the detection of fluorescent signals in the ~700 nm wavelength region is compromised by tissue optical properties and autofluorescence effects (10). In our series, autofluorescence was indeed observed, further hampering the delineation of the primary tumours.

In conclusion, NIR fluorescence imaging with methylene blue may improve intraoperative detection of metastatic lesions of SI-NETs, and in particular peritoneal- and liver metastases. Detection of the primary tumour and occult multiple primaries is not possible with this contrast agent. There is a clinical need for development and clinical validation of tumour-targeted tracers to improve intraoperative identification of SI-NETs and thereby improve the care of these patients with SI-NETs.

## REFERENCES


1. Wu L, Fu J, Wan L, Pan J, Lai S, Zhong J, Chung DC, Wang L. Survival outcomes and surgical intervention of small intestinal neuroendocrine tumours: a population based retrospective study. *Oncotarget* 2017;**8**(3): 4935-4947.
2. Keck KJ, Maxwell JE, Utria AF, Bellizzi AM, Dillon JS, O'Dorisio TM, Howe JR. The Distal Predilection of Small Bowel Neuroendocrine Tumours. *Ann Surg Oncol* 2018;**25**(11): 3207-3213.
3. Snorradottir S, Asgeirsdottir A, Rögnvaldsson S, Jonasson JG, Björnsson ES. Incidence and prognosis of patients with small intestinal neuroendocrine tumours in a population based nationwide study. *Cancer Epidemiol* 2022;**79**: 102197.
4. Gangi A, Siegel E, Barmparas G, Lo S, Jamil LH, Hendifar A, Nissen NN, Wolin EM, Amersi F. Multifocality in Small Bowel Neuroendocrine Tumours. *J Gastrointest Surg* 2018;**22**(2): 303-309.
5. Howe JR, Cardona K, Fraker DL, Kebebew E, Untch BR, Wang YZ, Law CH, Liu EH, Kim MK, Menda Y, Morse BG, Bergsland EK, Strosberg JR, Nakakura EK, Pommier RF. The Surgical Management of Small Bowel Neuroendocrine Tumours: Consensus Guidelines of the North American Neuroendocrine Tumour Society. *Pancreas* 2017;**46**(6): 715-731.
6. Niederle B, Pape UF, Costa F, Gross D, Kelestimur F, Knigge U, Öberg K, Pavel M, Perren A, Toumpanakis C, O'Connor J, O'Toole D, Krenning E, Reed N, Kianmanesh R, Vienna Consensus Conference p. ENETS Consensus Guidelines Update for Neuroendocrine Neoplasms of the Jejunum and Ileum. *Neuroendocrinology* 2016;**103**(2): 125-138.
7. Blažević A, Zandee WT, Franssen GJH, Hofland J, van Velthuysen MF, Hofland LJ, Feelders RA, de Herder WW. Mesenteric fibrosis and palliative surgery in small intestinal neuroendocrine tumours. *Endocr Relat Cancer* 2018;**25**(3): 245-254.
8. Folkestad O, Wasmuth HH, Mjønes P, Fougner R, Hauso Ø, Fossmark R. Survival and disease recurrence in patients operated for small intestinal neuroendocrine tumours at a referral hospital. *Surg Oncol* 2020;**35**: 336-343.
9. Mieog JSD, Achterberg FB, Zlitni A, Hutteman M, Burggraaf J, Swijnenburg RJ, Gioux S, Vahrmeijer AL. Fundamentals and developments in fluorescence-guided cancer surgery. *Nat Rev Clin Oncol* 2022;**19**(1): 9-22.
10. Keereweer S, Van Driel PB, Snoeks TJ, Kerrebijn JD, Baatenburg de Jong RJ, Vahrmeijer AL, Sterenborg HJ, Löwik CW. Optical image-guided cancer surgery: challenges and limitations. *Clin Cancer Res* 2013;**19**(14): 3745-3754.
11. Winer JH, Choi HS, Gibbs-Strauss SL, Ashitate Y, Colson YL, Frangioni JV. Intraoperative localization of insulinoma and normal pancreas using invisible near-infrared fluorescent light. *Ann Surg Oncol* 2010;**17**(4): 1094-1100.
12. Handgraaf HJM, Boogerd LSF, Shahbazi Feshtali S, Fariña Sarasqueta A, Snel M, Swijnenburg RJ, Vahrmeijer AL, Bonsing BA, Mieog JSD. Intraoperative Near-Infrared Fluorescence Imaging of Multiple Pancreatic Neuroendocrine Tumours: A Case Report. *Pancreas* 2018;**47**(1): 130-133.
13. Patel HP, Chadwick DR, Harrison BJ, Balasubramanian SP. Systematic review of intravenous methylene blue in parathyroid surgery. *Br J Surg* 2012;**99**(10): 1345-1351.
14. Azargoshasb S, Boekestijn I, Roestenberg M, KleinJan GH, van der Hage JA, van der Poel HG, Rietbergen DDD, van Oosterom MN, van Leeuwen FWB. Quantifying the Impact of Signal-to-background Ratios on Surgical Discrimination of Fluorescent Lesions. *Mol Imaging Biol* 2022.

**15.** Wu J. The Enhanced Permeability and Retention (EPR) Effect: The Significance of the Concept and Methods to Enhance Its Application. *J Pers Med* 2021;**11**(8).

**16.** Dijkstra BM, de Jong M, Stroet MCM, Andreae F, Dulfer SE, Everts M, Kruijff S, Nonnekens J, den Dunnen WFA, Kruyt FAE, Groen RJM. Evaluation of Ac-Lys(0)(IRDye800CW)Tyr(3)-octreotate as a novel tracer for SSTR(2)-targeted molecular fluorescence guided surgery in meningioma. *J Neurooncol* 2021;**153**(2): 211-222.

**17.** Elf AK, Johanson V, Marin I, Bergström A, Nilsson O, Svensson J, Wängberg B, Bernhardt P, Elias E. Evaluation of SSTR2 Expression in SI-NETs and Relation to Overall Survival after PRRT. *Cancers (Basel)* 2021;**13**(9).

**18.** Keereweer S, Mol IM, Vahrmeijer AL, Van Driel PB, Baatenburg de Jong RJ, Kerrebijn JD, Löwik CW. Dual wavelength tumour targeting for detection of hypopharyngeal cancer using near-infrared optical imaging in an animal model. *Int J Cancer* 2012;**131**(7): 1633-1640.

## SUPPLEMENTARIES

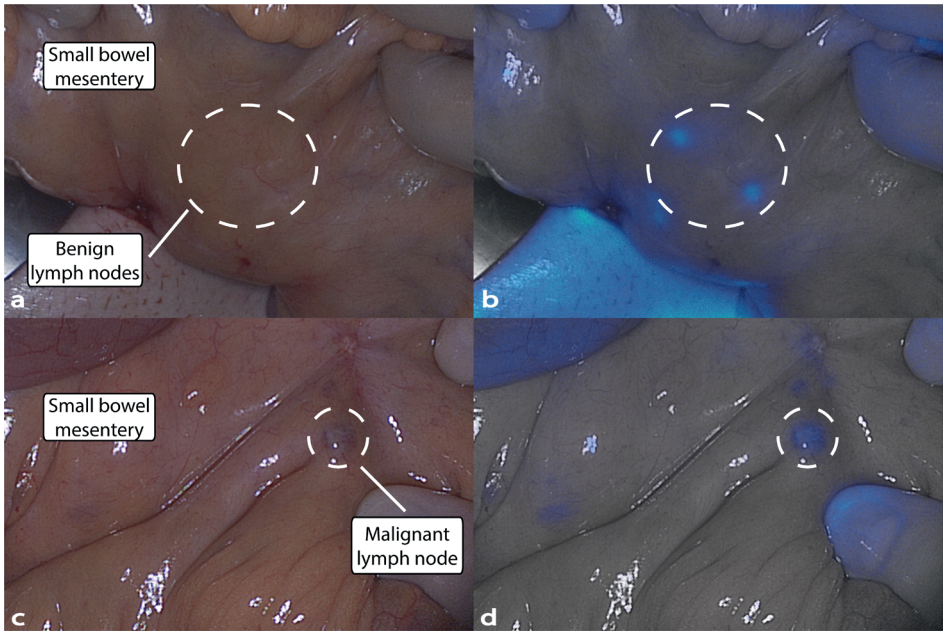


■ **Supplementary Figure 1:** Representative images of clinically non suspect, fluorescence positive lymph nodes that were benign (a,b, false positives) and malignant (c, d, true positives)
*white light view (left panels) and the gradient fluorescence overlay (right panels) images*

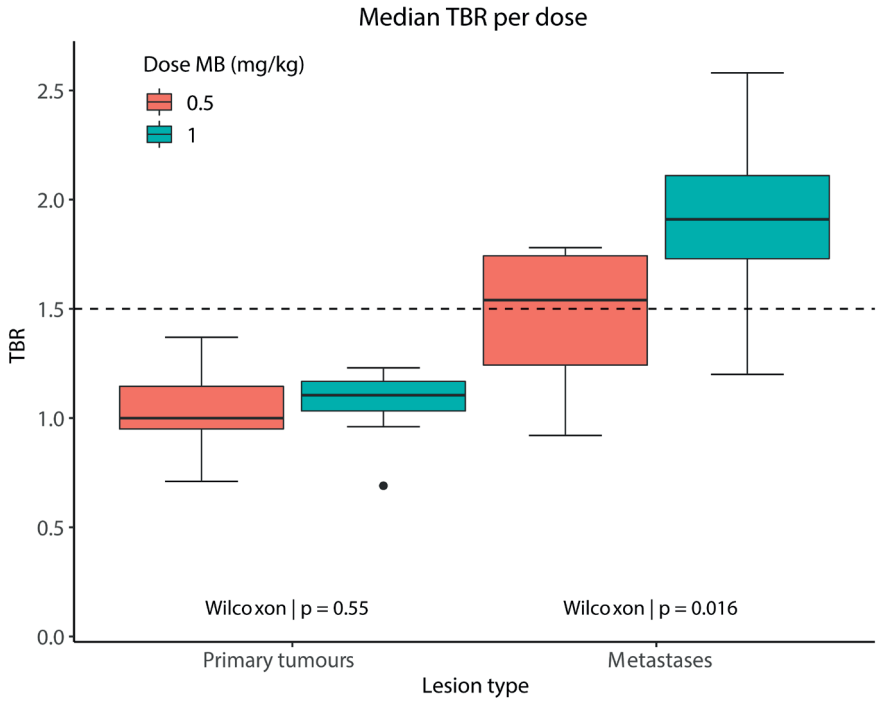


■ **Supplementary Figure 2:** Tumour-to-background ratios (TBR) stratified by dose for primary tumours and metastases

*The boxes represent medians with q1 and q3 and the error bars represent the range.*

# Chapter 8

# Intraoperative molecular imaging of colorectal lung metastasis with SGM-101: an exploratory study

Hidde A. Galema*, Ruben P.J. Meijer*, Robin A. Faber, Okker D. Bijlstra, Alexander P.W.M. Maat, Françoise Cailler, Jerry Braun, Stijn Keereweer, Denise E. Hilling, Jacobus Burggraaf, Alexander L. Vahrmeijer, Merlijn Hutteman

*Shared first authorship

**On behalf of the SGM-CLM study group:** Mats I. Warmerdam, Feredun Azari, Sunil Singhal, Dima D.A. Almandawi, Edris A.F. Mahtab, Ghada M.M. Shahin, Michail Doukas, Cornelis Verhoef, Bérénice Framery

European Journal of Nuclear Medicine and Molecular Imaging. 2023 Aug 8. doi: 10.1007/s00259-023-06365-3.

## ABSTRACT

### Purpose

Metastasectomy is a common treatment option for patients with colorectal lung metastases (CLM). Challenges exist with margin assessment and identification of small nodules, especially during minimally invasive surgery. Intraoperative fluorescence imaging has the potential to overcome these challenges. The aim of this study was to assess feasibility of targeting CLM with the carcinoembryonic antigen (CEA) specific fluorescent tracer SGM-101.

### Methods

This was a prospective, open-label feasibility study. The primary outcome was the number of CLM that showed a true positive fluorescence signal with SGM-101. Fluorescence positive signal was defined as a signal-to-background ratio (SBR) ≥ 1.5. A secondary endpoint was the CEA expression in the colorectal lung metastases, assessed with the immunohistochemistry and scored by the total immunostaining score.

### Results

Thirteen patients were included in this study. Positive fluorescence signal with *in vivo*, back table and closed-field bread loaf imaging was observed in 31%, 45% and 94% of the tumours respectively. Median SBRs for the three imaging modalities were 1.00 (IQR: 1.00 – 1.53), 1.45 (IQR: 1.00 – 1.89) and 4.81 (IQR: 2.70 – 7.41). All tumour lesions had a maximum total immunostaining score for CEA expression of 12/12.

### Conclusion

This study demonstrated the potential of fluorescence imaging of CLM with SGM-101. CEA expression was observed in all tumours and closed-field imaging showed excellent CEA specific targeting of the tracer to the tumour nodules. The full potential of SGM-101 for *in vivo* detection of the tracer can be achieved with improved minimal invasive imaging systems and optimal patient selection.

## INTRODUCTION

Around 5% of the patients with colorectal cancer (CRC) develop lung metastases after treatment with curative intent (1, 2). For selected, oligo-metastatic patients, metastasectomy is an important treatment option so long as the primary disease is under control. Tumour identification during metastasectomy is sometimes challenging, as nodules can be small. Positive margins are associated with decreased overall survival, which makes complete removal of the tumour of utmost importance (3). While the introduction of video-assisted thoracic surgery (VATS) has reduced surgical morbidity, tumour identification has become more challenging. Therefore, interest is growing in other methods for intraoperative detection of colorectal lung metastases (CLM).

Intraoperative, tumour-specific, near-infrared (NIR) fluorescence imaging is developed for several surgical procedures, including lung surgery (4). To realize NIR fluorescence tumour imaging, patients are administered intravenously with a tumour-specific tracer attached to a fluorophore. Imaging of these agents with a fluorescence imaging system allows for real-time intraoperative visualization of the tumour (5). SGM-101 is a fluorescent tracer that consists of a monoclonal antibody that targets carcinoembryonic antigen (CEA), labelled with a NIR fluorophore (BM-104). This fluorophore has an excitation and emission wavelength around 700 nm (6). CEA is overexpressed in >95% of the colorectal cancers and thus an excellent target for molecular imaging of CRC (7). NIR fluorescence imaging of CLM with SGM-101 may improve intraoperative detection of these tumours and thus increase the chance of a complete resection of the tumour.



Intraoperative NIR fluorescence imaging with SGM-101 has been studied in trials for locally advanced CRC, peritoneal metastases of CRC, colorectal liver metastases, and pancreatic cancer (8-12). In a phase II rectal cancer trial, NIR fluorescence imaging with SGM-101 resulted in a change in surgical plan in 7 out of 37 patients. Currently, two phase III trials are ongoing with SGM-101 for CRC and peritoneal metastases (13, 14). The aim of this study was to assess the potential of targeting CLM with SGM-101.

## METHODS

This study was reviewed and approved by the medical ethical committee ‘Leiden-Den Haag-Delft’ and conducted according to the declaration of Helsinki (10th version, Fortaleza, 2013). Informed consent was obtained from all study participants. The study was registered in Clinicaltrials.gov under identifier NCT04737213. The study was conducted in the Leiden University Medical Center (LUMC) and the Erasmus MC Cancer Institute (EMC).

## Study design

This was a prospective, open-label, non-randomized feasibility study to assess the ability of SGM-101 to target CLM. In this single arm trial, all patients were intravenously administered with SGM-101. SGM-101 was supplied by Surgimab (Montpellier, France). All patients received intravenous administration three to five days prior to surgery, based on earlier study protocols (10-12). The drug was administered over 30 minutes and patients were observed for three hours after infusion. Patients at least 18 years old, scheduled for resection of (suspected) CLM, and willing and able to give written informed consent were eligible for inclusion. Exclusion criteria were: history of any anaphylactic reaction, other malignancies either currently active or diagnosed in the last 5 years, hepatic or renal insufficiencies, blood count abnormalities, known positive test for HIV, hepatitis B surface antigen or hepatitis C virus antibody or patients with untreated serious infections, patients pregnant or breastfeeding, or any condition that the investigator considered to be potentially jeopardizing the patient's wellbeing or the study objectives.

## Outcomes

The primary outcome of this study was the number of CLM that showed a true positive fluorescence signal with SGM-101 and a NIR fluorescence imaging system. Secondary endpoints were the optimal dose of SGM-101 for fluorescence imaging of CLM, possible change in surgical management based on fluorescence imaging, and concordance between fluorescence imaging and CEA expression on the corresponding tissue slides.

For the primary outcome, lesions were considered fluorescent (i.e. a positive index test) if the signal-to-background ratio (SBR) was ≥ 1.5 (15). The reference standard for demonstrating CLM was final histopathological assessment. Imaging of the CLM was performed in three settings: *in vivo* imaging, *ex vivo* imaging of the whole specimen on the back table (back table imaging), and *ex vivo* imaging of bread loaf slides in a closed-field imaging device (closed-field imaging). *In vivo* and back table imaging was performed with the Quest spectrum V2 fluorescence camera (Middenmeer, The Netherlands). During VATS, the endoscopic camera of Quest spectrum V2 was used. Closed-field imaging was performed with the PEARL MSI imaging system (Li-Cor ,Lincoln, Nebraska, USA). SBRs were calculated with the 'Quest TBR tool' (Quest Medical Imaging, Middenmeer, The Netherlands) and Image Studio software (Li-Cor, Lincoln, Nebraska, USA). The SBR was defined as the mean fluorescence intensity of the signal derived from the tumour divided by the mean fluorescence intensity of the surrounding normal tissue.

Doses of 7.5, 10, and 12.5 mg were studied. The optimal dose was decided based on closed-field bread loaf imaging. As this was a feasibility study, no direct change in surgical management was performed, based on intraoperative fluorescence imaging alone. However, possible change in surgical management was noted as a secondary outcome measure (type D study (16)). CEA expression was assessed by immunohistochemistry with the monoclonal mouse antibody against CEACAM5 (clone number CI-P83-1, Santa Cruz Biotechnology) (12). Scoring of staining was done by multiplying the intensity score by the proportion score, to calculate the total immunostaining score (TIS) (17). A dedicated pathologist (MD) performed scoring of the immunohistochemistry-stained tissue slides.

### Statistics

R software (version 4.1.0, R Foundation for statistical computing, Vienna, Austria) was used for statistical analysis. Numerical data was described with median and interquartile range (IQR) or range. To assess SBR differences between dose groups, a Kruskal-Wallis test was performed. To assess the influence of overlying lung parenchyma on fluorescence signal intensity, tumours were categorized as closer or further distanced than 14 mm of the visceral pleura as defined by pre-operative computed tomography (CT) (18). $P < 0.05$ was considered significant. The sample size is based upon experience with this type of compounds and not on a formal power calculation. Using the 3+3 dose escalation design, a minimum of 9 and a maximum of 15 patients will be included, corresponding to a minimum of 3 patients per dose level. Patients were allocated in a chronological order.



## RESULTS

Between January-2021 and September-2022, 13 patients (ten males, three females) with a median age of 56 years (IQR: 54.5 – 66.5) were included. Patient and surgical characteristics are described in Table 1. There were no (serious) adverse events with any possible relationship to the administration of SGM-101.

■ **Table 1:** Patient- and surgical characteristics

| | | n (%)* |
|---|---|---|
| **Patients** | | 13 (100) |
| **Sex** | *Male* | 10 (77) |
| | *Female* | 3 (23) |
| **Hospital** | *LUMC* | 7 (46) |
| | *EMC* | 6 (54) |
| **Age (median [IQR])** | | 56 [54.5 - 66.5] |
| **Serum CEA (µg/ml) (median [IQR])** | | 5.8 [3.33 - 8.5] |
| **Location metastasis** | *RUL* | 5 (28) |
| | *ML* | 1 (6) |
| | *RLL* | 6 (33) |
| | *LUL* | 3 (17) |
| | *LLL* | 3 (17) |
| **Surgical procedure**** | *Lobectomy* | 4 (31) |
| | *Segment resection* | 2 (15) |
| | *Wedge resection* | 9 (69) |
| | *Lymphadenectomy* | 5 (38) |
| **Surgical approach** | *Thoracotomy* | 2 (15) |
| | *VATS* | 9 (70) |
| | *RATS* | 2 (15)*** |

** Percentages may not always add up to 100 due to rounding to full numbers*
*** Multiple patients underwent combined lobectomy and wedge/segment resections*
**** One converted to thoracotomy due to haemorrhage*
*LUMC = Leiden University Medical Centre | EMC = Erasmus Medical Centre | IQR = interquartile range | RUL = right upper lobe | ML = Middle lobe | RLL = right lower lobe | LUL = left upper lobe | LLL = left lower lobe | VATS = video assisted thoracic surgery | RATS = robot assisted thoracic surgery*

## Tumour lesions

Eighteen CLM were resected. Characteristics of all lesions are described in Table 2. *In vivo* imaging was performed on 16 lesions, back table imaging on 15 lesions, and closed-field imaging on 18 lesions. A positive fluorescence signal was observed in five lesions (31%) *in vivo*, in seven lesions (47%) with back table imaging and in 17 lesions (94%) with the closed-field imaging. Median SBRs for the three imaging modalities were 1.00 (IQR: 1.00 – 1.53), 1.45 (IQR: 1.00 – 2.05) and 4.81 (IQR: 2.70 – 7.41) respectively. All metastases were detected based on preoperative imaging and white light inspection. No lesions were identified solely based on NIR fluorescence imaging. Five metastases were located > 14 mm of the pleura, none of

which showed positive *in vivo* fluorescence (median SBR: 1.00, range 1.00 – 1.34). For lesions ≤ 14 mm of the pleura, 5 out of 11 (45%) were fluorescent *in vivo* (median SBR: 1.34, range: 1.00 – 2.15) and 6 out of 11 (64%) lesions on the back table (median SBR: 1.98, range 1.00 – 3.53). Figure 1 presents an example of *in vivo* and back table imaging (lesion 7).

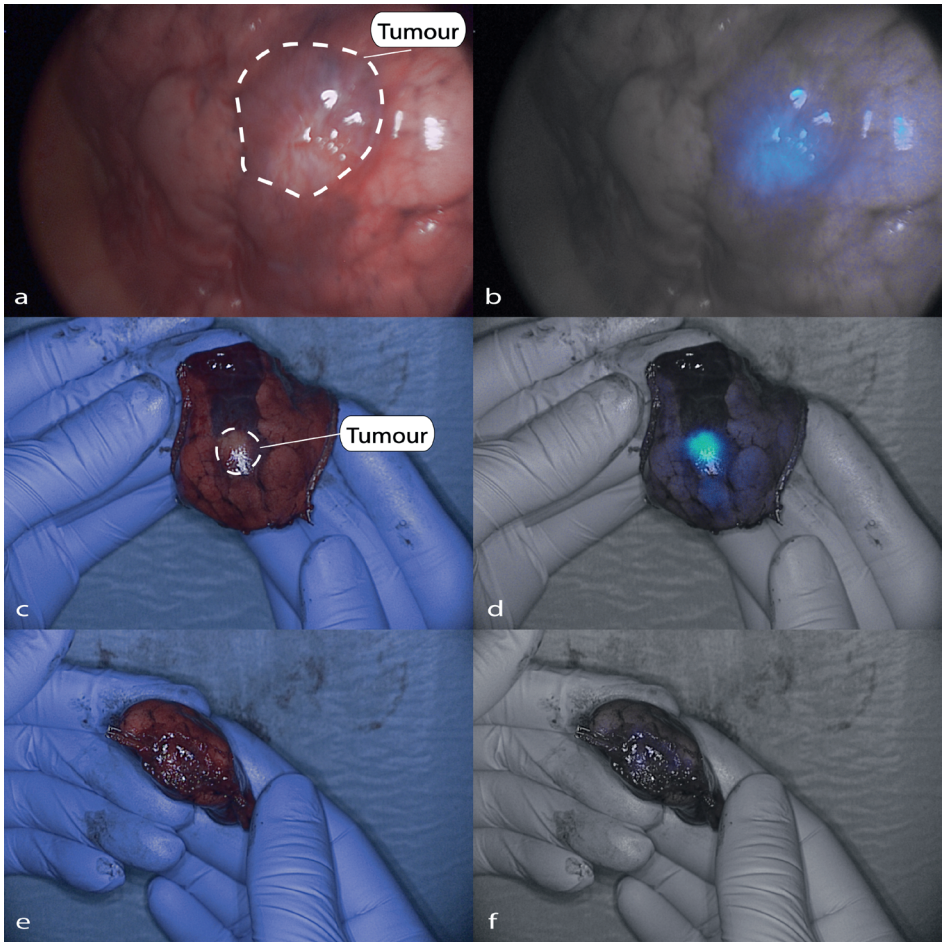


**Figure 1:** Representative in (a,b) and *ex vivo* (c, d, e, f) fluorescence images of a colorectal lung metastasis (lesion 7)
*White light (left panels) and gradient fluorescence overlay (right panels) images*

■ *Table 2: characteristics per lesion*

| | | | Preoperative | | | Intraoperative | | | Pathology | | | | IHC | | |
|---|---|---|---|---|---|---|---|---|---|---|---|---|---|---|---|
| ID | Dose SGM-101 | Lesion | Location | Distance to pleura (mm) | CT | WL | TBR (in vivo)* | TBR (ex vivo)* | Histopathology | Margin (mm) | TBR (bread loaf)* | Concordance ** | IS | PS | TIS |
| 1 | 7.5 | 1 | RLL | 6 | + | + | 2.15 | miss | metastasis crc | 4 | 6.1 | TP | 3 | 4 | 12 |
| | | 2 | station 11 | n/a | - | + | 1 | miss | benign LN | n/a | miss | TN | n/a | n/a | n/a |
| | | 3 | RLL | 17 | + | - | 1.34 | miss | metastasis crc | 20 | 5.91 | TP | 3 | 4 | 12 |
| 2 | 7.5 | 4 | RUL | 10 | + | + | 1.62 | 3.53 | metastasis crc | 5 | 6.43 | TP | 3 | 4 | 12 |
| 3 | 7.5 | 5 | LLL | 0 | + | + | 1.51 | 1.98 | metastasis crc | 10 | 4.09 | TP | 3 | 4 | 12 |
| | | 6 | LLL | 18 | + | + | 1 | 1.57 | metastasis crc | 23 | 5.07 | TP | 3 | 4 | 12 |
| 4 | 10 | 7 | RLL | 22 | + | + | miss | miss | metastasis crc | 2 | 10.44 | TP | 3 | 4 | 12 |
| 5 | 10 | 8 | LUL | 0 | + | + | 1.61 | 2.19 | metastasis crc | free | 4.54 | TP | 3 | 4 | 12 |
| 6 | 10 | 9 | RUL | 8 | + | + | 1 | 1 | fibrosis | n/a | miss | TN | n/a | n/a | n/a |
| | | 10 | RUL | 2 | + | + | 1 | 1 | fibrosis | n/a | miss | TN | n/a | n/a | n/a |
| | | 11 | RUL | n/a | - | + | 1 | 1 | fibrosis | n/a | miss | TN | n/a | n/a | n/a |
| | | 12 | RLL | 23 | + | + | 1 | 1 | metastasis crc | 3 | 1.52 | TP | 3 | 4 | 12 |
| | | 13 | ML | 0 | + | + | 1 | 1 | metastasis crc | 5 | 2.35 | TP | 3 | 4 | 12 |
| 7 | 12.5 | 14 | RLL | 3 | + | + | 1.34 | 1.19 | metastasis crc | 6 | 2.99 | TP | 3 | 4 | 12 |
| | | 15 | ML | 1 | + | + | 1 | 1 | metastasis crc | 1 | 2.01 | TP | 3 | 4 | 12 |
| | | 16 | RUL | 15 | + | + | 1 | 1 | metastasis crc | 10 | 1.23 | FN | 3 | 4 | 12 |
| | | 17 | station 11 | n/a | - | + | miss | 1 | benign LN | n/a | miss | TN | n/a | n/a | n/a |
| 8 | 12.5 | 18 | RUL | 9 | + | + | miss | 1.45 | metastasis crc | 26 | 9.93 | TP | 3 | 4 | 12 |

■ *Table 2: characteristics per lesion (continued)*

| | | | Preoperative | | | Intraoperative | | | Pathology | | | | IHC | | |
|---|---|---|---|---|---|---|---|---|---|---|---|---|---|---|---|
| ID | Dose SGM-101 | Lesion | Location | Distance to pleura (mm) | CT | WL | TBR (in vivo)* | TBR (ex vivo)* | Histopathology | Margin (mm) | TBR (bread loaf)* | Concordance ** | IS | PS | TIS |
| 9 | 12.5 | 19 | RLL | 7 | + | - | 1 | 2.04 | metastasis crc | free | 3.8 | TP | 3 | 4 | 12 |
| 10 | 7.5 | 20 | LUL | 20 | + | + | 1 | 1 | metastasis crc | 10 | 8.06 | TP | 3 | 4 | 12 |
| 11 | 7.5 | 21 | LUL | 10 | + | + | 1 | 2.13 | metastasis crc | free | 9.88 | TP | 3 | 4 | 12 |
| 12 | 12.5 | 22 | RUL | 2 | + | + | 1 | 1.37 | metastasis crc | free | 2.49 | TP | 3 | 4 | 12 |
| 13 | 10 | 23 | LLL | 0 | + | + | 1.6 | 2.06 | metastasis crc | free | 7.73 | TP | 3 | 4 | 12 |
| | | 24 | station 7 | n/a | - | + | miss | 1 | benign LN | n/a | miss | TN | 0 | 0 | 0 |
| | | 25 | station 8 | n/a | - | + | miss | 1.78 | malignant LN | n/a | miss | TP | 3 | 4 | 12 |
| | | 26 | station 9 | n/a | - | + | miss | 1 | benign LN | n/a | miss | TN | n/a | n/a | n/a |
| | | 27 | station 10 | n/a | + | + | miss | 1.63 | malignant LN | n/a | miss | TP | 3 | 4 | 12 |
| | | 28 | station 11 ventral | n/a | + | + | 1.59 | 1.69 | malignant LN | n/a | miss | TP | 3 | 4 | 12 |
| | | 29 | station 11 dorsal | n/a | - | + | miss | 1 | benign LN | n/a | miss | TN | n/a | n/a | n/a |

** a TBR of ≥ 1.5 is considered fluorescence positive ** concordance between fluorescence imaging and histopathology*
*CT = computed tomography | WL = white light suspect | n/a = not applicable | IS = intensity score | PS = proportion score | TIS = total immunostaining score | miss = missing | LN = lymph node | crc = colorectal cancer| TP = true positive | TN = true negative | FN = False negative*

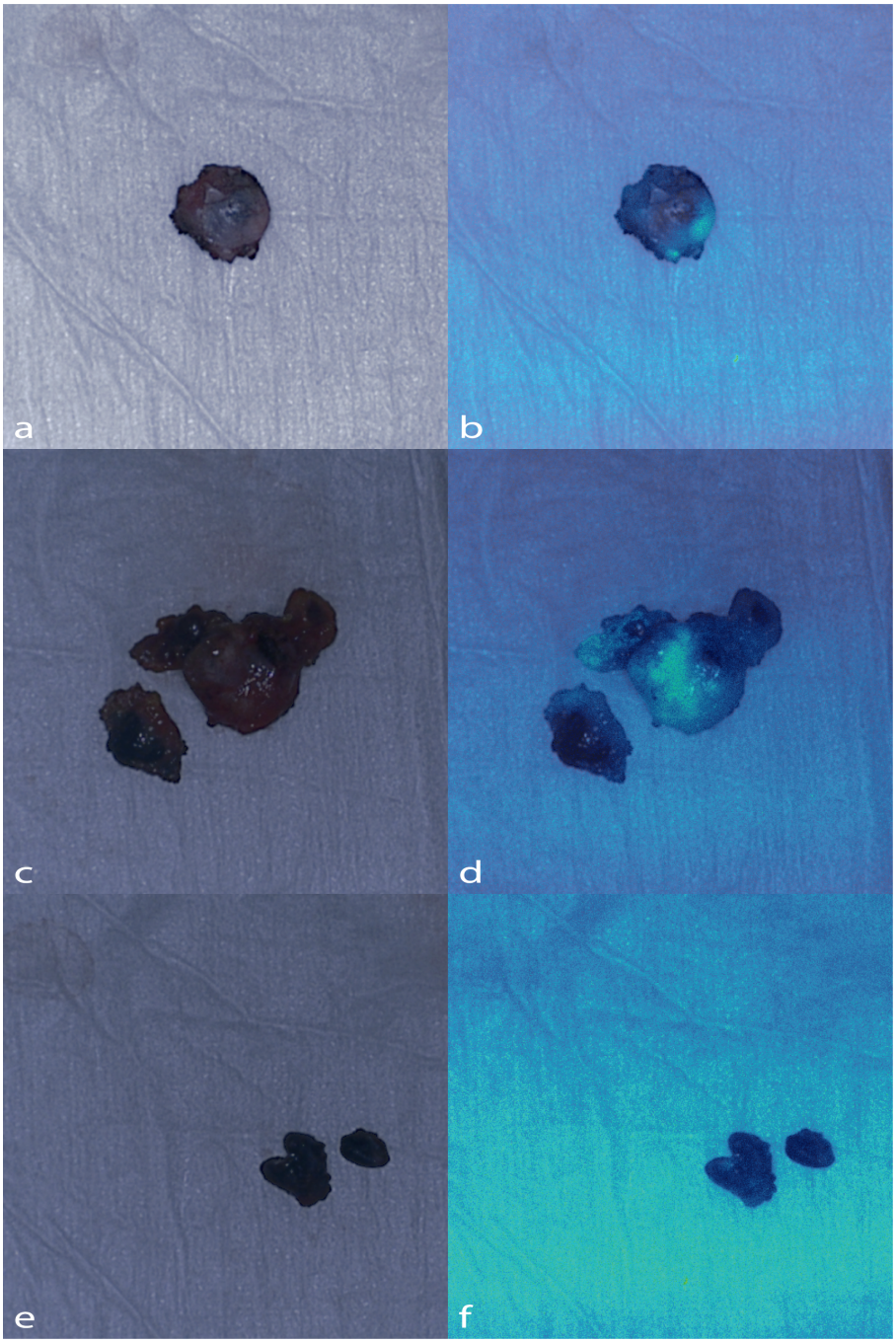


■ **Figure 2:** Fluorescence images of of malignant (a – d) and benign (e, f) lymph nodes
*White light (left panels) and gradient fluorescence overlay (right panels) images*

### Lymph nodes

In patient 1 and 7, two benign lymph nodes were resected based on white light suspicion, but were fluorescence-negative (true negatives). In patient 13, a lymphadenectomy was performed for preoperatively identified hilar lymph node metastases. Three malignant lymph nodes were fluorescent on the back table (lesions 25, 27, 28, true positives). Three other non-fluorescent lesions were resected based on clinical suspicion for tumour involvement. All three contained fibrosis without tumour (lesions 24, 26, 29, true negatives). Figure 2 presents the white light and gradient overlay fluorescence images of three lymph nodes (lesions 25, 26, 28).

### SGM-101 dose

Five patients (seven lesions) were injected with 7.5 mg SGM-101, four patients (five lesions) with 10 mg, and four patients (six lesions) with 12.5 mg. Median SBRs (closed-field imaging) for the dose levels were 6.1 (IQR: 5.50 – 7.25), 4.54 (IQR: 2.35 – 7.73), and 2.9 (IQR: 2.13 – 4.25) respectively (Figure 3a, p=0.20). There was no difference in absolute tumour or background mean fluorescence intensity (MFI) between the three dose groups (tumour: p=0.14, background: p=0.34, Figure 3b).

### Potential change in surgical management

In one patient, three clinically suspect, *in vivo* non-fluorescent nodules were resected (true negatives, lesions 9, 10, 11). In patient 5, the surgeon was unsure whether a complete removal of the tumour was achieved. Therefore, a small additional resection was performed. Fluorescence back table imaging of the primary specimen showed no tumour involvement of the resection margin (Figure 1, e and f). Final pathology assessment of primary resected specimen confirmed absence of tumour in the resection margin. In patient 9, tumour identification was based on the location on the CT scan and white light inspection. After resection, it was unclear whether the tumour was in the specimen, as the nodule was not palpable. After removing the staples, a clear fluorescent signal was observed in the specimen (Figure 4). The fluorescent tissue was sent for frozen section analysis and confirmed as malignant.

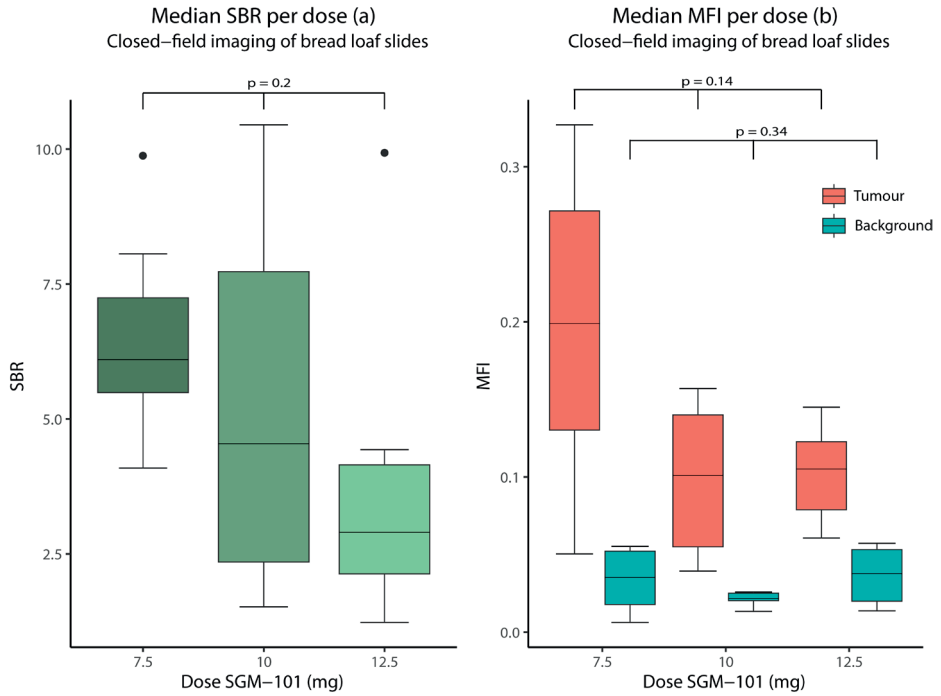


■ **Figure 3:** The signal-to-background ratios (a) and the mean fluorescence intensities (MFI) for tumour and background tissue per dose group (b) per dose group.
*The boxes represent medians with q1 and q3 and the error bars represent the range.*

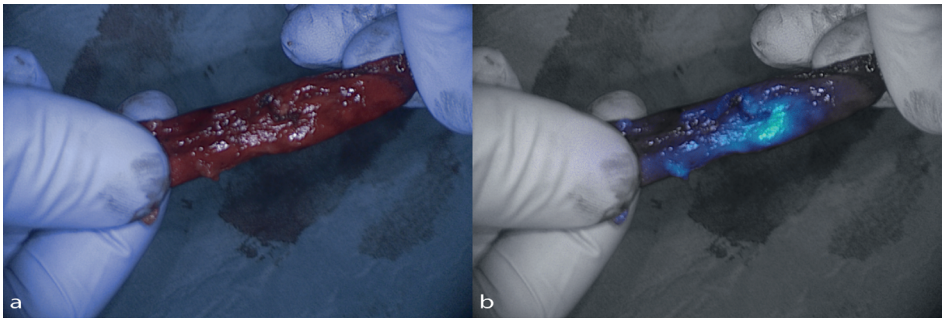


■ **Figure 4:** Images of an invisible and non-palpable tumour with a clear fluorescence signal (lesion 19).
*White light (a) and gradient fluorescence overlay (b) images*

### CEA immunohistochemistry

All 18 tumour lesions had a total immunostaining score (TIS) of 12 out of 12. Figure 5 represents a bread loaf tissue section of a CLM imaged with several imaging modalities. Figure 6 presents a slide from the same tissue block with the H&E and CEA immunohistochemistry staining. Three tumour containing lymph nodes had maximum CEA expression (TIS: 12). One normal control lymph node had no CEA expression (lesion 24, TIS: 0). CEA expression per lesion is shown in Table 2.

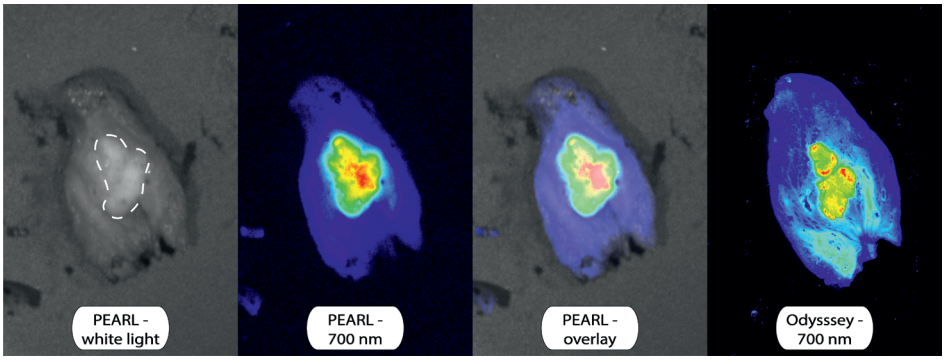


**Figure 5:** A tissue slide of a CLM imaged with the PEARL MSI and Odyssey CLx scanner.

## DISCUSSION

The present study shows that targeting of SGM-101 to CLM was accurate and that CEA is the target of choice for tumour-specific imaging of CLM. Challenges remain with *in vivo* detection of the tumour lesions, especially with the minimally invasive NIR fluorescence imaging system. The full potential of SGM-101 for in vivo detection of the tracer may therefore be achieved with improved minimally invasive imaging systems. Optimal patient selection may also further improve the efficacy of SGM-101. If intraoperative identification of the lesion is expected to be challenging, SGM-101 may help for the detection of superficial lesions. Identification of lesions deeper in the lung parenchyma is not expected to be possible with the technique, as overlying lung tissue negatively affects the observed fluorescence signal. An earlier study found a distance from the tumour to pleura of 14 mm as determined by pre-operative CT, to be the maximum tumour depth that can be imaged with an 800 nm fluorophore (18). For SGM-101 (700 nm) this might be slightly lower (5, 19). In the current study, five lesions had a distance to the pleura of more than 14 mm on CT and none of these were fluorescent *in vivo*. A second application of intraoperative NIR fluorescence imaging is margin assessment. When close or positive resection margins are expected during surgery (e.g. when the tumour infiltrates the chest wall or a bronchus), intraoperative fluorescence imaging with SGM-101 may also be beneficial. For margin assessment, tumour depth is not influential. This is due to the fact that margin assessment is performed by imaging of the resection margin on the specimen on the back table. When positive margins are suspected,

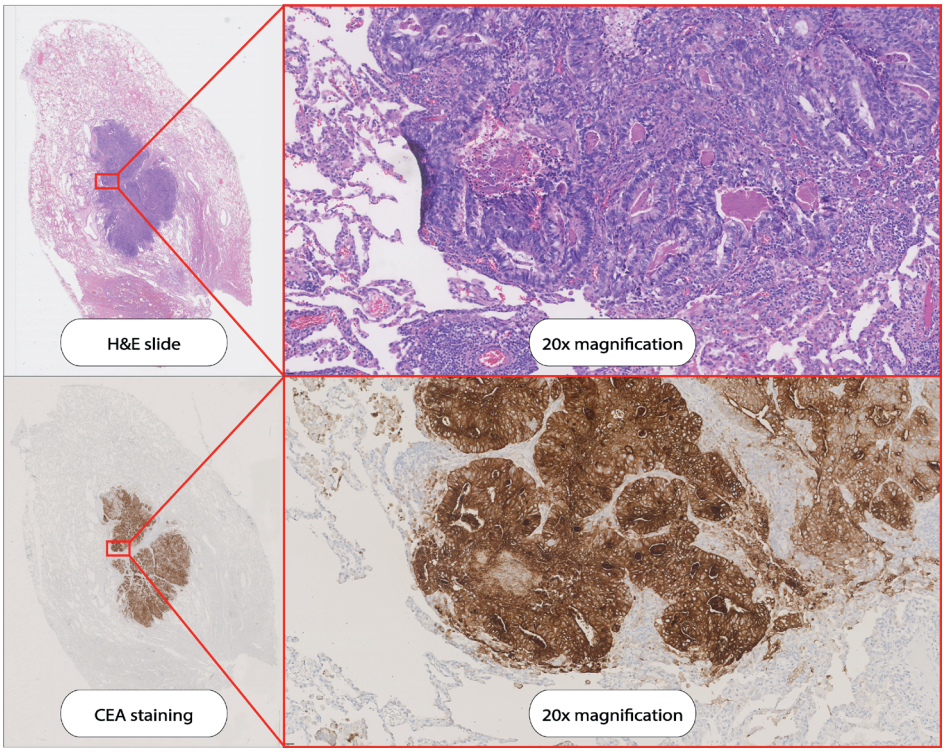


**Figure 6:** Haematoxylin and Eosin (HE) staining and Carcinoembryonic Antigen (CEA) immunohistochemistry staining on a the tissue slide as demonstrated in Figure 4.

the wound bed can also be imaged to assess for residual signal. Given that 94% of the tumour bread loaves showed a positive fluorescence signal, it is expected that when tumour positive margins occur, they can be detected with this technique. Thus, patients with superficial nodules which are expected to be challenging to identify, or patients with tumours with potential tumour positive margins are most likely to benefit from the use of SGM-101.

A secondary objective of this study was to find the optimal dose of SGM-101 for the identification of CLM. For primary colorectal cancer, a dose of 10 mg was found to be the optimal dose (10). Our study assessed three doses. In all dose groups sufficient SBRs were found. SBRs appeared to decrease with increasing doses but these differences were not significant. Therefore, a dose of 7.5 mg may be sufficient for pulmonary CLM imaging. The lowest dose is also preferable with regard to costs.

Recently, the first results were published on the use of SGM-101 for CLM and primary lung tumours (20). In this study, ten patients were included, of which four had CLM. A dose of 10 mg of SGM-101 was administered according to the standard dose for primary or recurrent

colorectal cancer. In the paper, only SBRs from the closed-field imaging were reported. When comparing SBRs from this trial to our results we find similar results, with mean SBRs of 3-4. For primary lung cancer surgery, several trials have been performed with other fluorescent tracers (4). OTL-38 is a folate-α targeted fluorescent tracer for pulmonary adenocarcinoma that has been used in several studies for intraoperative imaging of primary lung adenocarcinoma. However, OTL-38 is not a good candidate for imaging of most other adenocarcinomas, including colorectal cancers. Less than 30% of the colorectal cancers express folate-α, while CEA is expressed on 95% of tumours (7, 21, 22).

Several limitations of this study can be mentioned. The low number of patients might have affected dose finding. In addition, patients were not selected based on tumour location and distance to the pleura. This may explain why several nodules were not fluorescent when imaged intraoperatively. However, as we asked all eligible patients for participation, we most likely included a clinically representative cohort of patients.

In conclusion, the present study demonstrates the potential of fluorescence imaging of CLM with SGM-101. Closed-field imaging of bread loaves showed excellent targeting of the tracer to the tumour nodules, with maximum target expression on all tumour nodules. Challenges remain with *in vivo* detection of this tracer. Improving minimally invasive fluorescence imaging systems and optimal patient selection most likely enables the optimal efficacy of SGM-101 for CLM surgery.

## REFERENCES


1. Meyer Y, Olthof PB, Grünhagen DJ, de Hingh I, de Wilt JHW, Verhoef C, et al. Treatment of metachronous colorectal cancer metastases in the Netherlands: A population-based study. Eur J Surg Oncol. 2021.
2. Riihimäki M, Hemminki A, Sundquist J, Hemminki K. Patterns of metastasis in colon and rectal cancer. Sci Rep. 2016;6:29765.
3. Hao Z, Parasramka S, Chen Q, Jacob A, Huang B, Mullett T, et al. Neoadjuvant Versus Adjuvant Chemotherapy for Resectable Metastatic Colon Cancer in Non-academic and Academic Programs. Oncologist. 2022.
4. Neijenhuis LKA, de Myunck L, Bijlstra OD, Kuppen PJK, Hilling DE, Borm FJ, et al. Near-Infrared Fluorescence Tumour-Targeted Imaging in Lung Cancer: A Systematic Review. Life (Basel). 2022;12.
5. Keereweer S, Van Driel PB, Snoeks TJ, Kerrebijn JD, Baatenburg de Jong RJ, Vahrmeijer AL, et al. Optical image-guided cancer surgery: challenges and limitations. Clin Cancer Res. 2013;19:3745-54.
6. Gutowski M, Framery B, Boonstra MC, Garambois V, Quenet F, Dumas K, et al. SGM-101: An innovative near-infrared dye-antibody conjugate that targets CEA for fluorescence-guided surgery. Surg Oncol. 2017;26:153-62.
7. Tiernan JP, Perry SL, Verghese ET, West NP, Yeluri S, Jayne DG, et al. Carcinoembryonic antigen is the preferred biomarker for in vivo colorectal cancer targeting. Br J Cancer. 2013;108:662-7.
8. Meijer RPJ, de Valk KS, Deken MM, Boogerd LSF, Hoogstins CES, Bhairosingh SS, et al. Intraoperative detection of colorectal and pancreatic liver metastases using SGM-101, a fluorescent antibody targeting CEA. Eur J Surg Oncol. 2021;47:667-73.
9. Schaap DP, de Valk KS, Deken MM, Meijer RPJ, Burggraaf J, Vahrmeijer AL, et al. Carcinoembryonic antigen-specific, fluorescent image-guided cytoreductive surgery with hyperthermic intraperitoneal chemotherapy for metastatic colorectal cancer. Br J Surg. 2020;107:334-7.
10. de Valk KS, Deken MM, Schaap DP, Meijer RP, Boogerd LS, Hoogstins CE, et al. Dose-Finding Study of a CEA-Targeting Agent, SGM-101, for Intraoperative Fluorescence Imaging of Colorectal Cancer. Ann Surg Oncol. 2021;28:1832-44.
11. Hoogstins CES, Boogerd LSF, Sibinga Mulder BG, Mieog JSD, Swijnenburg RJ, van de Velde CJH, et al. Image-Guided Surgery in Patients with Pancreatic Cancer: First Results of a Clinical Trial Using SGM-101, a Novel Carcinoembryonic Antigen-Targeting, Near-Infrared Fluorescent Agent. Ann Surg Oncol. 2018;25:3350-7.
12. Boogerd LSF, Hoogstins CES, Schaap DP, Kusters M, Handgraaf HJM, van der Valk MJM, et al. Safety and effectiveness of SGM-101, a fluorescent antibody targeting carcinoembryonic antigen, for intraoperative detection of colorectal cancer: a dose-escalation pilot study. Lancet Gastroenterol Hepatol. 2018;3:181-91.
13. Vahrmeijer AL. SGM-101 in Locally Advanced and Recurrent Rectal Cancer (SGM-LARRC). ClinicalTrial.gov.
14. Vahrmeijer AL. Performance of SGM-101 for the Delineation of Primary and Recurrent Tumour and Metastases in Patients Undergoing Surgery for Colorectal Cancer. ClinicalTrials.gov.

**15.** Azargoshasb S, Boekestijn I, Roestenberg M, KleinJan GH, van der Hage JA, van der Poel HG, et al. Quantifying the Impact of Signal-to-background Ratios on Surgical Discrimination of Fluorescent Lesions. Mol Imaging Biol. 2022.

**16.** Lauwerends LJ, van Driel P, Baatenburg de Jong RJ, Hardillo JAU, Koljenovic S, Puppels G, et al. Real-time fluorescence imaging in intraoperative decision making for cancer surgery. Lancet Oncol. 2021;22:e186-e95.

**17.** Linders D, Deken M, van der Valk M, Tummers W, Bhairosingh S, Schaap D, et al. CEA, EpCAM, αvβ6 and uPAR Expression in Rectal Cancer Patients with a Pathological Complete Response after Neoadjuvant Therapy. Diagnostics (Basel). 2021;11.

**18.** Okusanya OT, Holt D, Heitjan D, Deshpande C, Venegas O, Jiang J, et al. Intraoperative near-infrared imaging can identify pulmonary nodules. Ann Thorac Surg. 2014;98:1223-30.

**19.** Kennedy GT, Azari FS, Chang A, Nadeem B, Bernstein E, Segil A, et al. Comparative Experience of Short Versus Long Wavelength Fluorophores for Intraoperative Molecular Imaging of Lung Cancer. Ann Surg. 2022.

**20.** Azari F, Meijer RPJ, Kennedy GT, Hanna A, Chang A, Nadeem B, et al. Carcinoembryonic Antigen-Related Cell Adhesion Molecule Type 5 Receptor-Targeted Fluorescent Intraoperative Molecular Imaging Tracer for Lung Cancer: A Nonrandomized Controlled Trial. JAMA Netw Open. 2023;6:e2252885.

**21.** D'Angelica M, Ammori J, Gonen M, Klimstra DS, Low PS, Murphy L, et al. Folate receptor-α expression in resectable hepatic colorectal cancer metastases: patterns and significance. Mod Pathol. 2011;24:1221-8.

**22.** Chen CI, Li WS, Chen HP, Liu KW, Tsai CJ, Hung WJ, et al. High Expression of Folate Receptor Alpha (FOLR1) is Associated With Aggressive Tumour Behavior, Poor Response to Chemoradiotherapy, and Worse Survival in Rectal Cancer. Technol Cancer Res Treat. 2022;21:15330338221141795.

# Chapter 9

# A quantitative assessment of perfusion of the gastric conduit after oesophagectomy using near-infrared fluorescence with indocyanine green

Hidde A. Galema*, Robin A. Faber*, Floris P. Tange*, Denise E. Hilling‡, Joost R. van der Vorst‡

* Shared first authorship ‡ Shared senior authorship

**On behalf of the Upper-GI ICG quantification study group:**

Wobbe O. de Steur, Henk H. Hartgrink, Alexander L. Vahrmeijer, Merlijn Hutteman, J. Sven. D. Mieog, Sjoerd M. Lagarde, Pieter C. van der Sluis, Bas P.L. Wijnhoven, Cornelis Verhoef, Jacobus Burggraaf, Stijn Keereweer

European Journal of Surgical Oncology. 2023 Mar 2:S0748-7983(23)00171-3. doi: 10.1016/j.ejso.2023.02.017.

## ABSTRACT

### Introduction

Anastomotic leakage is a severe complication after oesophageal resection with gastric conduit reconstruction. Poor perfusion of the gastric conduit plays an important role in the development of anastomotic leakage. Quantitative near-infrared (NIR) fluorescence angiography with indocyanine green (ICG-FA) is an objective technique that can be used for perfusion assessment. This study aims to assess perfusion patterns of the gastric conduit with quantitative ICG-FA.

### Methods

In this exploratory study, 20 patients undergoing oesophagectomy with gastric conduit reconstruction were included. A standardized NIR ICG-FA video of the gastric conduit was recorded. Postoperatively, the videos were quantified. Primary outcomes were the time-intensity curves and nine perfusion parameters from contiguous regions of interest on the gastric conduit. A secondary outcome was the inter-observer agreement of subjective interpretation of the ICG-FA videos between six surgeons. The inter-observer agreement was tested with an intraclass correlation coefficient (ICC).

### Results

In a total of 427 curves, three distinct perfusion patterns were recognized: pattern 1 (steep inflow, steep outflow); pattern 2 (steep inflow, minor outflow); and pattern 3 (slow inflow, no outflow). All perfusion parameters were significantly different between the perfusion patterns. The inter-observer agreement was poor – moderate (ICC:0.345,95%CI:0.164–0.584).

### Discussion

This was the first study to describe perfusion patterns of the complete gastric conduit after oesophagectomy. Three distinct perfusion patterns were observed. The poor inter-observer agreement of the subjective assessment underlines the need for quantification of ICG-FA of the gastric conduit. Further studies should evaluate the predictive value of perfusion patterns and parameters on anastomotic leakage.

## INTRODUCTION

Annually, around 600.000 patients are diagnosed with oesophageal or junctional cancer worldwide (1). For most patients with curable disease, neoadjuvant therapy followed by oesophagectomy with gastric conduit reconstruction is the treatment of choice. Major complications related to the gastric conduit or the anastomosis, such as anastomotic leakage, abscesses, gastric conduit necrosis, or fistulas are reported in 4-30% of the cases (2, 3). Occurrence of major complications increases postoperative mortality significantly and decreases long term survival (4-6). Poor perfusion of the gastric conduit is thought to play a significant role in the development of these complications. Therefore, interest in intraoperative perfusion assessment of the gastric conduit using optical imaging techniques is growing. The most commonly used technique is near-infrared fluorescence angiography with indocyanine green (ICG-FA) (7).

ICG-Fluorescence Angiography (ICG-FA) is being used extensively for perfusion assessment of tissue such as colorectal anastomoses. However, no high-quality evidence has been published proving the additional value of ICG-FA to prevent these anastomotic complications (8, 9). Evidence that ICG-FA reduces the risk of anastomotic leakage of the gastric conduit is also scarce (10, 11). This might be due to the subjective interpretation of the fluorescence signal, which depends on the 'real-time' interpretation of the surgeon. With this subjective approach, it can be challenging to distinguish well-perfused from poorly-perfused parts of the gastric conduit (12). We hypothesized that quantification of the NIR fluorescence signal could be used to objectively assess various perfusion patterns (13).

Few studies have performed quantitative ICG-FA of the gastric conduit (14-17). Time-intensity curves of proximal parts of the gastric conduit generally showed a steep inflow, with a peak immediately followed by a steep outflow. Distal parts showed a gradual increase of fluorescence intensity without reaching a peak intensity. However, in these studies, the location of the ROIs were pre-selected based on parts of the gastric conduit that were subjectively assumed by surgeons to be well perfused or poorly perfused. In addition, none of these studies plotted curves on the exact location of the anastomosis. This study aimed to identify perfusion patterns within the entire gastric conduit to differentiate between well and poorly perfused areas and to identify transition areas that could be of clinical relevance.



## METHODS

This study was reviewed and approved by the medical ethical committee 'Leiden-Den Haag-Delft' (MEC-2021-0876) and was performed according to the declaration of Helsinki (10th version, Fortaleza, 2013). Informed consent was obtained from all patients. The study

was conducted in the Leiden University Medical Centre (LUMC) and the Erasmus MC Cancer Institute (EMC).

## Study design and imaging protocol

This was a prospective cohort study. Twenty patients undergoing oesophageal resection with gastric conduit reconstruction with cervical anastomosis were included.

After creating the gastric conduit, it was placed on a flat surface. The Quest V2 Fluorescence imaging platform (Quest Medical Imaging, Middenmeer, The Netherlands) was positioned at a distance of 30 cm above the gastric conduit, at a 90 degrees angle. The gastric conduit was positioned in such a way that it could be imaged completely. All ambient light was switched off and the windows were blinded. Camera settings were as follows: the gain was set on 3.5 (colour) and 20 (ICG) decibels, exposure was set on 11 (colour) and 100 (ICG) milliseconds. Five mg (2 ml of 2.5 mg/ml) ICG solution was then rapidly injected in a peripheral intravenous catheter, followed by a flush of saline. After administration of ICG, a standardized ICG-FA video was recorded for 5 minutes.

## Outcome

The primary outcome measure was the time-intensity curve and its derived parameters. Secondary outcomes were the inter-observer agreement of subjective interpretation of the ICG-FA videos by every upper-GI surgeon separately (HH, WS, MH, PS, SL, BW). For the subjective interpretation, surgeons were asked to mark the most distal location of the gastric conduit where perfusion was still deemed sufficient based on the ICG-FA video (i.e. the location where they would create the anastomosis in order to save as much length as possible). Finally, anastomotic complications (defined as: anastomotic leakage, fistulas originating from the gastric conduit, gastric conduit necrosis, or abscesses near the anastomosis) within 30 days from surgery were recorded.

## Quantification

Postoperatively, continuous ROIs of approximately 1 cm width were drawn from proximal to distal across the gastric conduit using the Quest Research Framework (figure 1). Overexposed videos were excluded. From each ROI, a absolute- and normalised time intensity curve was plotted from which nine perfusion parameters were derived (18). The following five inflow and four outflow parameters were determined: time to maximum fluorescence intensity (time to max); maximum fluorescence intensity (Imax); mean slope of the inflow (ingress rate); maximum slope of the inflow (max ingress slope); normalised maximum slope of the inflow (normalised ingress slope); maximum slope of the outflow (maximum egress slope); and the area under the curve (AUC) after 30, 60, 120 seconds (auc30, auc60, auc120) starting from the Imax.

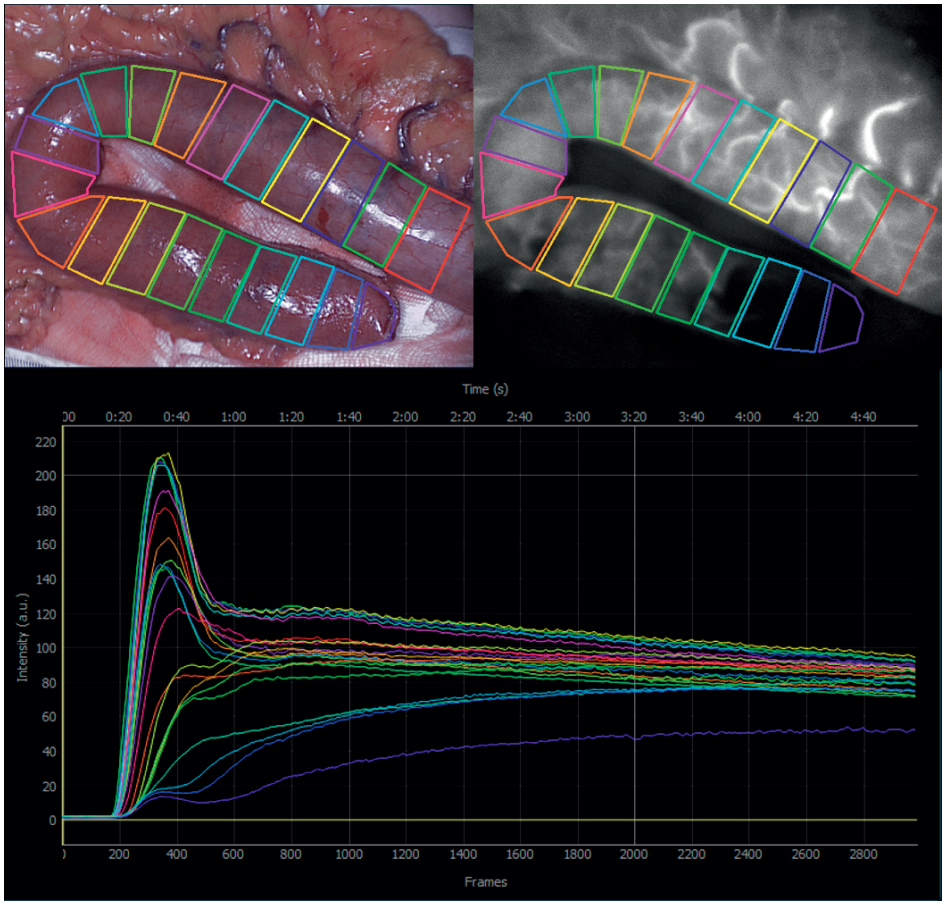


**Figure 1:** output of the Quest research framework with time-intensity curves of the corresponding ROIs

## Statistics

Statistical analyses were performed with R-studio software (version 4.1.0, R Foundation for statistical computing, Vienna Austria). Descriptive statistics were used to describe numerical data (mean with standard deviation (SD), median with interquartile range (IQR), or median with range). To calculate statistical differences in parameters between perfusion pattern groups (>2 groups, normal distribution), a one-way ANOVA was used. To test statistical difference in perfusion parameters between anastomotic leakage and non-leakage groups (2 groups, non-normal distribution), a Mann-Whitney U test was conducted. To assess inter-observer agreement, an intraclass correlation coefficient (ICC) with 95% confidence interval (CI) was calculated according to a two-way mixed modal, absolute agreement type, single measurement method. An ICC of < 0.5 was defined as 'poor agreement'; ≥ 0.5 to 0.75 was defined as 'moderate agreement'; > 0.75 to 0.90 was defined as 'good agreement'; and > 0.90 was defined as 'excellent agreement' (19). The distance between the chosen locations

was measured with ImageJ (version 1.53k, National Institutes of Health, USA) according to a previously published method (12). The most proximal selected location (i.e. the closest to the base of the gastric conduit) was used as the baseline measurement. Figures were created in Graphpad (version 9.3.1., Graphpad software Inc. San Diego, California, USA).

## RESULTS

### Patient characteristics

The study comprised of 20 patients, 17 (85%) males and 3 (15%) females. The median age was 63 years (IQR: 62 – 70.5). All patient characteristics are shown in table 1. In total, 427 curves were plotted. The median number of curves per gastric conduit was 22 (range 18 - 25).

**Table 1:** patient characteristics

| **Characteristic** | | **N (%)** |
|---|---|---|
| **Sex** | *Male* | 17 (85) |
| | *Female* | 3 (15) |
| **Age (median [IQR])** | | 63.00 [62.00, 70.50] |
| **Hospital** | *LUMC* | 12 (60) |
| | *EMC* | 8 (40) |
| **T stage** | *c1* | 1 (5) |
| | *c2* | 3 (15) |
| | *c3* | 13 (65) |
| | *c4* | 3 (15) |
| **Surgical approach** | *Transthoracic* | 9 (45) |
| | *Transhiatal* | 11 (55) |
| **Minimal invasive** | *Yes* | 12 (60) |
| | *No* | 8 (40) |
| **Days of admission (median [IQR])** | | 8.00 [7.00, 23.50] |

### Perfusion patterns

Based on qualitative and quantitative assessment of the time-intensity curves and the corresponding perfusion parameters, three distinctive perfusion patterns of the gastric conduits were observed. These patterns were present on every gastric conduit. Pattern 1: a steep inflow with a short peak and steep outflow. Pattern 2: a steep inflow but no/little egress and an immediate plateau phase. Pattern 3: a slow gradient inflow that does not or slowly reaches its peak fluorescence intensity. Pattern 1 was present at the base of the gastric conduit that

was clinically selected as a vital part of the gastric conduit. Pattern 2 displayed the transition zone and pattern 3 the ischemic zone at the tip of gastric conduit.

Based on qualitative interpretation of the curves with a quantitative check afterwards, cut-off values were established for each pattern. pattern 1: time to max ≤ 50 sec and max egress ≤ -1.5; pattern 2: time to max ≤ 50 sec and max egress > -1.5; and pattern 3: time to max > 50 sec. Figure 2 shows the mean curves per perfusion pattern and figure 3 shows the separate curves with the standard deviation (top row) and the normalised curves per perfusion pattern (bottom row). The mean perfusion parameters per pattern are presented in table 2. All perfusion parameters were significantly different between the perfusion patterns.

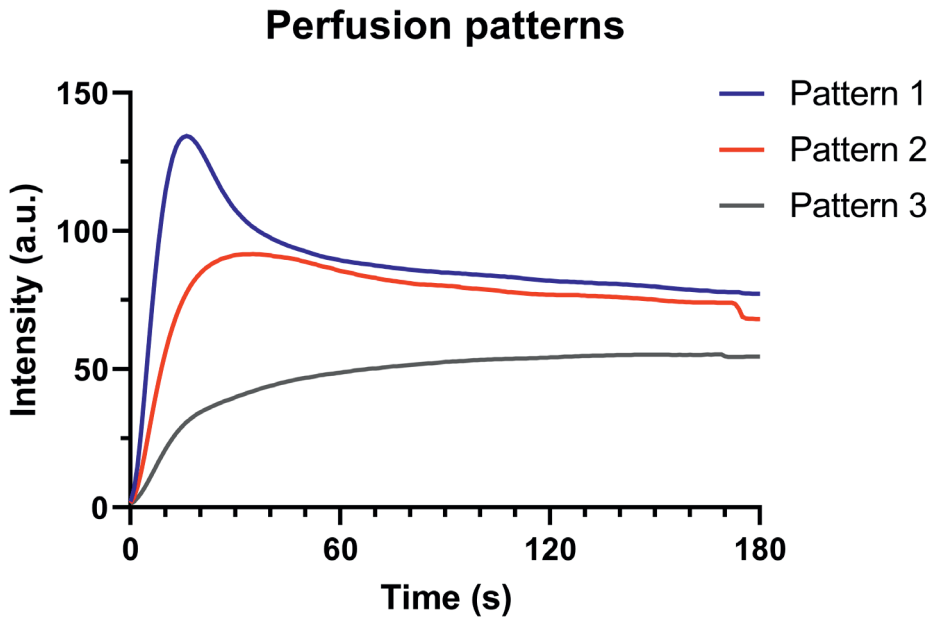


■ **Figure 2:** average curves of the three perfusion patterns

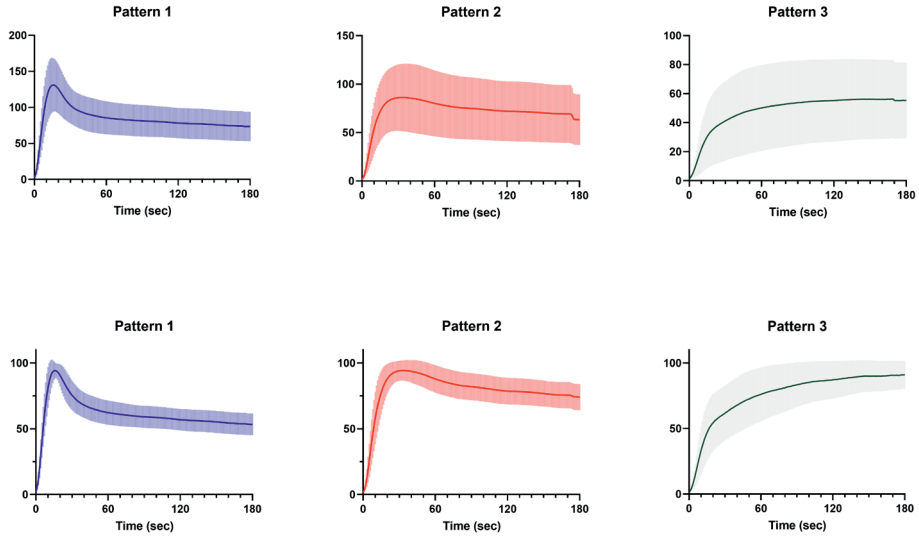


- **Figure 3:** the three separate perfusion patterns, with standard deviations. The bottom row represents the normalised curves

- **Table 2:** perfusion parameters of all ROIs, stratified by perfusion pattern

| Perfusion parameter | Pattern 1 (mean (SD)) | Pattern 2 (mean (SD)) | Pattern 3 (mean (SD)) | P |
|---|---|---|---|---|
| N (curves) | 211 | 92 | 124 | |
| Time to max (sec) | 15.47 (5.22) | 31.28 (11.30) | 173.92 (79.68) | * |
| Imax | 142.64 (33.90) | 96.09 (30.99) | 59.15 (27.76) | <0.001 |
| Ingress rate (a.u./sec) | 9.40 (3.44) | 3.27 (1.72) | 0.45 (0.39) | <0.001 |
| Max ingress slope (a.u./sec) | 16.06 (5.54) | 7.67 (3.48) | 3.08 (2.32) | <0.001 |
| Max egress slope (a.u./sec) | -4.34 (1.89) | -0.96 (0.29) | -0.53 (0.61) | * |
| Normalised max slope (a.u./sec) | 11.20 (2.70) | 7.96 (2.63) | 5.09 (2.33) | <0.001 |
| AUC 30 | 78.12 (6.59) | 93.19 (5.44) | 96.76 (6.21) | <0.001 |
| AUC 60 | 70.64 (7.16) | 88.61 (7.13) | 95.37 (8.38) | <0.001 |
| AUC 120 | 64.85 (7.47) | 83.91 (8.28) | 91.59 (10.45) | <0.001 |

** patterns are categorized based on the time to max and the max egress slope. Therefore, these parameters are not statistically compared.*
*Abbreviations: sec = seconds | a.u. = arbitrary units | AUC = area under the curve*

### Subjective interpretation of ICG-FA recordings

Six surgeons reviewed all ICG-FA videos and selected the location where they would place the anastomosis. Inter-observer agreement for this subjective evaluation was poor – moderate; ICC: 0.349 (95% CI: 0.164 – 0.584). Per gastric conduit, the median distance between the most proximal- and distal selected location was 2.79 cm (range 0.49 – 6.46 cm). Supplementary figure 1 shows the ICC dot plot with the distance (in centimetres) between the locations selected by the surgeons.

### Clinical outcome

In twelve patients (60%), quantitative analysis of the part of the gastric conduit that was used for the anastomosis showed perfusion pattern 2. In two patients (10%), pattern 1 was present at the location of the anastomosis and pattern 3 was present in six (30%) patients. Figure 4 displays all 20 curves at the location of the anastomosis. Anastomotic leakage occurred in three patients (15%) and all complications were clinically relevant (Clavien-Dindo ≥ 3). In two (67%) patients with anastomotic leakage the anastomosis location showed pattern 2, and in one patient (33%) pattern 3. The median Imax was significantly lower in the anastomotic leakage group compared to the non-leakage group (97.69 vs. 46.81, p=0.023). The ingress rate (2.13 vs. 0.85, p=0.101) and max ingress slope (7.58 vs. 1.63, p=0.153) did not significantly differ between the groups. Supplementary table 1 presents all perfusion parameters stratified by anastomotic leakage.

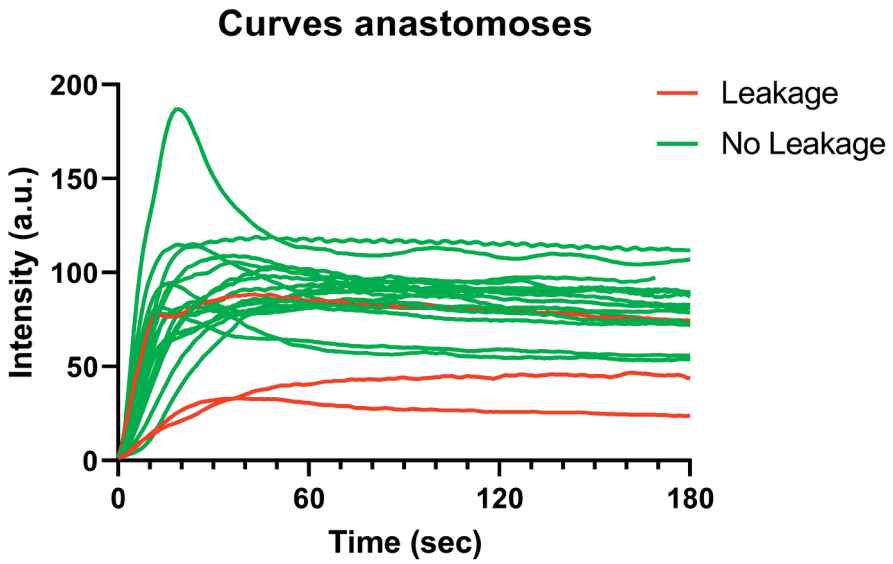


**Figure 4:** all curves on locations where the anastomosis was placed. The red lines represent the patients that developed anastomotic leakage

## DISCUSSION

This is the first study that used quantitative ICG fluorescence angiography to assess perfusion patterns of the complete gastric conduit after oesophageal resection. By plotting continuous ROIs on the gastric conduit, a clear representation of perfusion of the entire gastric conduit was obtained. Based on these curves, three distinct patterns were recognized. Pattern 1 generally presented on the base of the gastric conduit, whereas pattern 3 was usually found at the distal end, corresponding with the expected area of poorest perfusion. Pattern 2 was observed in the transition zone of the gastric conduit. These three perfusion patterns were clearly distinguishable in each patient and might adequately reflect the perfusion status of the gastric conduit. Although these results suggest that quantitative ICG-FA can objectively identify differences in perfusion throughout the gastric conduit, the clinical value of these perfusion patterns should be further explored.

Another important outcome of this study was the inter-observer agreement of the surgeons' subjective assessment of the ICG-FA videos, which was considered poor – moderate (ICC = 0.349, 95% CI: 0.164 – 0.584). This ICC is lower than an earlier study from Hardy et al. (12), where analysis of ICG-FA videos resulted in a moderate overall ICC of 0.717 for experts and 0.641 for non-experts. Our findings underline the need for standardization and quantification of these ICG-FA assessment videos. In particular in the gastric conduit, in which a trade-off between length of the conduit and corresponding tissue perfusion is present.

This study was not powered to assess the correlation between quantitative perfusion assessment and anastomotic leakage. Although there was only a small group of patients with anastomotic leakage (n=3), a significantly lower Imax was found in these patients, compared to patients without leakage. These findings should be interpreted with caution, as external factors such as ICG dose, administration method, and camera distance all influence Imax, even if they are standardized. Optical properties of the tissue may also influence Imax by causing scattering and absorption of the emitted photons (20). In addition, patient-related factors, such as cardiac output and vascular status, may be of importance. Still, it remains remarkable that the two patients with the lowest Imax both developed anastomotic leakage. Other parameters, such as the ingress rate, max ingress slope, and the normalised max slope also showed a non-significant difference between the groups. Further studies should explore the clinical significance of all perfusion patterns and parameters and normalisation of the curve, and their predictive value on anastomotic leakage.

This study only included patients with cervical anastomoses. This was due to the difficulty of making standardized recordings when the gastric conduit is located in the thorax. Intrathoracic gastric conduits require imaging with endoscopic or robotic NIR fluorescence cameras. In the intrathoracic setting, standardization of distance and angle can be challenging.

However, as there is more room to adjust the anastomosis location on the gastric conduit in intrathoracic anastomosis, ICG-FA assessment may have more direct clinical consequences in this group of patients.

Several studies have been published regarding quantitative ICG-FA of the gastric conduit. Due to the use of varying analysis software, a clear comparison of the results is difficult. Similar to our study, Yukaya *et al*. (15) reported perfusion patterns based on ICG-FA of the gastric conduit. In this study, only two ROIs were drawn. Interestingly, three perfusion patterns were reported: the 'normal flow' pattern that was similar to our pattern 1, the 'inflow delayed' pattern that was similar to our pattern 3, and the 'outflow delayed' pattern that was similar to our pattern 2. A study by Jansen *et al*. (14) analysed quantitative ICG-FA videos of 20 patients undergoing oesophagectomy with gastric conduit reconstruction. Four pre-selected ROI's were analysed. Slope and maximum intensity decreased at more distal locations of the gastric conduit. Von Kroge *et al*. (17) measured the slope, time-to-max and Imax on 20 gastric conduits. Perfusion patterns were not reported, but a decrease in all three parameters was seen in the most proximal compared to the most distal part of gastric conduit. In general, these findings are in line with our data. However, in our study, continuous series of ROIs were drawn on the gastric conduit. Furthermore, we used an extensive set of perfusion parameters and we applied curve normalisation.

The authors recognize that there remains a subjective factor in the determination of the cut-off values for categorizing perfusion patterns. Cut-off values were chosen based on qualitative interpretation of the curves with a quantitative check afterwards. Although these cut-off values were subjective, the method of categorizing the curves is reproducible. A general limitation of ICG-FA assessment of gastric conduits is that there is often not a possibility to reduce length of the gastric conduit in a way that an anastomosis with the proximal oesophagus is still feasible. Therefore, some patients have an anastomosis on a location of high risk of anastomotic leakage. However, even when it is not possible to reduce length of the gastric conduit, clinical value of ICG-FA exists. In these high-risk patients surgeons should be more alert to anastomotic leakage by rapidly performing radiological assessment. Also other surgical options can be taken into account or placement of a drain near the anastomosis.



Larger datasets are needed to assess the prognostic value of the perfusion patterns and parameters that were found in this study. A follow-up study should be sufficiently powered to assess whether these patterns and parameters are correlated with anastomotic leakage. Also, quantitative measurements should be performed intraoperatively to facilitate change in surgical management.

In conclusion, this study described three perfusion patterns of the gastric conduit by performing quantified ICG fluorescence angiography. These perfusion patterns were clearly recognized in every patient. The exact clinical meaning of these perfusion patterns, and the corresponding parameters, should be evaluated further. The poor inter-observer agreement of subjective analysis of the videos underlines the need for quantification of NIR fluorescence imaging with ICG. Larger studies should assess the predictive value of the observed perfusion patterns and parameters on the occurrence of anastomotic leakage.

## REFERENCES


1. Sung H, Ferlay J, Siegel RL, Laversanne M, Soerjomataram I, Jemal A, et al. Global Cancer Statistics 2020: GLOBOCAN Estimates of Incidence and Mortality Worldwide for 36 Cancers in 185 Countries. CA Cancer J Clin. 2021;71(3):209-49.
2. Voeten DM, Busweiler LAD, van der Werf LR, Wijnhoven BPL, Verhoeven RHA, van Sandick JW, et al. Outcomes of Esophagogastric Cancer Surgery During Eight Years of Surgical Auditing by the Dutch Upper Gastrointestinal Cancer Audit (DUCA). Ann Surg. 2021;274(5):866-73.
3. de Steur WO, Hutteman M, Hartgrink HH. Generalizability of the Results and Concerns About Leakage Rates of the ICAN Trial. JAMA Surg. 2022;157(2):176.
4. Alanezi K, Urschel JD. Mortality secondary to esophageal anastomotic leak. Ann Thorac Cardiovasc Surg. 2004;10(2):71-5.
5. Schlottmann F, Molena D. Anastomotic leak: an early complication with potentially long-term consequences. J Thorac Dis. 2016;8(10):E1219-E20.
6. Markar S, Gronnier C, Duhamel A, Mabrut JY, Bail JP, Carrere N, et al. The Impact of Severe Anastomotic Leak on Long-term Survival and Cancer Recurrence After Surgical Resection for Esophageal Malignancy. Ann Surg. 2015;262(6):972-80.
7. Hong ZN, Huang L, Zhang W, Kang M. Indocyanine Green Fluorescence Using in Conduit Reconstruction for Patients With Esophageal Cancer to Improve Short-Term Clinical Outcome: A Meta-Analysis. Front Oncol. 2022;12:847510.
8. Safiejko K, Tarkowski R, Kozlowski TP, Koselak M, Jachimiuk M, Tarasik A, et al. Safety and Efficacy of Indocyanine Green in Colorectal Cancer Surgery: A Systematic Review and Meta-Analysis of 11,047 Patients. Cancers (Basel). 2022;14(4).
9. Jafari MD, Pigazzi A, McLemore EC, Mutch MG, Haas E, Rasheid SH, et al. Perfusion Assessment in Left-Sided/Low Anterior Resection (PILLAR III): A Randomized, Controlled, Parallel, Multicenter Study Assessing Perfusion Outcomes With PINPOINT Near-Infrared Fluorescence Imaging in Low Anterior Resection. Dis Colon Rectum. 2021;64(8):995-1002.
10. Pather K, Deladisma AM, Guerrier C, Kriley IR, Awad ZT. Indocyanine green perfusion assessment of the gastric conduit in minimally invasive Ivor Lewis esophagectomy. Surg Endosc. 2022;36(2):896-903.
11. Van Daele E, De Bruyne N, Vanommeslaeghe H, Van Nieuwenhove Y, Ceelen W, Pattyn P. Clinical utility of near-infrared perfusion assessment of the gastric tube during Ivor Lewis esophagectomy. Surg Endosc. 2022;36(8):5812-21.
12. Hardy NP, Joosten JJ, Dalli J, Hompes R, Cahill RA, van Berge Henegouwen MI. Evaluation of inter-user variability in indocyanine green fluorescence angiography to assess gastric conduit perfusion in esophageal cancer surgery. Dis Esophagus. 2022.13.
13. Van Den Hoven P, Goncalves LN, Quax PHA, Van Rijswijk CSP, Van Schaik J, Schepers A, et al. Perfusion Patterns in Patients with Chronic Limb-Threatening Ischemia versus Control Patients Using Near-Infrared Fluorescence Imaging with Indocyanine Green. Biomedicines. 2021;9(10).
14. Jansen SM, de Bruin DM, Wilk LS, van Berge Henegouwen MI, Strackee SD, Gisbertz SS, et al. Quantitative Fluorescence Imaging of Perfusion-An Algorithm to Predict Anastomotic Leakage. Life (Basel). 2022;12(2)

**15.** Yukaya T, Saeki H, Kasagi Y, Nakashima Y, Ando K, Imamura Y, et al. Indocyanine Green Fluorescence Angiography for Quantitative Evaluation of Gastric Tube Perfusion in Patients Undergoing Esophagectomy. J Am Coll Surg. 2015;221(2):e37-42.

**16.** Ishige F, Nabeya Y, Hoshino I, Takayama W, Chiba S, Arimitsu H, et al. Quantitative Assessment of the Blood Perfusion of the Gastric Conduit by Indocyanine Green Imaging. J Surg Res. 2019;234:303-10.

**17.** von Kroge P, Russ D, Wagner J, Grotelüschen R, Reeh M, Izbicki JR, et al. Quantification of gastric tube perfusion following esophagectomy using fluorescence imaging with indocyanine green. Langenbecks Arch Surg. 2022.

**18.** Van Den Hoven P, Tange F, Van Der Valk J, Nerup N, Putter H, Van Rijswijk C, et al. Normalization of Time-Intensity Curves for Quantification of Foot Perfusion Using Near-Infrared Fluorescence Imaging With Indocyanine Green. J Endovasc Ther. 2022:15266028221081085.

**19.** Koo TK, Li MY. A Guideline of Selecting and Reporting Intraclass Correlation Coefficients for Reliability Research. J Chiropr Med. 2016;15(2):155-63.

**20.** Keereweer S, Van Driel PB, Snoeks TJ, Kerrebijn JD, Baatenburg de Jong RJ, Vahrmeijer AL, et al. Optical image-guided cancer surgery: challenges and limitations. Clin Cancer Res. 2013;19(14):3745-54.

# Chapter 10

## Quantification of indocyanine green near-infrared fluorescence bowel perfusion assessment in colorectal surgery

Hidde A. Galema*, Robin A. Faber*, Floris P. Tange*, Thomas C. Zwaan, Fabian A. Holman, Koen C. M. J. Peeters, Pieter J. Tanis, Cornelis Verhoef, Jacobus Burggraaf, J. Sven D. Mieog, Merlijn Hutteman, Stijn Keereweer, Alexander L. Vahrmeijer, Joost R. van der Vorst‡, Denise E. Hilling‡.

* Shared first authorship ‡ Shared senior authorship

Surg Endosc. 2023 Jun 7. doi: 10.1007/s00464-023-10140-8

## ABSTRACT

### Background

Indocyanine green near-infrared fluorescence bowel perfusion assessment has shown its potential benefit in preventing anastomotic leakage. However, the surgeon's subjective visual interpretation of the fluorescence signal limits the validity and reproducibility of the technique. Therefore, this study aimed to identify objective quantified bowel perfusion patterns in patients undergoing colorectal surgery using a standardized imaging protocol.

### Methods

A standardized fluorescence video was recorded. Postoperatively, the fluorescence videos were quantified by drawing contiguous region of interests (ROIs) on the bowel. For each ROI, a time-intensity curve was plotted from which perfusion parameters (n=10) were derived and analyzed. Furthermore, the inter-observer agreement of the surgeon's subjective interpretation of the fluorescence signal was assessed.

### Results

Twenty patients who underwent colorectal surgery were included in the study. Based on the quantified time-intensity curves, three different perfusion patterns were identified. Similar for both the ileum and colon, perfusion pattern 1 had a steep inflow that reached its peak fluorescence intensity rapidly, followed by a steep outflow. Perfusion pattern 2 had a relatively flat outflow slope immediately followed by its plateau phase. Perfusion pattern 3 only reached its peak fluorescence intensity after 3 minutes with a slow inflow gradient preceding it. The inter-observer agreement was poor-moderate (Intraclass Correlation Coefficient (ICC): 0.378, 95%-CI 0.210 – 0.579).

### Conclusion

This study showed that quantification of bowel perfusion is a feasible method to differentiate between different perfusion patterns. In addition, the poor-moderate inter-observer agreement of the subjective interpretation of the fluorescence signal between surgeons emphasizes the need for objective quantification.

## INTRODUCTION

Anastomotic leakage (AL) is a serious postoperative complication in colorectal surgery with an incidence ranging from 1 to 20% (1). It is associated with high morbidity and mortality, prolonged hospitalization, increased healthcare costs, and impaired oncological outcomes (2, 3). The etiology of AL is multifactorial, in which compromised bowel perfusion is considered as a major contributing factor. Conventionally, bowel perfusion is assessed intraoperatively based on subjective clinical indicators, including tissue color, peristaltic movements, active bleeding from marginal arteries and palpable mesenteric arterial pulsations. Additional tests that may be used to assess the integrity of the anastomosis are the air leak test, intraoperative endoscopy and doughnut inspection (4). However, the surgeon's judgement of these clinical indicators was found to have low predictive value for AL, which indicates the need for more accurate intraoperative diagnostic tests (5, 6).

Near-infrared (NIR) fluorescence imaging with indocyanine green (ICG) is a technique that enables real-time assessment of bowel perfusion. Several studies have shown its benefit to prevent AL (7). This is currently being validated in ongoing phase III randomized controlled trials, such as the AVOID trial (8) (NCT04712032), IntAct trial (9), and EssentiAL trial (jRCTs031180039), that should determine its clinical efficacy. However, the use of this technique is based on subjective visual interpretation of the fluorescence signal by the surgeon, which remains a limiting factor for the validity and reproducibility of these data in daily practice (10-13).

Quantitative evaluation of the fluorescence signal could increase the objectivity and accuracy of ICG NIR fluorescence bowel perfusion assessment. This method is based on the analysis of fluorescence intensity over time from which various inflow and outflow parameters can be derived. Some cohort studies have already investigated quantified bowel perfusion assessment using various generic quantification software (14-25). However, no consensus has been reached on which perfusion pattern and/or quantitative parameters can considered to be sufficiently reliable to assess bowel perfusion (26). This is partly due to the lack of a standardized imaging protocol, given the fact that intensity-based parameters are altered by camera-to-target distance, angle of camera to target tissue, type of imaging system and its settings (27).



This prospective cohort study aimed to identify quantified bowel perfusion patterns in patients undergoing colorectal surgery using a standardized imaging protocol. In addition, the inter-observer agreement of the surgeon's subjective interpretation of the fluorescence signal was assessed.

## METHODS

### Study design and population

This prospective, dual center, exploratory study was conducted at the Leiden University Medical Center (LUMC) and Erasmus MC Cancer institute (EMC), according to the declaration of Helsinki (10th version, Fortaleza, 2013). Twenty patients with colorectal cancer who underwent ICG NIR fluorescence-guided colorectal resection with a primary anastomosis were included in the study.

Medical ethical approval from the ethic committee Leiden-Den Haag-Delft was obtained (MEC-2021-0876). Informed consent was given by all patients.

### Surgical procedure

A standardized imaging protocol was used to obtain fluorescence videos for quantification of the fluorescence signal. Fluorescence videos were recorded using the Quest Spectrum 2.0 camera system (Quest Medical Imaging, Middenmeer, the Netherlands). ICG NIR fluorescence bowel perfusion assessment was performed extracorporeally in all patients regardless the surgical approach chosen (i.e., open or minimally invasive surgery). In patients undergoing minimally invasive surgery (i.e., laparoscopic or robotic), the ileum and/or afferent/efferent colon was extracted extracorporeally through a Pfannenstiel incision. Before extracorporeal ICG NIR fluorescence bowel perfusion assessment, the camera was fixed in the camera arm and positioned 30 centimeters above the target tissue at an angle of 90 degrees. Standardized camera settings (GAIN: color 3.5dB, ICG-fluor 20.0 dB; EXPOSURE: color 11.0 ms, ICG-fluor 50.0 ms) were maintained. After dissection of the vascular branch and prior to bowel transection, all patients received 5 mg ICG (2.5 mg/ml, Verdye, Diagnostic Green, Aschheim, Germany) intravenously followed by 10 mL saline flush according to standard care. Surgeons were allowed to change the surgical plan intraoperatively by performing an additional bowel resection based on their subjective interpretation of the fluorescence signal. Immediately after administration, a fluorescence video was recorded for 5 minutes. On each fluorescence video, the resection line was marked by the surgeon.

### Quantitative analyses

The Quest Research Framework (Quest Medical Imaging, Middenmeer, the Netherlands) was used for quantification of the fluorescence videos. Postoperatively, contiguous region of interests (ROIs; approximately of 1 cm length) from proximal to distal of the resection line were drawn on the ileum or afferent/efferent colon, depending on the surgical procedure performed (Figure 1). An example of a standardized fluorescence measurement is displayed in supplementary Video 1. The fluorescence signal as shown in Video 1 was quantified from multiple ROI's into corresponding time-intensity curves as illustrated in Figure 1. For each ROI, absolute (i.e., fluorescence intensity over time) and normalized (i.e., fluorescence intensity as a percentual change over time

by setting the maximum fluorescence intensity at 100 percent to minimize the influences of patient and camera-related factors (28)) time-intensity curves were plotted from which 5 inflow and 5 outflow parameters were derived. These time-intensity curves were analyzed separately for the ileum and colon. The inflow parameters included the maximum fluorescence intensity (Imax), maximum inflow slope (Ingress slope), mean slope from baseline to maximum fluorescence intensity (Ingress rate), maximum inflow slope in percentage per second (Normalized slope), and time to maximum intensity (Tmax); the outflow parameters included the maximum outflow slope (Egress slope), area under the curve in percentage after 30, 60, 120, and 180 seconds

## Outcomes

The primary outcome of this study was to identify quantified bowel perfusion patterns in patients undergoing colorectal surgery by analyzing the time-intensity curves plotted from each ROI and its derived inflow and outflow perfusion parameters. The secondary outcomes were to assess the inter-observer agreement of the surgeon's subjective interpretation of the fluorescence signal and ALs after 90 days (i.e., early and late AL). The colorectal surgeons (FH, KP, DH, AB, GF, PT, CV) all experienced with fluorescence-guided surgery, were individually asked to mark the intended resection line on all 20 fluorescence videos, based on their subjective interpretation of the fluorescence signal. from Tmax (AUC30, AUC60, AUC120, AUC180).

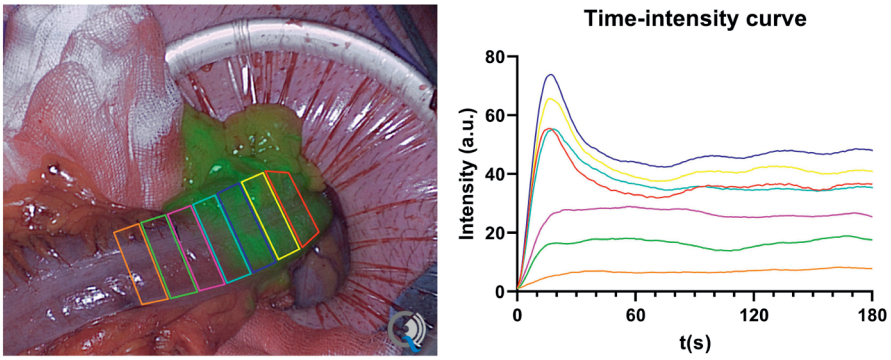


**Figure 1:** Quantification of a standardized fluorescence video using the Quest Research Framework quantification tool.
*Contiguous region of interests (ROIs) were drawn from proximal to distal of the resection line (located at the dark blue ROI) on the afferent colon. For each ROI, an absolute time-intensity curve was plotted. The color of each time-intensity curve corresponds to the color of the ROI.*

The distance between the markers (i.e., intended resection lines) on each fluorescence video was measured with ImageJ (National Institutes of Health, USA), in which the most proximal marker was used as the baseline measurement according to the previously published method of Hardy et al. [12, 13]. AL was defined as AL that required active therapeutic intervention but manageable without reoperation (Grade B) or AL that requires reoperation (Grade C), accord-

ing to the definition of the International Study Group of Rectal Cancer [29, 30]. To associate the quantified perfusion patterns with the occurrence of AL, the time-intensity curves plotted from the ROIs of the anastomosis were analyzed.

The time-intensity curves of the anastomosis from both the afferent ileum or colon and the efferent colon were analyzed when both could be imaged extracorporeally. If not, only the time-intensity curves of the afferent ileum or colon were analyzed.

### Statistical analyses

Patient characteristics were described using summary statistics. The distribution of all variables was assessed using histograms and verified with the Shapiro-Wilk test. Normally distributed variables were reported as means and standard deviation (SD) and skewed continuous variables were reported as medians and range. The inflow and outflow parameters from different perfusion patterns were compared using the One-way ANOVA or Kruskal Wallis test, depending on the distribution. The inter-observer agreement of the surgeon's subjective interpretation of the fluorescence signal was assessed by calculating the intraclass correlation coefficient (ICC) according to a two-way mixed model, consistency type, single measurement method. An ICC <0.50 indicated "poor agreement", ICC ≥0.50 up to 0.75 indicated "moderate agreement", ICC >0.75 up to 0.90 indicated "good agreement", and ICC >0.90 indicated "excellent agreement".

All statistical analyses were performed using SPSS Version 25.0. The statistical outcomes were considered significant if the p-value was <0.05.

## RESULTS

### Patient characteristics

Twenty patients (13 males; 7 females) with a median age of 63 years (range 46 – 83) were included in the analyses. Of these patients, 7 (35%) underwent a right-sided resection (i.e., ileocecal resection, right hemicolectomy or subtotal colectomy) and 13 (65%) patients underwent a left-sided resection (i.e., left hemicolectomy, sigmoid resection or low anterior resection). The majority (85%) of patients underwent surgery for a malignant tumour. Two (10%) patients received neo-adjuvant radiotherapy prior to surgical resection. A minimally invasive approach (i.e., laparoscopic or robotic) was performed in most patients (80%). The median in-hospital stay was 5 days (range 3 – 90). In total, 2 patients died during hospitalization of which 1 died due to an acute coagulation disorder and 1 patient died from an acute myocardial infarction. A detailed overview of all patient characteristics is shown in Table 1.

**Table 1:** Patient characteristics

| | | N (%) (n=20) |
|---|---|---|
| **Age,** *median (range)* | | 63 (46 – 83) |
| **Male** | | 13 (65%) |
| **BMI**[a] | *≥30* | 14 (70%) |
| | *<30* | 6 (30%) |
| **ASA-score** | *1* | 1 (5%) |
| | *2* | 14 (70%) |
| | *3* | 5 (25%) |
| **Smoking** | *Current* | 4 (20%) |
| | *Former* | 6 (30%) |
| | *Never* | 7 (35%) |
| **Neoplasm** | *Benign* | 3 (15%) |
| | *Malignant* | 17 (85%) |
| **Neo-adjuvant radiotherapy** | | 2 (10%) |
| **Type of surgery** | *Right-sided resection*[b] | 7 (35%) |
| | *Left-sided resection*[c] | 13 (65%) |
| **Surgical approach** | *Open* | 4 (20%) |
| | *Laparoscopic* | 11 (55%) |
| | *Robotic* | 5 (25%) |
| **Type of anastomosis** | *Side-to-side isoperistaltic* | 4 (20%) |
| | *Side-to-side antiperistaltic* | 4 (20%) |
| | *Side-to-end* | 10 (50%) |
| | *End-to-side* | 0 (0%) |
| | *End-to-end* | 1 (5%) |
| **Anastomosis technique** | *Handsewn* | 3 (15%) |
| | *Stapled* | 16 (80%) |
| **Hospitalization in days,** *median (range)* | | 5 (3 – 90) |
| **Anastomotic leakage** | | 4 (20%) |
| **Mortality** | | 2 (10%) |

[a] *Body Mass Index (weight per kilogram/length$^2$)*
[b] *Included ileocecal resection, right hemicolectomy, and subtotal colectomy.*
[c] *Included left hemicolectomy, sigmoid resection, and low anterior resection*

## Perfusion patterns

A total of 218 ROIs were drawn on the ileum or afferent/efferent colon, with a mean number of 11 ± 3.8 ROIs per patient. From these ROIs, 35 (16%) time-intensity curves of the ileum and 183 (84%) time-intensity curves of the colon were plotted and analyzed.

Based on qualitative assessment of the quantified time-intensity curves, three different perfusion patterns were identified. Similar for both the ileum and colon, perfusion pattern 1 was characterized by a steep inflow slope (Ingress slope) that reached its peak fluorescence intensity (Tmax) rapidly, followed by a steep outflow slope (Egress slope). In contrast, perfusion pattern 2 had a relatively flat outflow slope immediately followed by its plateau phase. Perfusion pattern 3 only reached its peak fluorescence intensity after 3 minutes with a slow inflow gradient preceding it.

Cut-off points were determined for each perfusion pattern based on the quantified perfusion parameters. For the ileum, the time-intensity curves were distributed among the three different perfusion patterns using the following cut-off values; pattern 1: Tmax <70 and Egress slope <-2.5; pattern 2: Tmax <70 and Egress slope ≥-2.5; pattern 3: Tmax ≥70.

The time-intensity curves of the colon were distributed using cut-off values such as pattern 1: Tmax <70 and Egress slope <-1; pattern 2: Tmax <70 and Egress slope ≥-1; pattern 3: Tmax ≥70. The mean normalized time-intensity curve with standard deviation of each perfusion pattern for both the ileum and colon are shown in Figure 2.

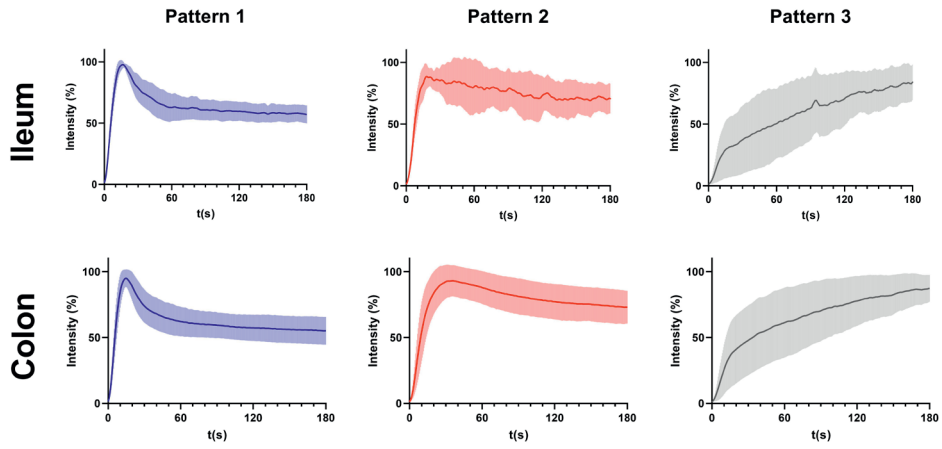


■ **Figure 2.** The mean normalized time-intensity curve with standard deviation of each perfusion pattern for both the ileum and colon.

The mean quantified perfusion parameters of each perfusion pattern were compared for both the ileum and colon. The Imax, Ingress slope, Ingress rate, Normalized slope, Tmax, and Egress slope of the ileum differed significantly between the three perfusion patterns. The AUC30, 60, 120 and 180 did not differ significantly. The perfusion parameters of the colon were all significantly different between the three perfusion patterns as shown in Table 2.

**Table 2.** In- and outflow parameters of the quantified time-intensity curves of the ileum and colon

| ILEUM | PATTERN 1 (n=17) | PATTERN 2 (n=8) | PATTERN 3 (n=10) | P-VALUE |
|---|---|---|---|---|
| **Imax**, *a.u. (range)* | 131.71 (70.07 – 162.21) | 48.75 (13.32 – 64.43) | 39.37 (4.15 – 77.85) | **<0.001** |
| **Ingress slope**, *a.u./sec (range)* | 15.45 (4.79 – 17.60) | 5.46 (1.55 – 7.41) | 1.18 (0.45 – 9.87) | **<0.001** |
| **Ingress rate**, *a.u./sec (range)* | 8.59 (2.49 – 10.17) | 1.14 (0.69 – 2.87) | 0.16 (0.02 – 0.56) | **<0.001** |
| **Normalized slope**, *%/sec (range)* | 11.99 (8.36 – 14.90) | 9.90 (5.75 – 15.22) | 4.66 (1.59 – 20.98) | **0.018** |
| **Tmax**, *sec (range)* | 14.50 (12.00 – 25.50) | 27.00 (13.00 – 60.00) | 215.25 (84.00 – 272.50) | **<0.001** |
| **Egress slope**, *a.u./sec (range)* | -4.18 (-8.59 – -2.51) | -1.26 (-2.31 – -0.58) | -0.54 (-8.42 – -0.06) | **<0.001** |
| **AUC 30**, *% (range)* | 78.12 (71.96 – 94.51) | 95.59 (68.39 – 96.99) | 96.46 (49.01 – 97.23) | 0.076 |
| **AUC 60**, *% (range)* | 68.39 (62.21 – 86.28) | 90.23 (57.68 – 95.86) | 96.84 (49.02 – 96.92) | 0.135 |
| **AUC 120**, *% (range)* | 62.14 (57.53 – 82.08) | 82.11 (53.45 – 92.56) | 95.91 (49.83 – 96.74) | 0.191 |
| **AUC 180**, *% (range)* | 60.12 (55.38 – 79.87) | 77.98 (52.38 – 91.61) | 94.07 (94.07 – 94.07) | 0.067 |
| **COLON** | **PATTERN 1 (n=95)** | **PATTERN 2 (n=32)** | **PATTERN 3 (n=56)** | **P-VALUE** |
| **Imax**, *a.u. (range)* | 87.49 (30.83 – 193.32) | 46.76 (2.61 – 88.61) | 25.22 (2.37 – 86.59) | **<0.001** |
| **Ingress slope**, *a.u./sec (range)* | 9.86 (3.73 – 35.03) | 3.41 (0.22 – 11.29) | 0.70 (0.11 – 10.98) | **<0.001** |
| **Ingress rate**, *a.u./sec (range)* | 5.51 (1.30 – 21.06) | 1.21 (0.12 – 5.12) | 0.10 (0.01 – 0.62) | **<0.001** |
| **Normalized slope**, *%/sec (range)* | 12.18 (6.58 – 19.38) | 8.16 (3.80 – 18.39) | 4.16 (1.43 – 12.68) | **<0.001** |
| **Tmax**, *sec (range)* | 13.00 (8.00 – 39.50) | 29.75 (8.00 – 63.00) | 231.00 (82.00 – 270.00) | **<0.001** |
| **Egress slope**, *a.u./sec (range)* | -2.44 (-12.06 – -1.04) | -0.59 (-0.97 – -0.14) | -0.26 (-4.30 – -0.00) | **<0.001** |
| **AUC 30**, *% (range)* | 77.56 (59.59 – 94.85) | 94.82 (52.69 – 98.08) | 96.91 (78.93 – 99.28) | **<0.001** |
| **AUC 60**, *% (range)* | 68.44 (52.78 – 91.08) | 89.52 (42.54 – 96.91) | 95.80 (80.53 – 98.11) | **<0.001** |
| **AUC 120**, *% (range)* | 61.85 (48.08 – 95.90) | 84.47 (38.40 – 96.70) | 93.35 (81.37 – 96.11) | **<0.001** |
| **AUC 180**, *% (range)* | 58.43 (45.96 – 85.49) | 81.09 (37.95 – 95.01) | 85.59 (81.32 – 93.49) | **<0.001** |

***White rows:*** *inflow parameters;* ***Grey rows:*** *outflow parameters;* ***a.u.:*** *arbitrary units;* ***sec:*** *second*
***Fmax:*** *maximum fluorescence intensity,* ***Ingress slope:*** *maximum inflow slope,* ***Ingress rate:*** *mean slope from baseline to maximum fluorescence intensity,* ***Normalized slope:*** *maximum inflow slope in percentage per second,* ***Tmax:*** *time to maximum intensity,* ***Egress slope:*** *maximum outflow slope,* ***AUC30:*** *area under de curve after 30 seconds,* ***AUC60:*** *area under de curve after 60 seconds,* ***AUC120:*** *area under de curve after 120 seconds,* ***AUC180:*** *area under de curve after 180 seconds.*

### Subjective interpretation of ICG NIR fluorescence imaging

All (n=20) ICG NIR fluorescence imaging videos were independently assessed by 7 colorectal surgeons. The inter-observer agreement of the intended resection lines determined by the surgeons based on their subjective interpretation of the fluorescence signal was poor – moderate, with an ICC of 0.378 (95% CI: 0.210 – 0.579). The median distance between the most proximal marker (i.e., baseline) and the most distal marker on the afferent and/or efferent ileum or colon was 1.122 cm (range 0.071 – 3.861). An overview of the distances (in centimeter) between the markers (i.e., intended resection lines) per fluorescence video are demonstrated in an ICC dot plot in Figure 3.

The surgical plan has been changed in 4 (20%) patients by performing an additional bowel resection based on the intraoperative subjective interpretation of the fluorescence signal by the surgeon (Figure 4.). In 1 patient, perfusion pattern 2 was observed at the location of the intended anastomosis. After performing additional bowel resection, perfusion pattern 1 was observed.

Perfusion pattern 3 was observed in the other 3 patients at the location of the intended anastomosis and after additional bowel resection, perfusion pattern 2 was observed in 2 patients and perfusion pattern 1 in another patient. In none of these patients an AL occurred after 90 days of follow-up.

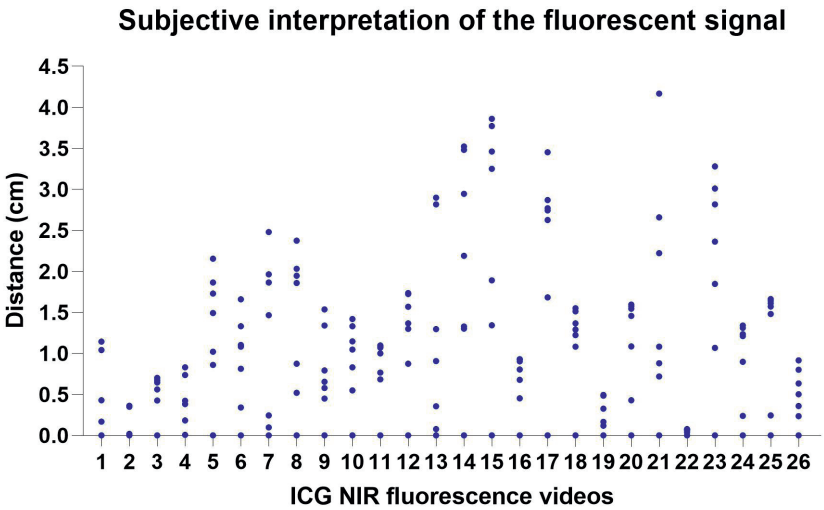


■ **Figure 3.** Inter-observer agreement of the surgeon's subjective interpretation of the fluorescent signal per ICG NIR fluorescence video.
*Each blue dot represents an intended resection line marked by the surgeon based on the fluorescence signal, with the most proximal marker used as the baseline. An ICG NIR fluorescence video of both the afferent ileum or colon and the efferent colon was analyzed separately. Intraclass correlation (ICC) of 0.378 (95%-CI 0.210 – 0.579).*

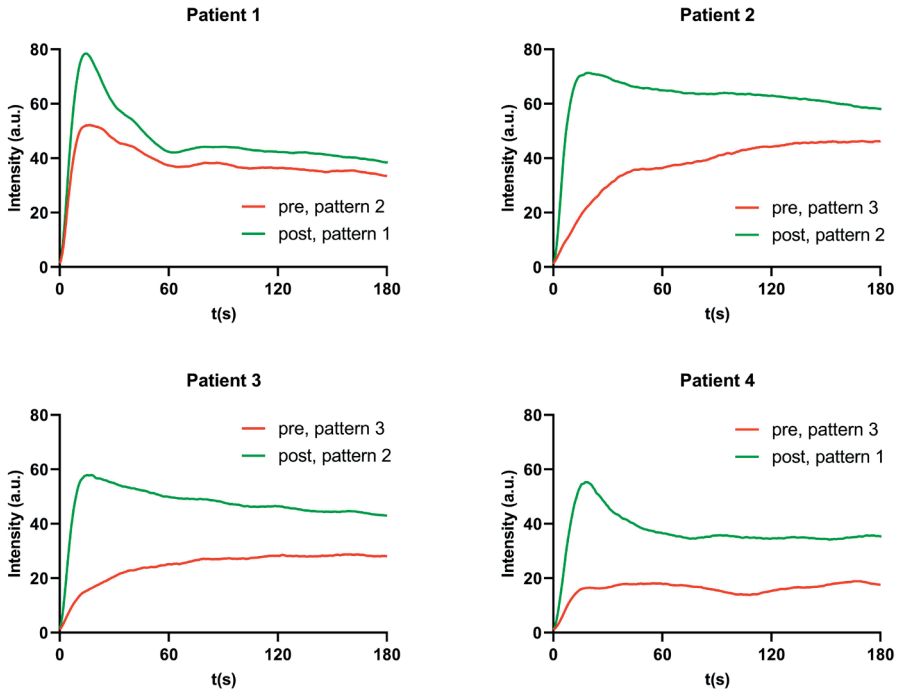


**Figure 4.** Time-intensity curves before and after additional bowel resection based on the surgeon's subjective interpretation of the fluorescence signal in 4 patients.
*The red time-intensity curves represent the fluorescence signal of the intended anastomosis and the green time-intensity curves represent the fluorescence signal of the actual anastomosis after additional bowel resection.*

## Clinical outcome

A total of 24 time-intensity curves plotted from the ROIs of the anastomosis (afferent ileum or colon and efferent colon in 5 patients (n=10); afferent ileum or colon alone in 14 patients (n=14)) were analyzed (Figure 5). Of all (n=24) time-intensity curves, 17 (71%) corresponded to perfusion pattern 1, 6 (25%) time-intensity curves to perfusion pattern 2, and 1 (4%) time-intensity curve corresponded to perfusion pattern 3.

AL occurred in 4 (20%) patients. In 1 patient who underwent a right hemicolectomy, the time-intensity curve of the anastomosis on the afferent ileum corresponded to perfusion pattern 3 and the efferent colon to perfusion pattern 1. Postoperatively, this patient developed an acute coagulation disorder with subsequent bowel ischemia and anastomotic leakage as was observed during relaparotomy, after which the patient died. The other 3 patients who developed anastomotic leakage, underwent left-sided resection and the time-intensity curve of the anastomosis on the afferent colon corresponded to perfusion pattern 1. In 1 of these 3 patients, macroscopic ischemia on the afferent colon was observed during relaparotomy.

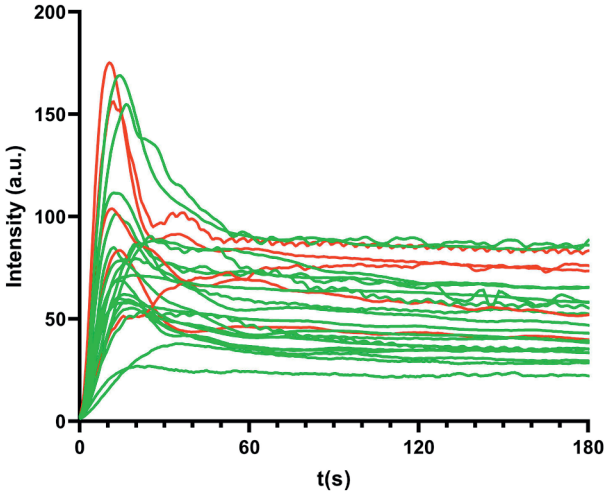


■ **Figure 5.** The absolute time-intensity curves plotted from the ROI of the anastomosis. The ***red*** absolute time-intensity curves represents the patients who developed an anastomotic leakage.

## DISCUSSION

This prospective dual center cohort study identified quantified bowel perfusion patterns in patients undergoing colorectal surgery by using a standardized imaging protocol. A clear overview of the bowel perfusion was obtained by drawing contiguous ROIs from proximal to distal of the resection line on the ileum and afferent/efferent colon. The quantified time-intensity curves plotted from these ROIs could be divided into three different perfusion patterns. Perfusion pattern 1 implied for well-perfused bowel tissue, as it was mainly observed at the most proximal side of the resection line on the afferent ileum or colon and at the most distal side of the resection line on the efferent colon. In contrast, perfusion pattern 3 implied for poorly perfused bowel tissue, since it was generally present at the avascular region of the ileum or colon from which the vascular branch was already dissected. Perfusion pattern 2 implied for the transition zone, where perfusion pattern 1 transitions to perfusion pattern 3. These three perfusion patterns were identified in each patient and might be a representation of the actual bowel perfusion.

Several cohort studies have investigated quantified bowel perfusion using various quantification methods (14-25). In contrast to our study, most of these studies did not use a standardized imaging protocol (i.e., inconsistency in camera-to-target distance, angle of camera on target tissue, type of imaging system and its settings, etc.). Moreover, the ROIs were selected based on the surgeon's subjective interpretation of the fluorescence signal (14-16, 18-21, 23-25). As a result, the study results were difficult to compare, which may negatively affect

the reproducibility of previously reported quantification methods. Although in our study cut-off values to divide the time-intensity curves among the three perfusion patterns were determined based on qualitative assessment of the quantified time-intensity curves, the subjective factor was limited. Therefore, our quantification method might be more reproducible, which should be validated in larger studies.

Currently, ICG NIR fluorescence bowel perfusion assessment relies on the surgeon's subjective interpretation of the fluorescence signal to guide clinical decision-making, which limits the reproducibility and validity of the technique (10-13). This is underlined in this study where a poor-moderate inter-observer agreement of the surgeon's subjective interpretation of the fluorescence signal was observed, with an ICC of 0.378 (95%-CI 0.210 – 0.579).

The ICC was lower compared to the previous published study by Hardy et al. (12), in which a good ICC of 0.753 (95% IC 0.510 – 0.932) for experts and a moderate ICC of 0.613 (95% IC 0.409 – 0.856) for non-experts were found. In this study, there were some outliers in the surgeon's subjective interpretation of the fluorescence signal (e.g., ICG NIR fluorescence videos 14, 15, and 21; Figure 3) for which no clear explanation was found. A possible explanation for this variability could be the different ways in which surgeons interpret the fluorescence signal, with one surgeon focusing on eventually the most distal fluorescent resection line, another surgeon assessing the fluorescence signal by focusing on the time to maximum fluorescence, and other surgeons being more cautious in defining the resection line based on the fluorescence signal. Although a low ICC is not necessarily detrimental to the clinical outcome (i.e., AL), this study demonstrates the need for quantification of ICG NIR fluorescence imaging to improve the objectivity and accuracy of the bowel perfusion assessment. Especially when bowel length preservation becomes more important, for example in re-resections, Crohn's disease, or in ultralow anterior resection.

The AL rate (20%) in this study was remarkably high when compared to the national AL rate of 6% in 2016 according to the Dutch Colorectal Audit (DCRA) (31). This AL rate is believed to be an overestimation due to the small sample size as both participating hospitals have annual AL rates that are comparable with the national AL rate by the DCRA. Moreover, the high AL rate could also be explained by the fact that all included patients underwent surgery in tertiary academic hospitals that provide healthcare in highly complex patients in whom the a priori risk of developing AL will be higher. This could also be an explanation of the mortality rate of 10% (n=2) in our study. One patient who developed AL was postoperatively admitted to the intensive care unit for respiratory insufficiency due to an aspiration pneumonia, followed by an acute coagulation disorder which resulted in an acute ischemic limb and bowel ischemia with AL as seen during relaparotomy, after which the patient died. The second patient (ASA-3 with cardiovascular risk factors such as smoking, obesity and diabetes mellitus 2) died of

acute myocardial infarction postoperatively. In the other patients with AL, one patient underwent robotic low anterior resection (LAR) and a relaparotomy was performed three days postoperatively to evacuate a hematoma in the small pelvis.

A vital anastomosis was observed during this procedure, however, nine days after primary surgery, the patient developed AL without any signs of ischemia on the afferent colon during relaparotomy. In another patient using long-term prednisolone for IgG4 cholangiopathy, an AL with macroscopic ischemia on the afferent colon was observed. The last patient developed AL in whom LAR was combined with a left nephrectomy. During relaparotomy, a limited AL was observed that required a diverting stoma. Given these highly complex cases, no firm conclusions can be drawn about the high AL and mortality rates found in this study.

Although this pilot study was too small to assess the correlation between the quantified perfusion patterns and AL, the perfusion patterns of the patients who developed AL (n=4) were analyzed. Interestingly, in three of these patients the time-intensity curves of the anastomosis corresponded to perfusion pattern 1. However, in only one of them macroscopic ischemia on the afferent colon was observed during relaparotomy. This may be explained by the fact that ICG NIR fluorescence bowel perfusion assessment has been implemented as standard care, allowing the surgeon to change the surgical plan intraoperatively based on subjective interpretation of the fluorescence signal. As a result, risk factors other than tissue perfusion might be overrepresented in this cohort, since the development of AL is known to have a multifactorial cause. Future studies should investigate the predictive value of each perfusion pattern on the development of AL.

This study has some limitations. First, the primary goal of this exploratory study was to identify quantified bowel perfusion patterns. Therefore, the study design does not allow for any firm conclusions to be drawn about the reliability of the determined cut-off values distributing the time-intensity curves among the three perfusion patterns and the correlation between each perfusion pattern and the development of AL. Thus, there might be a risk of random sampling errors. Additionally, variation in patient-specific hemodynamic factors or the use of vasopressors during the ICG NIR fluorescence measurement could affect the observed perfusion pattern which requires further evaluation because of limited evidence in literature [32]. Second, our standardized imaging protocol only allows for extracorporeal video recordings of the ICG NIR fluorescence bowel perfusion assessment. Therefore, in some patients undergoing laparoscopic or robotic left-sided resection, only quantification of the ICG NIR fluorescence imaging video of the afferent colon was possible. Standardization of the camera-to-tissue distance and angle of the camera to tissue can be challenging to maintain during intra-abdominal imaging. However, some studies have shown that quantification of the fluorescence signal using a laparoscopic imaging system might be possible, but the tech-

nique of this intracorporeal method is still in its early stages and needs further optimization [23, 33).

Lastly, even though the quantification tool is suited to produce proper time-intensity curves in most patients (n=18), the motion tracker of the quantification tool was unable to correct for severe breathing-related movements in two patients. These movements resulted in a fluctuating line in the time-intensity curve, which affected the accuracy of some perfusion parameters (e.g., Tmax or Egress slope). Although this effect was negligible in our study, the quantification software needs further improvement for daily use.

In the future, larger studies with powered sample sizes should investigate the variation in perfusion patterns and corresponding cut-off values within various bowel parts in correlation to the occurrence of an AL. In addition, these studies should give us a conclusive answer whether quantified perfusion patterns are a reflection of the actual bowel perfusion status and if these pattern could be of added value to predict AL intraoperatively. Moreover, quantification of ICG NIR fluorescence bowel perfusion assessment should be performed intraoperatively to guide the surgeon's clinical decision-making during surgery and to allow immediate modification of the surgical plan when needed.

## CONCLUSION

In conclusion, this prospective cohort study showed that quantification of ICG NIR fluorescence bowel perfusion assessment is a feasible method to differentiate between different perfusion patterns. The use of a standardized imaging protocol could improve the reproducibility of the quantification method. Moreover, the poor-moderate inter-observer agreement of the subjective interpretation of the fluorescence signal between surgeons emphasizes the need for quantification of the fluorescent signal to improve the objectivity and accuracy of the bowel perfusion assessment. Future studies should examine the clinical value of these different perfusion patterns by correlating each perfusion pattern with the development of AL.

## REFERENCES


1. Arron MNN, Greijdanus NG, Ten Broek RPG, Dekker JWT, van Workum F, van Goor H, Tanis PJ, de Wilt JHW (2021) Trends in risk factors of anastomotic leakage after colorectal cancer surgery (2011-2019): A Dutch population-based study. Colorectal Dis 23**:**3251-3261
2. McDermott FD, Heeney A, Kelly ME, Steele RJ, Carlson GL, Winter DC (2015) Systematic review of preoperative, intraoperative and postoperative risk factors for colorectal anastomotic leaks. Br J Surg 102**:**462-479
3. Ramphal W, Boeding JRE, Gobardhan PD, Rutten HJT, de Winter L, Crolla R, Schreinemakers JMJ (2018) Oncologic outcome and recurrence rate following anastomotic leakage after curative resection for colorectal cancer. Surg Oncol 27**:**730-736
4. Nachiappan S, Askari A, Currie A, Kennedy RH, Faiz O (2014) Intraoperative assessment of colorectal anastomotic integrity: a systematic review. Surg Endosc 28**:**2513-2530
5. Karliczek A, Harlaar NJ, Zeebregts CJ, Wiggers T, Baas PC, van Dam GM (2009) Surgeons lack predictive accuracy for anastomotic leakage in gastrointestinal surgery. Int J Colorectal Dis 24**:**569-576
6. Clifford RE, Fowler H, Manu N, Sutton P, Vimalachandran D (2021) Intra-operative assessment of left-sided colorectal anastomotic integrity: a systematic review of available techniques. Colorectal Dis 23**:**582-591
7. Song M, Liu J, Xia D, Yao H, Tian G, Chen X, Liu Y, Jiang Y, Li Z (2021) Assessment of intraoperative use of indocyanine green fluorescence imaging on the incidence of anastomotic leakage after rectal cancer surgery: a PRISMA-compliant systematic review and meta-analysis. Tech Coloproctol 25**:**49-58
8. Meijer RPJ, Faber RA, Bijlstra OD, Braak J, Meershoek-Klein Kranenbarg E, Putter H, Mieog JSD, Burggraaf K, Vahrmeijer AL, Hilling DE (2022) AVOID; a phase III, randomised controlled trial using indocyanine green for the prevention of anastomotic leakage in colorectal surgery. BMJ Open 12**:**e051144
9. Armstrong G, Croft J, Corrigan N, Brown JM, Goh V, Quirke P, Hulme C, Tolan D, Kirby A, Cahill R, O'Connell PR, Miskovic D, Coleman M, Jayne D (2018) IntAct: intra-operative fluorescence angiography to prevent anastomotic leak in rectal cancer surgery: a randomized controlled trial. Colorectal Dis 20**:**O226-o234
10. Degett TH, Andersen HS, Gogenur I (2016) Indocyanine green fluorescence angiography for intraoperative assessment of gastrointestinal anastomotic perfusion: a systematic review of clinical trials. Langenbecks Arch Surg 401**:**767-775
11. Galema HA, Faber RA, Tange FP, Hilling DE, van der Vorst JR, Upper GIICGqsg (2023) A quantitative assessment of perfusion of the gastric conduit after oesophagectomy using near-infrared fluorescence with indocyanine green. Eur J Surg Oncol 49**:**990-995
12. Hardy NP, Dalli J, Khan MF, Andrejevic P, Neary PM, Cahill RA (2021) Inter-user variation in the interpretation of near infrared perfusion imaging using indocyanine green in colorectal surgery. Surg Endosc 35**:**7074-7081
13. Hardy NP, Joosten JJ, Dalli J, Hompes R, Cahill RA, van Berge Henegouwen MI (2022) Evaluation of inter-user variability in indocyanine green fluorescence angiography to assess gastric conduit perfusion in esophageal cancer surgery. Dis Esophagus

**14.** Han SR, Lee CS, Bae JH, Lee HJ, Yoon MR, Al-Sawat A, Lee DS, Lee IK, Lee YS (2022) Quantitative evaluation of colon perfusion after high versus low ligation in rectal surgery by indocyanine green: a pilot study. Surg Endosc 36**:**3511-3519

**15.** Gomez-Rosado JC, Valdes-Hernandez J, Cintas-Catena J, Cano-Matias A, Perez-Sanchez A, Del Rio-Lafuente FJ, Torres-Arcos C, Lara-Fernandez Y, Capitan-Morales LC, Oliva-Mompean F (2022) Feasibility of quantitative analysis of colonic perfusion using indocyanine green to prevent anastomotic leak in colorectal surgery. Surg Endosc 36**:**1688-1695

**16.** D'Urso A, Agnus V, Barberio M, Seeliger B, Marchegiani F, Charles AL, Geny B, Marescaux J, Mutter D, Diana M (2021) Computer-assisted quantification and visualization of bowel perfusion using fluorescence-based enhanced reality in left-sided colonic resections. Surg Endosc 35**:**4321-4331

**17.** Gosvig K, Jensen SS, Qvist N, Nerup N, Agnus V, Diana M, Ellebaek MB (2021) Quantification of ICG fluorescence for the evaluation of intestinal perfusion: comparison between two software-based algorithms for quantification. Surg Endosc 35**:**5043-5050

**18.** Ahn HM, Son GM, Lee IY, Park SH, Kim NS, Baek KR (2021) Optimization of indocyanine green angiography for colon perfusion during laparoscopic colorectal surgery. Colorectal Dis 23**:**1848-1859

**19.** Amagai H, Miyauchi H, Muto Y, Uesato M, Ohira G, Imanishi S, Maruyama T, Tochigi T, Okada K, Maruyama M, Matsubara H (2020) Clinical utility of transanal indocyanine green near-infrared fluorescence imaging for evaluation of colorectal anastomotic perfusion. Surg Endosc 34**:**5283-5293

**20.** Iwamoto H, Matsuda K, Hayami S, Tamura K, Mitani Y, Mizumoto Y, Nakamura Y, Murakami D, Ueno M, Yokoyama S, Hotta T, Takifuji K, Yamaue H (2020) Quantitative Indocyanine Green Fluorescence Imaging Used to Predict Anastomotic Leakage Focused on Rectal Stump During Laparoscopic Anterior Resection. J Laparoendosc Adv Surg Tech A 30**:**542-546

**21.** Park SH, Park HM, Baek KR, Ahn HM, Lee IY, Son GM (2020) Artificial intelligence based real-time microcirculation analysis system for laparoscopic colorectal surgery. World J Gastroenterol 26**:**6945-6962

**22.** Seeliger B, Agnus V, Mascagni P, Barberio M, Longo F, Lapergola A, Mutter D, Klymchenko AS, Chand M, Marescaux J, Diana M (2020) Simultaneous computer-assisted assessment of mucosal and serosal perfusion in a model of segmental colonic ischemia. Surg Endosc 34**:**4818-4827

**23.** Hayami S, Matsuda K, Iwamoto H, Ueno M, Kawai M, Hirono S, Okada K, Miyazawa M, Tamura K, Mitani Y, Kitahata Y, Mizumoto Y, Yamaue H (2019) Visualization and quantification of anastomotic perfusion in colorectal surgery using near-infrared fluorescence. Tech Coloproctol 23**:**973-980

**24.** Son GM, Kwon MS, Kim Y, Kim J, Kim SH, Lee JW (2019) Quantitative analysis of colon perfusion pattern using indocyanine green (ICG) angiography in laparoscopic colorectal surgery. Surg Endosc 33**:**1640-1649

**25.** Wada T, Kawada K, Takahashi R, Yoshitomi M, Hida K, Hasegawa S, Sakai Y (2017) ICG fluorescence imaging for quantitative evaluation of colonic perfusion in laparoscopic colorectal surgery. Surg Endosc 31**:**4184-4193

**26.** Slooter MD, Mansvelders MSE, Bloemen PR, Gisbertz SS, Bemelman WA, Tanis PJ, Hompes R, van Berge Henegouwen MI, de Bruin DM (2021) Defining indocyanine green fluorescence to assess anastomotic perfusion during gastrointestinal surgery: systematic review. BJS Open 5

**27.** Lutken CD, Achiam MP, Osterkamp J, Svendsen MB, Nerup N (2021) Quantification of fluorescence angiography: Toward a reliable intraoperative assessment of tissue perfusion - A narrative review. Langenbecks Arch Surg 406**:**251-259

**28.** Van Den Hoven P, Tange F, Van Der Valk J, Nerup N, Putter H, Van Rijswijk C, Van Schaik J, Schepers A, Vahrmeijer A, Hamming J, Van Der Vorst J (2022) Normalization of Time-Intensity Curves for Quantification of Foot Perfusion Using Near-Infrared Fluorescence Imaging With Indocyanine Green. J Endovasc Ther**:**15266028221081085

**29.** Rahbari NN, Weitz J, Hohenberger W, Heald RJ, Moran B, Ulrich A, Holm T, Wong WD, Tiret E, Moriya Y, Laurberg S, den Dulk M, van de Velde C, Buchler MW (2010) Definition and grading of anastomotic leakage following anterior resection of the rectum: a proposal by the International Study Group of Rectal Cancer. Surgery 147**:**339-351

**20.** Kulu Y, Ulrich A, Bruckner T, Contin P, Welsch T, Rahbari NN, Buchler MW, Weitz J, International Study Group of Rectal C (2013) Validation of the International Study Group of Rectal Cancer definition and severity grading of anastomotic leakage. Surgery 153**:**753-761

**21.** de Neree Tot Babberich MPM, Detering R, Dekker JWT, Elferink MA, Tollenaar R, Wouters M, Tanis PJ (2018) Achievements in colorectal cancer care during 8 years of auditing in The Netherlands. Eur J Surg Oncol 44**:**1361-1370

**22.** Al-Taher M, Pruimboom T, Schols RM, Okamoto N, Bouvy ND, Stassen LPS, van der Hulst R, Kugler M, Hostettler A, Noll E, Marescaux J, Diemunsch S, Diana M (2021) Influence of intraoperative vasopressor use on indocyanine green fluorescence angiography: first evaluation in an experimental model. Sci Rep 11**:**9650

**53.** Osterkamp J, Strandby R, Nerup N, Svendsen M, Svendsen L, Achiam M (2021) Quantitative fluorescence angiography detects dynamic changes in gastric perfusion. Surg Endosc 35**:**6786-6795

# Part IV

## Summary, general discussion, and future perspectives

# Chapter 11

## English summary / Nederlandse samenvatting

## ENGLISH SUMMARY

The aim of this thesis was to further improve clinical implementation of intraoperative near-infrared (NIR) fluorescence imaging, with a focus on tumour imaging and perfusion assessment. In this section, the methodology and results of each chapter are summarised in order of appearance in this thesis.

### Part I: Current status of intraoperative imaging in surgical oncology

The first part of this thesis consists of systematic literature studies in order to review the status of (NIR fluorescence) imaging and to describe the challenges that needed to be addressed for further implementation of the technique in daily surgical practice. To gain more insights in the current clinical applications of NIR fluorescence imaging in colorectal cancer surgery, a systematic review was performed and presented in **chapter 2**. The following clinical applications were identified and discussed: imaging of primary and recurrent tumours, sentinel lymph node imaging, imaging of peritoneal and liver metastases, imaging of nerves, imaging of the ureters and the urethra, and perfusion assessment of anastomoses or an omentoplasty. Both experimental and FDA/EMA approved fluorescent agents are discussed in this chapter.

In **chapter 3** of this thesis, we describe the use of several imaging modalities that can be used intraoperatively for margin assessment of laryngeal cancer. Laryngeal cancer is a prevalent head and neck malignancy, with poor prognosis and low survival rates for patients with advanced disease. In order to improve surgical resection of laryngeal cancer and reduce local recurrence rates, various intraoperative optical imaging techniques have been investigated. In this systematic review, we identify these technologies, evaluating the current state and future directions of optical imaging for this indication. Narrow-band imaging and autofluorescence are established tools for early detection of laryngeal cancer. Nonetheless, their intraoperative utility is limited by an intrinsic inability to image beyond the mucosa. Likewise, contact endoscopy (CE) and optical coherence tomography (OCT) are technically cumbersome and only useful for mucosal margin assessment. Research on fluorescence imaging for this application is sparse, dealing solely with nonspecific fluorescent agents. Evidently, the imaging modalities that have been investigated thus far are generally unsuitable for deep margin assessment. We discuss two optical imaging techniques that can overcome these limitations and suggest how they can be used to achieve adequate margins in laryngeal cancer at all stages.

In **chapter 4** of this thesis we focus on fluorescence imaging for sentinel lymph node (SLN) mapping in colorectal cancer. SLN mapping can be a valuable addition to the treatment of colorectal cancer patients. Nevertheless, conventional lymph node mapping methods using blue dye are limited due to inadequate depth penetration, and the use of a radiocolloid tracer

has its logistic hurdles. With near-infrared (NIR) fluorescence imaging, the SLN can be accurately identified in most patients resulting in more accurate lymph node staging. Current technical challenges and the low negative predictive value of the SLN withhold surgeons from its use in daily practice.

## Part II: Tumour target expression in tumour tissue samples for NIR fluorescence imaging

In the second part of this thesis, we aimed to identify new tumour markers for NIR fluorescence imaging. Overexpression of these targets was assessed with immunohistochemistry (IHC). In **chapter 5**, we focussed on marker expression in oesophageal cancer. The expression of the following tumour markers was studied: CEA, c-MET, EGFR, EpCAM, and VEGF-α. Marker expression was quantified with the total immunostaining score (TIS) with a cut-off value of ≥ 6 for 'high expression'. The effect of neoadjuvant therapy on tumour marker expression was assessed by comparing the TIS from the paired pre- and post-treatment tissue samples. We found that EpCAM expression was high in 89% of the adenocarcinomas and EGFR expression was high in 100% of the squamous cell carcinomas SCC. Expression of all markers was not negatively affected by neoadjuvant therapy. Expression of all tumour markers was absent in tumour scar tissue after pathological complete response. Thus, these markers create opportunities for future studies assessing endoscopic NIR fluorescence imaging of oesophageal cancer during clinical response evaluation. Given that expression was not affected by neoadjuvant therapy, a patient specific tracer may be selected based on marker expression on the diagnostic biopsy.

## Part III: Clinical studies on intraoperative NIR fluorescence imaging in oncological surgery

In the third part of this thesis we present several clinical studies on intraoperative NIR fluorescence imaging. In **chapter 6** of this thesis we present a study in which we investigated whether NIR fluorescence imaging with methylene blue improves visualisation of small intestinal neuroendocrine tumours (SI-NETs). Seventeen patients undergoing open resection of SI-NETs were included in this prospective clinical trial. Intravenous methylene blue was intraoperatively administered followed by NIR fluorescence imaging. Seventeen primary tumour lesions, with a median TBR of 1.10 (IQR: 1.00 – 1.17), were identified. None of the primary tumours or the multiple primaries had a TBR ≥ 1.5. A total of 109 metastatic lesions were identified, of which 101 (93%) had a TBR ≥ 1.5 (median TBR: 1.90 (IQR: 1.71 – 2.01)). By using NIR fluorescence imaging, additional peritoneal metastases were found in three patients. Based on these results, it can be concluded that NIR fluorescence imaging using methylene blue allows for improved visualisation of peritoneal metastases, liver metastases, and mesenteric masses of SI-NETs. However, methylene blue does not appear to be useful for detection of the primary tumour or occult multiple primaries.

The presented study in **chapter 7** assesses binding of the CEA specific tracer SGM-101 to colorectal lung metastases (CLM). During CLM surgery, margin assessment and identification of small nodules can be challenging, especially with a minimally invasive approach. Intraoperative real time fluorescence imaging has the potential to overcome these challenges. We conducted a prospective open-label study, in which 13 patients undergoing surgical resection for CLM were included. Patients were administered with SGM-101 3 – 5 days prior to surgery. Eighteen CLM were identified and positive fluorescence signal with *in vivo*, back table and closed-field bread loaf imaging was observed in 31%, 45% and 94% of the tumour lesions. Median signal-to-background ratios (SBRs) for the three imaging modalities were 1.00 (IQR: 1.00 – 1.53), 1.45 (IQR: 1.00 – 1.89) and 4.81 (IQR: 2.70 – 7.41) respectively. Six resected benign lesions were all negative for fluorescence (true negatives). All tumour lesions had a total immunostaining score for CEA expression of 12/12. The study demonstrated the potential of fluorescence imaging of CLM with SGM-101. CEA expression was observed in all tumours and closed-field imaging showed excellent binding of the tracer to the tumour nodules. The full potential of SGM-101 for *in vivo* detection of the tumours can be achieved with improved minimally invasive imaging systems and optimal patient selection.

In **chapter 8** we graphically present the unique application of Indocyanine green fluorescence angiography (ICG-FA) to guide transection planes for a colon interposition. The case reported is a complicated course after oesophagectomy, in which eventually restoration of continuity was performed using a colon interposition. In order to assess perfusion of the colon interposition, we suggest an approach in which a situation is created where the colon is solely perfused by the middle colic artery, before transection of the colon and its vascularisation. This was done by placing forceps on the left colic artery and on the colon at the location of the future distal transection line, in order to prevent retrograde blood flow. After doing so, 10 mg ICG was intravenously injected, and an intense fluorescence signal over the whole left colon was observed. After transection of the colon, another 10 mg ICG was administered to assess perfusion of the colon interposition. Perfusion was deemed sufficient and adequate anastomoses were created. Postoperatively, the patient recovered well and was able to take full oral intake after 7 weeks.

In the last two chapters of this thesis we present two pilot studies in which we aimed to further improve outcomes of ICG-fluorescence angiography (ICG-FA). As stated in the introduction section of this thesis, the observed signal of ICG-FA can be affected by unstandardized imaging or administration protocols. Moreover, it was hypothesised that subjective interpretation of the signal leads to variation between surgeons in selection of locations to create an anastomosis. In **chapter 9** we focussed on the role of quantified ICG-FA in perfusion assessment of the gastric conduit, whereas in **chapter 10** bowel tissue was assessed. In both studies, standardized imaging and administration protocols were followed. Twenty patients

per study were included. For every patient, a standardized NIR ICG-FA video was recorded, with fixed camera settings and surrounding factors. Postoperatively, the signal was quantified in order to objectify the measurements. Primary outcomes were the time-intensity curves and nine perfusion parameters from contiguous regions of interest on the gastric conduit. A secondary outcome was the inter-observer agreement of subjective interpretation of the ICG-FA videos between six surgeons. The inter-observer agreement was tested with an intraclass correlation coefficient (ICC). For both the gastric conduit and the bowel, three distinct perfusion patterns were recognized: pattern 1 (steep inflow, steep outflow); pattern 2 (steep inflow, minor outflow); and pattern 3 (slow inflow, no outflow). All curves were systematically categorized in one of each patterns based on the time-to-max and max egress slope parameters. It was demonstrated for both applications that interpretation of intraoperative ICG-FA images by the surgeons was indeed subjective, as a poor – moderate inter-observer agreement (gastric conduit: ICC: 0.345, 95% CI: 0.164 – 0.584, bowel: 0.378, 95% CI: 0.210 – 0.579) was present. This underlines the need for quantification of the signal. Further studies are currently evaluating the predictive value of perfusion patterns and parameters on anastomotic leakage.

## NEDERLANDSE SAMENVATTING

Het doel van dit proefschrift was om de klinische implementatie van intra-operatieve nabij-infrarood (NIR) fluorescentiebeeldvorming verder te verbeteren, met de nadruk op tumour-beeldvorming en perfusiebeoordeling met indocyanine groen (ICG). In deze sectie worden de methodologie en resultaten van elk hoofdstuk samengevat in de volgorde van verschijning in dit proefschrift.

### Deel I: huidige status van intra-operatieve beeldvorming in de chirurgische oncologie

Het eerste deel van dit proefschrift bestaat uit systematisch literatuuronderzoeken om de status van (NIR-fluorescentie) beeldvorming te evalueren en om de uitdagingen te beschrijven die moeten worden beantwoord voor verdere implementatie van de techniek in de dagelijkse praktijk. Om meer inzicht te krijgen in de huidige klinische toepassingen van NIR-fluorescentiebeeldvorming voor colorectale kankerchirurgie, werd een systematische review uitgevoerd en gepresenteerd in **hoofdstuk 2**. De volgende klinische toepassingen werden geïdentificeerd en besproken: beeldvorming van primaire en recidiverende tumouren, beeldvorming van de schildwachtklier, beeldvorming van peritoneale en levermetastasen, beeldvorming van zenuwen, beeldvorming van de ureters en de urethra, en perfusiebeoordeling van anastomosen of een omentumplastiek middels ICG. Zowel experimentele als FDA/EMA-goedgekeurde fluorescente stoffen worden besproken in dit hoofdstuk.

In **hoofdstuk 3** van dit proefschrift beschrijven we het gebruik van verschillende beeldvormingstechnieken die intra-operatief kunnen worden gebruikt voor margebeoordeling van het larynxcarcinoom. Het larynxcarcinoom is een veel voorkomende maligniteit in het hoofd-hals gebied met een slechte prognose en lage overlevingspercentages voor patiënten met gevorderde ziekte. Om de chirurgische resectie van larynxkanker te verbeteren en het aantal lokale recidieven te verminderen, zijn verschillende intra-operatieve optische beeldvormingstechnieken onderzocht. In deze systematische review identificeren we deze technologieën en evalueren we de huidige staat en toekomstige richtingen van optische beeldvorming voor deze indicatie. Narrow-band imaging (NBI) en autofluorescentie (AF) zijn gevestigde hulpmiddelen voor vroege detectie van larynxkanker. Desalniettemin wordt hun intra-operatieve bruikbaarheid beperkt door een intrinsiek onvermogen om structuren dieper dan de mucosa af te beelden. Contactendoscopie (CE) en optische coherentietomografie (OCT) zijn technisch omslachtig en alleen nuttig voor de beoordeling van de mucosale marges. Onderzoek naar fluorescentiebeeldvorming voor deze toepassing is schaars en focust uitsluitend op niet-specifieke fluorescente stoffen. Het is duidelijk dat de beeldvormingsmodaliteiten die tot nu toe zijn onderzocht over het algemeen niet geschikt zijn voor beoordeling van diepe marges. We bespreken twee optische beeldvormingstechnieken die dit wel kunnen en stellen voor

hoe ze kunnen worden gebruikt om in alle stadia adequate marges te bereiken bij chirurgie voor larynxkanker.

In **hoofdstuk 4** van dit proefschrift richten we ons op fluorescentiebeeldvorming voor het in kaart brengen van schildwachtklieren (SLN-mapping) bij darmkanker. SLN-mapping kan een waardevolle aanvulling zijn op de behandeling van darmkankerpatiënten. Desalniettemin is de conventionele methoden voor het in kaart brengen van lymfeklieren met blauwe kleurstof beperkt vanwege onvoldoende dieptepenetratie. Ook het gebruik van een radiocolloïde tracer heeft zijn logistieke hindernissen. Met nabij-infrarood (NIR) fluorescentiebeeldvorming kan de SLN bij de meeste patiënten nauwkeurig worden geïdentificeerd, wat resulteert in een nauwkeurigere lymfeklierstadiëring. De huidige technische uitdagingen en de lage negatief voorspellende waarde van de SLN weerhouden chirurgen van het gebruik ervan in de dagelijkse praktijk.

## Deel II: Expressie van tumour markers in solide tumouren voor NIR-fluorescentiebeeldvorming

In het tweede deel van dit proefschrift hebben we getracht nieuwe tumour markers te identificeren voor NIR-fluorescentiebeeldvorming. Overexpressie van deze markers werd beoordeeld met immuunhistochemie (IHC). In **hoofdstuk 5** hebben we een studie uitgevoerd waarin we de expressie van CEA, c-MET, EGFR, EpCAM en VEGF-α in slokdarmkanker weefsel van 44 patiënten hebben beoordeeld. Marker expressie werd gekwantificeerd met de 'total immunostaining score' (TIS) met een afkapwaarde van ≥ 6 voor 'hoge expressie'. Het effect van neoadjuvante therapie op tumour marker expressie werd beoordeeld door de TIS van dezelfde weefsels voor en na de neoadjuvante therapie met elkaar te vergelijken. We vonden dat EpCAM expressie hoog was in 89% van de adenocarcinomen en dat EGFR expressie hoog was in 100% van de plaveiselcelcarcinomen SCC. De expressie van geen van de tumour markers werd negatief beïnvloed door neoadjuvante therapie. Alleen VEGF-α toonde enkele expressie in het tumourlittekenweefsel na een pathologische complete respons. Deze tumour markers zijn interessant voor toekomstige studies waarin endoscopische NIR-fluorescentiebeeldvorming van slokdarmkanker tijdens klinische responsevaluatie wordt onderzocht. Aangezien expressie niet werd beïnvloed door neoadjuvante therapie, zou een patiënt specifieke tracer kunnen worden geselecteerd op basis van markerexpressie op het diagnostische biopt.

## Deel III: Klinische studies naar intra-operatieve NIR-fluorescentiebeeldvorming binnen de oncologische chirurgie

In het derde deel van dit proefschrift presenteren we verschillende klinische studies naar intra-operatieve NIR-fluorescentiebeeldvorming. In **hoofdstuk 6** van dit proefschrift presenteren we een studie waarin we onderzoeken of NIR-fluorescentiebeeldvorming met methy-

leenblauw de visualisatie van dunne darm neuro-endocrine tumouren (NETs) verbetert. Zeventien patiënten die een open resectie van een dunne darm NET ondergingen werden geïncludeerd in deze prospectieve klinische studie. Intra-operatief werd intraveneus methyleenblauw toegediend gevolgd door NIR-fluorescentiebeeldvorming. Zeventien primaire tumourlaesies, met een mediane TBR van 1.10 (IQR: 1.00 - 1.17), werden geïdentificeerd. Geen van de primaire tumouren of de 'meerdere primaire' had een TBR ≥ 1.5. In totaal werden 109 metastasen geïdentificeerd, waarvan 101 (93%) een TBR ≥ 1.5 hadden (mediane TBR: 1.90 (IQR: 1.71 – 2.01)). Door gebruik te maken van NIR-fluorescentiebeeldvorming werd bij drie patiënten extra peritoneaal metastasen gevonden. Op basis van deze resultaten kan worden geconcludeerd dat NIR-fluorescentiebeeldvorming met behulp van methyleenblauw een verbeterde visualisatie van peritoneaal metastasen, levermetastasen en mesenteriale massa's van dunne darm NETs mogelijk maakt. Methyleenblauw lijkt echter niet bruikbaar te zijn voor de detectie van de primaire tumour of occulte 'meerdere primaire'.

In de gepresenteerde studie in **hoofdstuk 7** onderzoeken we de binding van de CEA-specifieke tracer SGM-101 aan colorectale longmetastasen (CLM). Tijdens CLM-chirurgie kunnen margebeoordeling en identificatie van kleine tumouren een uitdaging zijn, vooral tijdens minimaal invasieve chirurgie. Intra-operatieve fluorescentiebeeldvorming kan deze uitdagingen adresseren. We voerden een prospectieve open-label studie uit, waarin 13 patiënten werden geïncludeerd die chirurgische resectie voor CLM ondergingen. Patiënten kregen 3 – 5 dagen voorafgaand aan de operatie SGM-101 toegediend. *In vivo*, 'back table' en 'closed-field' fluorescentiebeeldvorming werd uitgevoerd van het resectie preparaat met de tumour. Achttien CLM werden geïdentificeerd en een positief fluorescentiesignaal met *in vivo*, 'back table' en 'closed-field' fluorescentiebeeldvorming werd waargenomen in 31%, 45% en 94% van de tumourlaesies. De mediane signal-to-background ratio's (SBR) voor de drie beeldvormingsmodaliteiten waren respectievelijk 1.00 (IQR: 1.00 – 1.53), 1.45 (IQR: 1.00 – 1.89) en 4.81 (IQR: 2.70 – 7.41). Zes gereseceerde goedaardige laesies waren allemaal negatief voor fluorescentie (waar negatief). Alle tumourlaesies hadden een TIS voor CEA-expressie van 12/12. De studie toonde het potentieel aan van fluorescentiebeeldvorming van CLM met SGM-101. CEA-expressie werd waargenomen in alle tumouren en 'closed-field' beeldvorming toonde een uitstekende binding van de tracer op de tumour laesies. Het volledige potentieel van SGM-101 voor *in vivo* detectie van de tumouren kan worden bereikt met verbeterde minimaal invasieve beeldvormingssystemen en optimale patiënten selectie.

In **hoofdstuk 8** presenteren we grafisch de unieke toepassing van indocyanine groen fluorescentie angiografie (ICG-FA) voor het selecteren van het optimale doorsnijdingsvlakken voor een coloninterpositie. De casus beschrijft een gecompliceerd beloop na slokdarmresectie, waarbij uiteindelijk herstel van de continuïteit met een coloninterpositie werd uitgevoerd. Om de perfusie van de coloninterpositie te beoordelen, stellen we een benadering voor waar-

bij een situatie wordt gecreëerd waarbij het colon uitsluitend wordt gevasculariseerd door de arteria colica media, voordat het colon en alle vascularisatie wordt doornomen. Dit werd gedaan door klemmen te plaatsen op de arteria colica sinistra en op het colon ter hoogte van de toekomstige distale doorsnijdingslijn, om retrograde doorbloeding te voorkomen. Hierna werd 10 mg ICG intraveneus geïnjecteerd en werd een intens fluorescentiesignaal waargenomen over het gehele linker colon. Na doornemen van het colon werd nog eens 10 mg ICG toegediend om de uiteindelijke doorbloeding van de coloninterpositie te beoordelen. Perfusie werd als afdoende beschouwd en er werden anastomosen gecreëerd. Postoperatief herstelde de patiënt goed en na 7 weken kon de patiënt volledig eten.

In de laatste twee hoofdstukken van dit proefschrift presenteren we twee pilotstudies waarin we de uitkomsten van ICG-FA verder proberen te verbeteren. Zoals vermeld in de inleiding van dit proefschrift kan het signaal van ICG-FA worden beïnvloed door niet-gestandaardiseerde beeldvorming- of toedieningsprotocollen. Bovendien werd verondersteld dat subjectieve interpretatie van het signaal leidt tot variatie tussen chirurgen in de selectie van locaties om een anastomose te creëren. Kwantificatie van ICG-FA signaal zou deze problemen kunnen oplossen. In **hoofdstuk 9** concentreren we ons op de rol van gekwantificeerde ICG-FA bij perfusie beoordeling van de buismaag, terwijl we ons in **hoofdstuk 10** concentreren op de darm. In beide onderzoeken volgden we gestandaardiseerde beeldvorming- en toedieningsprotocollen. Per studie werden er twintig patiënten geïncludeerd. Per patiënt werd een gestandaardiseerde NIR ICG-FA video opgenomen, met vaste camera-instellingen en omgevingsfactoren. Postoperatief werd het ICG signaal van de video's gekwantificeerd. De primaire uitkomstmaten waren de tijd-intensiteitscurven en de negen afgeleide perfusieparameters van aangrenzende ‘regions of interest’ op de buismaag. Een secundaire uitkomstmaat was de overeenstemming over de subjectieve interpretatie van de ICG-FA-video's tussen zes chirurgen. De inter-observer overeenstemming tussen de chirurgen werd getest met een intraclass correlatiecoëfficiënt (ICC). Voor zowel de buismaag als de darm werden drie verschillende perfusiepatronen herkend: patroon 1 (steile instroom, steile uitstroom); patroon 2 (steile instroom, geringe uitstroom); en patroon 3 (langzame instroom, geen uitstroom). Alle curves werden systematisch gecategoriseerd in een van elk patroon op basis van de ‘time-to-max’ en ‘max egress slope’ parameters. Voor beide toepassingen werd aangetoond dat de interpretatie van intra-operatieve ICG-FA-beelden door de chirurgen subjectief was, gezien een slecht tot matige inter-observer overeenstemming (buismaag: ICC: 0.345, 95% BI: 0.164 – 0.584, darm: 0.378, 95 % BI: 0.210 – 0.579). Dit onderstreept de noodzaak van kwantificatie van het signaal. Vervolgstudies onderzoeken op dit moment de voorspellende waarde van deze perfusiepatronen en parameters op naadlekkage.

# Chapter 12

## General discussion and future perspectives

## GENERAL DISCUSSION AND FUTURE PERSPECTIVES

The aim of this thesis was to further improve clinical implementation of intraoperative near-infrared (NIR) fluorescence imaging, with a focus on tumour imaging and perfusion assessment. Here, the results of this thesis are evaluated and placed in a broader perspective of current literature. Finally, we reflect on future perspectives leading to a broad implementation of intraoperative NIR fluorescence imaging in standard of care.

## TUMOUR IMAGING

To successfully implement the use of a tumour-specific NIR fluorescence tracer into standard of care, roughly three steps need to be taken. The first step involves identifying a suitable tumour marker for targeted imaging. The second step involves both preclinical and clinical trials to evaluate safety, toxicity, and binding of a specific fluorescent tracer to the tumour marker identified in step one. Several doses and timing intervals of the tracer can be studied in this step. In the third step, studies focus on evaluating whether the use of the tracer, with the optimal dose and timing, results in improved patient-related outcomes such as adequate surgical margins and survival rates. The studies presented in this thesis were mainly focussed on the first two steps.

### Identifying tumour markers for targeted imaging

In order to identify suitable tumour markers for targeted tracers, immunohistochemistry (IHC) experiments are typically performed on cancer tissue to assess overexpression. These tumour markers are specific characteristics of cells that ideally have higher expression on tumour cells compared to surrounding healthy tissue. In the study presented in **chapter 5** we found suitable tumour markers (EGFR and EpCAM) for NIR fluorescence imaging of oesophageal cancer. An important additional conclusion from this study is that marker expression in oesophageal cancer tissue remains unaffected after neoadjuvant therapy. This finding is consistent with earlier results from Boogerd et al., who observed unaffected tumour marker expression after neoadjuvant therapy in rectal cancer (1). In both rectal and oesophageal cancer, an organ preserving strategy is currently being explored in patients with a clinical complete response after neoadjuvant therapy (2, 3). These tumour markers offer opportunities for targeted NIR fluorescence imaging during endoscopic response evaluation. While ideally a single fluorescent tracer for all tumours would be used, this may not be possible due to heterogeneity in tumour marker expression between (and even within) tumours. For that reason, unaffected marker expression after neoadjuvant therapy is essential as it enables the selection of a patient-specific targeted tracer for fluorescence imaging, based on target expression on the diagnostic biopsy. Endoscopic spraying of the tracer on the lesion of interest (i.e. topical administration), opposed to conventional intravenous administration, appears to be feasible during endoscopic fluorescence imaging and this method is expected to be

more frequently used in future studies (4, 5). Topical administration is a major advantage, as it does not require an extra or earlier hospital visit, prior to endoscopy. While the required dose for topical tracer administration has not yet been reported, it is reasonable to assume that it would be lower, reducing costs and toxicity. Currently, the lack of commercially available flexible NIR fluorescence endoscopic imaging systems withholds the technique from being further integrated in clinical trials. Close collaborations with NIR fluorescence camera manufacturers should therefore be maintained.

### Assessing tracer binding to the associated tumour marker

Binding of a tumour-specific tracer to the earlier detected tumour markers is not guaranteed. Tracer dose, interval between administration and imaging, and pharmacokinetics all affect tracer binding to the tumour, subsequently affecting the fluorescent contrast. Moreover, clinical tracers may bind to different epitopes than the antibodies used for the immunohistochemistry staining. As such, the second step of tracer development is to evaluate its binding ability to the tumour, to assess the optimal dose and timing interval, and to assess toxicity. The two main applications of tumour imaging include detection of clinically invisible tumour lesions (i.e. occult lesions) and detection of inadequate resection margins. These applications require different approaches, and thus, different outcome measures should be considered when assessing the usability of the tracer and determining the optimal dose and timing strategy.

Detection of occult lesions is exclusively carried out through in vivo imaging. To this end, reporting in vivo Tumour-to-Background Ratios (TBRs) and the number of detected occult metastases is essential. In **chapter 6** we described the utility of methylene blue as a fluorescent agent for the detection of small intestinal neuroendocrine metastases (SI-NETs) to the liver and peritoneal surface. High TBRs in the smallest metastases were observed, which implicates that methylene blue is a useful contrast agent for the detection of occult lesions. Since large metastases are typically detected by palpation and inspection already, TBRs in small lesions are particularly relevant in this context. In general, detection of occult (peritoneal) metastases can lead to additional resection, or to refraining from resection at all when achieving complete resection is not possible anymore. In case of the latter, the use of NIR fluorescence imaging is used to for improved patient selection by withholding patients from useless operations. Improved patient selection is another important result of the use of NIR fluorescence imaging, though its importance is sometimes underestimated.

Opposed to peritoneal surface and liver metastases, primary tumours were not identified using methylene blue. As detection of occult primary and metastatic lesions is both important , we are currently exploring whether second window ICG results in sufficient TBRs in primary SI-NETs (OCEANS-II trial). Second window ICG, in which doses of up to 5 mg/kg are

intravenously injected 24 hours before surgery, has been demonstrated to enhance detection of several thoracic and intracranial malignancies (6, 7). The underlying mechanism is based on the enhanced permeability and retention effect (EPR) of tumours (8). If second window ICG, alone or combined with methylene blue, proves to enhance detection of all SI-NETs, a laparoscopic approach for patients with these tumours may be possible.

In **chapter 8** we present a study in which binding of the CEA specific antibody SGM-101 to colorectal lung metastases was assessed. The use of this tracer might be useful for margin assessment, as well as detection of occult or small lesions. We found sufficient binding of the tracer to the tumour with high TBRs with *ex vivo* black box imaging of the bread loaves. However, in- and *ex vivo* TBRs (of the whole specimen) were significantly lower, hampering the intraoperative detection of the tumours with fluorescence imaging. These low in vivo TBRs were attributed to the lack of high quality 700 nm minimally invasive imaging systems. Consequently, SGM-101 is currently suboptimal for the detection of small and occult lesions.

A different tracer, that may be superior to SGM-101 for colorectal lung metastases, is the integrin specific cRGD-ZW800-1 (hereafter referred to as 'cRGD'). It was already demonstrated that integrins are highly expressed in colon carcinomas and that the tracer binds to primary colorectal cancers (9). The cRGD molecule is relatively small, particularly compared to larger antibodies like SGM-101, bevacizumab-800CW, or panitumumab-IRDye800CW (10, 11). The use of small molecules is preferable to larger antibodies owing to the shorter time interval between administration and imaging. Consequently, imaging with small molecules does not necessitate an additional hospital admission for tracer administration, unlike the case for most antibodies. A second advantage of cRGD is that it is labelled with the 800 nm fluorophore ZW800-1, which has a higher wavelength than the 700 nm fluorophore (BM-104) of SGM-101. This may lead to a slight improvement in penetration depth, allowing for imaging of deeper seeded lesions (12). Moreover, multiple minimally invasive NIR fluorescence imaging systems already allow for imaging of 800 nm fluorophores, as opposed to 700 nm fluorophores. Given this, cRGD may be particular useful for intraoperative use during (minimally invasive) colorectal lung metastases surgery.

Binding of cRGD to tumour cells is also currently being explored by our research group in patients with oral squamous cell carcinoma (the Guided by Light trial, (13)). Moreover, continuing on our findings presented in **chapter 3**, the STELLAR trial will be carried out, in which efficacy and feasibility of targeting advanced laryngeal cancer with cRGD-ZW800-1 will be studied (14). Both the Guided by Light and STELLAR trial may provide us with valuable result regarding the optimal dose and timing strategy of cRGD and its efficacy of identifying inadequate resection margins. If the use of cRGD appears to improve identification of inadequate margins in these head and neck cancers, a subsequent study (third step of implementation)

will be conducted. Such a study will assess whether the use of cRGD increases the rate of adequate resection margins, potentially improving survival outcomes of these head and neck cancer patients.

### Assessing patient related outcomes

Though not part of this thesis, clinical trials in which direct patient benefit is explored are currently ongoing for multiple fluorescent tracers. Worth mentioning are two phase-III studies with SGM-101 (**chapter 8**) for advanced colorectal cancer and the studies that led to the recent registration by the Food and Drug Association (FDA) of OTL-38, a folate-α targeting tracer, for detection of ovarian and primary lung cancer (15-18). OTL-38 is now the first clinically approved tumour-specific NIR fluorescence tracer. It is expected that more of these phase-III studies will be conducted which eventually will lead to registration for clinical use by the FDA or European Medicine Agency (EMA).

### The sentinel margin approach

In recent years, it has become increasingly evident that standardised approaches are required for NIR fluorescence imaging, including margin assessment. For this purpose, the sentinel margin approach was introduced by van Keulen et al (19, 20). This approach involves imaging of the surgical specimen in a black box imager, which allows for standardised imaging with respect to camera distance, absence of surrounding light, and fixed gain and exposure settings. As a result, absolute fluorescence intensities can be measured more reliable. By imaging the resection margin of the specimen in this black box, the location with the highest fluorescence intensity can be identified. This location should correspond to the closest resection margin (i.e. the sentinel margin), assuming sufficient sensitivity and specificity of the tracer. The tumour-free margin at this location can then be measured using frozen section analysis to determine whether an adequate resection is achieved. Ideally, this final frozen section analysis will also become redundant, as it is time consuming and not available in every clinic. Therefore, multiple research groups are currently exploring whether absolute or relative fluorescence intensities at the location of sentinel margin can predict adequate or inadequate resection margin status (20, 21).

While the sentinel margin approach was initially introduced for oral cancer, it is currently validated for other tracers and tumour types as well. Examples are the earlier mentioned Guided by Light trial, STELLAR trial, and the SGM-LARRC trial. Overall, we believe that the sentinel margin approach shows great promise for detection of inadequate resection margins and should therefore be incorporated in every study with tumour-specific tracers assessing resection margin status.

## PERFUSION ASSESSMENT

The second application of NIR fluorescence imaging studied in this thesis is tissue perfusion assessment with Indocyanine Green Fluorescence Angiography (ICG-FA). This thesis focused on ICG-FA in gastrointestinal surgery, specifically perfusion assessment of the colon and gastric conduit. The first randomized controlled trials (RCTs) evaluating the efficacy of Indocyanine Green Fluorescence Angiography (ICG-FA) in reducing anastomotic leakage after colorectal surgery yielded negative results, as reported in **chapter 2**. The low incidence of anastomotic leakage might have resulted in underpowered trials, thereby necessitating larger randomized studies over recent years. The EssentiAL trial, which included 850 rectal cancer patients randomized to receive either ICG-FA or standard of care, recently finished accrual. Preliminary results showed that the incidence of anastomotic leakage was significantly lower in the ICG-FA group (7.6% vs. 11.8%) (22). The AVOID trial has recently reached full inclusion of 978 colorectal cancer patients, thereby making it the largest randomized controlled trial (RCT) conducted on this subject thus far (23). Definitive results of both trials are expected on short-term and these may definitively prove the value of ICG-FA in reducing anastomotic leakage.

### Standardisation of ICG-FA

Other important factors that may have contributed to the negative results reported in chapter 2 are the lack of standardized imaging protocols and the subjective interpretation of the signal. Therefore, we aimed to further standardise and improve interpretation of ICG-FA by conducting two pilot studies on quantitative ICG-FA, presented in **chapter 9 and 10**. Our findings demonstrate that the standard interpretation of the ICG-FA signal by surgeons for both the gastric conduit and bowel is highly subjective, highlighting the need for quantification of the signal. Standardisation of imaging, with fixed gain and exposure settings of fluorescence cameras, as well as a fixed distance to the tissue, is the first crucial step when performing (quantitative) ICG-FA. No standardisation of these factors leads to severely affected results and subsequently, incomparable data. It is therefore remarkable that in recent publications on quantitative ICG-FA these factors have not been standardised or reported (24, 25).

For the gastric conduit and the bowel we demonstrated feasibility of performing quantified ICG-FA and acquiring time-intensity perfusion curves. Currently larger datasets are being obtained, by which we aim to develop prediction models providing risk rates of anastomotic leakage per tissue location. With these prediction models, the surgeon can be guided more precisely in selecting an adequately perfused part to create an anastomosis. Quantitative ICG-FA also has a few challenges that need to be addressed for full integration into the clinic. The most important challenge is that quantification in real-time during surgery is not possible yet, which means that the surgical strategy cannot be altered based on the perfusion parameters. We expect that this will be resolved in the near future, as the first real-time

quantification software has been introduced recently (26). A specific limitation of **chapter 9** is that our results have solely been focussing on cervical anastomoses, as the gastric conduit is brought extracorporal during this procedure, facilitating standardised imaging with the open camera system. Nonetheless, we aim to introduce quantitative ICG-FA in intrathoracic procedures as well. The biggest challenges to address in this procedure is to maintain a standardized imaging protocol, in particular a fixed distance between the camera and gastric conduit. Moreover, most high quality NIR minimally invasive imaging systems are currently lacking a function to fix gain and exposure settings. The main advantage of procedures with intrathoracic anastomoses, opposed to cervical anastomoses, is that there is more room to reduce the length of the gastric conduit.

## NIR FLUORESCENCE IMAGING AND ARTIFICIAL INTELLIGENCE (AI)

Deep learning models using AI is currently a topic of interest in almost all scientific fields, including surgery. AI is an ideal tool to for image analysis, which makes its combination with NIR fluorescence imaging very promising. AI algorithms can analyse large amounts of complex data generated by NIR fluorescence imaging and can therefore assist in the identification and localization of specific targets within the tissue, such as cancer cells. This may be very beneficial during in vivo imaging, in which an AI model might be better in recognising the fluorescence signal of small occult lesions than the surgeon. This concept was recently introduced for the first time during endoscopic fluorescence imaging of the oesophagus (27). AI models can also be trained to recognize perfusion patterns and parameters within ICG-FA videos, which can then be used to generate more accurate and reliable prediction of anastomotic leakage per tissue location (28). Furthermore, AI models can aid in the identification of new tumour markers for new contrast agents that can improve the sensitivity and specificity of NIR fluorescence imaging (29).

The integration of AI in NIR fluorescence imaging also presents some challenges, such as the need for large and diverse datasets to train machine learning models and the potential for bias in the analysis of data. Collection of such datasets may take a long time as the technique is fairly new. However, due to the rapid expansions of the use of NIR fluorescence imaging (especially ICG-FA) this may go faster than expected. Additionally, the use of AI in medical imaging raises ethical and regulatory concerns regarding the safety and privacy of patients.

## NIR FLUORESCENCE IMAGING AND OTHER IMAGING TECHNIQUES

Interpretation of NIR fluorescence images poses a challenge in that the fluorescence signal is affected by absorption and scattering due to tissue optical properties (30). Additionally, the markers for tumour-specific tracers are also expressed in healthy tissue that can contrib-

ute to false positive or false negative signals. To resolve these problems, NIR fluorescence imaging can be combined with other imaging techniques. Raman spectroscopy (RS) is an optical technique that is used to characterise cancerous and non-cancerous tissue based on their molecular composition and water concentration. Measurements are typically acquired through point-based measurements with an optical fibre, which makes its use alone prone to sampling error. However, its uniquely high specificity for detecting tumour makes RS an ideal candidate for combination with wide-field NIR fluorescence imaging. For margin assessment, the optical fibre can be inserted in the tissue at the location of the sentinel margin in order to precisely measure the tumour free distance. It was recently shown for the first time by Lauwerends and Abbasi et al. that RS measurements can be performed in combination with the presence of a fluorescent agent (31). The combination of these two techniques may be very beneficial in further intraoperative tissue characterisation. Currently, two clinical trials in patients with oral cancer and rectal cancer are ongoing, in which we further aim to bring these two techniques together.

A second imaging method that may be combined with NIR fluorescence imaging is photoacoustic imaging. Photoacoustic imaging is a hybrid imaging technique that combines the imaging depth of ultrasound with the contrast of molecular imaging. Photoacoustic imaging allows for imaging of fluorescent agents located several centimetres below the surface. This may be useful for imaging of tumour targeted NIR tracers to detect lymph node metastases, for example in head and neck cancer (32). To date, it was demonstrated that two fluorescent tracers yield high sensitivity and specificity to detect lymph node metastases, when these nodes were imaged in an *ex vivo* setting (33, 34). However, due to the low penetration depth of NIR light, it is unlikely that these results can be translated to in vivo imaging. Accordingly, refraining from an elective lymph node dissection, based on absence of fluorescence signal, appears not realistic. Due to the relatively high imaging depth of photoacoustic imaging, this technique may offer better differentiation between malignant and benign lymph nodes. This may allow for an approach in which preoperative, tumour-specific, photoacoustic assessment of nodal status is performed in order to decide for an elective lymph node dissection.

## COST-EFFECTIVENESS

As healthcare costs continue to rise annually in the Netherlands, it is important to critically evaluate the feasibility of costly new therapies, including NIR fluorescence imaging. NIR fluorescence imaging, especially using tumour-specific tracers, is currently an expensive technique. Thus, it is imperative to remain vigilant regarding cost-effective methodologies or fluorescent tracers, for example methylene blue (**chapter 6**). In future studies, cost-effectiveness analyses of the use of the NIR fluorescence imaging will become increasingly important. Additional costs that should be considered in such analyses include the costs accompanied

with the production and administration of the tracer, and those of NIR fluorescence camera systems. Potential financial benefits include less adjuvant therapy, less recurrences and subsequent treatment, and less re-operations or interventions for surgical complications. So far, one cost-effectiveness study was published on the use of Bevacizumab-800CW to detect inadequate breast cancer margins (35). It was demonstrated that the use of this tracer saved €663 per patient, mainly due to the reduction of re-operations for inadequate resection margins. It should be noted that this analysis was based on a set presumptions and that changes in effectiveness of inadequate margins, or a change in costs of the tracer, will likely affect the results.

With regard to cost-effectiveness of ICG, a study by Nguyen et al. demonstrated cost-effectiveness of ICG-FA assessment in post-mastectomy breast reconstruction (36). Based on the break-even point analysis, 318 surgical cases with 18 prevented ischaemic complications are needed to recover the costs of the fluorescence camera, ICG, and other costs associated with operating room expenses. However, given the versatility of fluorescence cameras and their ability to be utilized in different surgical specialties, the actual break-even point may be lower. A second study found ICG to be a cost-effective option for bile duct identification during laparoscopic cholecystectomy (37). This was primarily driven by the reduction in operating time (21 minutes) and in conversion rate (1.6 vs. 6.7%). A cost-effectiveness analysis of the earlier mentioned AVOID trial is also expected (23).

## CONCLUSION

In conclusion, NIR fluorescence imaging has emerged as a powerful tool in surgical research and clinical applications, owing to its high sensitivity, resolution, and higher penetration depth than white light. With the development of AI algorithms, improved camera systems, and new contrast agents, NIR fluorescence imaging is expected to become even more advanced and versatile in the next decade. It is likely that AI-assisted NIR fluorescence imaging will enable real-time visualization and quantification of biological processes at the cellular and molecular level, paving the way for personalized medicine and precision surgery. Moreover, the integration of NIR fluorescence imaging with other imaging modalities will provide complementary and synergistic information for diagnosis and treatment monitoring. Challenges that need to be addressed in the following years are the further development of safe and effective contrast agents, the standardization of imaging protocols, the validation of AI algorithms, and proving efficacy in improving patient outcomes in third phase (randomized clinical) trials. Overall, NIR fluorescence imaging holds great promise for improving outcomes of surgically treated oncological patients.

## REFERENCES


1. Boogerd LS, van der Valk MJ, Boonstra MC, Prevoo HA, Hilling DE, van de Velde CJ, et al. Biomarker expression in rectal cancer tissue before and after neoadjuvant therapy. Onco Targets Ther. 2018;11:1655-64.
2. van der Valk MJM, Hilling DE, Bastiaannet E, Meershoek-Klein Kranenbarg E, Beets GL, Figueiredo NL, et al. Long-term outcomes of clinical complete responders after neoadjuvant treatment for rectal cancer in the International Watch & Wait Database (IWWD): an international multicentre registry study. Lancet. 2018;391(10139):2537-45.
3. Eyck BM, van der Wilk BJ, Noordman BJ, Wijnhoven BPL, Lagarde SM, Hartgrink HH, et al. Updated protocol of the SANO trial: a stepped-wedge cluster randomised trial comparing surgery with active surveillance after neoadjuvant chemoradiotherapy for oesophageal cancer. Trials. 2021;22(1):345.
4. Gabriels RY, van Heijst LE, Hooghiemstra WTR, van der Waaij AM, Kats-Ugurlu G, Karrenbeld A, et al. Detection of early esophageal neoplastic Barrett lesions with quantified fluorescence molecular endoscopy using cetuximab-800CW. J Nucl Med. 2023.
5. Nagengast WB, Hartmans E, Garcia-Allende PB, Peters FTM, Linssen MD, Koch M, et al. Near-infrared fluorescence molecular endoscopy detects dysplastic oesophageal lesions using topical and systemic tracer of vascular endothelial growth factor A. Gut. 2019;68(1):7-10.
6. Newton AD, Predina JD, Corbett CJ, Frenzel-Sulyok LG, Xia L, Petersson EJ, et al. Optimization of Second Window Indocyanine Green for Intraoperative Near-Infrared Imaging of Thoracic Malignancy. J Am Coll Surg. 2019;228(2):188-97.
7. Teng CW, Cho SS, Singh Y, De Ravin E, Somers K, Buch L, et al. Second window ICG predicts gross-total resection and progression-free survival during brain metastasis surgery. J Neurosurg. 2021:1-10.
8. Maeda H. Tumor-Selective Delivery of Macromolecular Drugs via the EPR Effect: Background and Future Prospects. Bioconjugate Chemistry. 2010;21(5):797-802.
9. de Valk KS, Deken MM, Handgraaf HJM, Bhairosingh SS, Bijlstra OD, van Esdonk MJ, et al. First-in-Human Assessment of cRGD-ZW800-1, a Zwitterionic, Integrin-Targeted, Near-Infrared Fluorescent Peptide in Colon Carcinoma. Clin Cancer Res. 2020;26(15):3990-8.
10. Lamberts LE, Koch M, de Jong JS, Adams ALL, Glatz J, Kranendonk MEG, et al. Tumor-Specific Uptake of Fluorescent Bevacizumab-IRDye800CW Microdosing in Patients with Primary Breast Cancer: A Phase I Feasibility Study. Clin Cancer Res. 2017;23(11):2730-41.
11. Lu G, van den Berg NS, Martin BA, Nishio N, Hart ZP, van Keulen S, et al. Tumour-specific fluorescence-guided surgery for pancreatic cancer using panitumumab-IRDye800CW: a phase 1 single-centre, open-label, single-arm, dose-escalation study. Lancet Gastroenterol Hepatol. 2020;5(8):753-64.
12. Kennedy GT, Azari FS, Chang A, Nadeem B, Bernstein E, Segil A, et al. Comparative Experience of Short-wavelength Versus Long-wavelength Fluorophores for Intraoperative Molecular Imaging of Lung Cancer. Ann Surg. 2022;276(4):711-9.
13. Keereweer S. Fluorescence-guided Surgery Using cRGD-ZW800-1 in Oral Cancer (GuidedbyLight): clinicaltrials.gov; 2022 [Available from: https://clinicaltrials.gov/ct2/show/NCT04191460?term=crgd-zw800-1&draw=2&rank=2.

**14.** Keereweer S. Fluorescence-guided Surgery in Laryngeal- and Hypopharyngeal Cancer: a Feasibility Trial (STELLAR): clinicaltrials.gov; 2023 [Available from: https://clinicaltrials.gov/ct2/show/NCT05752149?term=STELLAR&draw=2&rank=3.

**15.** Tanyi JL, Randall LM, Chambers SK, Butler KA, Winer IS, Langstraat CL, et al. A Phase III Study of Pafolacianine Injection (OTL38) for Intraoperative Imaging of Folate Receptor-Positive Ovarian Cancer (Study 006). J Clin Oncol. 2023;41(2):276-84.

**16.** Kennedy GT, Azari FS, Bernstein E, Marfatia I, Din A, Kucharczuk JC, et al. Targeted Intraoperative Molecular Imaging for Localizing Nonpalpable Tumors and Quantifying Resection Margin Distances. JAMA Surg. 2021;156(11):1043-50.

**17.** Vahrmeijer AL. SGM-101 in Locally Advanced and Recurrent Rectal Cancer (SGM-LARRC): ClinicalTrial.gov; [Available from: https://clinicaltrials.gov/ct2/show/NCT04642924.

**18.** Vahrmeijer AL. Performance of SGM-101 for the Delineation of Primary and Recurrent Tumor and Metastases in Patients Undergoing Surgery for Colorectal Cancer: ClinicalTrials.gov; [Available from: https://clinicaltrials.gov/ct2/show/NCT03659448.

**19.** van Keulen S, Nishio N, Birkeland A, Fakurnejad S, Martin B, Forouzanfar T, et al. The Sentinel Margin: Intraoperative Ex Vivo Specimen Mapping Using Relative Fluorescence Intensity. Clin Cancer Res. 2019;25(15):4656-62.

**20.** Krishnan G, van den Berg NS, Nishio N, Kapoor S, Pei J, Freeman L, et al. Fluorescent Molecular Imaging Can Improve Intraoperative Sentinel Margin Detection in Oral Squamous Cell Carcinoma. J Nucl Med. 2022;63(8):1162-8.

**21.** Witjes MJH. Image Guided Surgery for Margin Assessment of Head and Neck Cancer Using Cetuximab-IRDye800CW cONjugate (ICON): Clinicaltrials.gov; 2017 [Available from: https://clinicaltrials.gov/ct2/show/NCT03134846?term=ICON+fluorescence&draw=2&rank=1.

**22.** Watanabe J. Randomized phase 3 trial evaluating the efficacy of ICG fluorescence imaging on anastomotic leakage in laparoscopic surgery of rectal cancer.

**23.** Meijer RPJ, Faber RA, Bijlstra OD, Braak J, Meershoek-Klein Kranenbarg E, Putter H, et al. AVOID; a phase III, randomised controlled trial using indocyanine green for the prevention of anastomotic leakage in colorectal surgery. BMJ Open. 2022;12(4):e051144.

**24.** de Groot EM, Kuiper GM, van der Veen A, Fourie L, Goense L, van der Horst S, et al. Indocyanine green fluorescence in robot-assisted minimally invasive esophagectomy with intrathoracic anastomosis: a prospective study. Updates Surg. 2023;75(2):409-18.

**25.** Slooter MD, de Bruin DM, Eshuis WJ, Veelo DP, van Dieren S, Gisbertz SS, et al. Quantitative fluorescence-guided perfusion assessment of the gastric conduit to predict anastomotic complications after esophagectomy. Dis Esophagus. 2021;34(5).

**26.** [Available from: https://www.perfusiontech.com/.

**27.** van der Laan JJH, van der Putten JA, Zhao X, Karrenbeld A, Peters FTM, Westerhof J, et al. Optical Biopsy of Dysplasia in Barrett’s Oesophagus Assisted by Artificial Intelligence. Cancers. 2023;15(7):1950.

**28.** Park SH, Park HM, Baek KR, Ahn HM, Lee IY, Son GM. Artificial intelligence based real-time microcirculation analysis system for laparoscopic colorectal surgery. World J Gastroenterol. 2020;26(44):6945-62.

**29.** Meijer RPJ, Neijenhuis LKA, Zeilstra AP, Roerink SF, Bhairosingh SS, Hilling DE, et al. Data-Driven Identification of Targets for Fluorescence-Guided Surgery in Non-Small Cell Lung Cancer. Mol Imaging Biol. 2023;25(1):228-39.

**30.** Keereweer S, Van Driel PB, Snoeks TJ, Kerrebijn JD, Baatenburg de Jong RJ, Vahrmeijer AL, et al. Optical image-guided cancer surgery: challenges and limitations. Clin Cancer Res. 2013;19(14):3745-54.

**31.** Lauwerends LJ, Abbasi H, Bakker Schut TC, Van Driel P, Hardillo JAU, Santos IP, et al. The complementary value of intraoperative fluorescence imaging and Raman spectroscopy for cancer surgery: combining the incompatibles. Eur J Nucl Med Mol Imaging. 2022;49(7):2364-76.

**32.** Nishio N, van den Berg NS, Martin BA, van Keulen S, Fakurnejad S, Rosenthal EL, et al. Photoacoustic Molecular Imaging for the Identification of Lymph Node Metastasis in Head and Neck Cancer Using an Anti-EGFR Antibody-Dye Conjugate. J Nucl Med. 2021;62(5):648-55.

**33.** Nishio N, van den Berg NS, van Keulen S, Martin BA, Fakurnejad S, Teraphongphom N, et al. Optical molecular imaging can differentiate metastatic from benign lymph nodes in head and neck cancer. Nat Commun. 2019;10(1):5044.

**34.** Vonk J, de Wit JG, Voskuil FJ, Tang YH, Hooghiemstra WTR, Linssen MD, et al. Epidermal Growth Factor Receptor-Targeted Fluorescence Molecular Imaging for Postoperative Lymph Node Assessment in Patients with Oral Cancer. J Nucl Med. 2022;63(5):672-8.

**35.** Präger M, Kiechle M, Stollenwerk B, Hinzen C, Glatz J, Vogl M, et al. Costs and effects of intra-operative fluorescence molecular imaging - A model-based, early assessment. PLoS One. 2018;13(6):e0198137.

**36.** Nguyen CL, Dayaratna N, Comerford AP, Tam SKM, Paredes SR, Easwaralingam N, et al. Cost-effectiveness of indocyanine green angiography in postmastectomy breast reconstruction. J Plast Reconstr Aesthet Surg. 2022;75(9):3014-21.

**37.** Reeves JJ, Broderick RC, Lee AM, Blitzer RR, Waterman RS, Cheverie JN, et al. The price is right: Routine fluorescent cholangiography during laparoscopic cholecystectomy. Surgery. 2022;171(5):1168-76.

# Appendices

## LIST OF PUBLICATIONS

1. Current intraoperative imaging techniques to improve surgical resection of laryngeal cancer: a systematic review
   Galema HA, Lauwerends LJ, Hardillo JAU, Sewnaik A, Monserez D, van Driel PBAA, Verhoef C, Baatenburg de Jong RJ, Hilling DE, Keereweer S.
   *Cancers (Basel). 2021 Apr 15;13(8):1895. doi: 10.3390/cancers13081895*

2. Fluorescence-guided surgery in colorectal cancer; a review on clinical results and future perspectives
   Galema HA, Meijer RPJ, Lauwerends LJ, Verhoef C, Burggraaf J, Vahrmeijer AL, Hutteman M, Keereweer S, Hilling DE
   *European Journal of Surgical Oncology. 2022 Apr;48(4):810-821. doi: 10.1016/j.ejso.2021.10.005.*

3. Fluorescence-guided sentinel lymph node detection in colorectal cancer
   Meijer RPJ, Galema HA, Lauwerends LJ, Verhoef C, Burggraaf J, Keereweer S, Hutteman M, Vahrmeijer AL, Hilling DE
   *The Lymphatic System in Colorectal Cancer. Basic Concepts, Pathology, Imaging and Treatment Perspectives. 2022, Pages 245-255*

4. ICG-fluorescence angiography assessment of colon interposition for oesophageal cancer – a video vignette
   Galema HA, van Rees JM, Matthijsen RA, Hilling DE, Wijnhoven BPL, Lagarde SM
   *Colorectal Disease. 2022 May;24(5):665. doi: 10.1111/codi.16076. Epub 2022 Mar 2.*

5. Fluorescence-guided surgery using methylene blue to improve identification of small intestinal neuroendocrine tumours and peritoneal metastases
   Galema HA, van Ginhoven TM, Franssen GJH, Hofland J, Bouman CGOT, Verhoef C, Vahrmeijer AL, Hutteman M, Hilling DE, Keereweer S.
   *British Journal of Surgery. 2023 Apr 12;110(5):541-544. doi: 10.1093/bjs/znad043.*

6. A quantitative assessment of perfusion of the gastric conduit after oesophagectomy using near-infrared fluorescence with indocyanine green
   Galema HA, Faber RA, Tange FP, Hilling DE, van der Vorst JR; Upper-GI ICG quantification study group
   *European Journal of Surgical Oncology. 2023 Mar 2:S0748-7983(23)00171-3. doi: 10.1016/j.ejso.2023.02.017.*

7. Quantification of indocyanine green near-infrared fluorescence bowel perfusion assessment in colorectal surgery
   Galema HA, Faber RA, Tange FP, Zwaan TC, Holman FA, Peeters KCMJ, Tanis PJ, Verhoef C, Burggraaf J, Mieog JSD, Hutteman M, Keereweer S, Vahrmeijer AL, van der Vorst JR‡, Hilling DE‡.
   *Surgical Endoscopy. 2023 Jun 7. doi: 10.1007/s00464-023-10140-8*

8. Intraoperative molecular imaging of colorectal lung metastasis with SGM-101: an exploratory study
   Galema HA, Meijer RPJ, Faber RA, Bijlstra OD, Maat APWM, Cailler F, Braun J, Keereweer S, Hilling DE, Burggraaf J, Vahrmeijer AL, Hutteman M, On behalf of the SGM-CLM study group:
   *European Journal of Nuclear Medicine and Molecular Imaging. 2023 Aug 8. doi: 10.1007/s00259-023-06365-3.*

9. Effects of neoadjuvant therapy on tumour target expression of oesophageal cancer tissue for NIR fluorescence imaging
   Galema HA, Neijenhuis LKA, Lauwerends LJ, Dekker-Ensink NG, Verhoef C, Vahrmeijer AL, Bhairosingh S, Kuppen PJK, Rogallae S, Burggraaf J, Lagarde SM, Wijnhoven BPL, Hutteman M, Doukas M, Keereweer S, Hilling DE
   *Submitted*

## Not in this thesis

10. Huidige behandeling sinus pilonidalis in Nederland
    Galema HA, Vles, WJ, Gosselink MP, Schouten R, Smeenk RM, Toorenvliet BR
    *Het Nederlands Tijdschrift voor Heelkunde*

11. Intraoperative Near-Infrared Fluorescence Imaging with Indocyanine Green for Identification of Gastrointestinal Stromal Tumors (GISTs), a Feasibility Study.
    Kalisvaart GM, Meijer RPJ, Bijlstra OD, Galema HA, de Steur WO, Hartgrink HH, Verhoef C, de Geus-Oei LF, Grünhagen DJ, Schrage YM, Vahrmeijer AL, van der Hage JA.
    *Cancers (Basel). 2022 Mar 18;14(6):1572. doi: 10.3390/cancers14061572.*

12. Assessment of Surgical Strategies for Pilonidal Sinus Disease in the Netherlands
    Huurman EA, Galema HA, de Raaff C, Toorenvliet B, Smeenk R
    *Cureus. 2022 May 16;14(5):e25050. doi: 10.7759/cureus.25050*

## CONTRIBUTING AUTHORS

Dima D.A. Almandawi
Feredun Azari
Robert Jan Baatenburg de Jong
Shadhvi Bhairosingh
Okker D. Bijlstra
Claire G.O.T. Bouman
Jerry Braun
Jacobus Burggraaf
Françoise Cailler
Wobbe O. de Steur
N. Geeske Dekker - Ensink
Michail Doukas
Robin A. Faber
Bérénice Framery
Gaston J.H. Franssen
José A.U. Hardillo
Henk H. Hartgrink
Denise E. Hilling
Johannes Hofland
Fabian A. Holman
Merlijn Hutteman
Stijn Keereweer
Sjors Koppes
Peter J.K. Kuppen
Sjoerd M. Lagarde
Lorraine J. Lauwerends
Alexander P.W.M. Maat
Edris A.F. Mahtab
Robert Matthijsen
Ruben P.J. Meijer
J. Sven D. Mieog
Dominiek Monserez
Lisanne K.A. Neijenhuis
Koen C.M.J. Peeters
Stephan Rogalla
Aniel Sewnaik
Ghada M.M. Shahin
Sunil Singhal
Floris P. Tange
Pieter J. Tanis
Alexander L. Vahrmeijer
Pieter C. van der Sluis
Joost R. van der Vorst
Pieter B.A.A. van Driel
Tessa M. van Ginhoven
Jan M. van Rees
Cornelis Verhoef
Mats I. Warmerdam
Bas P.L. Wijnhoven
Thomas C. Zwaan

## PHD PORTFOLIO

| | |
|---|---|
| **Name PhD student:** | H.A. Galema |
| **Erasmus MC Department**: | Surgical oncology and gastrointestinal surgery & Otorhinolaryngology, Head and neck surgery |
| **PhD period:** | 01/06/2020 – 31/05/2023 |
| **Promotors:** | Prof. dr. C. Verhoef<br>Prof. dr. R.J. Baatenburg de Jong |
| **Co-promotors:** | Dr. D.E. Hilling<br>Dr. S. Keereweer |

| **Research Courses** | **Year** | **EC** |
|---|---|---|
| Scientific Integrity | 2020 | 0.3 |
| Erasmus MC – BROK | 2020 | 1.5 |
| Biostatistical Methods I: Basic Principles | 2020 | 5.7 |
| ESHCC – Data management | 2020 | 1.0 |
| In-house training Castor EDC | 2021 | 1.0 |
| Basic course on 'R' | 2021 | 1.8 |
| Translational imaging workshop by AMIE 'from mouse to man' | 2022 | 1.0 |
| Biomedical writing for PhD candidates | 2023 | 1.5 |
| **Other Courses** | | |
| Advanced Trauma Life Support | 2023 | 2.0 |
| **Oral Presentations** | | |
| Science day, dept. of Otorhinolaryngology, Head and neck surgery, Erasmus MC | 2022 | 1.0 |
| ESSO 41, Bordeaux (poster in the spotlight presentation) | 2022 | 0.5 |
| ESSO 41, Bordeaux | 2022 | 1.0 |
| Science day, dept. of Surgery, Erasmus MC | 2023 | 1.0 |
| Chirurgendagen 2023, Veldhoven | 2023 | 1.0 |
| WCP Zuid West Nederland, Dordrecht | 2023 | 1.0 |
| **Poster Presentations** | | |
| ESSO 40, Lisbon | 2021 | 0.5 |
| WMIC 2022, Miami (2 posters) | 2022 | 1.0 |
| ESSO 41, Bordeaux | 2022 | 0.5 |
| ESDE 2023, Leuven | 2023 | 0.5 |
| Erasmus MC Cancer Retreat, Rotterdam | 2023 | 0.5 |

| | | |
|---|---|---|
| **Conference Attendance** | | |
| ESSO Webinar Fluorescence Guided Surgery | 2021 | 0.3 |
| Chirurgendagen 2022, Den Haag | 2022 | 0.6 |
| Dutch Fluorescence Guided Surgery (DFGS) conference, Zeist | 2022 | 0.3 |
| ESSO 41, Bordeaux | 2022 | 0.9 |
| Erasmus MC Cancer Retreat, Rotterdam | 2023 | 0.6 |
| Chirurgendagen 2023, Veldhoven | 2023 | 0.6 |
| **Teaching and supervision** | | |
| Educating medical students on colorectal cancer | 2021 | 0.3 |
| Master student – M.G. Been | 2023 | 1.0 |
| **Organisation** | | |
| Focusgroup fluorescence guided surgery, 2 monthly | 2020 – 2023 | 3.0 |
| Dutch Fluorescence Guided Surgery (DFGS) conference (1st edition) | 2022 | 2.0 |
| Het Wondcongres (22nd edition) | 2022 – 2023 | 2.0 |
| **Other** | | |
| Peer reviewing for the following scientific journals | 2020 -2022 | 2.1 |
| - European Journal of Surgical Oncology | | |
| - World Journal of Surgical Oncology | | |
| - British Journal of Surgery | | |
| - Oral Oncology | | |
| - Cancers | | |
| **Total EC** | | 38 |

## ACKNOWLEDGEMENTS | DANKWOORD

Dit proefschrift heeft niet tot stand kunnen komen zonder de actieve deelname van vele patiënten. Deze patiënten bevinden zich vaak in een emotioneel en lichamelijk zware periode in hun leven. Veelal zonder enig eigen gewin, en puur uit motivatie om de zorg voor toekomstige patiënten met eenzelfde aandoening te verbeteren, nemen zij deel aan wetenschappelijk onderzoek. Enorm veel dank gaat uit naar hen allen.

Daarnaast wil ik een aantal personen persoonlijk bedanken:

Geachte promotor, Prof. dr. C. Verhoef, Beste Kees, toen ik als 6e jaars geneeskunde student eens bij je op de koffie mocht om te praten over een eventuele onderzoeksplek, vroeg je waarom ik onderzoek wilde doen. Uiteraard had ik die vraag zien aankomen en noemde ik een paar (hele slechte) argumenten. Je prikte daar gelijk doorheen en antwoordde: 'Nee, je wilt gewoon chirurg worden'. Hier had je natuurlijk volkomen gelijk in, en dat heb ik dan ook maar toegegeven. Toch durfde je de gok met mij te wagen en heb je me aanbevolen bij Stijn en Denise. Waarschijnlijk heb je ze iets gezegd als: 'Ik heb hier nog wel een geinig ventje rondlopen' (meer zal het niet geweest zijn in ieder geval). Dat de afgelopen 3 jaar op deze manier zouden verlopen had ik zelf ook niet verwacht, en dat komt mede door jou en de mensen die je om je heen verzamelt. Ondanks dat ik 'gewoon chirurg wilde worden' heb ik een fantastische tijd gehad als onderzoeker bij de OGC. Dank voor alles en ik ga zelfs de klappen op mijn schouder missen.

Geachte promotor, Prof. dr. R.J. Baatenburg de Jong, Beste Rob, wellicht heeft onze kennismaking door COVID en beetje een trage start gekend, maar dat is in de 2e helft van mijn onderzoeksperiode zeker ingehaald. Ik waardeer de moeite die u steekt in de band met uw onderzoekers door het organiseren van borrels, uitjes en etentjes. Hierbij denk ik aan de wetenschapsdag met aansluitend borrel en diner en de lunch voor onderzoekers en ANIOS bij Marseille. Ik heb onze samenwerking altijd als bijzonder prettig ervaren en zie de combinatie van KNO en Chirurgie zeker als een mooie toevoeging aan mijn promotie onderzoek, ondanks dat ik nog steeds chirurg wil worden. Mooi dat de 'hoofd-hals studies' nu dan toch eindelijk begonnen zijn.

Geachte copromotoren, Dr. D.E. Hilling & Dr. S. Keereweer, het gouden duo en de drijvende kracht achter dit proefschrift. Jullie vullen elkaar perfect aan en dat maakt dat er maar weinig promovendi zijn die de begeleiding krijgen die jullie mij (ons) hebben gegeven. Mede door jullie enthousiasme en bereikbaarheid heb ik dit proefschrift in 3 jaar af kunnen ronden. De meeste dank gaat uit naar jullie.

Beste Denise, je bent een van de meest relaxte personen die ik de afgelopen jaren heb leren kennen en dat maakt de samenwerking de laatste jaren erg prettig. Ik kon altijd even bellen voor overleg of om gewoon even te praten. Daarnaast was je bijzonder goed inzetbaar als aanjager van Merlijn om naar mijn stukken te kijken! De afgetrape spiegel van de Mercedes (taxi) na het DFGS congres was wellicht een dieptepunt maar ik ben blij dat we veilig thuis zijn gekomen die avond. Ik ben blij dat jullie eindelijk wat meer vastigheid hebben gevonden en uiteraard is het een grote winst voor het EMC dat je toch nog in Rotterdam blijft. Ik kom snel een keer langs in Nijmegen, je kan er toevallig ook nog heel mooi fietsen!

Beste Stijn, jouw enthousiasme en doorzettingsvermogen zijn de belangrijkste reden voor het succes van de Image Guided Surgery Group van het EMC. Je weet kritiek of commentaar op zo'n positieve manier te brengen dat het mij de afgelopen jaren veel heeft gebracht. Daarnaast heb je ook altijd ruimte gelaten voor mijn eigen ideeën, wat enorm veel motivatie gaf. Je bent niet alleen als begeleider, maar vooral ook als persoon enorm fijn om mee samen te werken. Vanaf de eerste dag heb je er op aangedrongen dat onze onderzoeksgroep elkaar ook af en toe buiten het ziekenhuis spreekt, want 'het moet ook een beetje leuk blijven'. Ondanks dat ik geen KNO-arts wil worden heb ik een fantastische tijd gehad en hebben we mooie dingen voor elkaar gekregen, met als kers op de taart de Guided by Light studie en binnenkort de STELLAR. Ongetwijfeld tot snel in het EMC en wie weet kan ik je ooit nog eens het verschil tussen een buismaag en een colon laten laten zien.

Geachte leden van de beoordelingscommissie Prof. dr. M. Smits, Prof. dr. C.W.G.M. Löwik en Prof. dr. S. Kruijff, hartelijk dank voor jullie bereidheid om zitting te nemen in de beoordelingscommissie en mijn proefschrift te beoordelen.

Geachte Dr. A.L. Vahrmeijer, Beste Lex, als in Leiden geboren Rotterdammer ben ik meer dan trots dat ik het eerste Rotterdamse GreenLight Leiden lid mocht zijn. Je zorgt met jouw bevlogenheid en humor voor een ontzettend goede sfeer binnen je groep. Dank dat ik deel mocht uitmaken van een van de meest vooruitstrevende onderzoeksgroepen op het gebied van fluorescentie beeldvorming.

Beste Sandra en Esmee, eigenlijk zouden jullie bovenaan dit dankwoord moeten staan. Wat jullie allemaal voor ons onderzoekers regelen is ongekend. Veel dank voor alles en voor de prettige samenwerking.

Alle chirurgen van de OCG die hebben bijgedragen aan de inclusie van patiënten en daarbij de totstandkoming van dit proefschrift. Alexandra, Bas, Dirk, Eva, Gaston, Joost, Linetta, Pieter van der Sluis, Pieter Tanis, Sjoerd, Tessa en Thijs. Bedankt voor jullie eeuwige geduld tijdens

de fluorescentie metingen; ik besef me dat jullie bijna nooit direct iets aan deze metingen hadden. Des te meer dank voor de gezelligheid op OK, maar ook op de afdelingsuitjes.

Hoofd-hals chirurgen Hetty, Brend, Atilla, Dominiek, José, Aniel en longchirurgen Lex, Edris, Sabrina en Amir. Ook jullie bedankt voor jullie bijdrage aan inclusie van de studies in dit proefschrift en de nog lopende studies.

Geachte Dr. Hutteman, Beste Merlijn, ook jij veel dank voor je bijdragen aan nagenoeg alle stukken in dit boekje. Sorry dat ik Denise af en toe heb ingezet om jou naar mijn stukken te laten kijken, maar het werkte vaak wel erg goed. Uiteraard ben ik blij dat je (eindelijk) een vaste plek in een academisch centrum hebt gevonden. Het is je meer dan gegund.

Geachte Dr. Doukas, beste Michail, ik denk dat er in het Erasmus MC weinig mensen rondlopen die een groter hart hebben dan jij. De ochtenden coupes scoren om 8:00 waren altijd gezellig. Je hebt daarmee een belangrijke rol gespeeld in de totstandkoming van het lastigste hoofdstuk van dit proefschrift. Zeer veel dank daarvoor.

Collega 'fluorescentie onderzoekers' Lorraine en Bo, het is mooi om te zien dat jullie de klinische projecten zo goed hebben opgepakt en hier gaan ongetwijfeld een paar fantastische papers uit voort komen. Lorraine, ik weet dat het niet altijd makkelijk voor je is om als 'techneut' in een ziekenhuis rond te lopen. Toch is het bewonderingswaardig hoe je dit hebt opgepakt de laatste jaren. Je creatieve en taalkundige kwaliteiten hebben menig artikel aanzienlijk verbeterd. Daarnaast heeft je creativiteit ook geleid tot het ontwerp van de cover van dit proefschrift. Dank voor alles en succes met de afronding van je eigen proefschrift. Bo, als mijn opvolger ben je voortvarend van start gegaan en heb je (zoals Kees het noemde) al mijn 'corvee taken' over genomen. Uiteraard dank daarvoor en mede daardoor is het mij gelukt om dit proefschrift binnen de full-time termijn af te ronden. Mooi om te zien dat je je draai ook helemaal hebt gevonden op Na-21.

Dear Hamed, thanks for the nice collaboration in the past years and I'm happy to hear that you settled in Breda with your wife. I enjoyed working together and I'm curious to hear your Dutch speaking in the following months. Dear Dom and Riette, although I have seen your formulas to calculate scattering and absorption at least ten times, I still don't understand them. Therefore, I'm very glad that you two were on our team and you both have contributed a lot to the Guided by Light trial. Thanks for everything!

Alle huidige en voormalig collega onderzoekers van Na-21, alle borrels, congressen en uitjes hebben de afgelopen 3 jaar bijzonder veel glans gegeven. Een aantal mensen wil ik in het bijzonder bedanken: Job, Ben, Berend: dank voor het warme welkom toen als verdwaalde

onderzoeker op de 21e aankwam. Mooi om te zien dat deze vriendschap zich nog steeds voortzet en onthoud: 'Please stop repyling to all'. Jan, het samen mogen coördineren van de Surgimab studie, met als hoogtepunt de vrouw van een patiënt die jou telefonisch bedreigde ('als je tegenover me had gezeten had ik je een klap gegeven'), zal ik nooit vergeten. Mooi om onze samenwerking voort te zetten in het Ikazia! Stassen en Sam (van Dick), prijzenwinnaars van de ESSO en bewakers van 'de mannenkamer', dank voor de lol de afgelopen jaren. Mannen van de leverkamer: Huppie, Boris, Wills, Yannick en Stijn: het is de hoogste tijd dat Huppie weer eens op zijn handen gaat staan. Hakan, Het waren drie fantastische maanden. Evalyn, Marloes, Ivona, Anne-Rose, Kelly en Michelle, zelfs het geschreeuw uit jullie kamer ga ik missen! Gelukkig wordt de herrinerering aan deze klanken nog eens opgehaald in de Fame. Ev, het was sowieso de best georganiseerde chirurgencup ooit, ondanks de 7e plaats….

Collega's van de GreenLight Leiden, Ruben, Mats, Robin, Floris, Okker, Martijn en Lisanne, mooi dat ik onderdeel mocht uitmaken van de GreenLight en dank voor het altijd warme welkom in Leiden! We gaan elkaar ongetwijfeld nog vaak tegenkomen.

Chirurgen en assistenten van het Ikazia Ziekenhuis: van Forgeron naar co-assistent, naar oudste co-assistent en nu ANIOS. Terugkomen voelt altijd weer als een warm bad. Ik kijk ontzettend uit naar mijn eerste echte stappen in de kliniek.

Boudewijn en Robert, stelling 9 komt van jullie en deze weerspiegelt de mooie periode waarin ik onder julie supervisie mijn eerste wetenschappelijke stappen kon zetten. Dank dat jullie mij toen het vertrouwen gaven. Helaas toen nog niet zo succesvol in het binnenhalen van subsidies, maar mooi om te zien dat jullie deze projecten ondertussen aardig op gang hebben.

Free en Marijn, studiematen van het eerste uur. Sinds de eerste colleges in 2012 waarbij Free graag de goede antwoorden wilde geven ('tumor!') tot Swirls halen met extra 'crunch' voor Marijn, en '1 pinnen, 2 chippen'. Ik wacht nog steeds op het moment tot de oude hoofdingang wordt hersteld. Op jullie kan ik altijd terugvallen.

De schoonfamilie en (mede)aanhang, ontzettend blij dat ik als nieuwste lid heb mogen toetreden tot de gezelligste groepswhatsapp van Nederland, de PH5 partycrew. Het is elke keer weer genieten in Utrecht en natuurlijk ook in Cadzand. Ontzettend mooi dat ik (hopelijk) als 3e dit jaar mag promoveren.

Mijn twee broertjes (en tevens Paranimfen), Jouke en Geert, alleen al het idee dat jullie in rokkostuum een uur lang aan mijn zijde staan tovert een glimlach op mijn gezicht. Hoewel we (volgens sommige mensen) heel veel op elkaar lijken, hebben we ook heel veel verschillen,

wat onze chemie alleen maar versterkt. Ik geniet van het feit dat jullie je eigen pad bewandelen. Gelukkig is dat geen Geneeskundig pad, want anders zou het wel heel saai worden binnen ons gezin.

Lieve papa en mama, dat ik als 3e gezinslid een PhD kan afronden maakt het extra speciaal en het maakt mij meer dan trots. Ik besef me dat dit allemaal niet mogelijk was geweest zonder de stabiele basis die jullie ons hebben gegeven, thuis in Rotterdam. Mijn dank is oneindig.

Lieve Elies, het laatste woord is voor jou. Nooit gedacht dat jij het mooiste 'hoofdstuk' van mijn promotietijd zou zijn. Jij kan het saaiste nog leuk maken en je gekke maniertjes fleuren alles op. Er is geen fijnere plek om elke dag te zijn dan bij jou. Ik ben blij dat alles voor jou op zijn plaats is gevallen en kijk enorm uit naar de komende jaren samen in Rotterdam in ons nieuwe huis.

## ABOUT THE AUTHOR

Hidde Ake Galema was born on April 13th, 1994 in Leiden, The Netherlands as the oldest son of Tjebbe Galema and Annette Boers. He grew up in Rotterdam in a family of five with his two younger brothers Jouke and Geert. After graduating from secondary school in 2012 (VWO, Montessori Lyceum Rotterdam) he started Medical School at the Erasmus University Rotterdam. During his studies he joined the medical student team ('Les Forgerons') of the Surgery department at the Ikazia Hospital which triggered his interest in Surgery. In 2017, he conducted his master research at the department of Plastic- and Reconstructive Surgery of the SickKids Hospital in Toronto, Canada on congenital craniofacial abnormalities which only increased his enthusiasm about surgical disciplines.

In 2020 Hidde obtained his medical degree after which he started as a PhD-candidate at the Erasmus MC Cancer Institute on intraoperative NIR fluorescence imaging (Prof. C. Verhoef & Prof. R.J. Baatenburg de Jong). Given the multidisciplinary nature of the subject, this research project was a joined effort between the department of Surgical Oncology and Gastrointestinal Surgery and the department of Otorhinolaryngology, Head and Neck Surgery, and in close collaboration with the GreenLight Leiden group led by Dr. A.L. Vahrmeijer.

From July 2023 onwards, Hidde is working as a Resident (ANIOS) at the Department of Surgery of the Ikazia Hospital in Rotterdam (Dr. W.J. Vles and Dr. P.T. den Hoed).